University of Liège
Faculty of Medicine
GIGA Cancer

Tregs independent GARP functions

in the tumor microenvironment

Loïc ROUAUD

Promotor: Pr Agnès Noël
Laboratory of Tumor and Development Biology

Thesis presented to obtain the degree of
Doctorate of Biomedical and Pharmaceutical Sciences

2023 – 2024

Université de Liège
Faculté de Médecine
GIGA Cancer

Les fonctions de GARP indépendantes des Tregs dans le microenvironnement tumoral

Loïc ROUAUD

Promoteur : Prof. Agnès Noël
Laboratoire de Biologie des Tumeurs et du développement

*Thèse présentée en vue de l'obtention du grade de
Doctorat en Sciences Biomédicales et Pharmaceutiques*

2023 – 2024

SUPERVISOR

Pr Agnès Noël

JURY

Internal members	External members
Pr Chantal Humblet	Pr Pierre Coulie
Dr Ingrid Struman	Pr Bernard Mari
Dr Christophe Deroane	
Dr Nicolas Van Baren	

"On fait la science avec des faits, comme on fait une maison avec des pierres : mais une accumulation de faits n'est pas plus une science qu'un tas de pierres n'est une maison."

Henri Poincaré

"Parce que la science nous balance sa science, science sans conscience égale science de l'inconscience."

Mc Solaar

Acknowledgment

Après 4 ans et demi, mon chapitre au sein du LBTD se termine, mais il laisse place à de nouvelles aventures. En repensant à mon doctorat, je ne peux qu'être reconnaissant d'avoir fait partie de cette équipe de recherche accueillante et dynamique. Un travail de recherche ne peut être mené à bien sans le soutien et l'accompagnement de toutes les personnes qui nous entourent.

Je tiens dans un premier temps à exprimer ma profonde gratitude envers la professeure Agnès Noël, ma promotrice, pour m'avoir accueilli au sein de son laboratoire et pour m'avoir offert l'opportunité de réaliser ce projet sur GARP. Pendant ces quatre dernières années, Agnès m'a accordé sa confiance et m'a soutenu dans ce qu'elle qualifie de projet « fantasme », comme elle aime à le dire. Bien que parfois ses idées semblent difficiles à suivre, elle a toujours une longueur d'avance et une vision tournée vers l'avenir. Je tiens à exprimer ma reconnaissance à la fois sur le plan professionnel, pour ses connaissances scientifiques, et sur le plan personnel, pour son écoute attentive. C'est ainsi qu'elle a contribué à mon développement tant sur le plan personnel que scientifique.

Ce projet n'aurait pas été réalisable sans le soutien de nos collaborateurs de l'UCL que sont la professeure Sophie Lucas et le Dr Nicolas Van Baren. Merci encore, Sophie, pour ton accueil, ton soutien et ton expertise en immunologie, notamment sur le sujet de GARP. Nos échanges scientifiques ont toujours été un plaisir, non seulement en raison de ta passion pour transmettre ton savoir, mais aussi grâce à ta pédagogie toujours efficace. Merci Nicolas pour m'avoir guidé à mes débuts dans l'apprentissage de R et pour avoir renforcé mon attrait pour l'analyse de données. Mais aussi pour le partage de tes connaissances sur GARP et ta patience pour la correction de ce manuscrit. Je tenais également à remercier Pierre pour son accueil chaleureux, son sourire contagieux, sa joie de vivre et son enthousiasme pour la recherche. Ce fut un plaisir de pouvoir échanger avec toi lors de nos rencontres à l'UCL ou aux soirées Télévie. Je te souhaite tout le meilleur pour la suite. Je tiens aussi à remercier tous les membres ou anciens membres de l'équipe de Sophie : Charlotte, Nicolas, Grégoire et bien d'autres.

Je suis reconnaissant envers les membres de mon jury pour la lecture de mon manuscrit, leurs remarques pertinentes et tous leurs précieux conseils qui m'ont permis de m'améliorer. Merci encore aux professeurs Bernard Mari et Pierre Coulie pour avoir généreusement rejoint mon jury en tant que membres externes. De même qu'aux professeurs Chantal Humblet, Ingrid Struman, Nicolas Van Baren et Christophe Deroanne pour avoir participé à mes comités de thèse et m'avoir suivi pendant ces quatre longues années.

Je n'oublierai pas non plus le bureau des 6 (cru 2019) que sont Isabelle, Amélie, Alice, Sébastien et Fabrice. Nous avons tous commencé en même temps et nous arrivons à la fin de cette belle aventure. Nous avons traversé le COVID, non sans difficulté, mais nous avons bravé la vague. Merci encore pour nos discussions et nos échanges aussi bien scientifiques que non-scientifiques, ah ah.

Je tiens à exprimer ma gratitude envers mes super collègues de bureau, Dada et Léa, qui ont été mes compagnons de route pendant les deux dernières années de cette thèse. Merci encore à vous deux pour m'avoir soutenu et supporté tant durant la rédaction que lors de la préparation de mes présentations. Leurs encouragements m'ont permis de traverser la thèse de manière plus relaxe, car parfois, « JPP », n'est-ce pas Léa ?

Merci à mes compagnons de voyage, Flo, Louis, Séb et Fabrice, qui ont été d'excellents partenaires dans nos périples scientifiques. Je me souviendrai de la joie de participer à un séminaire après une dizaine d'heures de vol et quatre heures du matin, heure de Belgique ☺. En plus des connaissances scientifiques acquises, ces voyages nous ont également permis de mieux nous connaître les uns les autres.

Je remercie par ailleurs tous les anciens membres ou membres actuels de la Team Lymphangio, Alizée, Sophie, Sébastien, Florence, Louis, Fatine, Léa, Jonathan, Eva, Elitsa et Chloé. J'ai partagé de très bons moments de bench en votre compagnie, même si Séb prend quatre benchs à lui tout seul. Vous avez été d'un très grand soutien lors de nos grandes (et longues) réunions ^^.

Merci à tous mes collègues du LBTD : Charles, Coline, Alice, Robin, Mohammad, Amélie, Thomas, Aimée, Isabelle B, Daphnée, Jules, Marlyne, Laetitia, Isabelle DDS,

Vincent, Manon, Silvia, Erika, Sheila et Isabelle D. Je remercie aussi tous les PI de toutes les équipes qui y sont associées. Il en va de même pour les équipes de notre étage, ainsi que tous leurs membres (Eh oui, vous êtes nombreux et je ne voudrais pas en oublier).

Ma reconnaissance va également à notre super secrétaire, Hélène, qui effectue un travail remarquable. Elle répond toujours présent pour nous aider afin de résoudre nos problèmes administratifs, ainsi que pour prendre soin de nos commandes.

De plus, je souhaite remercier les différentes plateformes scientifiques qui ont contribué à la réalisation de ce travail. Leurs équipements, leur assistance technique et leur expertise facilitent grandement notre quotidien de chercheur. Je suis, bien évidemment, reconnaissant envers les différentes sources de financements du laboratoire (Télévie, Welbio et EOS) pour leur soutien. Ce sont elles qui ont permis la réalisation de ce travail.

Un tout grand merci va à ma famille, ainsi qu'à ma maman pour son soutien indéfectible tout au long de ce parcours. Même si je suis conscient que mes explications sur mes travaux peuvent parfois être aussi claires qu'un manuel de montage IKEA (sans les images). Ce que j'ai pu réussir plus jeune et aujourd'hui, c'est également grâce à ton soutien et à tes efforts, et je te remercie pour ce que tu as fait et feras à l'avenir.

Enfin, un très grand merci à Eva, mon petit chou, qui m'a été d'un très grand soutien durant ces 8 dernières années. Je ne regrette toujours pas de t'avoir rejoint en Belgique afin de reprendre mes études. Cela n'a pas été très facile tous les jours, mais nous avons tenu bon, malgré le COVID, la thèse ou tout autre périple de la vie. Tu as fait en sorte que cette thèse se passe pour le mieux et je t'en remercie.

Un grand merci aussi à Iris, amie et collègue d'Eva. Même si tu n'as pas contribué directement à ce travail, ta connaissance « scientifique » m'a grandement aidé ^^. Toi qui n'es pas scientifique, mais qui t'y connais très bien sur le sujet 😊, tu sauras aider mon collègue dans la suite du projet, ah ah. J'espère que ces travaux t'aideront à prendre conscience du cancer.

Les derniers remerciements iront à mes deux grands-parents, Pépé et Mémé, comme nous aimions les appeler. Si vous n'avez pas pu me soutenir durant ces dernières années, je sais que vous seriez fiers de moi. C'est votre cancer qui a motivé mon choix de

reprendre mes études et de continuer dans ce domaine. Vous m'avez rendu plus fort et permis de garder mon objectif en vue, aussi bien dans les moments difficiles que dans les meilleurs moments.

Table Of Content

List of Figures and Tables

Figures

Tables

Abbreviations

ALK	Activin receptor-like kinase
AMH	anti-Müllerian hormone
BAX	Bcl-2-associated X
Bcl-2	B-cell leukemia/lymphoma 2
BEC	Blood endothelial cell
bFGF	Basic fibroblast growth factor
BMP	Bone morphogenic protein
CAF	Cancer-associated fibroblast
CAM	Cell-cell adhesion molecule
CCL	C-C motif chemokine ligand
CCR	C-C motif chemokine receptor
CDK	Cyclin-dependent kinase
CTC	circulating tumor cells
DC	Dendritic cell
DTC	Disseminating tumor cells
ECM	Extracellular matrix
FACS	Fluorescence-associated cell sorting
FDC	Follicular dendritic cell
FFPE	Formalin-fixed paraffin-embedded
FGF-1/2	Acidic/basic fibroblast growth factors
FOXC2	Forkhead box protein C2
FRC	Fibroblast reticular cell
GARP	Glycoprotein A repetitions predominant
GDF	Growth differentiation factors
HEV	Hugh endothelial venule
HUVEC	Human umbilical cord endothelial cells
i.p.	Intraperitoneal
ICAM-1	Intercellular adhesion molecule 1
Ig	Immunoglobulin
IL	Interleukin
Integrin α	ITGA
IPEX	Immune dysregulation, polyendocrinopathy, enteropathy, X-linked
I-SMAD	Inhibitory SMAD
JAM-A	Junctional adhesion molecule A

LEC	Lymphatic endothelial cell
LN	Lymph node
LOX	Lysyl oxidase
LTBP	Latent TGF-β1 binding protein
LTi	Lymphoid-tissue inducer
Lto	Lymphoid-tissue organizer
LTαβ	Lymphotoxin-αβ
LTβR	Lymphotoxin receptor-β
LYVE-1	Lymphatic vessel endothelial hyaluronan receptor 1
mAbs	Monoclonal antibodies
MADCAM-1	Mucosal addressin cell adhesion molecule 1
MDSC	Myeloid-derived suppressor cell
MEK/MAPK	Mitogen-activated protein kinase pathway
MER	Myeloid-epithelial-reproductive tyrosine kinase
MHC	Major histocompatibility complex
MIS	Müllerian inhibiting substance
MMP	Metalloproteinase
MS	Medullary sinus
n-cadherin	Neural cadherin
NFAT	Nuclear factor of activated T cells
NF-κB	Nuclear factor-kappa B
NK	Natural killer
NO	Nitric oxide
p21	Cyclin-dependent kinase inhibitor 1
p53	Tumor protein p53
PAI-1	Plasminogen inhibitor 1
PD-1	Programmed cell death protein 1
PDGF	Platelet-derived growth factor
PD-L	PD-1 ligand
PECAM1/CD31	Platelet endothelial cell adhesion molecule
PI3K	Phosphoinositide 3-kinase
PMN	Pre-metastatic niche
PNAd	Peripheral node addressin
pRB	Retinoblastoma protein
pSMAD	Phospho-SMAD
R-SMAD	Receptor SMAD
rTGF-β1	Recombinant TGF-b1

scRNA-Seq	Single-cell RNA sequencing
SCS	Subcapsular sinus
sGARP	Soluble GARP
SLN	Sentinel lymph node
SpArC	Osteonectin
STAT3	Signal transducer and activator of transcription 3
TCR	T cell receptor
TGF-β1	Transforming growth factor β1
TGF-βRI or RII	Type I or type II TGF-β receptor
Th	Helper T cell
TME	Tumor microenvironment
TMLEC	Transforming mink lung endothelial cell
Treg	Regulatory T cell
VEGF	Vascular endothelial growth factor
VEGFR	VEGF receptor
αSMA	α-smooth muscle actin

Abstract

The lymphatic system and the sentinel lymph node (SLN) are a spreading relay for cancer cells in several cancer types, such as breast, cervical, head and neck, and pancreatic carcinomas, as well as melanomas. Before metastatic colonization, the tumor-draining LN undergoes remodeling, forming a pre-metastatic niche (PMN) associated with an increased number of Foxp3+ regulatory T cells (Tregs). These modifications lead to the creation of an immune-suppressive microenvironment. One of the factors leading to immunosuppression is the transforming growth factor beta 1 (TGF-β1), secreted or bound at the cell surface to a transmembrane receptor known as glycoprotein A repetitions predominant (GARP). Several immune and non-immune cells are known to express GARP, and Tregs are the best studied GARP+ cells. Non-immune cells are known to play a significant role in the structure, organization, and function of LN. The cellular sources and the spatial distribution of GARP in LNs during the metastatic process have not been studied extensively. Through data mining of scRNA-Seq datasets of human and mouse LNs, we revealed GARP expression in blood (BEC) and lymphatic (LEC) endothelial, fibroblastic, and perivascular cells. Consistently, through immunostaining and in situ RNA hybridization approaches, GARP was detected in and around blood and lymphatic vessels, in αSMA+ fibroblasts, and in the ECM. GARP was also detected in LECs forming the subcapsular sinus and in high endothelial venules (HEVs), two vascular structures localized at the interface between LNs and the afferent lymphatic and blood vessels, respectively. Altogether, we provide the first report about the spatial distribution of non-immune cells expressing GARP in human and murine metastatic LNs. These results suggest a role for these cell populations in the immunosuppressive microenvironment in the LN and open new perspectives for studying the secretion of active TGF-β1 by these cells.

Résumé

Le système lymphatique et le ganglion sentinelle sont des relais de propagation des cellules cancéreuses dans plusieurs types de cancer, tels que les carcinomes du sein, du col de l'utérus, de la tête et du cou et du pancréas, ainsi que les mélanomes. Avant la colonisation métastatique, les ganglions drainant la tumeur subissent un remodelage, formant une niche pré-métastatique associée à un nombre accru de lymphocytes T régulateurs Foxp3+ (Tregs). Ces modifications conduisent à la création d'un microenvironnement immunosuppresseur. L'un des facteurs conduisant à l'immunosuppression est le facteur de croissance transformant bêta 1 (TGF-β1), sécrété ou lié à la surface cellulaire à un récepteur transmembranaire connu sous le nom de glycoprotein A repetitions predominant (GARP). Il est établi que plusieurs cellules immunitaires et non immunitaires expriment GARP, et les Tregs sont les cellules productrices les mieux étudiées. Les cellules non immunitaires sont connues pour jouer un rôle important dans la structure, l'organisation et la fonction du ganglion. Les sources cellulaires et la distribution spatiale de GARP dans les ganglions au cours du processus métastatique sont encore méconnues et n'ont pas été étudiées auparavant. Grâce à l'exploration de données de scRNA-Seq de ganglions humains et murins, nous avons observé l'expression de GARP dans les cellules endothéliales sanguines (BEC) et lymphatiques (LEC), fibroblastiques et périvasculaires. De même, grâce à des approches d'immunomarquage et d'hybridation d'ARN in situ, GARP a été détecté dans des vaisseaux sanguins et autour de vaisseaux lymphatiques, dans les fibroblastes (αSMA+) et dans la matrice extracellulaire. GARP est exprimé en particulier dans les LEC formant le sinus sous-capsulaire et des vaisseaux sanguins spécialisés (HEV), deux structures vasculaires localisées à l'interface entre les ganglions et respectivement les vaisseaux lymphatiques ou sanguins afférents. En résumé, nous rapportons la première observation de distribution spatiale de cellules non immunitaires exprimant GARP dans des ganglions métastatiques humains et murins. Ces résultats mettent en évidence un rôle de ces populations cellulaires dans la participation du microenvironnement immunosuppresseur dans les ganglions et ouvrent de nouvelles perspectives pour l'étude de la sécrétion de TGF-β1 actif par ces cellules.

Part-1 INTRODUCTION

1 Cancer and metastases

1.1 Definition of Cancer

1.1.1 The biological nature of Cancer

Cancer, called the "Emperor of All Maladies"[1], is a multifactorial disease in which some cells develop abnormally and acquire common features. Among them, cancer cells differ from normal cells in their ability to grow abnormally and uncontrollably, ignoring the regulatory signals that limit cell growth and division. While normal cells strictly follow the cell division rules, the acquired capabilities of cancer cells allow them to become autonomous and divide abnormally and continuously. Uncontrolled growth leads to the formation of tumors and, in the most severe cases, the dissemination and invasion of other organs. Cancer is a pathology with diverse origins, behaviors, and treatment responses. However, through extensive research, common characteristics among different types of cancer have been identified. These characteristics are referred to as the "Hallmarks of Cancer", a term first proposed by Hanahan and Weinberg in 2000 (**Fig. 1**)[2].

1.1.2 The hallmarks of Cancer

Tumoral progression is a **dynamic process** characterized by the continuous evolution of the tumor and its microenvironment. This dynamic aspect is underscored by the work of Bert Vogelstein and colleagues, who proposed a multistep genetic model for colorectal cancer initiation and progression[3]. The initiation and progression involve the acquisition of driver mutations. These events endow normal cells with the potential for uncontrolled growth. Understanding the sequence and timing of these mutations is essential in comprehending tumor initiation. Tumors can evolve, acquiring additional genetic alterations that drive progression and lead to the distant dissemination known as metastasis.

INTRODUCTION
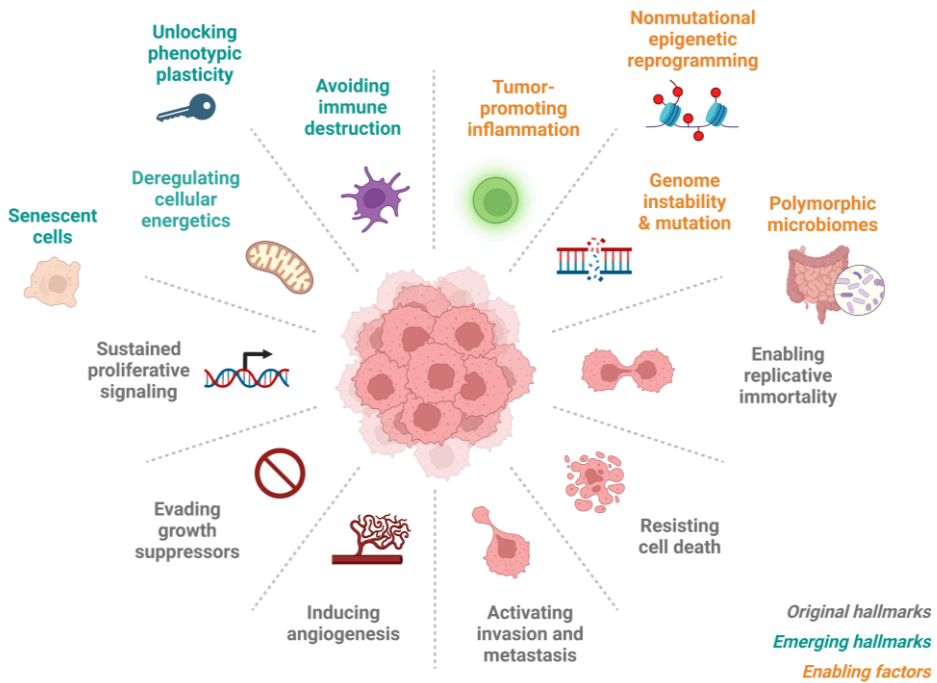
Figure 1. Overview of Cancer Hallmarks
Representation of the fundamental characteristics and key biological processes that define cancer cells. The six original cancer hallmarks (in grey) identified by Hanahan and Weinberg, are highlighted together with additional emerging hallmarks recently reported and the enabling factors (Adapted from[4]).

Cancer cells are known for their adaptability through a process known as **clonal evolution.** The idea of clonal evolution was introduced by Peter Nowell in 1976 as the driving force behind cancer progression[5]. Within a tumor, cancer cells display a range of genetic changes, including mutations, deletions, and rearrangements of chromosomes. This diversity enables the selection of subclones with survival advantages contributing to the progression of the tumor. The process of clonal selection leads to the dominance of specific clones in the genetic composition of the tumor. It happens when some clones have advantages, such as resistance to treatment or a higher potential for metastasis. This process is similar to Charles Darwin's theory of natural selection, but it occurs on a smaller scale within the context of cancer[5,6].

INTRODUCTION

Healthy tissues are subjected to **mechanisms of regulation** that keep a **balance between cell division and cell death**. Normal cells have a limited lifespan and undergo apoptosis in response to DNA damage or aging[7]. However, this mechanism disturbs cancer cells, leading to uncontrolled cell growth and continuing to divide indefinitely. Cancer cells cannot limit their development and division, which usually occurs due to cellular regulatory signals and responses to the cellular environment[8]. **Apoptosis**, a programmed cell death, is a physiological process that controls cell proliferation as a barrier to uncontrolled cell growth[9]. Evidence from experimental models and clinical observations emphasize that cancer cells often acquire the ability to evade apoptosis. This resistance involves altering key regulator genes such as the tumor suppressor protein p53, *c-MYC*, B-cell leukemia/lymphoma 2 (Bcl-2) family members and ndm23[10]. p53 is a cellular gatekeeper that regulates the Bcl-2/Bcl-2–associated X (Bax) balance by down-regulating the expression of Bcl-2[11] and up-regulating Bax in favor of apoptosis[12]. Many types of cancer exhibit an alteration of this equilibrium, such as colorectal carcinoma, brain and lung cancer, mammary carcinoma, skin and bladder carcinomas[13,14]. *C-MYC* is a major regulator gene that plays a role in this regulation. The deregulation of the *C-MYC* gene often leads to its overexpression, affecting cell cycle entry, ribosome biogenesis and metabolism[15].

In the environment of healthy tissue, the proliferation of normal cells is meticulously regulated by a network of **antiproliferative signals**. These signals include cell growth inhibitors such as transforming growth factor beta (TGF-β) and the interleukin 10 (IL-10), present in the extracellular matrix (ECM). They are essential to maintain cellular quiescence and tissue homeostasis. At the cellular level, p53, the cyclin-dependent kinase inhibitor 1 (p21), and the retinoblastoma protein (pRb) are involved. It ensures that normal cells are either maintained in the G0 phase of the cell cycle or abandon their proliferative potential permanently. A key component of this regulation is the phosphorylation of the pRB, which governs the release of E2F transcription factors. E2F protein controls the transition from the G1 to the S phase of the cell cycle. The disruption of this regulatory pathway under abnormal conditions allows cancer cells to proliferate uncontrollably[16]. Furthermore, TGF-β plays a crucial role in preventing the deactivation of pRb by inhibiting its phosphorylation[16]. In certain neoplastic conditions,

these regulatory signals are compromised, leading to a loss of the ability of pRBb to regulate the cell cycle. Intriguingly, TGF-β, despite its antiproliferative role, can also facilitate the epithelial-to-mesenchymal transition in advanced tumors, highlighting the complex and context-dependent nature of signaling pathways in cancer biology (**Fig. 2**)[17].
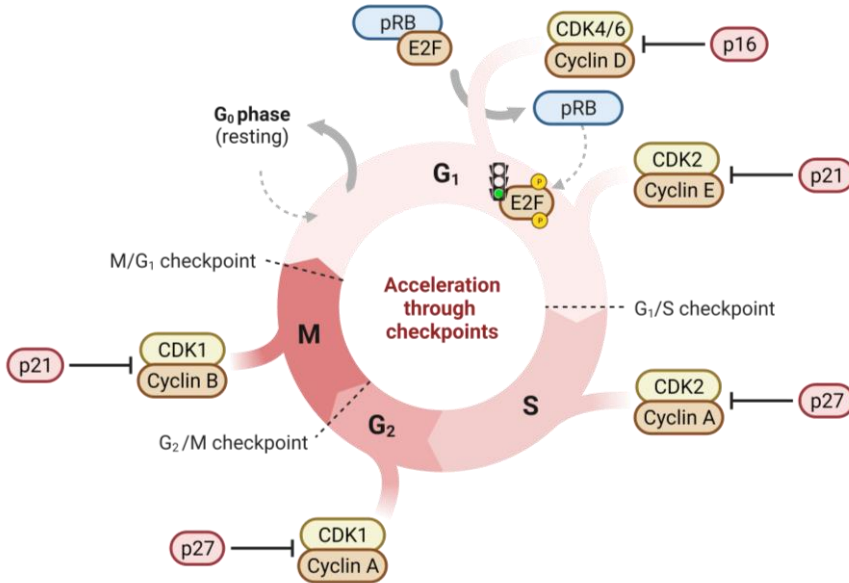
Figure 2. Cell cycle regulation
See the explanation in the text. Adapted from[18].

Cancer cells escape from regulation and **become autonomous** by secreting their growth factors or inducing surrounding cells to produce tumor-promoting factors[19,20]. It includes basic fibroblast growth factor (bFGF), members of the vascular endothelial growth factor (VEGF) family, platelet-derived growth factor (PDGF), epidermal growth factor receptor ligands, ILs, colony-stimulating factors (CSFs) and TGFβ[21,22]. The expression of integrins by cancer cells is correlated by a switch toward the pro-growth balance side and metastatic potential. For example, α2β1 in rhabdomyosarcoma or β1 integrin in mammary carcinoma cells are overexpressed. Other integrins like α5β1 and α3β1 participate in the protection from apoptosis by the activation of the Shc protein[23,24]. Some target pathways triggered by growth signals implicating MEK/MAPK kinase are constitutively activated due to somatic mutation implicated in human melanoma tumors

with B-Raf protein modifications[25]. Besides these modifications, some other somatic mutations of phosphoinositide 3-kinase (PI3K)/PTEN and AKT or the loss of mTOR lead to the perturbation of its dedicated pathway[26].

The reactivation of the telomerase enzyme that maintains telomere size during cell division permits **limitless proliferation in cancer cells**[27,28]. Mice with a mutation in the p16INK4A gene are more likely to develop tumors[29]. Usually, during senescence, the shortening of the telomeres protects against abnormal cell growth, and cells stop dividing. The perturbations in cell death reveal modifications in DNA repair processes or the accumulation of oncogenes such as p53, c-MYC or E2F[30]. In a mouse model with B-cell lymphoma, dysfunctional telomeres induce the senescence of premalignant cells decreasing the tumorigenesis potential[31].

Within the intricate **tumor microenvironment (TME)**, cancer cells interact with diverse stromal cells, immune cells, and ECM components. These interactions shape tumor behavior and progression[2]. The presence of cancer-associated fibroblasts (CAFs), immune cells, and endothelial cells is referred to as TME. CAFs are a type of mesenchymal-like cell residing in proximity or direct contact with tumoral cells[32]. The tumor growth is enhanced by regulatory T cells (Tregs) and macrophages by the secretion of CSF, IL-10 and TGF-β. Macrophages associated with the tumor, called tumor-associated macrophages in the TME, can either promote (M2) or inhibit tumor growth (M1) depending on their polarization[33]. The ECM provides structural support and serves as a reservoir of signaling molecules. Alterations in the ECM composition and stiffness impact tumor progression where enzymes like matrix metalloproteinases (MMPs) such as MMP-3, MMP-7, and MMP-14 play pivotal roles in ECM remodeling[34].

Blood vessels play a critical role in delivering oxygen and nutrients to cells during development. The formation of new vessels is a normal process. In adulthood, the vasculature is quiescent. The growth of new blood vessels is an abnormal process called angiogenesis. Some factors, such as VEGF-A and acidic/basic fibroblast growth factors (FGF-1/2), are promoting angiogenesis. The VEGF signaling pathway is regulated through multiple VEGF receptors (VEGFR-1-3). Moreover, thrombospondin-1 can counteract this effect with its suppressive signal through the activation of TGF-β[35–37]. Tumors activate

the angiogenic switch by altering the balance between angiogenesis inducers and inhibitors. Targeting angiogenesis can be an effective therapy for different tumor types but may require a combination of treatments[38]. Pericytes also play an essential role in neovascularization, where they are less present around tortuous vessels and are observed in almost all tumors[39,40].

1.1.3 Distinction between benign and malignant tumors

During tumor growth, a subset of cancer cells undergoes alterations that impact their adhesive properties, enabling them to acquire a migratory phenotype. This shift facilitates the invasion of surrounding tissues. Tumors that exhibit such invasive behavior are classified as malignant and can proliferate, extend, and penetrate adjacent tissues. Cancer cells can disseminate to distant organs and this process, known as metastasis, is a critical factor in cancer progression. Indeed, metastasis is implicated in up to 90% of cancer-related deaths, highlighting its role in cancer lethality[41,42]. Cell-cell adhesion molecules (CAM) can be affected. The partners of these modifications are immunoglobulin proteins and the calcium-dependent cadherin families that mediate cell-cell attachment[43]. E-cadherin is a key adhesion molecule in epithelia frequently lost in human epithelial cancers and is implicated in carcinogenesis. Restoring the E-cadherin complex can reverse the cancer phenotype, leading to a switch from invasive to benign tumors. A study of pancreatic beta-cell carcinogenesis in a mouse model Rip1Tag2 revealed that E-cadherin loss expression coincided with the transition from well-differentiated adenoma to invasive carcinoma. Additionally, the expression of a dominant-negative form of E-cadherin in this model led to early invasion and the formation of metastases[44].

The invasion capacity is supported by the upregulation of a panel of proteases (MMPs and serine proteases)[45] and the downregulation of protease inhibitors PAI-1 and TIMP-1. This leads to the degradation of ECM and the shedding of transmembrane proteins from the surface of cells. Due to their multiple roles in cancer progression, proteases were a target of anti-cancer drug development. Proteases are also produced by the stromal and inflammatory cells in the TME[46].

1.2   Metastasis: a key stage in tumor progression

Metastasis is the deadliest occurrence during the progression of tumorigenesis that can happen at an early or late stage[47]. The process of metastasis is not random; it is a highly organized, multi-stage process, and metastases are organ-specific[48]. This multi-step mechanism is one of the reasons explaining therapeutic failure in the establishment of effective therapies. A lot of actors promoting metastasis have been identified[49]. The different steps have been established as follows: the escape of cancer cells from the primary tumor, intravasation, survival maintenance, and finally, extravasation (secondary site seeding) and outgrowth (colonization) (**Fig. 3**)[49].
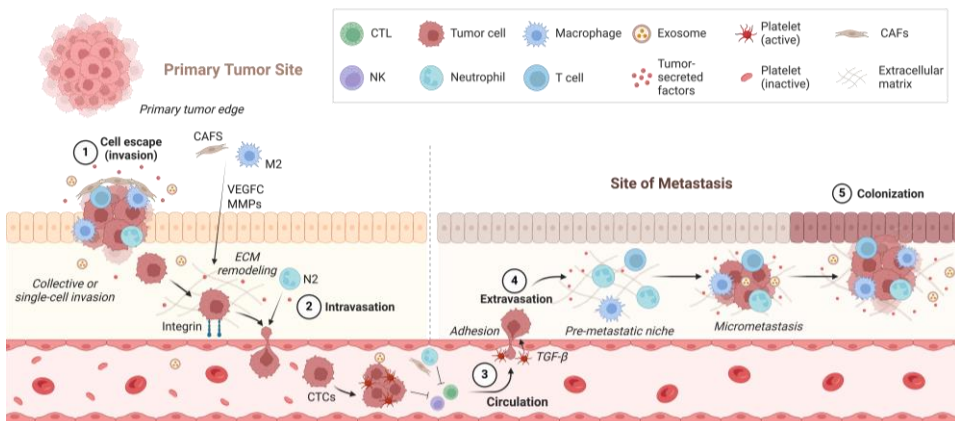
Figure 3. Steps of metastasis
(1) During the cellular escape, tumor cells acquire an epithelial-mesenchymal transition (EMT) due to the secretion of TGF-β by cancer-associated fibroblasts (CAFs), leading to their invasion phenotype. Macrophage M2 and CAFs modify the extracellular matrix (ECM), making it permissive to cell migration. (2) Vascular entry is possible via intravasation, and tumoral cells acquire circulating tumoral cells (CTC) phenotype. (3) The CTCs circulate in the bloodstream surrounded by CAFs and platelets, forming a protective shell. (4) Trans-endothelial migration permits access to the distant site during extravasation. (5) The CTCs colonize the new site, invading the pre-metastatic niche, and after a MET phenotype acquisition, the CTCs become distant tumoral cells (DTCs). Adapted from[49].

1.2.1   Cell escape (invasion)

Tumor cells become invasive by adopting plasticity, with somatic mutations or abnormal chromosome numbers selecting cells with metastatic potential[50,51]. The invasion starts at the interface between the tumor and the stroma by a cell alone or a

group of cells[52]. E-cadherin, a marker of cell-cell adhesion, is downregulated and correlated with epithelial-mesenchymal transition activation, leading to the invasiveness of the tumor cells[53,54]. The decrease in E-cadherin depends at least on the TGF-β-Smad signaling pathway[55]. The study of invasive ductal breast cancer reveals a correlation between E-cadherin expression and metastasis[56]. Epithelial-mesenchymal transition is a process known to be the start of metastasis[57], where tumor cells communicate with CAFs[58]. Loss of E-cadherin is accompanied by the acquisition of markers such as vimentin, α-smooth muscle actin (αSMA), neural cadherin (n-cadherin), cadherin 11, osteonectin (SPARC), laminin and fascin. The physical barrier of the stroma made by the basal membrane can be mechanically deformed by the contractile forces of CAF cells, which help the invasion of group or single cells[59]. Various studies have observed CAF transformation, where normal or cancer epithelial cells undergo transdifferentiation[60].

1.2.2 Intravasation

Once tumor cells enter the bloodstream, they become circulating tumor cells (CTCs). The process of entering the bloodstream, known as intravasation, involves internal and external signals. The intrinsic signals received are epithelial-mesenchymal transition and protease production, while external signals come from pro-tumoral N2 neutrophils, CAFs and M2 macrophages[61]. Intravasation occurs when tumor cells pass through permeable vessels guided by chemokine gradients of CSF-1, EGF and TGF-β secreted by tumor-associated macrophages attracting tumoral cells and creating an immunosuppressive microenvironment[62]. Cancer cells use invadopodia to release proteases MMP-2 and MMP-9[63]. They pass through the ECM, which is degraded by CAFs[64] and tumor-associated macrophages[65]. This creates paths for invading tumor cells and promotes angiogenesis[66], lymphangiogenesis[67], and cancer cell extravasation[68]. For example, it is worth noting that the malignancy is supported and enhanced by CAFs PDGF receptors (PDGFR)α/β+ and integrin α11 (ITGA11), leading to the aggressiveness of breast cancer cells by activating Jun kinase (JNK) signaling. PDGFRα/β[high] CAFs are implicated in LN metastasis and invasion of lymphatic vasculature in ovarian cancer and pancreatic cancer leading to a poor prognosis[69].

1.2.3 Survival maintenance

CTCs have a short half-life of 2.4h in human circulation. During this time, they are exposed to a rich environment and various stressors in the circulation. The CTCs face oxidative stress, shear forces, and immune cell attacks. As a result, only a small number of CTCs can reach their destination. These stresses induce cell death in some tumor cells[70,71]. CTCs are shielded by platelets, protecting against immune attacks and environmental stress, and facilitating their colonization of secondary sites. When platelets meet tumor cells, it causes a mesenchymal-like phenotype which promotes metastasis. The TGF-β1/Smad and nuclear factor-kappa B (NF-κB) pathways control metastasis efficiency in cancer cells[72]. To prevent the attack from immune cells for instance natural killer (NK) cells, CTCs interact with NK cells and neutrophils to protect them. To suppress the immunogenicity of tumor cells in prostate cancer, tumoral cells inhibit interferon 1 signaling[70]. TGF-β1 maintains epithelial-mesenchymal transition and anoïkis in CTCs cells through the extracellular-signal-regulated kinase (ERK) activity [73]. Due to the maintenance of an epithelial-mesenchymal transition state in circulating tumor cells (CTCs)[17], the pathway promotes the upregulation of Slug and leads to the inhibition of E-cadherin[74].

1.2.4 Extravasation and colonization

Upon reaching the distant organ, CTCs interact with the endothelium of the colonization site, along with partners that express CAMs[75]. The low-binding adhesion by integrin β3 and CD44 initiates transient vascular arrest. Then, a stronger adhesions by integrin β1 lead to stable bonds with the endothelium and extravasation[76,77]. CTCs create protrusions called invadopodia between cells at the junctions between endothelial cells to help trans-endothelial or transepithelial migration. The CTCs become disseminating tumor cells (DTCs) during invasion and acquire a MET phenotype for proliferation into forming secondary tumors[78].

It is estimated that only 0.01% of the cancer cells that enter the bloodstream survive to form the distant site of a secondary tumor[79]. DTCs will either become dormant or proliferate. Actin assembly plays a role in transitioning from a dormant to a

proliferative state, involving various factors. Indeed, actin cytoskeleton regulator myocardin-related transcription factor have a role in tumor cell survival and growth in breast cancer. Loss of this factor induces a reduction in the activity of Profilin-1, which is essential for actin network dynamics[80]. Other factors are involved in this process, such as 6-phosphofructo-2-kinase/ fructose-2,6-biphosphatase 3 (Pfkfb3) and the p38/ERK ratio. The latter leads to dormancy when p38 is more present than ERK and, conversely, suppresses metastasis in breast cancer[81]. In addition, glypican-3 is involved in the p38-mediated mesenchymal to epithelial switch[82].

Metastases follow two main dissemination routes: either through the bloodstream or through the lymphatic system. In this second route, metastases first reach LNs and then eventually return to the bloodstream. Pereira et al. and Brown et al. conducted studies and utilized different techniques to track the movement of tumor cells within LN[83,84]. They discovered that tumor cells could enter local blood vessels within the LN, exit the LN by entering the bloodstream, and eventually establish themselves in the lung. Furthermore, the presence of metastases in the sentinel LN (SLN) is often highlighted as a poor prognosis for the patient. These observations underline the importance of knowing the dissemination pathway, i.e., the lymphatic system and the LN, to understand how this dissemination is orchestrated.

2 The lymphatic system and cancer dissemination

2.1 The lymphatic system network

Multicellular organisms such as mammals require circulatory systems to distribute oxygen, nutrients, fluid, signaling molecules, hormones, cells and to collect waste products like carbon dioxide. The blood system comprises the heart and blood vessels, where blood pressure allows plasma to filtrate continuously into the interstitial space[85]. In parallel, the lymphatic system (**Fig. 4**), a unidirectional, blind-ended vascular network, comprises lymphatic capillaries, larger collecting vessels, and secondary lymphoid organs such as LNs, spleen and tonsils.

The lymphatic system is essential for maintaining fluid homeostasis, absorbing dietary lipids, and transporting immune cells and soluble antigens from peripheral tissues toward LNs and the central circulatory system[86,87]. The reabsorption of interstitial fluid is permitted at 90% by the blood system and the other 10% by the lymphatic system. The left thoracic duct drains (i) both lower limbs, pelvis, and abdomen; (ii) the left half of the head, neck, and thorax; (iii) the left upper limb. The right lymphatic duct drains (i) the right half of the head, neck, and thorax (ii) the right upper limb. It terminates and goes back to blood at the junction of the right internal jugular vein and the right subclavian vein[85].
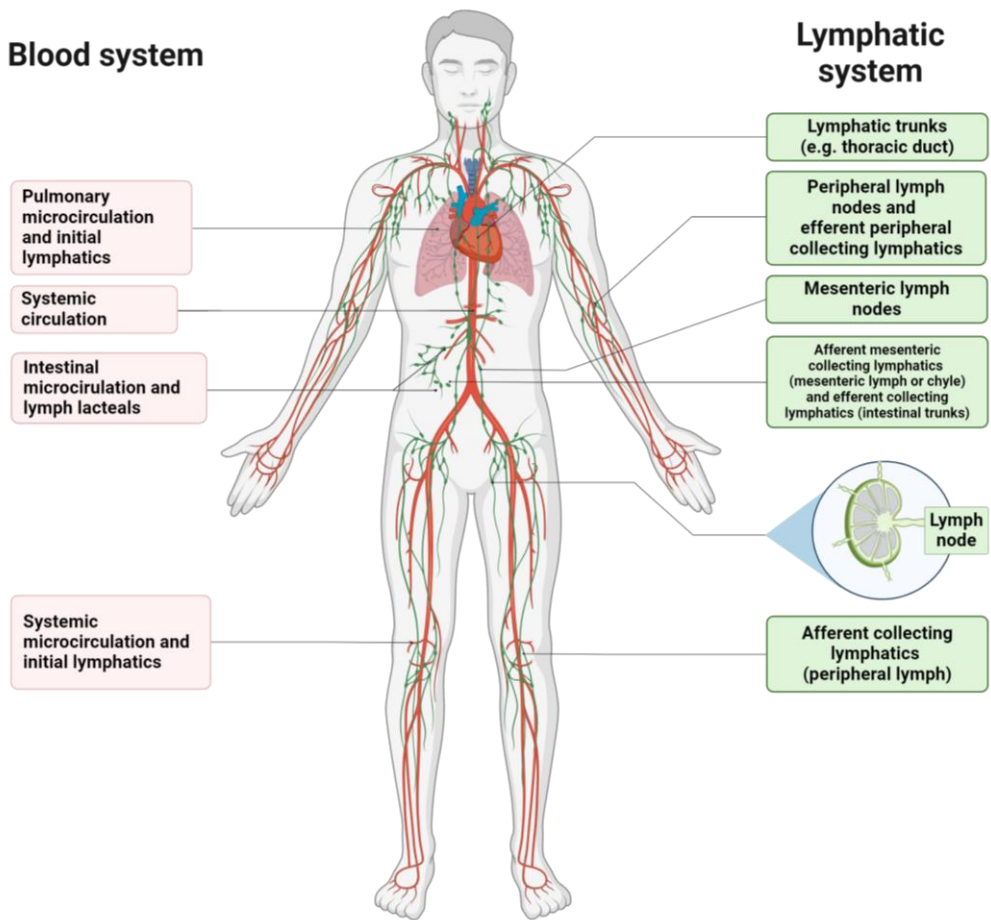
Figure 4. The circulations of blood and lymph in mammals
The filtered plasma creates interstitial fluid, which is transformed into lymph when entering the initial lymphatics. The lymph is mixed with dietary lipids in the intestine, resulting in a milky lymph called chyle. The lymph is carried by afferent collecting lymphatics to the LN for immune surveillance. It exits by efferent collecting lymphatics to larger trunks and returns to veins. Adapted from[88].

2.1.1 Lymphatic vessels

Lymphatic vessels are present in many tissues, except for avascular tissues such as the cartilage, cornea, hair, and nails, as well as specific vascularized tissues such as the brain, spinal cord, bone and retina[85,89]. More recently, a lymphatic system in the eyes called Schlemm's canal was discovered, which shared endothelial characteristics of initial lymphatics. Moreover, lymphatic-like vessels have been reported in the central nervous

system, such as glymphatic formed by the glial network and meningeal lymphatics, contributing to inflammatory reactions and immune surveillance[90,91]. The lymphatic vascular network consists of blind-ended capillaries that absorb interstitial fluid and cells connected to collecting vessels for the transport of the lymph to return into the bloodstream[92] (**Fig. 5**).
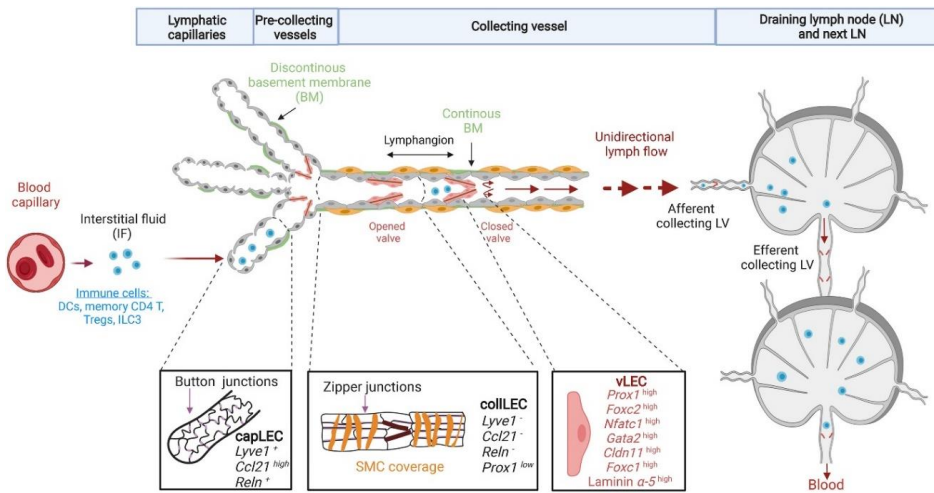
Figure 5. Schematic representation of the lymphatic system organization
Blind-ended lymphatic capillaries remove fluid and immune cells from the interstitial space. Capillary LECs (capLECs) contain button-like intercellular junctions and a discontinuous basement membrane. Pre-collecting and collecting vessels effectively transport lymph toward the draining lymph node through zipper-like LEC junctions, continuous basement membranes, and intraluminal valves. In addition, contractile smooth muscle cells surround collecting LVs. Specific molecular markers of LECs from lymphatic capillaries (capLECs), collectors (collLECs), and vessels (vLECs) are shown. Once the lymph reaches the draining lymph node, it is transported to the following lymph nodes until it reaches the blood circulation. Issue from[92].

2.1.2 Lymphatic capillaries

The **lymphatic capillaries** are the first initial part of the lymphatic network, consisting of blind-ended vessels, also characterized as a plexus of interconnected vessels. Their structural characteristics are defined by incomplete or absent intercellular junctions[93]. At the end of the capillaries, the lymphatic endothelial cells (LECs) have the shape of an oak leaf. They lack junctions at the tip with overlapping membrane extensions called flaps. Flaps act as valves referred to as "primary lymphatic valves" in contrast with the "secondary lymphatic valves" present in precollecting vessels (**Fig. 5**).

Discontinuous button-like junctions attach the lateral part of the capillary. All these structures and gaps allow influx through the LECs in one way due to the hydrostatic pressure[94]. LECs are in contact with the interstitial matrix, to which they are attached to elastic anchoring filaments[95] (**Fig. 6**). The separation with the pre-collecting vessels is formed by LECs and connective tissue forming intraluminal valves. Capillaries in the lymphatic system comprise one layer of LECs and a non-continuous basal lamina. Although the lymphatic's composition is similar to blood capillaries, they differ in their basal membrane and lumina structure and the absence of pericytes in their walls[96,97].
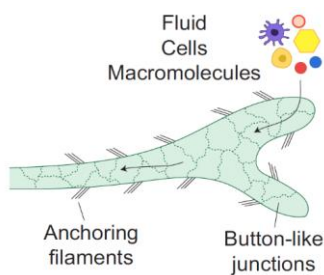
Figure 6. The initial lymphatics

It comprises one layer of lymphatic endothelial cells (LECs) with an oak leaf shape and no continuous basement membrane. The LECs are loosely connected by button-like junctions, which help to absorb interstitial fluid and macromolecules from the peripheral tissues. The initial lymphatics are anchored to the extracellular matrix by anchoring filaments, which open the primary valves formed by the button-like junctions in response to an increase in interstitial pressure. Issue from[98].

Despite the lack of a continuous basal lamina, intermittently "button-like" junctions form a barrier made of VE-cadherin and several tight junctions composed of Occludin, Claudin-5, zonula occludens-1, endothelial cell-selective adhesion molecule, and Junctional adhesion molecule A (JAM-A)[88]. In the tip region, where junctions are absent, two proteins are present: lymphatic vessel hyaluronan receptor-1 (LYVE-1) and PECAM-1 (CD31). PECAM-1 is known to be involved in the diapedesis process of leukocytes and has been demonstrated that dendritic cells (DCs) enter through these discontinued capillaries[94,99].

The **connection between the LEC cytoskeleton and the ECM** is mediated by anchoring filaments where fibrillin is the main component[100] in addition to Collagen VII[101,102], and Elastin Microfibril Interfacer 1 (EMILIN1)[95]. Those components connect with focal adhesion kinase simultaneously with the presence of the integrin α3β1[100]. Furthermore, EMILIN1 coupled with α9β1 is essential for forming and maintaining the lymphatic capillaries where its absence causes hyperplastic vessels[95,103]. Under physiological conditions, most lymphatic capillaries collapse. However, the anchoring

filaments allow these capillaries to open by transmitting physical forces when the surrounding pressure increases[104] (**Fig. 7**).
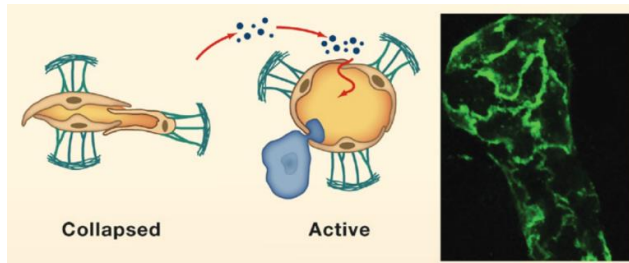
Figure 7. Mechanism of the opening of lymphatic capillaries
Interstitial fluid, macromolecules and cells enter through the permeable gaps formed by oak-leaf-shaped LECs sealed by filled vessels. Immunostaining of LYVE-1 in green shows a blind-ended capillary in a whole-mount preparation of the mouse ear skin. Issue from[85].

2.1.3 Lymphatic pre-collecting vessels

The pre-collector lymphatic vessels serve as a connection between the lymphatic capillaries and the collector vessels. They consist of endothelial cells arranged in a single layer, with secondary valves that prevent the backflow of lymph. The shape of the cells in this area tends to be oak-leaf-like near the capillary tip, while they adopt a round shape near the collector. Furthermore, the junctions composed of LYVE-1 and VE-cadherin become more continuous as they progress toward the collector. Lymphatic pre-collecting vessels are the transition from vessels permeable to lymph fluid to non-permeable lymphatics which transport the lymph[85,88].

2.1.4 Lymphatic collecting vessels

The lymphatic collecting vessels are lymphatic vessels like tiny veins in their composition. The LEC has a thick basal membrane and a spindle shape, a layer of circular SMC, and continuous "Zipper-like" cell junctions to avoid any leakage into the interstitial space. To ensure that lymph only flows in one direction and to prevent any backflow, valves are present along the length of the collecting vessels[88,94,105]. These valves create compartments within the vessels and are bicuspid valves that effectively counteract any backward flow of lymph. The valves consist of two leaflets of endothelial cells folded in a bilayer, with their apical sides facing each other. Elastin fibers are present in the inner

supporting ECM that divides the basal sides of intraluminal valve endothelial cells[88]. The vessel is segmented into multiple small units separated by secondary valves. These units, known as *lymphangions*, can either contract independently or be synchronized with each other. The previous one synchronizes with the next one. The lymph travels from the collecting lymphatic vessel and enters the LN by afferent lymphatic vessels (**Fig. 5**).

2.2   Lymph nodes (LNs)

During immunosurveillance, the LN filters the lymph containing debris from apoptotic cells, proteins and peptide antigens and antigen-loaded DCs[106]. The B and T lymphocytes initiate and regulate adaptive immune responses in reaction to foreign pathogens[107]. Antigen presentation is controlled by specialized cells DCs called antigen-presenting cells[108].

2.2.1 Lymph node development

LN formation during fetal development is a topic of ongoing research. While the process is still not fully understood, various gene-deficient mice have been used to explore it in detail[109]. Lymphoid-tissue inducer (LTi) cells cluster from the earliest event in LN development and are attracted by CXCL13 expression. The first expression of CXCL13 depends essentially on the metabolic degradation product of retinoic acid. Lymphotoxin-αβ (LTα1β2) expression by LTi cells is necessary for interaction with lymphotoxin receptor-β (LTβR)-expressing stromal organizer cells or lymphoid-tissue organizer (LTo)[110,111]. The differentiation of LTi cells from precursors in the fetal liver and their local differentiation into LTαβ-expressing cells requires cytokines, such as TRANCE or IL-7. These cells are attracted to sites of lymphoid organ development by homeostatic chemokines, including CXCL13, CCL19, and CCL21, which also maintain surface LTαβ expression on LTi cells. The lymphotoxin signaling pathway is essential for the development of secondary lymphoid organs, leading to the differentiation of mesenchymal cells, the production of homeostatic chemokine expression, and the promotion of the differentiation of high endothelial venules (HEVs), stromal cells and DCs[112] (**Fig. 8**).
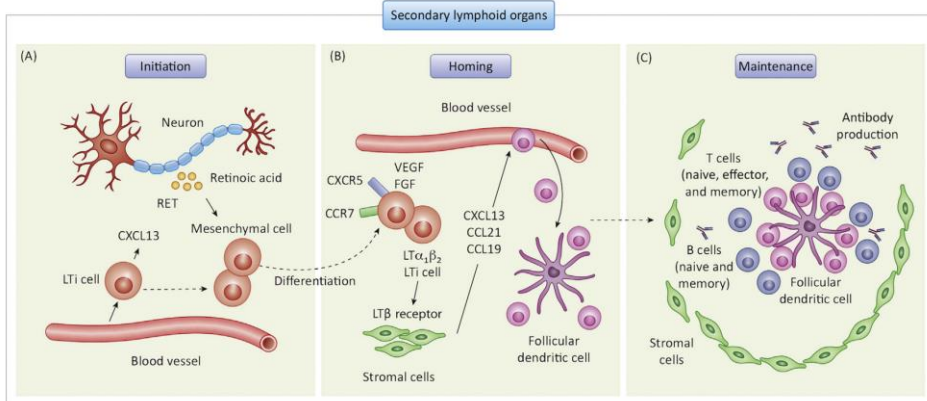
Figure 8. Onset and Development of Secondary Lymphoid Organs
(**A**) The events in the development of secondary lymphoid organs involve the release of initiating factors like retinoic acid (RET). (**B**) This leads to the expression of lymphoid chemokines and adhesion molecules, promoting the influx of various hematopoietic cells. (**C**) B and T cells are essential in maintaining the structure of lymphoid organs, as they regulate the expression of lymphoid chemokines, which is necessary for lymphoid tissue homeostasis. Issue from[113].

Using a mouse model, the LTi cells were shown to exploit gaps in venous mural coverage to transmigrate from veins to LN development sites. The lymphatic vessel transports LTi cells from blood capillaries and is a reservoir for LN expansion. The expansion leads to a lymphatic capsule comprising a LN capsule and a subcapsular sinus (SCS). Retention of CXCR5+ LTi cells is possible with the cooperation between LTαβ signaling and amplification of CXCL13 production[114]. The retention of LTi cells expressing LTα1β2 at their surface is permitted by communication with stromal cells that express the LTβR. This signalization leads to an upregulation of adhesion molecules such as intercellular adhesion molecule 1 (ICAM-1) and vascular cell adhesion molecule1 present on mesenchymal LTo[112,115]. LTβR signaling induces VEGF-C secretion by LTo cells, potentially attracting LECs into the developing organ. LECs surround LTi and LTo clusters and express CCL21, further drawing in LTi cells and activating LECs[112]. This activation was attributed to the expression of the receptor (RANK) activator of the NF-κB by LECs. Accordingly, the ablation of RANK expression in LECs blocks LTi organization and lymph node formation[115]. Collecting lymphatic vessels are essential for transporting LTi cells, forming the LN capsule, and SCS specialization in embryonic stages. Indeed, SCS specialization coincides with lymphatic vascular maturation and LECs are organized in a

bilayer. The outer LECs layer expressed FOXC2 (a marker for collecting vessels). In contrast, the inner layer expresses LYVE1, ITGA2B, and mucosal vascular addressin cell adhesion molecule 1 (MADCAM-1), specific markers of LECs lining the floor called floor LECs (fLEC). Furthermore, the absence of Foxc2 gene expression, in *Foxc2*[lecKo] mouse embryos, results in the absence of ITG2A expression in the SCS. This results in a defect of the LN capsule formation and a lack of smooth muscle cell coverage of lymphatic vessels (**Fig. 9**)[114].
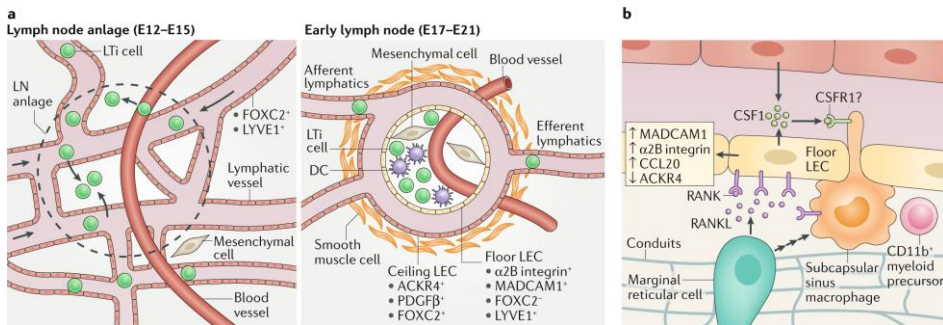
Figure 9. Organization and development of lymph nodes
(**a**) LECs of the collecting lymphatics in the future LN area (LN anlage) begin to form a cup around the anlage at embryonic day 12 (E12) in mice. LTo cells attract the first hematopoietic LTi cells to the anlage. Alternatively, the first LTi cells can enter the anlage through blood vessels and are later transported to the anlage by LEC-lined lymphatic vessels. By E17, LECs have completely engulfed the LN anlage and the LEC layers of the floor and the ceiling can be detected and begin to express the characteristic markers. LN LECs are also necessary to recruit smooth muscle cells to form the LN capsule. (**b**) The macrophage colony-stimulating factor 1 (CSF1) required for the SCS macrophages survival is produced by the floor and ceiling LECs. The marginal reticular cells, stromal cells located below the floor LECs (fLECs), synthesize receptor activators of nuclear factor-κB ligand (RANKL). This RANKL binds to its receptor RANK expressed by the fLECs, which supports their differentiation and allows them to maintain the subcapsular sinus (SCS) macrophages. Moreover, RANKL can directly bind to SCS macrophages and recruit myeloid precursor cells (CD11b+ cells) to the subfloor area. These pathways have been identified in mice LNs. ACKR4, atypical chemokine receptor 4; CSFR1, macrophage colony-stimulating factor receptor 1; CCL20, CC-chemokine ligand 20; DC, dendritic cell (DC); FOXC2, forkhead box C2; LYVE1, lymphatic vessel endothelial hyaluronic acid receptor 1; MADCAM-1, mucosal addressin cell adhesion molecule 1; PDGFβ, platelet-derived growth factor-β. Issue from[116].

2.2.2 Lymph node organization

LNs are immune organs with a complex network of lymphatic sinuses surrounding a highly organized parenchyma. The parenchyma comprises reticular fibers, supporting immune cells, specialized blood vessels, and fibroblast reticular cells (FRCs).

INTRODUCTION

FRCs compartmentalize B and T cells within the LNs. Together, they represent between 20 and 50% of the non-hematopoietic components. These specialized cells express molecules commonly found in myofibroblasts, such as desmin, vimentin, CD90, CD73, CD103, αSMA and the ERTR7 antigen[117]. FRCs form stellar-shaped cells connecting with other cells, creating a 3D network that allows leukocyte migration. This network enables smaller antigens and soluble molecules to reach the interfollicular zone and the paracortex of the SCS in the LN[118]. They also produce fibroreticular fibers, which play a role in transporting molecules and facilitating cell migration. These reticular fibers consist of collagen I[119], III, IV[120] and collagen VI (ER-TR7)[121] core surrounded by microfibrils and a basement membrane[119]. In murine LNs, high heterogeneity in FRCs has been identified based on single-cell RNA sequencing (scRNA-Seq) by classifying them into nine subsets[122]. Marginal reticular cells, which produce CXCL13, were identified as a subset for B cell homing towards follicles[123]. In the paracortex, two different subsets with distinct levels of CCL19 expression, which regulates lymphocyte migration[122], have been identified. This organization provides an optimal environment for immune response induction and regulation[107]. The LN is divided into three areas: the cortex, paracortex and medulla. Furthermore, recent studies have shown that these conduits can transport even larger molecules, such as immunoglobulins or virions[124]. (**Fig. 10**).
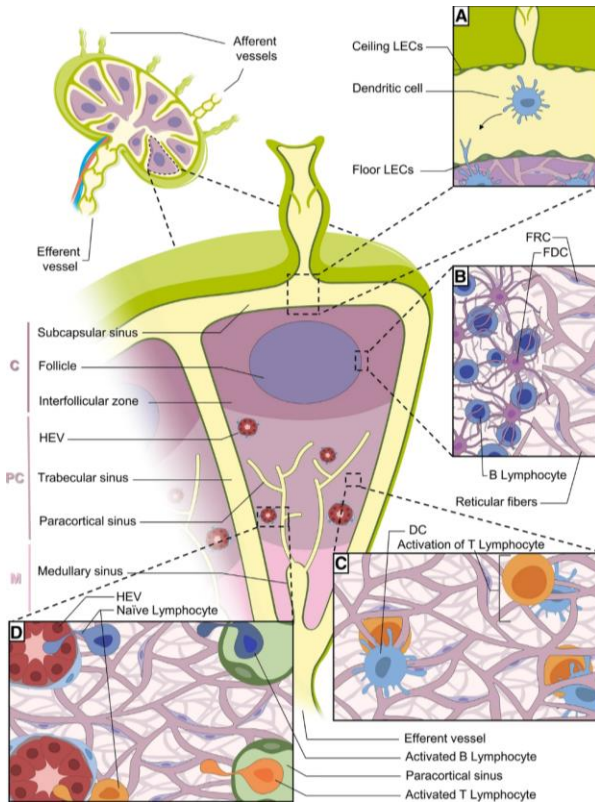
Figure 10. Lymph node (LN) organization

The LN is divided into three parts: the cortex (C), paracortex (PC) and medulla (M). (**A**) Dendritic cells (DCs) from all over the body arrive at the LN via afferent vessels and then migrate into the cortex (C). (**B**) B lymphocytes are in germinal follicles and interact with follicular dendritic cells (FDCs). (**C**) T lymphocytes are in the paracortex to interact with DCs. (**D**) DCs migrate on reticular fibers to the high endothelial venules (HEVs), interacting with naïve lymphocytes entering the LN from the HEV. Activated B and T lymphocytes crawl along the medullary sinus (MS) to leave the LN. Issue from[125] (*Annex 2*).

The cortex contains follicular dendritic cells (FDCs) and B cells mainly associated with germinal follicles. FDCs present antigens to naïve B lymphocytes, leading to antibody production by activated B cells. An interfollicular zone in the cortex separates the germinal follicles and the T cell zone in which antigen-presenting DCs prime naïve T lymphocyte forms the paracortex. The medulla contains a complex network of medullary sinuses, which converge into the efferent lymphatic vessel at the hilum [107,126]. This region includes blood vessels, antibody-secreting B cells and macrophages expressing markers such as CD169, F4/80, MARCO and CD206[127,128].

Recent research revealed some interesting findings regarding LECs' plasticity, heterogeneity, and origins[129,130]. In humans and mice, different LEC subtypes have been identified in various anatomical sites[131–134]. Distinct features are observed in SCS LECs and medullary sinus LECs, such as differences in cellular organization, expression profiles, and roles[131]. Mouse SCS LECs produce macrophage scavenger receptors, which are involved in the transmigration of lymphocytes entering LNs from peripheral tissues. Medullary sinus LECs, which express high levels of programmed cell death-ligand 1 (PD-

L1), contribute to the deletion of alloreactive CD8+ T cells[135]. An additional subset expressing the C-type lectin CD209, which helps in the adhesion of neutrophils to the medulla, was identified in the medullary and cortical sinuses of humans. The NT5E, LYVE1 and MFAP4 genes are expressed by the LECs lining the ceiling of the medulla, while the expression of PDPN, LYVE1 and CCL21 characterizes those from lymphatic capillaries[134]. Transcriptomic analysis of mouse LNs suggests the presence of two distinct LEC subsets in the SCS, indicating functional specialization[131]. fLECs of the SCS secrete neutrophil chemoattractant CXCL1-CXCL5, and cLECs express CCRL1, a chemokine receptor, creating a gradient favorable for DC migration[136]. In humans, these subsets can be distinguished by the expression of caveolin-1 in cLECs, while fLECs express TNFRSF9[134]. These data demonstrate a specific signature of LECs that varies depending on their location within the LN. The lymph enters the LN via the afferent lymphatic vessels, which penetrate in the SCS. The lymph contains lymphocytes, antigens and DCs scanned by macrophages when they arrive in the SCS[137]. It filters through the trabeculae, cortical sinuses and medullary sinus before leaving the LN via the efferent lymphatic vessel (**Fig. 11 and Table 1**)[119].

The HEVs are involved in the recruitment of naïve B and T lymphocytes and the exit of metastatic cells[83,138]. The meshwork of FRCs progresses from fLECs towards the HEVs[130], surrounded by pericytes embedded in a thick basement membrane[139]. HEV endothelial cells with a cuboidal shape express general endothelial markers including CD31, CD34, VE-cadherin and VEGFR-2, specific blood endothelial cell (BEC) markers like von Willebrand factor and peripheral node addressin (PNAd) and VEGFR1 (**Table 1**)[140]. This structural micro-anatomy, where hematopoietic cells can circulate, survive, and interact with each other and with their environment, allows the LN to carry out its task of an initial immune response site. FRCs produce CCL19/CCL21, which assists in the directional cell migration of naïve T cells, B cells and DCs expressing CCR7. During homeostasis and infection, this chemokine gradient helps lymphocyte homing and mediates interactions between T cells and DCs[141].
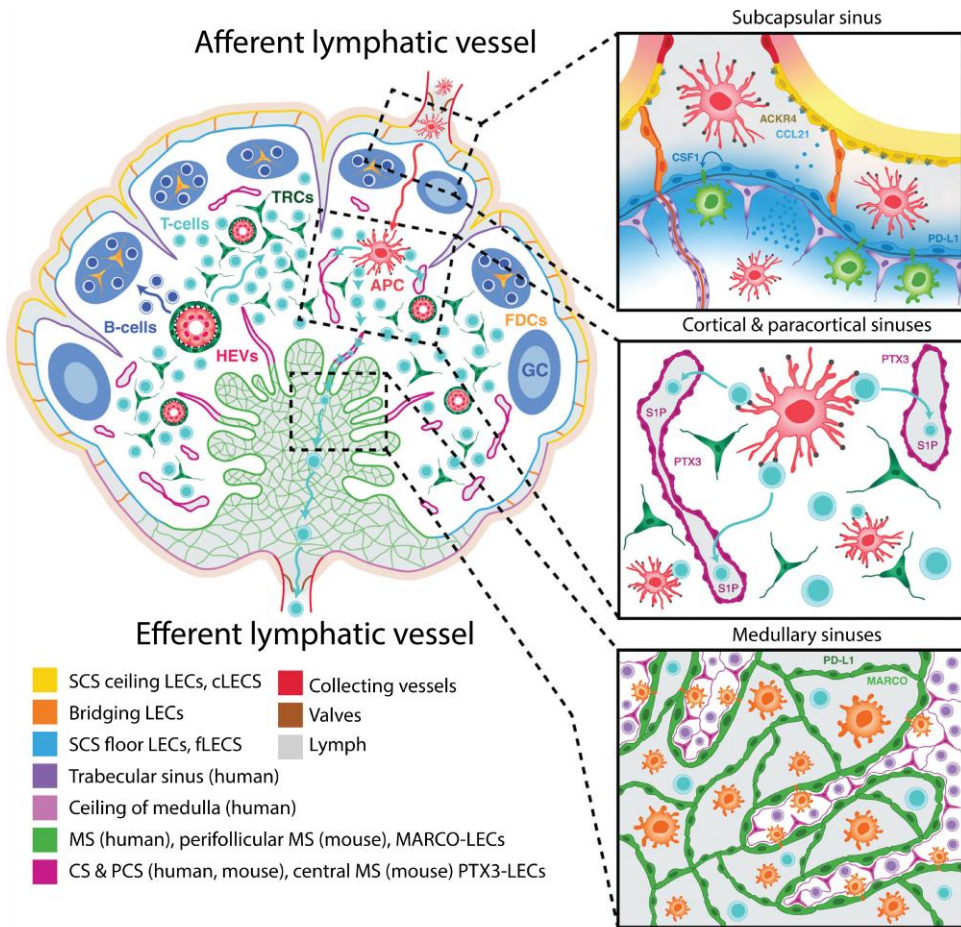
Figure 11. Localization of lymphatic endothelial cell (LECs) subsets in human and mouse LN
See explanations in the text (Adapted from[142]).

Table 1. Location, Functions and Genes Expression of the Different LEC Subsets in LNs

Location	LEC subset	Functions	Human[133,134]	Mouse[132,133]
Lymphatic valves	vLECs	Prevent backflow of lymph[97,143,144]	*FOXC2high CLDN11high*	*Foxc2high Cldn11high*
Subcapsular Sinus (+ trabecular sinuses in humans)	cLECs	Structural role, chemokine gradient formation[136], neuronal input sensory neurons[145]	*ACKR4, MMRN1, FOXC2, PDGFB, EDN1, CAV1, RANK (TNFRSF11A), NT5E*	*Ackr4, Mmrn1, Foxc2, Pdgfb, Edn1, Cav1, Rank (Tnfrsf11a), Cd36high*
	fLECs	Immune cell trafficking (entry and shuttling[132–134]), maintaining MF niche[146–148], Ag-presentation (tolerance[149,150]), antigen archiving[151,152]	*CCL20, CD74, MHC-II: (HLA-DRA/HLA-DRB1), PDL1 (CD274), CSF1, LYVE1+/-, MADCAM1+/-, ACKR1*	*Ccl20, Cd74, MHC-II: (H2-Ab1), Pdl1(Cd274), Csf1, Lyve1, Glycam1, Itga2b, Madcam1*
Paracortical sinuses (+ central MSs in mouse)	PTX3-LECs	Exit routes for lymphocytes[153], proliferation, and expansion in LN hypertrophy[132–134]	*PTX3, ITIH3, LYVE1, FLT4 (VEGFR3)high, NRP2high, PDPN high, CD36high*	*Ptx3, Itih5, Lyve1, Flt4 (Vegfr3)high, Nrp2high*
Medullary sinuses (perifollicular MSs in mice)	MARCO-LECs	Maintain MF niche[146,147], scavenging of virus[154], antigen archiving[151,152], recruitment neutrophils (human[134])	*MARCO, PDL1 (CD274), CSF1, LYVE1, ACKR1, CD209, CLEC4M*	*Marco, Pdl1(Cd274), Csf1, Lyve1, Itga2b*
Ceiling of the medulla (human)	MFAP4+ LECs	Structural role?[134]	*MFAP4*	*Not present*

Taken from[142].

2.2.3 The extracellular matrix of the lymph node

The ECM provides structural scaffolding, biochemical support for tissue function and mechanical integrity and regulates the availability of growth factors and cytokines. It comprises a network of biochemically distinct components, including fibrous proteins, glycoproteins, proteoglycans and matricellular proteins[155]. Although it has always been described as a support structure for tissue architecture, it is, in fact, a highly dynamic compartment that regulates many cell functions. One of the features of the ECM is its constant remodeling as ECM components are deposited, degraded, or modified by ECM-modifying enzymes such as MMP and lysyl oxidase (LOX).

Collagen accounts for the most significant ECM proteins, but its composition and structure vary across tissue types[156]. For instance, the basement membrane surrounding endothelial cells mainly consists of collagen type IV, while the fibroreticular stroma is, for the most part, composed of fibrillar types I[119], III[120], and VI (ER-TR7) collagen embedded in a meshwork of fibrillin collagen microfibers. In LNs, reticular fibers form the principal ECM fibers and support the lymphoid organ architecture. The reticular arrangement of those fibrils is particularly suited to form conduits, transport antigen and signaling molecules, and guide migrating cells[157]. Reticular fibers begin at the SCS and extend to the medullar sinus. fibrillin-1 and fibrillin-2 are essential matricellular proteins in the LN that connect collagen fibers and the basement membrane in tubular structures[157]. Fibrillin constitutes the structural backbone of microfibrils, found in many elastic and non-elastic tissues, carrying out diverse functions, including interactions with latent transforming growth factor binding proteins (LTBP) described below[158].

In the majority of organs, fibroblasts are the main source of ECM components, including at least type I and III collagens, elastin, fibronectin, tenascin-c and periostin (POSTN)[159]. Under physiological conditions, these cells produce fibrillary types I and III collagen, collagen type IV, laminin, fibronectin and tenascin-c, which allow cell migration within the LN[160]. A transcriptional analysis performed on murine LNs confirmed that FRCs expressed integrin subunits such as αV, α4, α5, α6, α9, β1, β3, and β5, enabling their adhesion to many ECM components[161]. For example, integrin α5β1 can bind to fibronectin, and αVβ3 interacts with fibronectin, vitronectin, fibrinogen,

thrombospondin and POSTN[162,163]. tenascin-c can attach to numerous integrins, including α2β1 and αvβ3, but the tenascin-c/integrin α9β1 interaction is considered to be of higher avidity[164].

2.3   Cancer dissemination through the lymphatic system

Different types of cancer can spread through the lymphatic system, including melanoma, breast, oral, pancreatic, and cervical cancer[165–169]. The presence of cancer cells in the first draining LN also known as sentinel LN (SLN), is a sign of a poorer patient outcome[170]. Tumors induce changes in their microenvironment that facilitate their growth and dissemination to distant organs from the primary site to distant organ[171]. One of the most important modifications is the induction of angiogenesis and lymphangiogenesis, which consist of the formation of new blood and lymphatic vessels[172]. The two systems represent the two possibilities for tumor cells to enter the blood and lymphatic system and metastasize (**Fig. 12**).

2.3.1   Tumor lymphangiogenesis and lymphatic metastases

Metastases result from direct intravasation of tumor cells into the bloodstream associated with angiogenesis. However, LN metastases can be the initial stage of lymphatic vascular dissemination for some carcinomas, lymphomas and melanoma[85,96,173]. Several studies have highlighted a correlation between lymphatic vessel density in the primary tumor and the presence of LN metastases, leading to an unfavorable survival prognosis[174,175]. Indeed, in adults, the processes of angiogenesis and lymphangiogenesis occur in numerous pathological situations: wound healing, graft rejection, tumor development and metastasis[176,177]. Various studies show that the density of blood and lymphatic vessels increases in cancerous tissue[178,179].
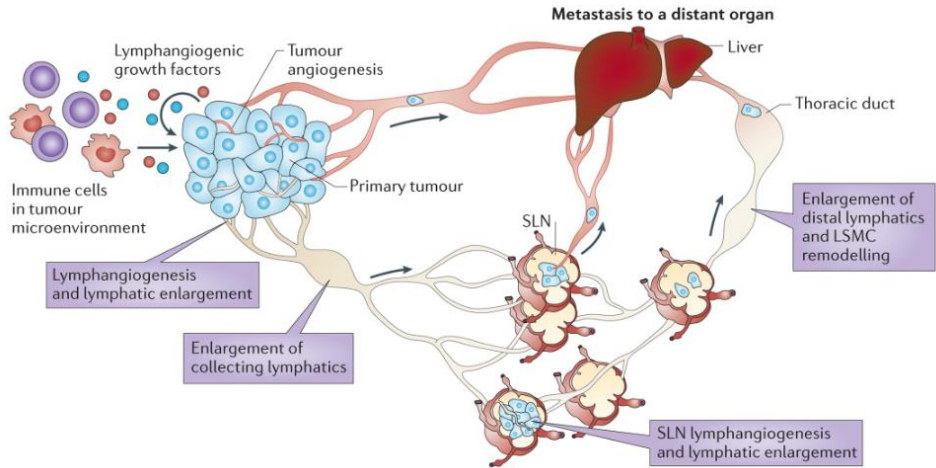
Figure 12. Pathways of Cancer Cell Dissemination: A Schematic Overview.
Originating from the primary tumor, tumor cells orchestrate the assembly of various cell types to construct the local TME. The primary tumor excretes factors that promote the formation of new blood and lymphatic vessels, known as angiogenesis and lymphangiogenesis. The newly formed vessels serve as conduits for the cancer cells to disseminate. The black arrows indicate the direction of cancer cell circulation. These invasive cells have the potential to enter the bloodstream directly, migrating to distant secondary organs. Alternatively, they may infiltrate the lymphatic capillaries, journeying through the collecting vessels to reach the sentinel LN (SLN)—the initial LN that drains the site from which they emerged. Lymphangiogenesis, the new lymphatic vessel formation process, may also occur within this SLN. Subsequently, tumor cells can transition into the bloodstream via lymphatic vessels (Issue from Stacker et al.[180]).

In addition to draining tissue fluids, lymphatic vessels linked to tumor lymphangiogenesis contribute to metastasis[181,182]. Tumor cells find the structure of lymphatic capillaries to be an ideal path for spreading. The lymphatic endothelium lacks a continuous basement membrane and has intermittent intercellular junctions, making it easier for leukocytes to enter and, therefore, providing favorable entry conditions for tumor cells. Passive dissemination also promotes the colonization of LNs by tumor cells. Tumor growth is associated with angiogenesis, leading to the formation of disorganized and permeable neo-blood vessels[177]. This abnormal structure increases the hydrostatic pressure responsible for the entry of the various elements supported by the lymphatic system[183]. This results in a semi-passive intravasation of the tumor cells into the lymphatic system[184,185].

2.3.2 Distant lymphangiogenesis and role of lymphangiogenic factors

In 2005, a study was conducted by Michael Detmar using transgenic mice that developed skin tumors due to an excess of VEGF-A. It revealed that lymphangiogenesis was present in the SLN even before the arrival of tumor cells, which gave rise to a "pre-metastatic lymph node niche"[186]. Two years later, this hypothesis was confirmed using a model of transgenic mice overexpressing VEGF-C[187]. Several factors promoting lymphangiogenesis have been found to induce a premetastatic LN niche formation. This, in turn, increases the frequency of metastatic events in the SLN and promotes the formation of distant metastases. Additionally, studies have confirmed that injecting tumor cells can establish a premetastatic LN niche[188,189].

Pro-lymphangiogenic factors play a role in shaping the immunological phenotype of the surrounding environment. One such factor, VEGF-A has been found to have a significant impact on DC maturation. Specifically, DC exposed to conditioned tumor cell media or VEGF-A display a tendency toward generating immature DC[190]. LECs can secrete various immunosuppressive factors such as TGF-β[93,191]. LECs express high levels of the inhibitory receptor PD-L1, which represses T-cell activation and controls inflammation[149]. PD-L1 is overexpressed by tumor cells, which minimizes the immune response during tumor progression[192,193]. LEC can contribute to immunotolerance in the tumor microenvironment, by interacting with cytotoxic T-cells via PD-1/PD-L1 interaction and antigens cross-presentation **(Fig. 13)**[150]. These T cells are rapidly oriented either towards a process of apoptosis, or to secrete fewer inflammatory cytokines and remain inactivated.
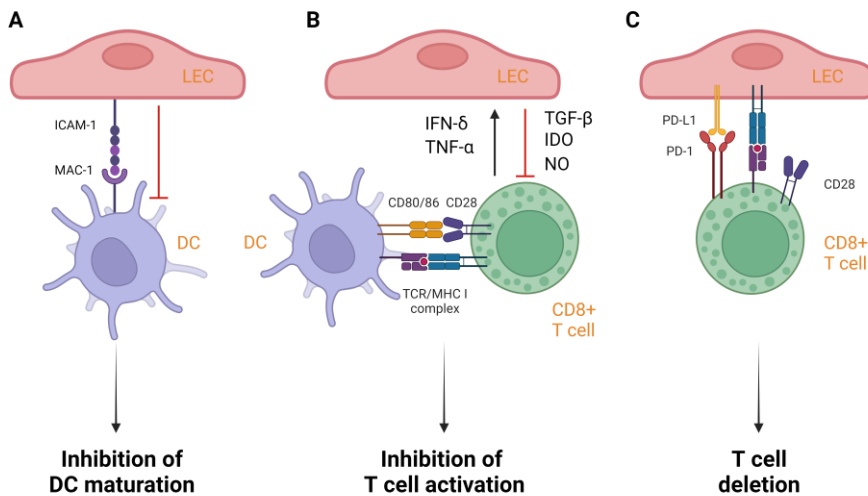
Figure 13. Diagram representing the interactions between LECs and immune cells inducing immunotolerance during tumor progression
(A) LECs use ICAM-1 to interact with dendritic cells (DCs) expressing MAC-1, inhibiting their maturation and ability to activate new lymphocytes. (B) Pro-inflammatory cytokines like TNF-α and IFN-γ activate LECs, causing them to produce immunosuppressive substances such as TGF-β, indoleamine2,3-dioxygenase (IDO), and NO that prevent the activation of cytotoxic T cells. (**C**) LECs can present tumor antigens directly to naïve T cells, leading to dysfunction of their activation and tolerance due to the expression of the inhibitory receptor PD-L1 (Adapted from Card et al.[106]).

2.4 Consequences of metastasis on patient health and treatment options

Metastatic disease has serious consequences, often indicating advanced cancer and a poor prognosis, with an increased risk of complications for patients[194]. Metastases can result in organ dysfunction, compromising vital physiological processes and causing severe patient symptoms. Moreover, the presence of metastatic disease poses complex treatment challenges, requiring a comprehensive approach that addresses both the primary tumor and the disseminated lesions. Understanding the impact of metastases on patient health and exploring innovative treatment strategies is crucial for improving patient outcomes. Understanding the formation of metastases is a key step[171], and by knowing their consequences on patients' health. This will enable us to develop therapeutic options[194]. This knowledge forms the basis for further exploration of the complex mechanisms governing tumor evolution and the spread of metastases. This will

open new avenues for the development of new therapeutic approaches in cancer research.

3 The pre-metastatic niche and lymph node colonization

3.1 First observations and definition of the pre-metastatic niche in lymph node

At the end of the 19th century, Stephen Paget, a surgeon, reported his observations on breast cancer cases, revealing that the location of metastasis was not random. He proposed the hypothesis of Seed and Soil according to which tumoral cells can form metastases referred to as "seed" and invade well-defined organs referred to as "soil"[195]. Forty years later, J. Ewing disclaimed this idea and argued that the dissemination is attributable to the structure of vasculature and purely due to mechanical factors[195].

Fifteen years ago, the seed and soil hypothesis was confirmed by the first formulation of a pre-metastatic niche (PMN) concept by David Lyden and colleagues[196]. The authors discovered that tumor cells release factors that create an environment within the organ where metastases can grow. These factors prepare the target organ to support the survival and growth of disseminated tumor cells. The process includes the secretion of growth factors and chemokines/cytokines that promote metastasis and the release of extracellular vesicles (EVs) by the primary tumor. The factors transported by EVs recruit specific cell types, increase the number of immunosuppressive cells, and remodel the ECM in the PMN[197,198]. These changes create a unique environment that supports subsequent metastatic growth[199,200]. PMN formation has been previously described in detail for different organs such as lung[201], liver[202] and bone[203]. However, less is known about the PMN in LNs. Hirakawa et al. were the first to observe LN remodeling at a premetastatic stage in 2005[204] and 2007[205]. VEGF-A and VEGF-C are crucial in inducing lymphangiogenesis in SLNs. Researchers have identified several distinct characteristics of premetastatic LNs, such as increased lymphangiogenesis and lymph flow, remodeling of HEVs, recruitment of myeloid cells, and reduced numbers and functionality of effector lymphocytes[196,205,206].

3.2 Factors influencing the formation of the pre-metastatic niche

3.2.1 Contribution of tumor-derived factors and extracellular vesicles

EVs, including exosomes, are released by various cells and contain proteins and nucleic acids. Tumor cells produce them in larger quantities than normal cells (**Fig. 14**)[207,208]. Metastatic cancers produce EVs that can prime a PMN. Cancer-derived EVs are thought to be involved in the suppression of innate immune responses through the mobilization of myeloid-derived suppressor cells (MDSCs) and the activation of tumor-associated macrophages and neutrophils[209,210].

Metastatic breast cancer cells are known to express and secrete miRNA (microRNA or miR) 105 via extracellular vesicles which can be transferred to endothelial cells. Tumor-secreted miR-105 targets zonula occludens-1, leading to increased vascular permeability and metastasis. This miR has been detected in the blood of tumor-bearing mice during the PMN formation[211]. miR-25-3P, helps to form a PMN by improving vascular permeability and angiogenesis. Additionally, miR-25-3P secreted by tumors can be transmitted to vascular endothelial cells, targeting KLF2 and KLF4. KLF2 reduces VEGFR2 promoter activity, while KLF4 regulates the integrity of the endothelial barrier[212].
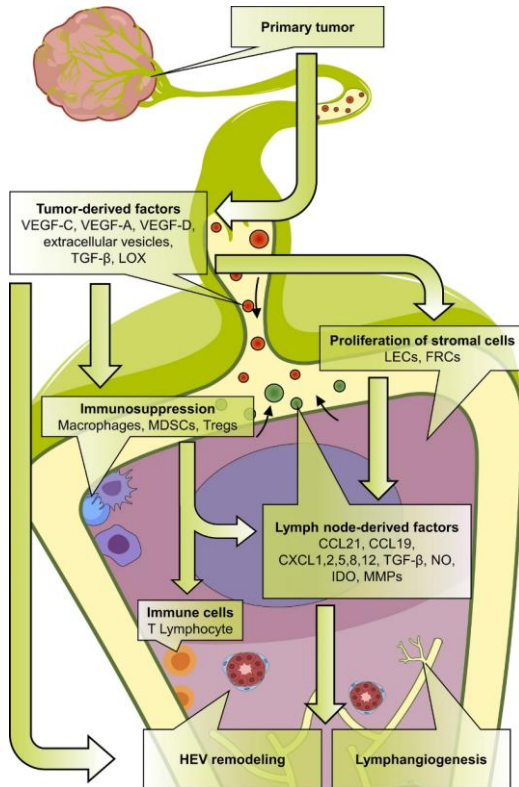
Figure 14. Establishment of the lymph node (LN) pre-metastatic niche (PMN)

Tumor-derived factors, including vascular endothelial growth factor (VEGF-A, VEGF-C and VEGF-D), extracellular vesicles, TGF-β and lysyl oxidase (LOX), induce an immunosuppressive microenvironment by recruiting macrophages, myeloid-derived suppressor cells (MDSCs) and regulatory T cells (Tregs). The proliferation of lymphatic endothelial cells (LECs) and fibroblastic reticular cells (FRCs) drives the production of LN factors such as chemokines (CCL19; CCL21; CXCL1, 2, 5, 8, and 12); TGF-β; matrix metalloproteinases (MMPs); indoleamine2,3-dioxygenase (IDO); and nitric oxide (NO), which induce high endothelial venule (HEV) remodeling, stimulate lymphangiogenesis and regulate tumor cells chemoattraction at the metastatic stage. Issue from[125] (*Annex 2*).

A recent prospective study has shown that tumor-derived extracellular vesicles from afferent lymphatic vessels can inhibit the maturation of DCs. These extracellular vesicles pass through LN subcapsular macrophages in the premetastatic SLN. By performing a proteomic analysis on lymphatic exudates taken from patients with primary melanoma, a signature of 18 immune-modulating proteins that include S100A9 was identified[213,214]. S100A9 is known to exert an inhibitory effect on DCs. In patients with melanoma, extracellular vesicles found in draining lymphatics can participate in forming the PMN. In early-stage melanoma, low S100A9 content in extracellular vesicles has been correlated with the non-metastatic stage of LNs[213]. In melanoma patients with metastatic disease, lymphatic exudate had an increased number of S100A9-containing extracellular vesicles as compared to plasma. This underlines the role of EVPs and S100A9 in PMN formation and provides a possible explanation for tumor progression[215].

Extracellular vesicles derived from early and advanced melanoma express protein signatures associated with different stages of the metastatic process. In the patient with melanoma, the lymphatic exudate contains more melanoma-derived

products such as lactate dehydrogenase, S100B, S100A8 and compared to extracellular vesicles in the plasma. In mice, lymphatic drainage or extracellular vesicles have been studied using transgenic mice (K14-VEGFR3-Ig) known to have a lymphatic drainage defect[216]. Injection of fluorescently labeled extracellular vesicles into the mouse ear dermis showed an absence at the distance from the injection compared with WT mice. Lymphatic vessels play an active role in the transport of extracellular vesicles. LECs were the primary stromal cells responsible for the uptake of extracellular vesicles in the tumor-draining LNs[215]. Similar results were observed by Garcia-Silva et al.[217], where lymphatic exudate had a higher level of S100A9 than plasma. Interestingly, the BRAF[V600E] mutation was detected in EV-associated nucleic acids from the exudate[217]. It is suggested that exudate-derived extracellular vesicles could represent a new prognostic tool for melanoma progression and the detection of melanoma mutations[218]. Moreover, active PD-L1 inhibiting activated T cells can be found in extracellular vesicles in plasma from individuals with head and neck cancer[219].

3.2.2 Creation of an immunosuppressive microenvironment in pre-metastatic lymph node

The LN is a dynamic organ with significant changes in size, cellular composition and molecular structure when exposed to pathological conditions. In cancer, tumor antigens trigger an anti-tumoral response in the LNs, blocking tumor growth and metastasis formation. However, as the tumor progresses, immunomodulatory factors are drained to prime an immunosuppressive environment in the draining LN, leading to the survival of the tumor and its outgrowth (**Fig. 14**)[220]. Different types of immunosuppressive cells, such as MDSCs, tumor-associated macrophages, Tregs, and immature DCs promote tumor growth and metastasis. These cells accumulate in the LNs and inhibit the anti-tumor immune response of CD4, CD8 T cells, and NK cells[221–223]. The MDSCs are precursors of macrophages, DCs, granulocytes and other myeloid cells. They have an important role in the support of immunosuppression. A wide variety of molecules, such as granulocyte-macrophage colony-stimulating factor, macrophage CSF, IL-3, IL-6, and VEGF produced by tumor cells can promote myeloid differentiation and the expansion of MDSCs[224]. MDSCs exert immunosuppressive activity through various

mechanisms, including arginase 1, indoleamine-2,3-dioxygenase (IDO), nitric oxide synthase (NOS), reactive oxygen species (ROS), peroxynitrite, TGF-β and IL-10[225,226]. Different cell types, including DCs, can express IDO enzymes that metabolize tryptophan. IDO reduces T cell immune responses and promotes an immunosuppressive microenvironment in the LNs[227]. In SLNs, the co-expression of IFN-γ and IL-10 has already been correlated with the expression of IDO[228].

3.2.3 Contribution to the pre-metastatic niche by immune cells

Macrophages are present throughout the LN but are classified into different subtypes according to location. A distinction is made between macrophages present in the SCS and medullary sinus from those residing in the LN parenchyma[127]. SCS macrophages can capture antigens and appear poorly phagocytic[128]. LECs play a role in maintaining these macrophages via RANKL production. Indeed, macrophages are lost with RANKL deficiency[146]. LECs produce CSF-1, which is crucial in maintaining the macrophages, especially the medullary sinus macrophages[147]. Macrophages are also present in the parenchyma adjacent to the medullar, known as the medullary cords[127]. The last subset of parenchymal macrophages resides in the T cell zone. They express CD11c, CX3CR1, CD64, and MER proto-oncogene tyrosine kinase but test negative for CD169 and F4/80[229]. Modifications in the CD169+ macrophage density have also been reported in premetastatic LNs. These macrophages capture tumor-derived antigens in the SCS and transfer them to CD8+ T cells to elicit an anti-tumor response. They can also capture extracellular vesicles derived from tumor cells[218]. In a pre-clinical model, mice lacking CD169+ macrophages failed to induce anti-tumor immunity[230]. The decreased presence of CD169 in premetastatic LNs has been associated with the advancement of metastatic disease and an undesirable prognosis in different types of tumors[231]. Tumor-derived extracellular vesicles bind SCS CD169+ macrophages in tumor-draining lymph nodes. Macrophages interact significantly with extracellular vesicles in mice with tumors. In line with fewer tumor-derived macrophages in LNs, 3D imaging showed that extracellular vesicles can penetrate the cortex of LNs more efficiently. These findings indicate that macrophages in SCS play a crucial role in preventing cancer progression by acting as scavengers of extracellular vesicles[232].

B cells and immunoglobulins (Igs) are studied in spontaneous breast cancer mice model to understand their roles in LN metastasis. Primary tumors were found to cause the accumulation of B cells in pre-metastatic tumor-draining LNs and the production of pathogenic IgG. This IgG targeted HSPA4, a glycosylated membrane protein in tumor cells, and led to the activation of integrin β5. The activation of integrin β5, in turn, triggers Src-NF-κB activation in cancer cells, which further promoted metastasis mediated by CXCR4/SDF1a[233].

PMN is an essential step in the establishment and colonization of LNs by metastatic cells. All immune cells mentioned in this section contribute to create a permissive environment within the LN and thus facilitate their colonization by metastatic cells[222,234]. In addition, the release of inflammatory cytokines, growth factors, pro-angiogenic molecules and matrix-remodeling enzymes such as LOX and MMPs can remodel the LN microenvironment[235].

3.2.4 Lymphatic immunosuppression in the pre-metastatic lymph node

LECs can play a role in the survival of metastatic cells and in creating an immunosuppressive environment in the PMN. Indeed, LECs express PD-L1, causing a marked reduction in the cytotoxic activity of CD8+ lymphocytes[236]. LECs in the LN may also present tumor antigens, helping to promote CD4 suppression. In addition, they produce immunosuppressive molecules such as NO, TGF-β1 and IDO[106,237]. They express major histocompatibility complexes class I and II (MHC-I and II)[116,212], which play an important role in immunotolerance and immune response. They can modify thus the CD8+ T-cell response by cross-presenting tumor antigens via MHC-I[116,238,239]. In addition, fLECS expressing CD74 is involved in forming and transporting MHC-II antigenic complexes[133].

3.2.5 Clinical study of the pre-metastatic niche as a biomarker of tumor progression

Studying human lymphatic fluid may reveal valuable information about the body's immune responses. Sentinel LN samples from cancer patients were used in some clinical studies to observe PMN. These LN are frequently removed for staging and serve as reliable indicators of patient outcomes as they represent a common site of metastasis for most solid tumors. One of the defining features of PMNs, VEGFR1+ myeloid clusters, has been identified in premetastatic LNs of cancer patients[196,240]. A correlation was observed between lymphatic metastasis in oral cancer and ECM-remodeling enzyme MT1-MMP and LOX expression in LN macrophages[241]. In the early stage of cervical and oral squamous cell carcinoma, a comparison was made between non-metastatic and metastatic SLNs and non-metastatic distal LNs. It has been found that both non-metastatic and metastatic SLNs had similar characteristics that were not present in distal LNs. The high lymphatic vessel density in both SLN groups suggested this trait could be a biomarker for LNs metastasis[169,242]. LNs exhibit high endothelial vessel remodeling linked to the aggregation of CCL21+ lymphocytes[243]. Nevertheless, the immunosuppression associated with LN pre-metastatic niche in patients is poorly understood[244].

3.3 Lymph node colonization by tumoral cells

LNs drain soluble antigens, proteins and DCs passing through the afferent lymphatic vessels to enter the SCS. In this way, the drained elements meet fLECs and cLECs lining the SCS. Collagen scaffold formed by FRCs permits transport and leucocyte migration to cortical areas [245]. The numerous lymphatic vessels in the tumor facilitate the drainage of the LNs. LN remodeling is characterized by the SCS expansion, LEC proliferation[246], dilatation[189] and dedifferentiation[247] of the HEVs. It is also characterized by fibrosis adjacent to FRCs[248]. Lymphangiogenesis and, hence, the proliferation of LECs at different LN sites are mainly driven by VEGF (A, C, and D) produced both locally and in the primary tumor[249]. This leads to LEC proliferation in the SCS, interfollicular zone and medulla[250]. This proliferation occurs during inflammation, permitting the increase of DC migration, which is exacerbated during tumor drainage.

Subsequently, the SCS is an entry point for tumor cells into LNs [251], which can interact with LECs and macrophages. Despite strong immunosurveillance, it has been shown that CD169+ macrophages present in the SCS progressively disappear, favoring deeper drainage of tumor-derived vesicles reaching B lymphocytes. The drainage of factors induces changes in B cell response, promoting tumor progression[252]. The directional migration of tumor cells from SCS towards the paracortex is enabled by the expression of the chemokine CCL21 and ACKR4 expressed by cLECs[253].

In a tumor context, the directional migration is exploited by tumor cells expressing CCR7, enabling them to migrate along CCL21+ lymphatic vessels[254]. CD11c+ DCs participate in the metastatic potentiation of SCS by expressing cyclooxygenase 2 (COX-2). COX-2-mediated production of prostaglandin E2 (PGE2) in SCS is used by tumor cells to migrate. The production of PGE2 in the SCS causes an accumulation of immunosuppressive Tregs cells in the draining LN[255]. It leads to an increase in reduced maturation of DCs[256] and effector T cell activity, as well as an accumulation of Tregs[256,257]. This immunosuppressive environment in SCS has been observed in many cancers, including carcinomas and melanoma. The accumulation of Tregs in tumor draining lymph nodes increase with tumor burden, limiting adaptive antitumor immune responses[258,259]. Tregs can suppress the expansion and cytotoxic activity of CD8+ T lymphocytes in a TGFβ-dependent manner, suggesting a suppressive function in draining LNs[257,260]. However, the accumulation of Tregs within draining LNs remains unresolved.

In humans, tumor Tregs possess specificity for tumor antigens, and this is shown by analysis of their TCR receptor repertoire. Moreover, this diversity and expansion of Tregs with a TCR repertoire are also found in the tumor-draining LNs[257]. Moreover, TGF-β in this context plays an important role by setting up the immunosuppressive environment represented by Tregs. Tumor cells can migrate and proliferate through the ganglion and reach the HEVs. HEVs in the paracortex of the LN express transmembrane glycoproteins required for adhesion, rolling and transmigration of naive CCR7+CD62L+ lymphocytes. Glycoproteins[261] are peripheral lymph node addressins (PNAds). Dilation of the HEV at the tumor stage is well described, both before and upon arrival of tumor cells in LNs. This dilatory remodeling results in the loss of PNAds and perivascular expression of CCL21-related chemokine, which may block the recruitment of naive lymphocytes to

this site[261]. Ultimately, remodeling of the HEVs enables tumor cells to exit through the HEVs into the bloodstream and colonize another organ. Alternatively, the tumor cells will continue their journey, exiting the lymph node via the afferent lymphatic vessel to establish themselves in another LN in the lymphatic chain.

Furthermore, despite numerous in-depth analyses of the origin of TGF-β in LN and given the secretion of TGF-β by LECs (chapter 2.3.3), no description has been made of the exact origin of TGF-β in LN apart from by immune cells and LECs. And thus, the exact nature of TGF-β secreted by LECs and its precise role in immunosuppression in LN.

4 Transforming growth factor beta 1 (TGF-β1)

TGF-β is present in various species, including vertebrates and invertebrates. It involves multiple biological functions, particularly cell proliferation, tissue repair, cell growth, embryologic development, tissue homeostasis, epithelial-mesenchymal transition, and immune system regulation[262].

4.1 The TGF-β superfamily

The TGF-β family comprises thirty-three human genes that encode homodimeric or heterodimeric cytokines[263]. These various members are separated into two sub-family members composed of the TGF-β-like cytokines and bone morphogenetic proteins (BMP). The former sub-family comprises the three isoforms of the TGF-β, TGF-β1, TGF-β2, and TGF-β3[264], activins A and B, Nodal, the growth differentiation factor 8 (GDF-8) or myostatin and some other members of GDFs (GDF-1, 3, 9 and 11)[265]. The BMP sub-family includes six BMPs (BMP-2, BMP-4, BMP-6, BMP-7, BMP-9 and BMP-15), GDFs: GDF-5 and 9[266] and the Müllerian inhibiting substance (MIS) also called anti-Müllerian hormone (AMH). Among those members, most of them are homodimers but several heterodimers exist such as TGF-β1/TGF-β2, TGF-β2/TGF-β3, BMP-2/BMP-7, BMP-2/BMP-6, BMP-4/BMP-7, BMP-15/GDF-9, inhibin βA/inhibin βB (activin AB), and inhibin βB/inhibin βC (activin AC). They have been studied in vivo and in vitro[267,268]. In the induction of cellular functions, heterodimers are generally much more biologically active than homodimers[268,269].

4.2 The different isoforms of TGF-β

TGF-beta cytokines are produced in three different isoforms, TGF-β1, TGF-β2, and TGF-β3, encoded by three separate genes on three different chromosomes (19q13, 1q41, and 14q24). These isoforms share a sequence identity of 71-80%. The three isoforms have non-redundant and different functions. Indeed, replacing one isoform with another in the in vivo model did not restore the phenotype generated by the loss of one of the isoforms[270]. In addition, TGF-β1 is the most abundant isoform expressed in humans, the most widely expressed in the TME and among immune cells, and abundant

in serum. TGF-β2 and TGF-β3 are involved in embryonic development, and they have been shown to have essential roles in processes such as palate development and lung formation[271,272].

4.3 Transforming Growth Factor Beta 1 (TGF-β1)

4.3.1 TGF-β1 protein synthesis

All TGF-β isoforms are produced as pre-propeptide precursors during translation, and a N-terminal signal peptide enables its localization and trafficking. After removing the signal peptide, homodimerization occurs by forming interchain disulfide bonds. The resulting pro-TGF-β1 dimer is cleaved by the furin enzyme, a trans-Golgi network pro-protein convertase. This proteolytic event produces two homodimer fragments, which stay non-covalently connected in the so-called latent TGF-β1: the carboxy-terminal dimer (the mature TGF-β1) and the amino-terminal dimer LAP. The LAP is wrapped around the mature TGF-β1 to prevent its binding to its receptors. The complex of mature TGF-β1 and LAP is called "latent TGF-β1". It is produced in an inactive form that must be activated to exert biological effects (**Fig. 15**)[273].
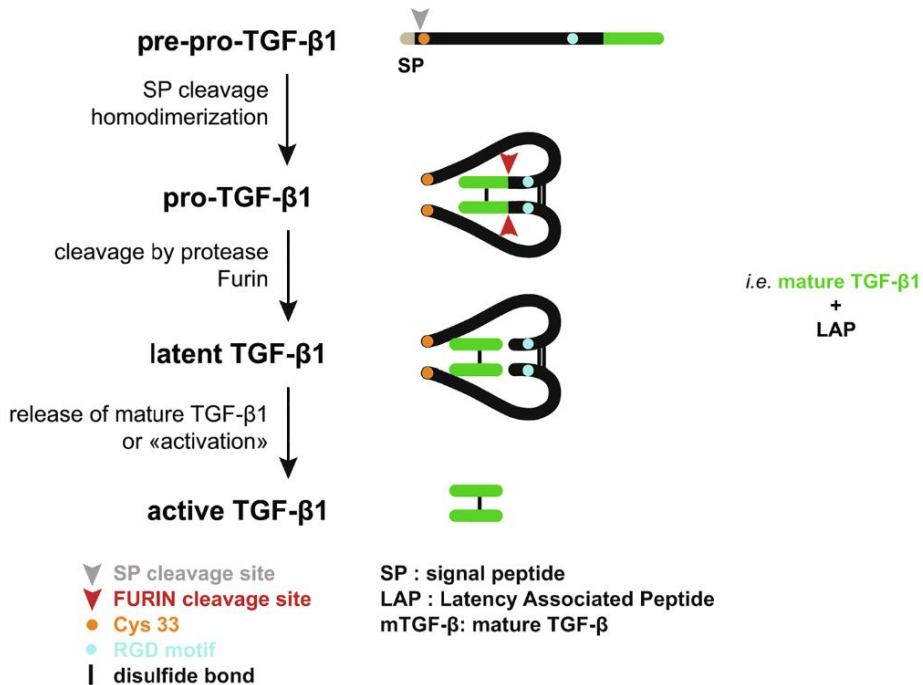
Figure 15. Schematic representation of TGF-β1 processing
TGF-β1 is produced as a pre-pro-precursor, and after the signal peptide is cleaved and removed, it homodimerizes through disulfide bond formation. Furin, a pro-protein convertase, then cleaves pro-TGF-β1. The N-terminal dimer, also known as the Latency Associated Peptide (LAP), stays bound to the C-terminal dimer, or mature TGF-β1, to create latent TGF-β1, which is inactive. For mature TGF-β1 to connect to its receptor, it must be released from LAP, known as "TGF-β1 activation" (Issue from[274]).

4.3.2 Stored and secreted forms of latent TGF-β1

Hematopoietic and immune cells are the primary sources of latent TGF-β1. It can exist in soluble forms or bound to other proteins through a residue Cys 33 to the LAP[275]. TGF-β1 can be attached to ECM components in a latent form with latent TGF-β1 binding proteins 1, 3, and 4 (LTBP-1, LTBP-3, and LTBP-4), with the contribution of fibronectin and fibrillin. It can also exist attached to two different extracellular membrane proteins called GARP (encoded by the gene LRRC32) or LRRC33. TGF-β1 is present in a free form attached to the LAP or a soluble form of GARP (sGARP)[276].

LTBP-1, LTBP-3, and LTBP-4 are synthesized concomitantly with TGF-β1 covalently attached to LAP. They lack a transmembrane cellular attachment domain. The

three distinct extracellular LTBP proteins are associated with the latent TGF-β1 to form a complex LTBP: latent TGF-β1. The complex formed by syndecan-4 and heparan sulfate at the cell surface captures the LTBP-1 to form multimers. LTBP4 binds fibulin-4 and -5 to assist in depositing elastin aggregates on fibrillin microfibrils during elastogenesis[277,278].

GARP is a member of the LRR (leucine-rich repeat) protein superfamily and is characterized by its horseshoe-shaped 3D structure[279] due to leucine repeats. GARP facilitates the presentation of latent TGF-β1 at the cell surface. GARP covalently binds to the TGF-β1:GARP complex by forming disulfide bonds with LAP. GARP:latent TGF-β1 complexes are expressed on the surface of TCR-stimulated Tregs[280,281], B cell receptor stimulated B cells[282], endothelial cells[283,284], fibroblasts[285], megakaryocytes and platelets[281,284], mesenchymal stromal cells[286,287], and hepatic stellate cells[288]. The group of Sophie Lucas has demonstrated that Tregs, B cells, and platelets can activate TGF-β1 in a GARP-dependent manner[280,282] (**Fig. 16**).

LRRC33 is a protein that belongs to the LRR family and is highly similar to the protein GARP. It is responsible for facilitating the presentation of latent TGF-β1 on macrophages and microglia cells, i.e., macrophage-like cells in the nervous system[289] (**Fig. 16**).
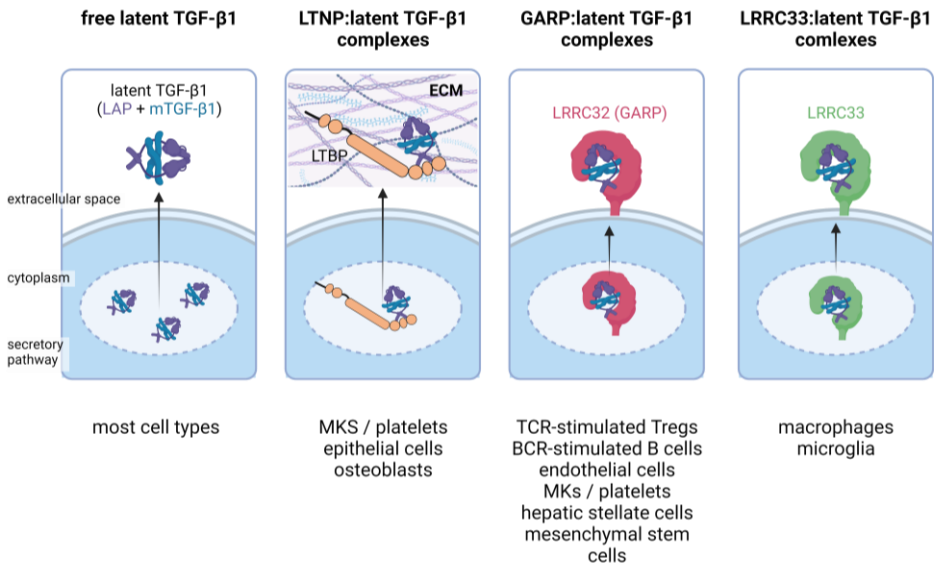
Figure 16. The stock of TGF-β1 in different cell types
Latent TGF-β1 is secreted by most cells. In certain cell types, latent TGF-β1 binds to proteins like LTBPs, which anchor it to the extracellular matrix (ECM). On the other hand, some cells can display latent TGF-β1 on their surface with the help of proteins such as LRRC32 (GARP) or LRRC33 (Inspired by the work of Charlotte Bertrand).

4.3.3 TGF-β1 activation and signaling pathways

After being activated and released from the LAP, the mature form of TGF-β1 can bind to the TGF-β receptors. These receptors consist of heteromeric transmembrane TGF-β receptor serine-threonine kinase. The complex is formed by the dimeric TGF-β type I receptor (RI, TβRI) (also known as activin receptor-like kinase or ALK), ALK5 and the dimeric TGF-β type II receptor (RII) TβRII[273,290,291]. After binding to TGF-β1, the RI receptor dimer is phosphorylated and recruits the RII receptors to form stable multimers. The RII serine/threonine kinase phosphorylates the GS domain composed of 30 amino acids (TSGSGSG sequence) of RI, leading to cross and autophosphorylation. This complex can be stabilized by co-receptors such as beta glycan (TGF-β type III receptor, TβRIII) or endoglin (CD105), which binds the TGF-β ligand and boosts the signaling. On the contrary, a protease can shed the co-receptors and decrease TGF-β1 signaling with scavenger properties[290].

In the canonical TGF-β1 pathway, TβRII is a constitutively active receptor that phosphorylates the TβRI receptor. Phosphorylated ALK5/TβRI or ALK4 or 7 can phosphorylate R-Smad proteins, such as Smad2 and Smad3. Conversely, negative feedback leads to pathway regulation with the action of inhibitory (I-) Smads, Smad7 through binding the GS domains of the RI receptor when the ligand is absent[292]. The phosphorylated dimer interacts with Smad4 and is transported into the nucleus to act as a transcription factor and regulate many target genes related to cycle arrest. The complex formed by Smad2/3/4 modifies DNA configuration at specific sites by modifying histones with acetyl and methyltransferases[293–295]. It is worth noting that in endothelial cells, TGF-β1 binding to its receptor composed of TβRI (ALK1 or 3 or 6), TβRII and the Endoglin co-receptor can induce the phosphorylation of Smad1/5/8, leading to cell proliferation and angiogenesis[296]. pSMAD 1/5/8 can also be activated by the receptor formed by BMPRI and BMPRII which bind other members of the TGF-beta family like BMPs[297]. Furthermore, the co-receptor called endoglin, or type III receptor, can modulate the activation of the TGF pathway in a SMAD-independent manner, regulating cell proliferation and adhesion only in endothelial cells[298,299] (**Fig. 17**).
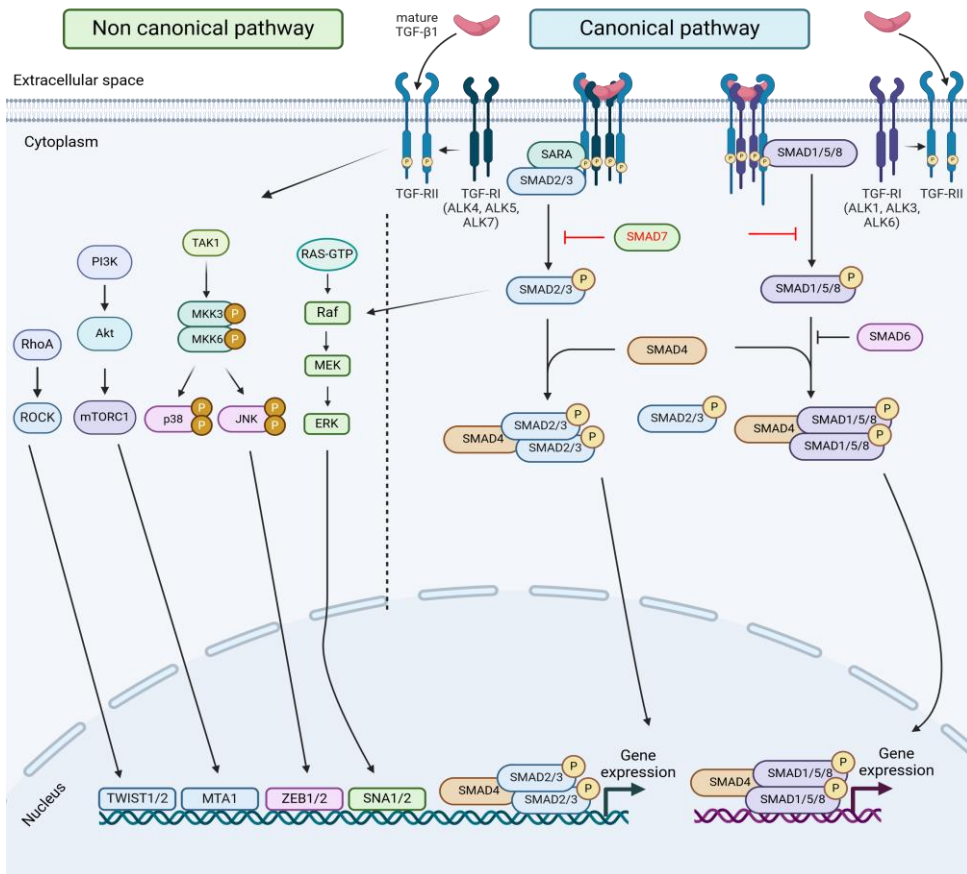
Figure 17. Canonical pathway of TGF-β1 signaling
Mature TGF-β1 binds to the type II receptor (TGF-BRII), its phosphorylation leads to a heteromeric complex with the type I receptor, either ALK (left) or ALK1 (right). Depending on the ALK involved, a cascade of SMAD activation proteins is triggered, with either SMADs 2/3 and 4 for ALK5, or SMADs 1/5/8 and 4 for ALK1. The phosphorylated SMAD proteins then migrate into the nucleus via SMAD4 and regulate target gene expression. Adapted from[264,296,298].

  In the non-canonical pathway, TGF-β receptors can activate MAP-ERK pathways through their tyrosine kinase activities. TAK1, or RAC1 then activate the MAPK pathway, phosphorylating the p38 and ERK effectors[300,301]. Furthermore, some non-canonical TGF-β signaling pathways are independent of Smad, such as Jun kinase (JNK), p38 MAPK, NF-κB, PI3K-Akt-mTOR, Raf-MEK1/2-ERK1/2 and Rho/Rho-dependent kinase[302]. Indeed, the canonical and non-canonical pathways are interconnected[265]. This is due to the low affinity for DNA binding at the activating and/or inhibiting sites of the protein complexes formed by Smad signaling proteins. Other independent transcription factors, such as T

cell factor and lymphoid enhancer factor (LEF), are involved in the downstream signaling of Wnt, YAP/TAZ, and myocardin-related transcription factor-A pathways[294]. Other pathways downstream of TGF-β signaling are regulated, including CDK and MAP kinase pathways through post-translational phosphorylation and dephosphorylation[303].

The opposite effects observed for TGF-β1 may be attributed to a diverse range of activated signaling pathways even within cells in the same environment. Consequently, while TGF-β1 inhibits the proliferation of epithelial cells, it stimulates the proliferation and growth of fibroblast and tumoral cells[304].

5 Glycoprotein A Repetitions Predominant (GARP)

5.1 The GARP protein encoded by the LRRC32 gene

The protein GARP is encoded by the Leucine Rich Repeats Containing protein 32 (LRRC32) gene, first identified in 1992 by Ollendorf et al. The gene was first discovered in human, in an altered chromosomal region located on chromosome 11 (11q13.5-q14). A cloning performed in mouse lead to identify the identification homologous sequence of this gene in the chromosome 7 (region 7E-7F)[293,305]. Using BLAST, nucleotide sequence analysis of the human LRRC32 and murine Lrrc32 genes shows over 81% sequence homology[306]. In 1994, Ollendorf et al. discovered two splice variants of GARP by cloning them from a human placental cDNA library. GARP comprises two coding exons, and the two splicing variants differ in their 5'UTR sequence. Northern blot analysis reveals the presence of a 4.4 and 2.8 kb transcript, which is strongly expressed in the placenta, lungs, and kidney. Lower expression was demonstrated in the heart, skeletal muscle, and pancreas but not in the brain[307]. After discovering the GARP gene, Ollendorf and colleagues provided evidence of GARP expression in different tissues, such as the placenta, lungs, and kidneys. The expression is less present in the heart, liver, skeletal muscle, and pancreas[307].

5.2 GARP protein domains

The LRRC32 gene encodes a human GARP protein of 662 amino acids long with a molecular weight of 72 kD[307], a leucine-rich repeat receptor. GARP is a type I transmembrane protein with a short cytoplasmic tail domain composed of 14 amino acids with no signaling activity and a large extracellular domain of 608 amino acids. The protein contains a PDZ-like domain formed by four amino acids, Gln-Tyr-Lys-Ala, located at the C-terminal region (homology with the PDZ class II binding motif)[308]. The extracellular domain of GARP contains two series of 10 Leucine Rich Repeats (LRRs) with a LRR C-terminal region (LRRCT)[309]. LRR domains comprise 2 to 45 LRRs with highly conserved regions of the sequence LxxLxLxxNxL or LxxLxLxxCxxL[310]. A form characterized by extracellular domain and LRR repeats is particularly described as interacting with

proteins[311]. Human proteins containing LRR domains perform multiple functions in innate immune responses with toll-like receptors to the proteins implicated in mRNA transport (NXF1 or proteins present in the synapses of neurons, LRRTM)[312]. GARP protein's folding and surface localization is supposed to be enhanced in the endoplasmic reticulum by a chaperone called gp96 (GRP94) like toll-like receptor[313]. GARP is linked to the LAP with disulfide bound between Cys-192 and Cys-331 present in two LRR regions and Cys-4 from LAP[314].

5.3   Tregs and the GARP:TGF-β1 complex

Tregs are a specialized subset of CD4+ T cells that play a crucial role in suppressing the activation and proliferation of effector T cells, preventing excessive immune responses and autoimmunity. Thus, Tregs maintain immune homeostasis. In contrast, they can have a detrimental effect on cancer patients by reducing anti-tumor immune responses[315]. Treg function and differentiation require the expression of the forkhead box P3 (FoxP3) marker[316], which is induced by the TGF-β1[317]. In immune cells, particularly immunosuppressive Tregs, TGF-β1 is the main TGF-β isoform expressed under normal physiological conditions[279]. Indeed, the expression of FoxP3 provokes the differentiation of T cells into induced Tregs (iTregs)[318]. It is also worth noting that TGF-β1 can modulate the expression of cell cycle regulators (p21 and p27), preventing the proliferation of naïve T lymphocytes[319]. In the absence of TGF-β1 signaling, Treg differentiation is impaired, leading to the development of autoimmune diseases. In humans, FoxP3 deficiency leads to the development of a very serious disease known as IPEX syndrome (Immunodysregulation Polyendocrinopathy Enteropathy X-linked), characterized by autoimmune-mediated multi-organ inflammation. In mice, this deficiency leads to the development of the same phenotype known as "scurfy"[316].

Multiple research groups, including Sophie Lucas' team, have conducted studies demonstrating that Tregs in both humans and mice can activate TGF-β1 following TCR stimulation. This activation occurs through a mechanism that involves GARP and integrin αvβ8. Immunoprecipitation assays have shown that GARP and αvβ8 integrin interact with each other in human Tregs. In vitro, the activation of TGF- β1 by TCR-stimulated human Tregs is blocked by antibodies directed against the GARP-TGF-β complex or the β8

subunit. Additionally, these antibodies can block human Treg-mediated immunosuppression in a murine model of xenogeneic graft versus host disease (GvHD)[285,320].

5.4   Regulation of the protein GARP

5.4.1   Relation between GARP and FoxP3

An inactivation by RNA interference of FoxP3 in Tregs cells leads to the reduction of surface GARP, while the reverse does not affect the expression of FoxP3[321]. Other cells, such as human and mouse platelets and megakaryocytes, have been shown to constitutively express both GARP and the GARP/LAP complex. Thus, upon their activation, these cells show an increase in GARP and FoxP3. The presence of GARP at the surface of cells is enhanced by Protease-activated receptor 4 activating peptide, and the augmentation of FoxP3 expression is boosted by phorbol ester myristate acetate[284]. Moreover, GARP and FoxP3 were found recently to be expressed simultaneously in human melanocytes[322]. The use of shRNA against FoxP3 affects the expression of GARP, but if conversely, a shRNA against GARP is used, then the expression of FoxP3 is not affected as seen previously with knockdown[321]. Another marker, Helios has also been shown to identify Tregs, which express the transmembrane complex GARP/LAP[323]. The transcription factor, signal transducer, and activator of transcription 3 (STAT3) also regulate the expression of GARP. IL6 on CD4+ naive cells causes a decrease in the transcription and expression of GARP through the STAT3 signaling pathway[324]. As seen previously, GARP is a latent TGF-β receptor, and its expression is independent of both TGF-β and furin, which is involved in TGF maturation by the cleavage of pro-TGF-β[325].

5.4.2   Transcriptional Regulation of LRRC32

The regulation of GARP also takes place at the level of its gene by the presence of two alternative promoters. GARP expression is induced in Tregs following TCR stimulation, but it is absent at the surface of human and mouse helper T (Th) cells[308]. These two promoters are called upstream promoter 1 (P1) and downstream promoter 2 (P2) and pilot the transcription of the GARP gene. They show differences by their

methylation states, the P2 promoter is almost entirely demethylated in Tregs and Th cells and the P2 promoter is blocked only in Th cells by the presence of methylated CpGs islands in the downstream P1 promoter. Thus, the transcription factors cannot bind to the promoter sequence found in a closed chromatin configuration due to methylated CpG islands. This contrasts with Tregs cells, which have much less methylated CpGs that allow the binding of the transcription factor FoxP3 by remodeling the promoter region in an open configuration. An open configuration allows the fixation of the nuclear factor of activated T cells (NFAT) and NF-κB, which leads to the transcription of the GARP gene[326]. GARP is considered as a transdifferentiation-associated marker proving the involvement of FoxP3 in the induction of GARP expression with the change of Th17 cell from tumor in ex-Th17 FoxP3+ cells with augmentation of GARP at their surface[327].

5.4.3 Post-Transcriptional Regulation of the GARP mRNA

GARP expression is known to be highly regulated at the post-transcriptional level. One such regulation involves small, single-stranded non-coding RNA (micro RNA or miRNAs), which are conserved between species. The translation inhibition occurs after the binding of the miRNA to the 3' UTR sequence of the mRNA by partial complementarity[328]. Within Tregs, numerous miRNAs have been shown to regulate various cell functions, such as differentiation, proliferation and immunosuppressive functions. This immunosuppressive function is regulated by miRNA miR-142-3p, which is negatively regulated by FoxP3[329]. Interestingly, miRNA regulation of GARP expression has been reported in activated Tregs. Following Treg activation, GARP mRNA synthesis is increased and a subsequent decrease is explained by the targeting of the mRNA by miR-142-3p. The expression of miR-142-3p is particularly high in Tregs, as compared to Th cells and contributes to explain GARP regulation in Tregs [330]. Other miRNAs such as miR-24 and miR-335 can bind the GARP 3'UTR sequence. Different sets of miRNAs can explain differences in GARP regulation according to the cell and tissue types [331].

5.5 Release of TGF-β1 from GARP

In vivo, two mechanisms exist for the activation and the release of TGF-β1, which involve either thrombospondin-1 or RGD-binding integrins. Among the various

integrins that exist, only those that can bind to an RGD domain can activate TGF-β1[332]. In vitro, the latent-TGF-β1 can be bound by different integrins containing RGD domain, such as integrins αVβ1, αVβ3, αVβ5, αVβ6, and αVβ8. In the context of cancer, many cell types express RGD-binding integrins. Integrin αVβ1 is expressed by fibroblasts, αVβ3 and αVβ5 are expressed by tumor cells and endothelial cells, αVβ6 by epithelial cells, and αVβ8 by DCs, monocytes, fibroblasts, tumor cells and Tregs[320,333].
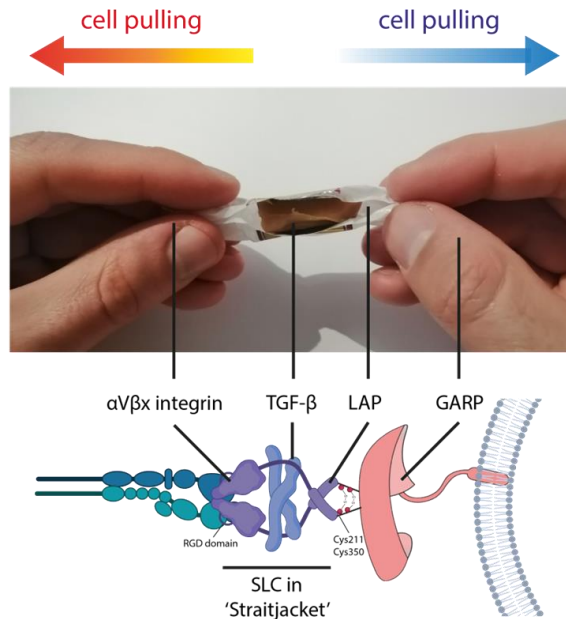
Figure 18. The TGF-β1 release is like unwrapping a candy
The small latent complex (SLC) is formed by the latency-associated peptide (LAP) and TGF-β1 complex. One end of the LAP wrapper is crosslinked to the 8-Cys domain of GARP through two cysteine residues such as Cys211 and Cys350, which are linked to the protein GARP. This linkage provides resistance, and when the other end of the LAP wrapper is pulled via αvβ6 or αvβ8 integrins, the TGF-β1 candy is released (Inspired by the work of Lodyga and Hinz[294]).

Pulling forces exerted by integrin αVβ6 on immobilized latent TGF-β1 are believed to result from the cytoskeleton's contraction. It causes the formation of the latency lasso of LAP to unfold, which in turn leads to the release of mature TGF-β1[334–336]. For the integrin αVβ8, a different process is proposed, and the binding of these integrins to the LAP provokes a conformation change that unmasks the binding site of mature TGF-β1[337]. Lodyga and Hinz suggest that activating latent TGF-β1 can be compared to

unwrapping a candy. The RGD domains present on the LAP are recognized by integrin αVβ6 and αVβ8 (**Fig. 18**)[294].

5.6 Role of GARP in disease

The GARP protein is implicated in both autoimmune diseases and cancer. Thus, different treatments have been proposed depending on the pathology, as shown in **figure 19**[338].
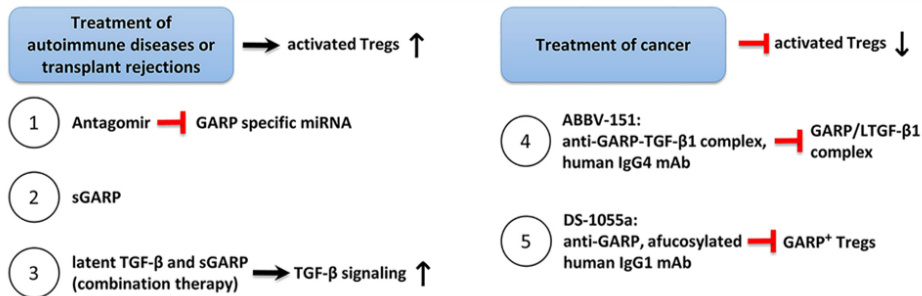
Figure 19. Potential therapies for targeting GARP in autoimmune diseases, transplant rejection and cancer
(Issue from[338]).

5.6.1 Role of GARP in immune-related disease

Single nucleotide polymorphisms present in the non-coding regions of GARP are related to the development of numerous diseases, which are immune-related diseases like asthma, allergic rhinitis, atopic dermatitis, or Crohn's disease[338]. One of the most frequent variants in the coding region of GARP has been proposed to be associated with developing atopic dermatitis (rs79525962, C/T, T allele frequency in the 1000 genomes project = 0.04). In this variant, position 407 is implicated with a change of A to a T that affects the presence of GARP at the surface of transfected cells, such as CD4+CD25- T cells transfected with A407T-LRRC32[339]. Another variant (rs201431152, G/A, A allele frequency = 0.00023), changing an R in W at position 414, is segregated with Usher syndrome in an isolated inbred population cohort[340].

5.6.2 Cancer and clinical trial

LRRC32 is amplified in several cancers with an area encompassing 40kb around GARP in breast cancer, but has not been demonstrated as an oncogene[305,341]. A pronounced increase in the number of copies of GARP has been found in primary and metastatic neck LNs in oral squamous cell carcinoma[342]. In prostate cancer, genetic instability increases in many genes, including GARP, during the progression from hormone-sensitive to hormone-resistant cancer[343]. A large heterozygous deletion and rearrangement of the Lrrc32 locus region has been reported in two cases of benign hibernoma cancer[344]. Further work is required to determine the secretion and the contribution of GARP-TGF-β1 in this context and the contribution in LNs. It has been recently demonstrated that the use of blocking anti-GARP:TGF-β1 monoclonal antibodies to target Tregs expressing GARP can produce a positive outcome in terms of anti-tumor efficacy in mice. The tridimensional structure of GARP:TGF-β1 complexes bound to the antigen-binding fragment (Fab) of a blocking anti-human GARP:TGF-β1 mAb has been determined using X-ray crystallography. This development provides a better understanding of how these antibodies block TGF-β1 activation by Tregs[283]. Furthermore, when blocking anti-GARP:TGF-β1 mAbs are used, interactions between the Latency Associated Peptide (LAP) and integrin aVβ8 remain unaffected. It has been suggested that the anti-GARP:TGF-β1 mAbs are effective via targeting complex conformational epitopes that include amino acids from the GARP:LAP:mature-TGF-β1 complex. The hypothesis is that these antibodies prevent LAP from deforming following integrin aVβ8 binding by restricting the movement of mature TGF-β1, which is bound by LAP[279]. Indeed, the development of monoclonal antibodies against GARP:TGF-β1 leads to the blockade of TGF-β1 activation and immunosuppression by GARP-expressing Tregs but not by cells that do not express GARP[274,279,285]. They are currently tested for the immunotherapy of cancer in patients with locally advanced metastatic solid tumors (clinicaltrials.gov NCT03821935 and NCT05822752)[345]. The immunomodulatory role of TGF-β1 in LNs has not been extensively studied. Understanding the role of GARP in Treg biology could have significant implications for the development of novel immunotherapeutic approaches

and the treatment of immune-related diseases. Thus, by extension, all the other cell populations in the LNs will be presented in the paper in the result section.

AIMS OF THE STUDY

Aims of the study

Our research team is investigating the tissue remodeling associated with the elaboration of pre-metastatic (PMN) and metastatic (MN) niches in the LNs of cancerous patients. We use human residual samples from a biobank (Biothèque Hospitalo-Universitaire de Liège, BHUL) and a mouse ear sponge assay model using melanoma B16F10Luc cells[346], with the aim to identify new actors implicated in the LN remodeling and immunosuppression. Previous studies by different teams, including our laboratory, have highlighted changes in the lymphatic network in the primary tumor. Such lymphangiogenic responses also occur in the SLN during the establishment of the PMN[83,138]. Indeed, a denser lymphatic network has been revealed in patients with cervical, lung, breast, and oral cancer both in the primary tumor and the SLN[167,169,347]. We here focus our interest on TGF-β1 as a key immune suppressor. Most of the studies on TGF-β1 are investigating its role in the primary tumor, while TGF-β1 in the LNs is less studied. In LNs, the main described cellular source of TGF-β1 is the Tregs, which produce it as a GARP:LAP:TGF-β1 complex. Our aim is to address the possibility that non-immune cells could be additional sources of this complex in the LN. Thus, these cell populations could be novel actors of the immunosuppressive environment to be considered within the LNs, in addition to the classical Tregs.

Our specific objectives are to:

❖ Explore and map the GARP sources in non-immune cells within metastatic LNs of patients suffering from breast or cervical cancer.

❖ To identify and cartograph the non-immune cell populations that express GARP in an experimental metastatic model using ear sponges containing B16F10 melanoma cells.

❖ To determine whether GARP production by non-immune cells (fibroblasts, endothelial cells) can contribute or not to TGF-β1 activation.

The results of this work are organized in two parts:

❖ The two first objectives are presented as an article published in 2023 in Cancers[348], describing the spatial distribution of the different non-immune cell

populations that express GARP. We revealed for the first time that beyond Tregs, GARP is expressed in several types of non-immune cells in LN, including specialized LEC subtypes in the SCS such as cLECs and fLECs, HEVs, and matrix-associated fibroblastic and perivascular cells. Through a combination of scRNA-Seq data mining, immunostaining and in situ RNA hybridization approaches, a precise mapping of GARP expression is provided in murine and human (breast and cervical cancer) samples.

❖ The results related to the third objective for the putative activation of TGF-β1 by GARP in endothelial and fibroblastic cells in vitro are presented as additional data.

During this thesis work, I also contributed to two articles that are presented in the Annexes:

❖ An article published by Bertrand C, Van Meerbeeck P, de Streel G, Vaherto-Bleeckx N, Benhaddi F, **Rouaud L**, Noël A, Coulie PG, van Baren N, Lucas S. in Frontiers in Immunology in 2021 entitled: "*Combined Blockade of GARP:TGF-β1 and PD-1 Increases Infiltration of T Cells and Density of Pericyte-Covered GARP⁺ Blood Vessels in Mouse MC38 Tumors*". The blockade of GARP:TGF-β1 was combined with the blockade of PD-1 in MC38 tumor-bearing mice. This combination exerted anti-tumor activity and resulted in a densification and a normalization of intratumoral blood vasculature associated with increased T cell infiltration into the tumors. These data might be significant for the identification of cancer patients who could benefit from the combined blockade of GARP:TGF-β1/PD-1 in clinical trials. The results are presented in **Annex 1**.

❖ A review authored by Lionel Gillot, Louis Baudin, **L. Rouaud**, Frédéric Kridelka and Agnès Noël: "*The pre-metastatic niche in lymph nodes: formation and characteristics*" published in 2021 in Cellular and Molecular Life Sciences. This review is presented in **Annex 2**.

Part-2 RESULTS

1 Spatial Distribution of Non-Immune Cells Expressing Glycoprotein A Repetitions Predominant in Human and Murine Metastatic Lymph Nodes

Loïc Rouaud [1], Louis Baudin [1,†], Marine Gautier-Isola [1,2,†], Pierre Van Meerbeeck [3], Emilie Feyereisen [1], Silvia Blacher [1], Nicolas van Baren [3], Frédéric Kridelka [4], Sophie Lucas [3,5,‡] and Agnes Noel [1,5,*,‡]

Question 1: Which non-immune cells in the LN express the GARP protein in humans and mice?

The presence or absence of metastatic tumor cells in the SLN, and thus the first tumor-draining LN, is a parameter clinicians use to establish the LN status, and it is strongly associated with poor clinical outcomes[180]. Various factors, such as cytokines and growth factors secreted by the tumor, are drained by the SLN, triggering its remodeling before the arrival of the tumor cells[138,349]. Changes in the proportions of immune cells have been reported [169], and an increase in the proportion of FoxP3+ Tregs in LNs contributes to the suppression of antitumoral immunity. The immunosuppressive microenvironment can be at least promoted by the secretion of TGF-β1 from Tregs. TGF-β1 is known to be presented at the surface of Tregs by the protein GARP[350]. GARP is also expressed by other immune and non-immune cells, including megakaryocytes and platelets[281], B cells[282], mesenchymal cells[351], and BECs[284,345,352]. Although GARP-expressing immune and non-immune cells have been characterized, GARP production and distribution in human and murine LNs remains unexplored.

The first objective was to identify non-immune cells expressing the protein GARP and, by extension, the GARP:TGF-β1 complex. These non-immune cells could potentially participate in the regulation of immunosuppressive tumor immunity and contribute to the spread of tumor cells through LNs.

We mapped here GARP expression in non-immune cells in metastatic LNs of humans and mice. We used various techniques and analyses of both human and murine samples, combining bioinformatics, in-vitro and in-vivo analyses and immunolabeling. Through the study of existing scRNA-Seq datasets, it has been discovered that various types of cells, such as BECs and LECs, fibroblasts, and perivascular cells, express the gene encoding GARP in both humans (*LRRC32*) and mice (Lrrc32). In human scRNA-Seq analyses, we found very low GARP expression in LECs. The GARP protein was found by immunostaining in BECs forming CD34+/PDPN- blood vessels and not in, but around CD34-/PDPN+ lymphatic vessels, forming a shield-like structure. Furthermore, our study has revealed that GARP is also expressed by αSMA+ fibroblasts around blood vessels and in fibroblasts

closely associated within the ECM. In mice, we used Lrrc32 (Garp) mRNA hybridization (RNA scope approach) to overcome the lack of anti-mouse GARP antibodies suitable for immunostaining. An almost identical map of GARP expression was found in the ear sponge assay, highlighting similarities between species, and further supporting the relevance of the experimental model for further investigation. The mapping of new non-immune cells expressing GARP opens new perspectives on the function of TGF-β1 in LNs.

Article

Spatial Distribution of Non-Immune Cells Expressing Glycoprotein A Repetitions Predominant in Human and Murine Metastatic Lymph Nodes

Loïc Rouaud [1], Louis Baudin [1,†], Marine Gautier-Isola [1,2,†], Pierre Van Meerbeeck [3], Emilie Feyereisen [1], Silvia Blacher [1], Nicolas van Baren [3], Frédéric Kridelka [4], Sophie Lucas [3,5,‡] and Agnes Noel [1,5,*,‡]

[1] Laboratory of Tumor and Development Biology, GIGA, University of Liège (ULiège), Sart-Tilman, 4000 Liège, Belgium; loic.rouaud@uliege.be (L.R.); louis.baudin@uliege.be (L.B.); marinegautier06@gmail.com (M.G.-I.)
[2] Université Côte d'Azur, CNRS UMR7275, IPMC, 06560 Valbonne, France
[3] de Duve Institute, UCLouvain, 1200 Brussels, Belgium; nicolas.vanbaren@uclouvain.be (N.v.B.); sophie.lucas@uclouvain.be (S.L.)
[4] Department of Obstetrics and Gynecology, CHU Liège, Sart-Tilman, 4000 Liège, Belgium
[5] WELBIO Department, WEL Research Institute, Avenue Pasteur, 6, 1300 Wavre, Belgium
*   Correspondence: agnes.noel@uliege.be; Tel.: +32-4-366-25-68
†   These authors contributed equally to this work.
‡   These authors contributed equally to this work.

Simple Summary: Glycoprotein A repetitions predominant (GARP) is expressed at the surface of regulatory T lymphocytes (Tregs) in human and murine primary tumors and was shown to mediate TGF-β1 activation and immunosuppression by Tregs in tumor-bearing mice. The cellular sources and the implication of GARP in lymph nodes (LNs) during the metastatic cascade are still elusive. Here, we mined available scRNA-Seq datasets and conducted immunohistochemistry and in situ hybridization analyses of metastatic LNs from mice and patients with cervical or breast cancer. We found GARP expression not only in Tregs, but also in blood/lymphatic vessels, fibroblastic cells, and perivascular cells. Our study highlights for the first time GARP expression by specialized lymphatic endothelial cells in the subcapsular sinus, high endothelial venules (HEVs), and matrix-associated (fibroblastic/perivascular) cells.

Abstract: Several types of cancer spread through the lymphatic system via the sentinel lymph nodes (LNs). Such LN-draining primary tumors, modified by tumor factors, lead to the formation of a metastatic niche associated with an increased number of Foxp3+ regulatory T cells (Tregs). These cells are expected to contribute to the elaboration of an immune-suppressive environment. Activated Tregs express glycoprotein A repetitions predominant (GARP), which binds and presents latent transforming growth factor beta 1 (TGF-β1) at their surface. GARP is also expressed by other non-immune cell types poorly described in LNs. Here, we mapped GARP expression in non-immune cells in human and mouse metastatic LNs. The mining of available (human and murine) scRNA-Seq datasets revealed GARP expression by blood (BEC)/lymphatic (LEC) endothelial, fibroblastic, and perivascular cells. Consistently, through immunostaining and in situ RNA hybridization approaches, GARP was detected in and around blood and lymphatic vessels, in (αSMA+) fibroblasts, and in perivascular cells associated with an abundant matrix. Strikingly, GARP was detected in LECs forming the subcapsular sinus and high endothelial venules (HEVs), two vascular structures localized at the interface between LNs and the afferent lymphatic and blood vessels. Altogether, we here provide the first distribution maps for GARP in human and murine LNs.

Keywords: LRRC32; GARP mRNA; glycoprotein A repetitions predominant (GARP); transforming growth factor beta 1 (TGF-β1); lymph node; tumor microenvironment; metastases; cancer

65

RESULTS

1. Introduction

Many types of cancer, such as breast, cervical, head and neck, and pancreatic carcinomas, as well as melanomas, are prone to disseminate through the lymphatic system [1–6]. Lymph nodes (LNs) are thus the first metastatic relay. The presence or absence of metastatic tumor cells in the sentinel LN, the first tumor-draining LN, is strongly associated with poor clinical outcomes and thus a crucial parameter for clinicians [7]. After colonizing LNs, metastatic tumor cells can seed distant organs and form systemic metastases [8,9]. The mechanisms underlying the cascade of events leading to LN metastases remain poorly understood.

Before nodal dissemination, the primary tumor modulates the microenvironment of its draining LN by secreting soluble factors (growth factors, cytokines) or releasing extracellular vesicles transported by lymphatic vessels [9–13]. This tissue remodeling occurs before the arrival of the first tumor cells. It leads to elaborating a so-called pre-metastatic niche permissive for subsequent metastatic cell survival and growth. The main features of this pre-metastatic LN niche include increased lymphangiogenesis and lymph flow, the recruitment of myeloid cells, and a reduction in effector lymphocyte numbers and function [11,14–16]. Strikingly, reported modifications of the immune landscape (changes in the proportion of CD8, Foxp3, CD20, or PD-1-expressing cells) suggest the elaboration of an immunosuppressive microenvironment in LNs [2]. In this context, an increased proportion of Foxp3+ regulatory T cells (Tregs) in LNs is expected to contribute to the suppression of anti-tumor immunity.

Upon activation of the T cell receptor, Tregs express a transmembrane protein called glycoprotein A repetitions predominant (GARP, encoded by the *LRRC32* gene). GARP covalently binds and presents latent transforming growth factor beta 1 (TGF-β1) on the Treg surface [17]. TGF-β1 is a pro-fibrotic and potently immunosuppressive cytokine that plays major roles in maintaining immune tolerance [18]. TGF-β1 is produced by virtually all cell types in a latent, inactive form (latent TGF-β1), in which the mature TGF-β1 dimer is non-covalently bound to the latency-associated peptide (LAP), preventing the binding of the cytokine to its receptor. To become active, TGF-β1 must be released from the LAP. In cells that do not express GARP, latent TGF-β1 is produced and secreted in association with latent TGF-β binding proteins (LTBPs), to which it associates via a disulfide linkage. Secreted LTBP:(latent)TGF-β1 complexes are deposited in the extracellular matrix, constituting a reservoir of latent TGF-β1 ready for activation by other cells. In cells that express GARP, in contrast, latent TGF-β1 associates preferentially with GARP via the formation of disulfide bonds, implicating the same LAP cysteine as that implicated in binding to LTBPs in other cell types [17]. GARP:(latent)TGF-β1 complexes are presented on the surface of human Tregs, where they can bind and be activated by integrin αVβ8 [17]. Monoclonal antibodies against GARP:TGF-β1 have been developed to block TGF-β1 activation and immunosuppression by GARP-expressing Tregs, but not by cells that do not express GARP [17,19,20]. They are currently tested for the immunotherapy of cancer in patients with locally advanced metastatic solid tumors [21] (clinicaltrials.gov NCT03821935 and NCT05822752).

Intriguingly, GARP is also expressed by other immune and non-immune cell types, including megakaryocytes and platelets [22], B cells [23], mesenchymal cells [24], and blood endothelial cells [21,25,26]. The spatial distribution of GARP-expressing non-immune cells in the LNs has not been studied previously. Non-immune cells contribute to the LN's architecture, compartmentalization, and function in the anti-tumoral immune response [27].

Blood and lymphatic endothelial cells (BECs and LECs, respectively) constitute two vascular networks implicated in antigen and cell transport. Of note, high endothelial venules (HEVs) are specialized blood vessels expressing the peripheral node addressin (PNAd). They are involved in the recruitment of naive lymphocytes [9,28] in lymphoid tissues and also contribute to the egress of metastatic cells from the LN [8,9]. Fibroblastic reticular cells (FRCs) and LECs elaborate a three-dimensional reticular meshwork important for the transport of antigens and signaling molecules into the LN parenchyma, as

well as for immune cell trafficking, priming and activation [27,29]. Recent advances in single-cell RNA sequencing have highlighted the heterogeneity of FRCs [30] and vascular cells (BECs, HEVs, and LECs), both in murine and human LNs [31–34]. Which of these cells express GARP in LNs is unclear.

Our study was carried out to identify and localize the different non-immune cell types expressing GARP and thus GARP:TGF-β1 complexes in non-metastatic and metastatic LNs. We here combined the analyses of publicly available scRNA-Seq datasets, immuno-histological stainings (IHCs), and in situ RNA hybridization approaches to map GARP expression in fibroblastic and vascular components of human and murine LNs. For the first time, we provide the spatial distribution of GARP expressing by perivascular, blood, and lymphatic endothelial cells in tumor-draining LNs.

2. Materials and Methods

2.1. Single-Cell RNA Sequencing of Human LN Cells

Human LN data (EGAD00001008311, European Genome-Phenome Archive database from Abe et al. were processed and analyzed using the R package Seurat (v.4.3.0) in RStudio (v.4.1.3) [31]. After removing ribosomal genes from cells that were apoptotic or lysed (more than 5% of mitochondrial genes), we filtered out genes expressed in fewer than three cells and cells expressing fewer than 200 unique features (low-quality cells). Cells with unique feature counts higher than 7500 genes (more than twice the median number, likely corresponding to doublets) were also removed. We then normalized data using the NormalizeData function and extracted highly variable features using the FindVariableFeatures function. Normalized data underwent a linear transformation (scaling, ScaleData function) and a principal component analysis (PCA) based on variable features using the RunPCA function. Graph-based clustering was then performed according to gene expression profiles using the FindNeighbors (dims = 1:50) and FindClusters (resolution: 0.8) functions. Results were visualized using a UMAP nonlinear dimensional reduction technique by running RunUMAP and DimPlot functions. The clustering of cells was annotated through the differentially expressed genes (DEGs) by running the FindAllMarkers function and the previous annotation described by Rodda et al. Cell clusters were illustrated using canonical cell type markers for lymphatic endothelial cells (LEC: *PROX1+*, *PDPN+*), blood endothelial cells (BEC: *CD34+*, *PECAM1+*), mesenchymal stromal cells (SCs: *COL1A1+*, *PDGFRB+*) expressing PTX3 (SCs-PXT3), SCs expressing C7 (SCs-C7), SCs expressing SFRP4 (SCs-SFRP4), SCs expressing AGT (SCs-AGT), adventitial/medullary reticular cells (ACs-MedRCs: *PCOLCE2+*, *MFAP5+*, *IGFBP6+*), and perivascular cells (PvCs: *MYL9+*, *ITGA7+*, and *ACTA2+*).

2.2. Single-Cell RNA Sequencing of Mouse LN Cells

Murine LN pre-processed data (GEO GSE202068 [35]) were processed and analyzed using the R package Seurat (v.4.3.0) in RStudio (v.4.1.3). After removing ribosomal genes from cells that were apoptotic or lysed (more than 5% of mitochondrial genes), we filtered out genes expressed in fewer than three cells and cells expressing fewer than 200 unique features (low-quality cells). Cells with unique feature counts higher than 7500 genes (more than twice the median number, likely corresponding to doublets) were also removed. We then normalized data using the NormalizeData function and extracted highly variable features using the FindVariableFeatures function. Normalized data underwent a linear transformation (scaling, ScaleData function) and a principal component analysis (PCA) based on variable features using the RunPCA function. Graph-based clustering was then performed according to gene expression profiles using the FindNeighbors (dims = 1:20) and FindClusters (resolution: 0.4) functions. Results were visualized using a nonlinear dimensional reduction UMAP technique by running RunUMAP and DimPlot functions. The clustering of cells was annotated through the differentially expressed genes (DEGs) by running the FindAllMarkers function and the previous annotation described by Rodda et al. Cell clusters were illustrated using canonical cell type markers for lymphatic endothelial

cells (LEC; Prox1, Flt4, and Lyve1), subdivided into two clusters LEC I (*Ackr4*, *Foxc2*, and *Cdln11*) and LEC II (*Madcam* and *Bmp2*), blood endothelial cells (BEC: *Pecam1* and *Cdh5*), marginal reticular cells (MRCs: *Enpp2* and *Cxcl13*), T cell reticular cells (TRCs: *Ccl19* and *Ccl21a*), adventitia cells (Acs: *Igfbp6* and *Mfap5*), medullary reticular cells (MedRCs: *Penk* and *Tmeff2*), and perivascular cells (PvCs: *Myl9*, *Notch3*, and *Acta2*).

2.3. In Vitro Cell Culture

We used primary human dermal lymphatic microvascular endothelial cells (HMVEC-dLyAd, CC-2810, Lonza, Verviers, Belgium) and human umbilical vein endothelial cells (CC-2519A, Lonza, Verviers, Belgium), herein referred to as LECs and HUVEC, respectively. These cells were cultured as a monolayer in EGM2-MV medium (complete medium) (CC-3202 for LECs and CC-3162 for HUVEC, Lonza, Verviers, Belgium) until confluence. Primary human lymphatic fibroblasts (HLFs from ScienCell, #2530, Carlsbad, CA, USA) were cultured in complete fibroblast medium (FM, Cat. #2301, ScienCell) until confluence was achieved, according to the manufacturer's instructions. Jurkat cells (clone E6-1) were obtained from the American Type Culture Collection (Manassas, VA, USA). As previously described, Clone E6-1 was transduced with a lentivirus encoding GARP to generate neomycin-resistant Jurkat + GARP cells [36]. Jurkat + GARP cells were cultured in RPMI medium (Gibco) supplemented with 10% fetal bovine serum (10270-106, Thermofisher, Waltham, MA, USA), 1% glutamine (25030-123, Thermofisher), and 1% penicillin–streptomycin (15140-122, Thermofisher), in the presence of neomycin (1 mg/mL) (N6386, Sigma-Aldrich, Darmstadt, Germany).

2.4. Western Blot

Cells were lysed with cell lysis buffer 1x composed of 20 mM Tris-HCl pH 7.5, 150 mM NaCl, 1 mM Na2EDTA, 1 mM EGTA, 1% Triton, 2.5 mM sodium pyrophosphate, 1 mM β-glycerophosphate, 1 mM Na3VO4, 1 μg/mL leupeptin (#9803, Cell Signaling, Danvers, MA, USA), and 1× protease/phosphatase inhibitor cocktail (Complete and phosSTOP, Roche, Indianapolis, IN, USA). Lysate samples were separated on acrylamide gels (10%) in a reducing condition with SDS at 20 μg/well and then transferred onto PVDF transfer membranes (88518, ThermoScientific, Waltham, MA, USA). Membranes were probed by overnight incubation at 4 °C with the indicated antibodies followed by 1 h incubation at room temperature with horseradish peroxidase-coupled secondary antibody (7076, Cell Signaling, Danvers, MA, USA) and enhanced chemiluminescent substrate (NEL104001EA, PerkinElmer, Waltham, MA, USA) using an Amersham ImageQuant 800 (GE Healthcare, Chicago, IL, USA). The following antibodies were used: GARP (1/1000; LRRC32 monoclonal antibody, Plato-1, ALX-804-867-C100, Enzo Life Sciences, Farmingdale, NY, USA) and GAPDH (1/10,000; MAB 374, Millipore, Burlington, MA, USA).

2.5. Flow Cytometry

Cell suspensions were harvested using Accutase (#07922, Stemcell Technologies, Vancouver, BC, Canada) at 37 °C for 5 to 10 min. The single-cell suspensions obtained were counted and immediately stained with antibodies against the following surface markers: GARP PE (clone Plato-1, Enzo Life Sciences, Farmingdale, NY, USA), integrin αV (clone NKI-M9; CD61), integrin β3 (clone VI-PL2) (Biolegend, San Diego, CA, USA), integrin β6 (clone #437211), integrin β8 (clone #416922, R&D Systems, Minneapolis, MN, USA) in the presence of a viability dye (Invitrogen, Waltham, MA, USA) and anti-CD16/32 to block FcgRs (Biolegend). Analyses were performed on an FACSCanto™ II flow cytometer (DIVA, BD Biosciences, San Jose, CA, USA), and data were computed using the FlowJo software vX.0.7 (Tree Star, Ashland, OR, USA).

2.6. Multiplexed Immunofluorescence on Human LN Sections

Human LN samples from breast or cervical cancer patients were obtained from CHU ULiège Biobank. Seven μm thick cryosections from human LNs were mounted on a

Superfrost microscope slide and fixed in formaldehyde 4% for 5 min, washed with demineralized water (ddH_2O) and phosphate-buffered saline (PBS), and then incubated with 3% H_2O_2 (8070-4, Carl Roth, Karlsruhe, Germany) to block endogenous peroxidases. Sections were blocked with animal-free blocking solution (15019 L, Cell Signaling), followed by an incubation with either 5 µg/mL of mouse monoclonal anti-human GARP antibody (clone MHG-6 [20]) in Dako antibody diluent or no primary antibody (negative control) for 90 min. After two washes with PBS supplemented with Tween20 (PBS-T), the EnVision-HRP secondary antibody (K4001, Dako Agilent, Diegem, Belgium) was incubated at room temperature for 30 min. Staining was amplified using tyramide signal amplification working solution (TSA, NEL741001KT, PerkinElmer) containing fluorescein isothiocyanate dye (1:500, FITC) for 10 min, washed thrice with PBS-T. The following antibodies were used in combination with GARP (following the same steps as above): rabbit monoclonal anti-FoxP3 antibody (clone EPR15038-69, Abcam, Cambridge, UK) (1:200), mouse monoclonal anti-CD34 antibody (clone Qbend 10, Abcam) (1:200), sheep polyclonal anti-PDPN (AF3670, R&D Systems) (1:200), monoclonal rat anti-PNAd Alexa Fluor 488 (High Endothelial Venule Marker, clone MECA79, eBioscience, San Diego, CA, USA) (1:100), αSMA (ab5694, Abcam) (1:200), and CD31 (ab24590, Abcam) (1:200). Ready-to-use EnVision+ System-HRP Labelled Polymer anti-Rabbit (K4003, Dako), anti-mouse IgG1 coupled with HRP (115-035-205, Jackson ImmunoResearch, Cambridge, United Kingdom) (1:1000), and anti-sheep coupled with HRP antibody (1:3000) were used as secondary antibodies, followed by TSA incubation with Cy3 or Cy5 (1:2000) instead of fluorescein. For the dual immunostaining GARP/HEV (PNAd), amplification of GARP with TSA was made with Cy3. A last wash with PBS-T was made before mounting the slides with Fluoromount containing DAPI (0100-20, SouthernBiotech, Birmingham, AL, USA).

2.7. Ear Sponge Assay

C57Bl6 female mice (6 to 8 weeks old) were used throughout this study. The animals were maintained under a 12 h light–dark cycle with free access to food and water. Gelatin sponges were incubated with tumor cells (2×10^5 B16F10 cells/sponge) or control medium (serum-free DMEM without tumor cells) for 30 min in serum-free-DMEM, embedded with collagen, and implanted into mouse ears as previously described [32,33]. Bioluminescence was detected in animals bearing ear sponges soaked with luciferase-expressing cells using the in vivo Imaging System IVIS 200 (Xenogen Corp.; Alameda, CA, USA). At the end of the experiment, the sponges and cervical LNs were harvested, incubated in 4% formol (11699408, VWR, Leuven, Belgium) for 16 h, dehydrated in ethanol, and fixed in paraffin (X881.2, Leica, Frankfurt, Germany).

2.8. In Situ RNA Hybridization

The mRNA in situ hybridization of *Lrrc32* (Garp) and *Prox1* was measured on mice LN tissue sections using the RNAscope assay according to the manufacturer's instructions (Advanced Cell Diagnostics, Bioké, Leiden, The Netherlands). Tissue sections (10 µm) were deparaffinized/rehydrated and hybridized with Mm-Lrrc32-C1 (#592941-C1, Bioké, Leiden, The Netherlands) probes and/or Mm-Prox1-C2 (#488591-C2, Bioké, Leiden, The Netherlands) with an RNAscope 3-plex negative control probe (#320871, Bioké, Leiden, The Netherlands). The hybridization signal was amplified with RNAscope Multiplex Fluorescent reagent kit V2 (#323135, Bioké, Leiden, The Netherlands) and with OPAL (Opal 520, PN FP1487001KT; Opal 570, PN FP1488001KT; Opal 620, PN FP1495001KT).

After hybridization, immunostaining was performed with one of the following antibodies incubated overnight at 4 °C: Alexa Fluor 488-PNAd (MECA-79, eBioscience), FoxP3 (ab191416, Abcam), Lyve-1 (AF2125, R&D Systems), CD31 (ab28364, Abcam), or αSMA (ab5694, Abcam).

2.9. Slide Scanning and Image Analysis with Olyvia and QuPath

For human samples, digital 3 or 4-color images of the stained tissue sections were digitalized using a NanoZoomer 2.0-HT system (Hamamatsu Photonics, Hamamatsu, Japan) at 20× magnification with a resolution of 0.23 μm/pixel. Mice samples of digital 3 or 4-color images were acquired with the SLIDEVIEW VS200 research slide scanner (Olympus, Anvers, Belgium) equipped with a UPlan-XApo 20× 0.8× objective (Olympus) and with a Hamamatsu ORCA-Flash camera, using DAPI, FITC, Cy3, and Cy5 filter sets. Some high-magnification images were generated with a confocal Zeiss LSM880 Airyscan microscope (Zeiss, Oberkochen, Germany) and a 40× or 63× objective lens. The relative quantity of GARP immunostaining in human LN samples was quantified with QuPath software (v0.4.3, [37]) using a deep learning model composed of 6 layers of different nodes (8, 10, 10, 10, 10, and 10 nodes) with the library OpenCV (module ann_mlp) and the Gaussian Laplacian features with an output of classification method.

2.10. Statistics

Statistical analyses were performed with GraphPad Prism 9.0 software using the Mann–Whitney test or one-way ANOVA, two-tailed as indicated in the figure legends. Data are shown as mean $\pm$ SD, and differences were considered statistically significant when $p < 0.05$, as indicated by asterisks with $p < 0.05$ (*), $p < 0.01$ (**), and $p < 0.001$ (***).

2.11. Study Approval

Animal experiments complied with the Animal Ethical rules of the University of Liège (Liège, Belgium) after approval from the local Animal Ethical Committee. Human LN samples were stored in the biobanks of the University of Liège (CHU, Liège, Belgium) after study approval by local ethics committees. The use of human body material from the biobank does not require consent forms under the Belgian law of 19 December 2008.

3. Results

3.1. Single-Cell RNA Sequencing Analysis of Human LNs Uncovers the LRRC32 Gene Expression by Subpopulations of Endothelial and Perivascular Cells in Human LNs

The LN, the main organ in which immune response takes place, comprises immune and non-immune cells, such as BECs, LECs, and FRCs, as well as other mesenchymal cells. In order to identify which non-immune cells express *LRRC32* (the gene encoding GARP) in human LNs, we started our analysis by examining available single-cell RNA sequencing (scRNA-Seq) datasets from human LN samples [31] (Figure 1a). In one of the datasets [31], non-sentinel non-enlarged LNs were taken from patients with a neoplasm ($n = 9$) and their malignancy-freeness was verified with a pan-cytokeratin marker. LN CD45- cells were separated into non-endothelial stromal cells (NESCs), BECs/HEVs, and LECs. Different subclasses were clustered through differentially expressed genes (DEGs) to highlight their specificity of expression and functionality (Figure 1b,c). Cells were classified into eight groups (Figure 1a–c): blood endothelial cells (BECs: *PECAM1+*, *CD34+*), lymphatic endothelial cells (LECs: *PROX1+*, *PDPN+*, *PECAM1+*), mesenchymal stromal cells (SCs: *COL1A1+*, *PDGFRB+*) expressing PTX3 (SCs-PXT3), SCs expressing C7 (SCs-C7), SCs expressing SFRP4 (SCs-SFRP4), SCs expressing AGT (SCs-AGT), adventitial/medullary reticular cells (ACs-MedRCs: *PCOLCE2+*, *MFAP5+*, *IGFBP6+*), and perivascular cells (PvCs: *ACTA2+*, *MYL9+*, *ITGA7+*). The violin plot provides an insightful visualization of the scRNA-Seq expression profiles of the *LRRC32* gene within the different subclasses of stromal cells (NESCs, BECs/HEVs, LECs, and PvCs) (Figure 1d). Of note, *LRRC32* was expressed by PvCs and BECs/HEVs, and was detected at a very low level in NESCs and LECs (Figure 1d). A focus on PvCs and NESCs confirmed a higher *LRRC32* expression level in PvCs as compared with NESCs (Figure 1e). Interestingly, *LRRC32* expression was detected in almost all BEC/HEV subtypes: large arteries (ABECs), arteries surrounding the LN capsule (caBECs), arterioles (aBECs), capillary BECs (cBECs), transitional BECs between capillary BECs and activated HEVs (C-aHEVs), large veins (VBECs), activated

HEVs (aHEVs), and homeostatic HEVs (hHEVs) (Figure 1f). In sharp contrast, *LRRC32* was not or only faintly expressed in the different LEC subtypes (Figure 1g). Collectively, these data suggest a role of GARP in different subpopulations of human blood endothelial cells and perivascular cells [38].
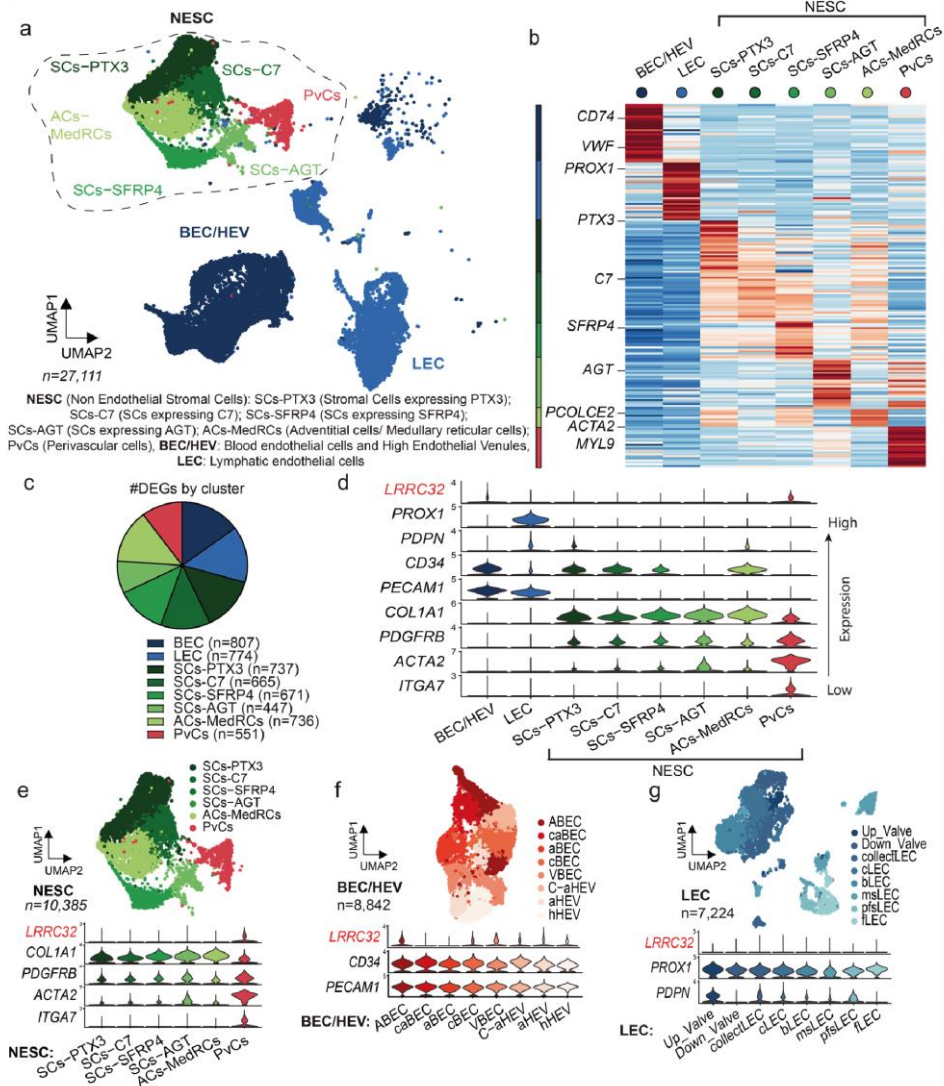
Figure 1. LRRC32 gene expression analysis in individual cells derived from metastasis-free human LNs. (**a**) UMAP plot clusters 27,111 cells from 9 metastasis-free LNs into 8 distinct groups (BECs/HEVs, LECs, SCs-PTX3, SCs-C7, SCs-SFRP4, SCs-AGT, ACs-MedRCs, and PvCs). (**b**) Heatmap showing the expression levels of the top-ranking marker genes in each cluster. Key genes are indicated on the left. (**c**) Number of DEGs in each cluster (**d**). Violin plot showing expression of genes of interest including *LRRC32* (in red) in each cluster. (**e**–**g**) UMAP plot clusters (**e**) non-endothelial stromal cells (NESCs), (**f**) BECs/HEVs, and (**g**) LECs, and violin plots showing expression of genes of interest, including *LRRC32* (in red) in each cluster.

3.2. Expression of GARP and Integrins Are Produced In Vitro by Human Endothelial Cells and LN Fibroblasts

We next assessed GARP protein expression in various primary cultures, including human umbilical vein endothelial cells (HUVECs), human LECs, and human lymphatic fibroblasts (HLFs) in basal conditions. Jurkat cells transduced to express the human GARP protein (h-GARP) were used as a positive control. Western blot analyses revealed similar levels of GARP expression in the different primary cells (Figures 2a and A1). Flow cytometry analyses under non-permeabilizing conditions further validated these findings and confirmed the presence of GARP on the cell surface of HUVECs, LECs, and HLFs (Figure 2b). Given the potential contribution of integrins $\alpha V \beta 6$ and $\alpha V \beta 8$ to the activation of latent TGF-β1 presented by GARP on the cell surface [17], we examined the presence of these integrins at the surface of the different cell types, as well as that of the more common integrin $\alpha V \beta 3$. Flow cytometry detected almost similar and important levels of αV and $\beta 3$ subunits in the three primary cell cultures (Figure A2). The $\beta 6$ and $\beta 8$ integrin subunits were also detected in HUVECs, LECs, and HLFs. These results established that, in basal culture conditions, protein GARP, $\alpha V \beta 6$, and $\alpha V \beta 8$ are co-expressed at the surface of primary HUVEC, LEC, and HLF cultures.
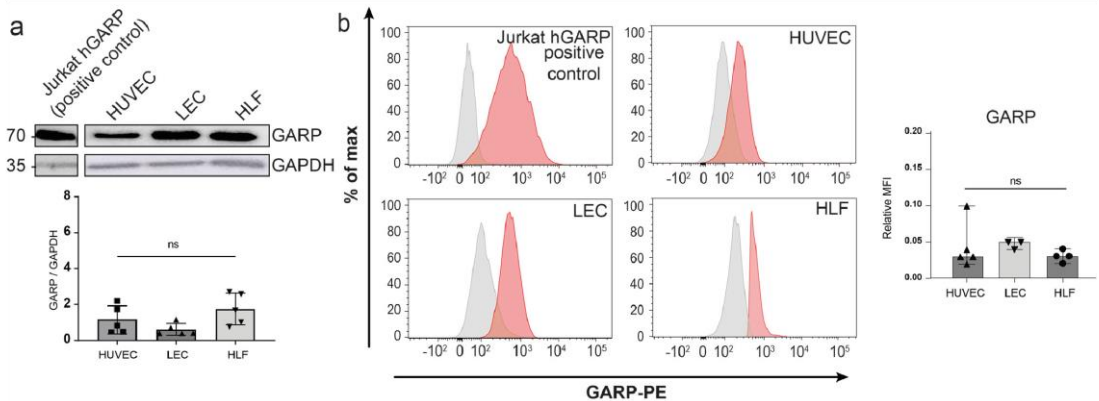
Figure 2. Evaluation of GARP in HUVEC, LEC, and HLF cells cultured under basal conditions. (**a**) Western blot analysis of GARP expression. The blot is a representative blot out of 4 independent experiments. The bar graph shows the quantification of GARP protein levels relative to the GAPDH protein signal (GARP/GAPDH signals) ($n = 4$, means $\pm$ SD, n.s. determined by one-way ANOVA). (**b**) Flow cytometry analysis of GARP at the surface of primary cells. Jurkat cells overexpressing GARP (Jurkat$-$hGARP) were used as a positive control. The isotype control is represented in grey, and the positive signal is depicted in red as a percentage of the maximum. The relative MFI of GARP in flow cytometry is represented with a bar graph ($n \geq 3$, means $\pm$ SD, n.s., no significance, determined by one-way ANOVA).

3.3. Detection and Mapping of GARP in Human Metastatic LN Samples

We next investigated the spatial distribution of GARP-expressing cells and GARP-positive areas in LNs of patients with breast (BC, $n = 14$) or cervical (CC, $n = 4$) cancer. Immunohistochemical analyses were conducted on non-metastatic (MLN$-$) (total $n = 3$) and metastatic LNs (MLN+) ($n = 18$). It is worth noting that the anti-GARP antibody (clone MHG-6) can only be used on frozen tissue sections, which limited the number of (normal and metastatic) human tissue samples amenable to analyses. Interestingly, the density of GARP staining was higher in MLN+ than in MLN$-$ (Figure 3a). Despite the reduced number of MLN$-$ samples, we noticed an approximative five-fold increased density of GARP staining in MLN+ compared to MLN$-$ (** $p = 0.0053$) (Figure 3b). As expected, we found GARP+/FoxP3+ cells, corresponding to activated Tregs, and GARP-/FoxP3+ cells, corre-

sponding mostly to non-activated Tregs, in both MLN+ and MLN− samples (Figure S1a–c). Areas with strong GARP staining but without FoxP3 staining were found in both types of samples, indicating the presence of non-Treg GARP-expressing cells (Figure S1a–c). Most GARP+FOXP3- areas were found around vessels and in the extracellular matrix. This observation prompted us to postulate that peri-vascular and vascular cells express GARP in LNs (Figure S1b,c).
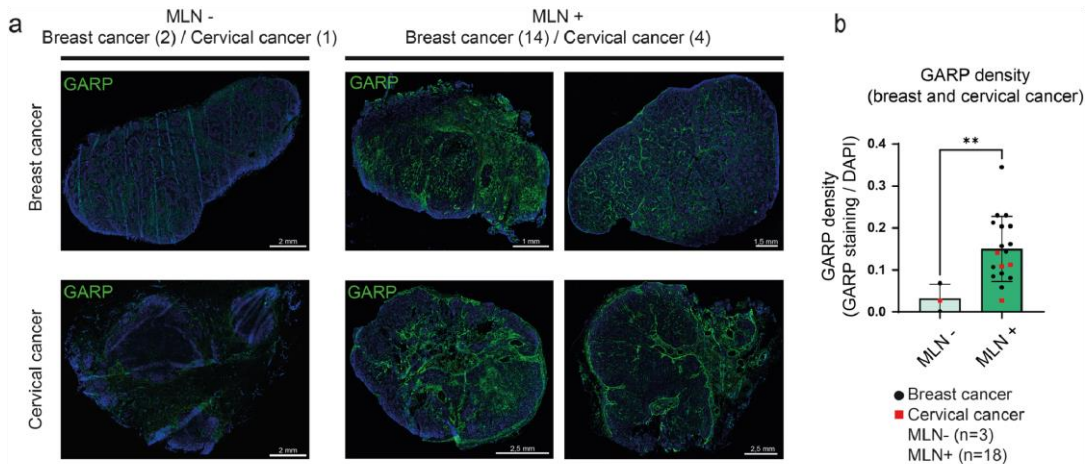
Figure 3. Multiplex immunofluorescence identifies GARP expression in human LN. (**a**) Immunofluorescence was conducted on frozen sections of human LN derived from metastatic-negative (MLN−, *n* = 3) and metastatic-positive (MLN+, *n* = 18) LNs from patients diagnosed with breast cancer (BC; 3 MLN− and 14 MLN+) or cervical cancer (CC; 1 MLN− and 4 MLN+). The sections were stained with anti-GARP antibody (in green) and DAPI for nuclei (in blue). Scale bar = 2, 1, 1.5, or 2.5 mm (**b**) Computer-assisted quantification of GARP density using QuPath (relative density with DAPI area) in MLN− and MLN+. The bar graph is represented with individual data points, and results are expressed by mean ± SD (** *p* = 0.0053 determined by the Mann–Whitney test).

To investigate GARP protein expression in the blood and lymphatic LN vasculatures, a triple co-staining of GARP, CD34 (a marker of blood vessels), and podoplanin (PDPN, a marker of lymphatic vessels) was performed and analyzed by confocal microscopy (Figure 4a). GARP staining was detected in the cell wall of CD34+/PDPN− blood vessels and around CD34-/PDPN+ lymphatic vessels. (Figure 4a). We also detected GARP staining in the subcapsular sinus (SCS), both in the layer directly in contact with the LN parenchyma (floor LECs) and in the external layer (ceiling LECs) (Figure 4b). In line with the detection of *LRRC32* expression in HEVs in scRNA-Seq data, GARP positivity was also found in PNAd+ HEV vessels (Figure 4c). Given the scRNA-Seq analysis identifying perivascular cells as a putative cellular source of GARP, we next focused on those cells identified by *ACTA2* (αSMA) expression. IHC with an anti-αSMA antibody confirmed the presence of GARP+/αSMA+ cells surrounding blood vessels or isolated in the ECM, likely corresponding to fibroblastic cells (Figure 4d,e). In contrast to the scRNAseq data suggesting *Itga7* expression by perivascular cells, only a few ITGA7+ cells were noted, in contrast to a widespread expression of αSMA (Figure A4). Collectively, our analyses lead to the mapping of GARP in human LNs (Figure 4a–e), revealing the presence of GARP in blood vessels, HEVs, and the SCSs, as well as αSMA+ perivascular and fibroblastic cells.
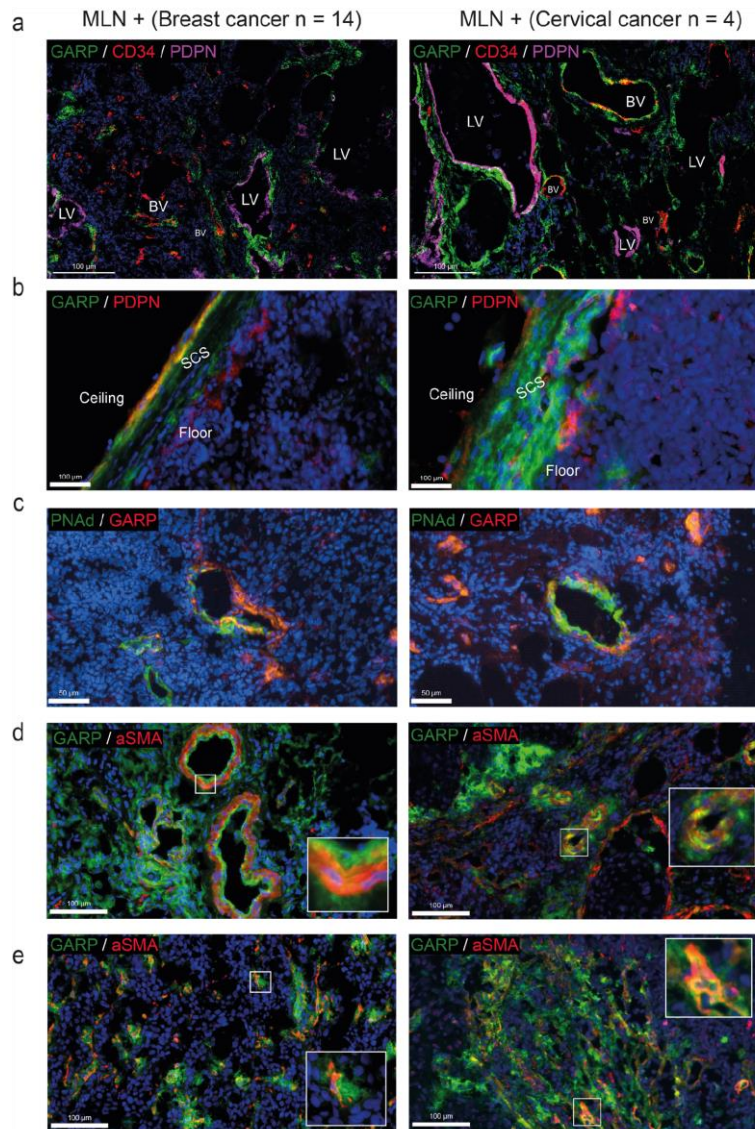
Figure 4. Multiplex immunofluorescence identifies GARP expression in lymphatic and blood vessels in human LNs. (**a**) Multiplex immunofluorescence staining of GARP (in green), CD34 (in red), podoplanin (in pink), and nuclei (DAPI, in blue) on MLN+ from patients with breast cancer (*n* = 14) or with cervical cancer (*n* = 4). LV: lymphatic vessel, BV: blood vessel. Scale bar = 100 μm. (**b**) Multiplex immunofluorescence staining of GARP (in green), PDPN (in red), and nuclei (DAPI, in blue) focused on the LN capsule on MLN+ from patients with breast cancer (*n* = 14) or with cervical cancer (*n* = 4). SCS: subcapsular sinus. Scale bar = 100 μm. (**c**) Multiplex immunofluorescence staining of GARP (in red), PNAd (in green), and nuclei (DAPI, in blue) on MLN+ from patients with breast cancer (*n* = 14) or with cervical cancer (*n* = 4). Scale bar = 50 μm. (**d**) Multiplex immunofluorescence staining of GARP (in green), αSMA (in red), and nuclei (DAPI, in blue) of MLN+ from patients with breast cancer (*n* = 14) or with cervical cancer (*n* = 4) or (**e**) in the ECM. Scale bar = 100 μm.

3.4. Single-Cell RNAseq Analysis Uncovers the Lrrc32 Gene Expression in Endothelial and Peri-Vascular Cells of Murine LNs

We next analyzed murine LN datasets of scRNA-Seq (Figure 5a,b) and focused our interest on FRCs (*Col1a1+*, *Pdgfrb+*), BECs/HEVs (*Pecam1+*, *Cd34+*), BECs/HEVs, and LECs (*Prox1+*, *Pdpn+*, *Pecam1+*). In each cell type, subclusters co-exist, characterized by distinct gene expression profiles related to their specific functions [31]. The exploration of the previously published dataset of naive mice LNs revealed different FRC subtypes: (i) marginal reticular cells (MRCs; *Enpp2+*, *Cxcl13+*) dispersed at the basis of the SCS, which are supposed to play a role in barrier defense; (ii) T cell reticular cells located near lymphocyte follicles (TRCs; *Ccl19+*, *Ccl21a+*); (iii) medullary reticular cells (MedRCs; *Inmt+*, *Penk+*, *Tmeff2+*), which are niche-restricted in the medullary sinus; (iv) adventitial cells in the medullary sinus (ACs; *Mfap5+*, *Igfbp6+*), which may support large vessels and secrete pro-(lymph)angiogenic factors; and (v) perivascular cells (PvCs; *Notch3+*, *Myl9+*, *Acta2+*, *Itga7+*) which are in the periphery of large blood vessels and have multiple functions of blood vessel support (Figure 5a,b) [30,35]. In this dataset, LECs were separated into LEC I (*Flt4+*, *Foxc2+*, *Ackr4+*, *Cldn11+*), which correspond to valve, collector, and ceiling lymphatic vessels, and LEC II (*Lyve1+*, *Madcam+*, *Bmp2+*), which are localized in the medullar and floor of the LN sinus. These different subclasses were clustered through differentially expressed genes (DEGs) to highlight their specificity of expression and functionality (Figure 5c). In line with the human data, *Lrrc32* mRNA expression was detected in BECs/HEVs and PvCs (Figure 5e). Furthermore, a LEC subpopulation, namely LEC I, corresponding mainly to collector lymphatic vessels and ceiling LECs, expressed *Lrrc32* at levels almost similar to that in PvCs (Figure 5d). These data indicate that GARP is expressed in murine BECs and PvCs, and a subpopulation of murine LECs [38].

3.5. Mapping of Lrrc32 mRNA Expression in Mouse LNs

To determine the spatial distribution of *Lrrc32* expression in murine LNs, we used the pre-clinical ear sponge assay to induce LN metastasis [39]. In this model, gelatin sponges soaked with melanoma B16F10 melanoma cells were transplanted into the ears of mice. This leads to the formation of a local tumor and dissemination of metastatic tumor cells to the draining LNs 3 weeks post-implantation. Histological analyses confirmed the presence of metastases. Given the absence of suitable anti-murine GARP antibodies, we used the RNAscope technique to localize the *Lrrc32* (*Garp*) mRNA. First, we observe FOXP3+ cells surrounded by *Lrrc32* mRNA, used as a positive control (Figure A3). We concomitantly used a *Prox1* probe (a transcription factor expressed by lymphatic cells) and Lyve1 immunostaining to localize LECs. In the parenchyma of the LN, the *Lrrc32* mRNAs were found in *Prox1+* lymphatic vessels in both control and metastatic LNs (Figure 6a,b). Lyve-1 staining confirmed *Lrrc32* mRNA expression in lymphatic vessels (Figure 6a,b). We next focused on the SCS, in which floor LECs (fLECs) are Lyve1+ while ceiling LECs (cLECs) are negative for Lyve-1. Lrrc32 mRNAs were detected in *Prox1+/Lyve1+* cells (fLEcs) in contact with the parenchyma, as well as in external *Prox1+/Lyve1-* cells (fLECs) (Figure 7a,b). Interestingly, we also observed *Lrrc32* mRNA within PNAd+ HEVs (Figure 8a,b). Furthermore, the immunostaining of CD31 and αSMA indicated Lrrc32 expression in αSMA+ perivascular cells surrounding both blood (*Prox1−/CD31+*) and lymphatic vessels (*Prox1+/CD31+*). We also detected *Lrrc32+/αSMA+* fibroblastic cells. A similar staining of blood endothelial cells, perivascular cells, and fibroblasts was detected in both control and metastatic mice LN samples (Figure 9a,b).
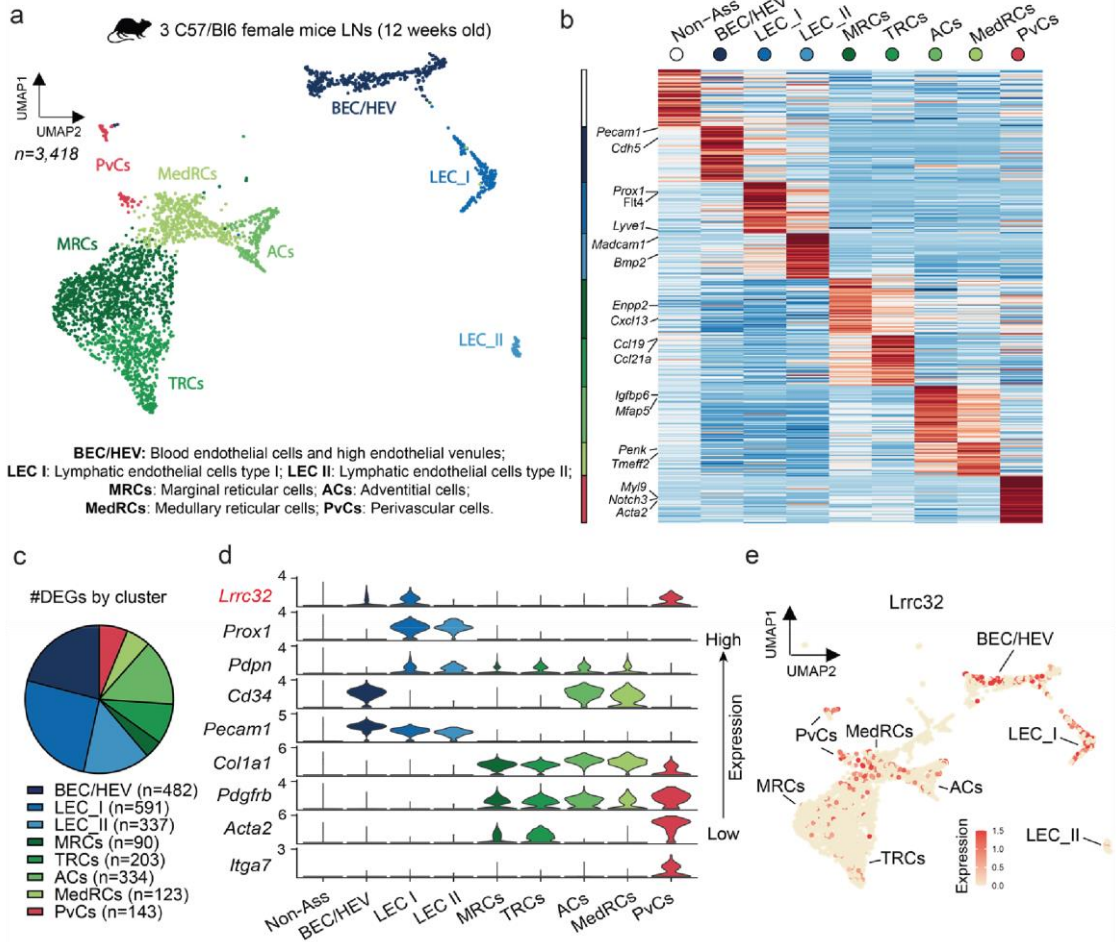
Figure 5. Lrrc32 gene expression analysis in individual cells derived from metastasis-free mice LNs. (**a**) UMAP plot clusters 3,418 cells from 3 C57/Bl6 female mice LNs cells into 8 distinct groups (BEC/HEV, LEC I, LEC II, MedRCs, ACs, MRCs, TRCs, and PvCs). (**b**) Heatmap showing the expression levels of the top-ranking marker genes in each cluster. Key genes are indicated on the left. (**c**) Number of DEGs in each cluster. (**d**) Violin plot showing expression of genes of interest including Lrrc32 (in red) in each cluster. (**e**) UMAP plot of Lrrc32 expression level in each cluster.
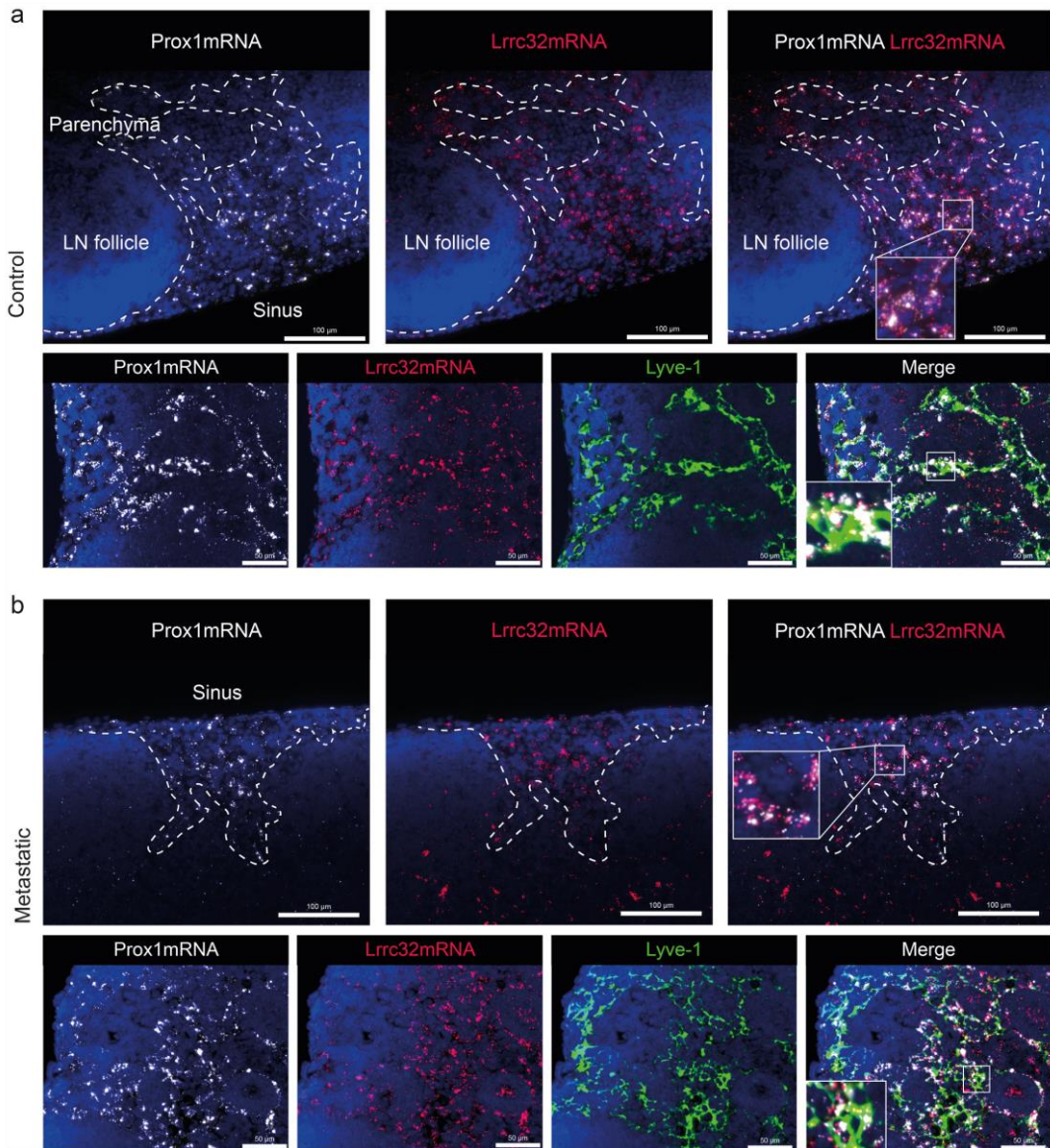
Figure 6. Mapping of *Lrrc32* mRNA (encoding Garp) in mouse LN parenchyma with hybridization. (**a**) mRNA detection by RNAscope of *Prox1* mRNA (white), *Lrrc32* mRNA (red), and/or coupled with Lyve-1 immunostaining on mouse cervical LN with a focus on the parenchyma area in control condition; (**b**) mRNA detection by RNAscope of *Prox1* mRNA (white), *Lrrc32* mRNA (red), and/or coupled with Lyve-1 immunostaining in a metastatic LN 3 weeks after B16F10 transplantation. Scale bar = 100 and 50 μm.
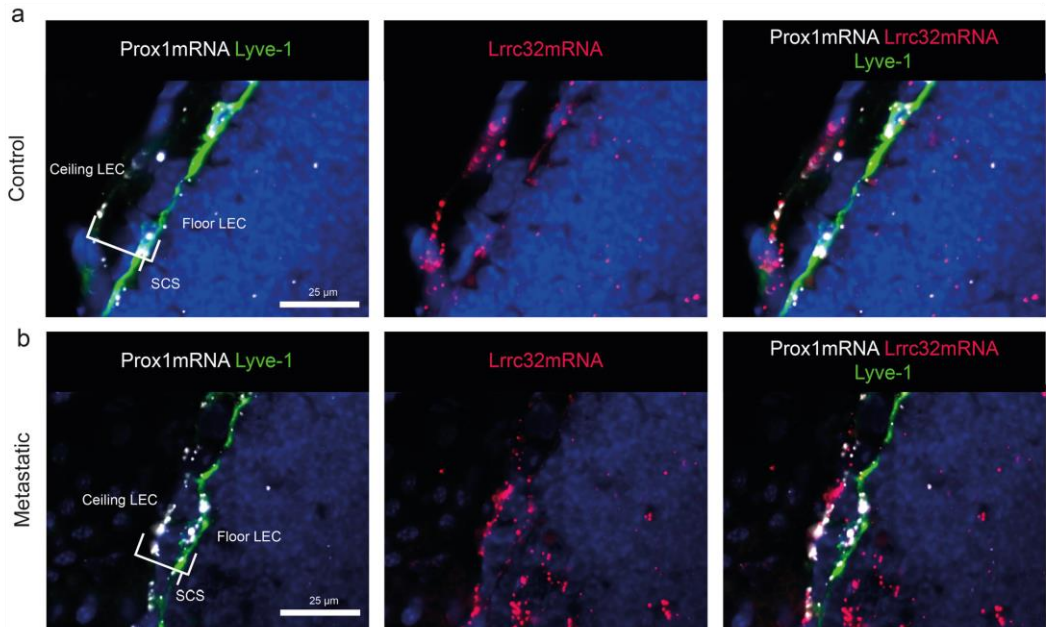
Figure 7. Mapping of *Lrrc32* mRNA (encoding Garp) in mouse LN SCS with hybridization. (**a**) mRNA detection by RNAscope of *Prox1* mRNA (white), *Lrrc32* mRNA (red) coupled with Lyve-1 immunostaining on mouse cervical LN with a focus on the SCS area in the control condition and (**b**) metastatic LN 3 weeks after B16F10 transplantation. Scale bar = 25 μm.
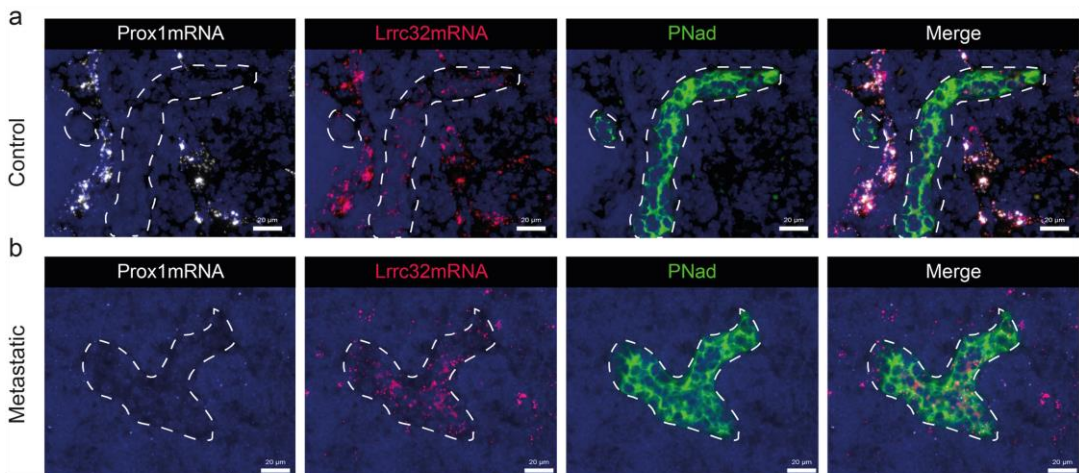
Figure 8. *Lrrc32* (encoding Garp) mRNA is expressed in HEV in mouse LN detected by hybridization. (**a**) mRNA detection by RNAscope of *Prox1* mRNA (white), *Lrrc32* mRNA (red) coupled with PNAd (HEV, in green) immunostaining on mouse cervical LN in control and (**b**) a metastatic LN 3 weeks after B16F10 transplantation conditions. The dashed line highlights HEV vessel sections. Scale bar = 20 μm.
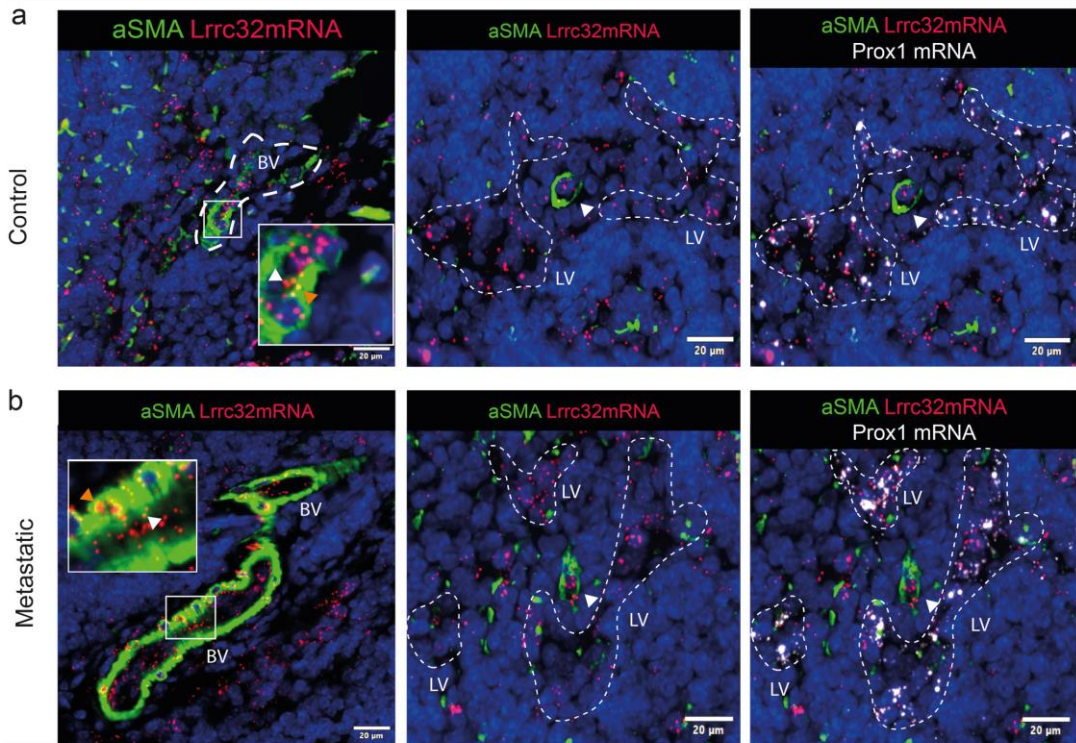
Figure 9. *Lrrc32* (encoding Garp) is expressed in blood and lymphatic vessels in mouse LN detected by hybridization. (**a**) mRNA detection by RNAscope of *Prox1* mRNA (white), *Lrrc32* mRNA (red) coupled with αSMA (in red), and CD31 (in pink) immunostaining on mouse cervical LN in control and (**b**) a metastatic LN 3 weeks after B16F10 transplantation conditions. The dashed line highlights the lymphatic vessel network. LV: lymphatic vessel, BV: blood vessel. White arrowheads show blood endothelial cells inside the vessel, and orange arrowheads indicate perivascular cells (PvCs). Scale bar = 20 μm.

We thus mapped the expression of *Lrrc32* mRNA in mouse LNs (Figures 5 and 8) and found *Lrrc32* expression in the lymphatic network (*Prox1*+/Lyve1+) of the SCS (including the ceiling and floor) and the parenchymal areas, as well as in perivascular αSMA+ cells around blood and lymphatic vessels.

4. Discussion

The originality of our study relies on investigating *LRRC32* mRNA and GARP protein expression in non-Treg cells in LN metastases, rather than in primary tumors. GARP was reported to mediate TGF-β1 activation and immunosuppression by Tregs in tumor-bearing mice, as blocking antibodies against GARP:TGF-β1 complexes induced regressions of tumors otherwise resistant to anti-PD-1 immunotherapy [40]. A Foxp3–GARP–TGF-β axis was proposed to represent an important signaling pathway in the primary tumor microenvironment for different types of cancer [41]. GARP is thus a target of interest for immunotherapeutic approaches. A blocking anti-GARP:TGF-β1 mAb, which blocks the release of active TGF-β1 without inducing an antibody-dependent cellular toxicity (ADCC)- or antibody-dependent cellular phagocytosis (ADCP)-mediated depletion of GARP expressing cells, is currently tested in clinical trials in patients with advanced or metastatic solid tumors (NCT03821935 and NCT05822752). Yet, GARP expression in LNs

has received very little attention despite the important role of this organ in the elaboration of the immune response. To fill this gap, we examined *LRRC32* and GARP expression by non-immune cells, including endothelial cells constituting different vascular structures (LECs, BECs, and HEVs) and fibroblastic/reticular cells forming a mesh of collagen fibers. Our observations that these non-immune and non-cancerous cells in metastatic LNs can express GARP may suggest that antibodies blocking TGF-β1 activation without inducing the depletion of GARP-expressing cells might bear less risks of undesired side effects that could be associated with a reduction in Treg numbers and destruction of vascular structures.

Our study has some limitations related to technical issues. First, anti-human GARP mAbs are suitable for staining frozen tissue sections but not on formalin-treated paraffin-embedded sections. This restricts analyses to a limited number of human tissue samples. Second, we lack an anti-murine GARP mAb that is suitable for IHC analyses in the pre-clinical model. We overcame this difficulty by conducting in situ mRNA hybridization to detect *Lrrc32* using the RNAscope approach, combined with multiple immunostainings of other markers, but this did not allow for quantitative analyses. Third, the depth of scRNA-Seq makes it possible to visualize only the most highly expressed genes in each cluster, and GARP appeared expressed at a low level in non-immune cells.

Recently, scRNA-Seq analyses have highlighted the heterogeneity of endothelial and fibroblastic cells in LNs [30–32,34]. This holds particularly true for human LECs. Indeed, human LECs were separated into eight different subtypes, among which three subtypes are located in the SCS, namely ceiling LECs (cLECs), floor LECs (fLECs), and bridge LECs (bLECs) located between cLECs and fLECS [31]. These scRNA-Seq data revealed very low levels or no *LRRC32* expression by all the different LEC subpopulations. In contrast, GARP expression at the protein level was found around lymphatic vessels (CD34-, PDPN+) in human samples. It is worth noting that protein GARP was detected in both fLECs and cLECs in the SCS. In the murine scRNA-Seq dataset, mRNA *Lrrc32* was detected in the LEC I cluster corresponding to ceiling, collector, and valve LECs. *Lrrc32* mRNA expression in murine LECs was confirmed by RNAscope imagery (Prox1+/Lrrc32+ cells) in both parenchymal LECs and in the SCS. Lrcc32 mRNA was found in Lyve1^{low}/Prox1+ cLECs and Lyve1+/Prox1+ fLECs, delineating the SCS. This is in line with the data obtained with human LN tissue sections. The cLECs expressed several matrix proteins deposited close to the collagenous matrix of the LN capsule [40]. It is currently considered that fLECs could serve as a receptive surface for antigen-presenting cells entering the SCS by the afferent lymph [42]. Our data raise the possibility that GARP plays a role in the SCS, a specialized area of the LN involved in the entrance of immune and/or cancer cells, as well as soluble tumor antigens derived from the primary tumor. The apparent discrepancy between the scRNA-Seq data (lack or faint Lrrc32 mRNA detection in LECs) and LN tissue section analysis (IHC and RNAscope revealing GARP and Lrrc32 expression in LECs, respectively) may be related, at least, to the sequencing depth of the datasets.

The analyses of the human and murine scRNA-Seq datasets confirmed the known *LRRC32/Lrcc32* expression by BECs [21,25] and revealed expression by different types of BECs forming large arteries and veins, capillaries, and HEVs. Accordingly, our IHC analyses performed on human and murine tissue samples confirmed the expression of protein GARP by BECs (CD34+/PDPN− in human, CD31+/Prox1− in mice). In line with previous studies [21,25], we also confirmed the expression of the *LRRC32* mRNA and the presence of the GARP protein at the surface of human BECs primary cells (HUVECs). Interestingly, we provide for the first time evidence for GARP expression in PNAd+ HEVs in human and mouse samples. These specialized vessels are involved in the entrance of circulating lymphocytes in the LN and the exit of metastatic cells from the LN to distant organs [8,9]. The functional importance of HEV-associated GARP in the control of immune responses and in the metastatic process is still to be elucidated. GARP in HEVs could play a role in the escape of metastatic cells from immune surveillance.

A striking finding from scRNA-Seq data mining is the detection of a particular subpopulation of perivascular cells (PvCs) expressing ITGA7, αSMA, and GARP. Integrin α7β1,

comprising ITGA7 and the ITGB1 subunit, is the primary receptor for laminin on skeletal myoblasts and adult myofibers [43]. It is also produced by vascular smooth muscle cells. Notably, α7 null mice that survive to birth exhibit vascular smooth muscle defects [44]. In our IHC analyses of LNs, we found only a few perivascular cells positive for ITGA7. In sharp contrast, an important population of αSMA+ cells surrounding blood vessels was detected and they expressed GARP. These perivascular cells are likely pericytes and/or smooth muscle cells. This perivascular distribution of GARP around blood vessels is intriguing and raises the question of the function of GARP in these areas. One could postulate that GARP exerts a "shielding" role around vessels involved in the entrance and/or exit of immune/metastatic cells.

The sometimes-extended GARP immunoreactivity in the extracellular matrix surrounding vessels (particularly blood vessels) suggests that fibroblastic cells also contribute to GARP production. Accordingly, we found GARP expression by human primary lymphatic fibroblasts (HLFs) in culture. Notably, GARP staining was also detected in parenchymal fibroblastic cells. The presence of GARP in the cLECs adjacent to the LN capsule, together with GARP expression by matrix-associated αSMA+ cells in the parenchyma, points to a putative relationship between GARP and matrix-producing cells. Although the *Lrrc32* mRNAs were detected by RNAscope in those cells, we cannot exclude the possibility that a soluble form of GARP (sGARP) is shed from the surface of these cells or other surrounding cells and deposited in the ECM. The shedding of sGARP from the cell surface of Tregs and platelets has been previously reported [45], and sGARP was reported to exert immunosuppressive properties [21]. The matrix could thus constitute a reservoir for sGARP bound to latent TGF-β1, which could be released during tissue remodeling associated with inflammatory and metastatic processes. However, whether active TGF-β1 can be released from sGARP:TGF-β1 complexes stored in the matrix is speculative and remains to be demonstrated. Indeed, the GARP transmembrane domain and anchorage of GARP:TGF-β1 complexes at the cell surface were shown to be required for TGF-β1 activation by integrins [46]. One cannot exclude TGF-β-independent functions for sGARP in the matrix.

Our data support the concept that GARP could mediate functions of cells other than Tregs [21]. Activated B cells and platelets were reported to express GARP:TGF-β1 complexes and produce active TGF-β1 in a GARP-dependent manner [23,47,48]. In mice, the GARP:TGF-β1 axis in B cells was shown to be a key factor for immune tolerance and the prevention of lupus-like autoimmune diseases [49] and, in platelets, it was shown to play a role in the immune evasion of cancer cells [47]. In multipotent mesenchymal stromal cells (MSCs), GARP was shown to be involved in their resistance to DNA damage and apoptosis in a TGF-β1 dependent manner, as well as in their immunomodulatory activities [50]. Finally, it was recently shown that GARP expressed on hepatic stellate cells drives the development of liver fibrosis via the activation of latent TGF-β1 [24].

The use of cell-specific *Lrrc32* KO mice provided evidence that targeting Garp on Tregs, but not on platelets, with a blocking anti-GARP:TGF-β1 antibody induced tumor regression and overcame resistance to PD1 blockade in tumor-bearing mice [40]. Indeed, the blocking anti-GARP:TGF-β1 mAb exerted anti-tumor efficacy in platelets-specific *Lrrc32* KO mice, but lost its activity in Tregs-specific *Lrrc32* KO mice. The activity of TGF-β1 produced by GARP-expressing Tregs was thus required for anti-GARP:TGF-β1 to exert anti-tumor activity. These findings also suggested that blocking the action of TGF-β1 emanating from GARP-expressing platelets or endothelial cells was neither necessary nor sufficient, at least for primary tumor progression. In vitro, under basal culture conditions, GARP and the αVβ6 and αVβ8 integrins were detected at the surface of HUVECs, LECs, and HLFs by flow cytometry. Despite several attempts in different experimental settings, we failed to observe TGF-β1 activation in BEC, HLF, and LEC cultures. This is in line with the previous study of Bertrand et al. [25]. Thus, functional studies remain essential to determine the GARP function, if any, in endothelial and fibroblastic cells in LNs. Due to the high levels of GARP protein detected in the LNs, one is expecting a function(s) that remain(s) to be determined.

5. Conclusions

The identity, spatial distribution, and cellular sources of GARP-expressing cells in normal and metastatic LNs have remained elusive. Here, we provide the first mapping of GARP expression in human and murine metastatic LNs. In addition to confirming GARP expression in BECs and Tregs in LNs, our data provide striking evidence for GARP production by specialized LEC subtypes in the SCS (cLECs and fLECs) in HEVs and matrix-associated (fibroblastic/perivascular) cells. Our findings suggest a role for GARP in two vascular structures localized at the interface between the LN and the afferent/blood vessels, as well as in matrix-associated cells, that is worth considering for future studies.

Appendix A

Figure A1. Full scans of Western blot images shown in Figure 2a. (**a**) Western blot membrane of GARP in Jurkat hGARP used as a positive control. The red rectangle corresponds to the first lane in Figure 2a. (**b**) Western blot membrane of GARP on HUVECs, LECs, and HLFs in which the red rectangle corresponds to the right part of Western blot shown in Figure 2a.
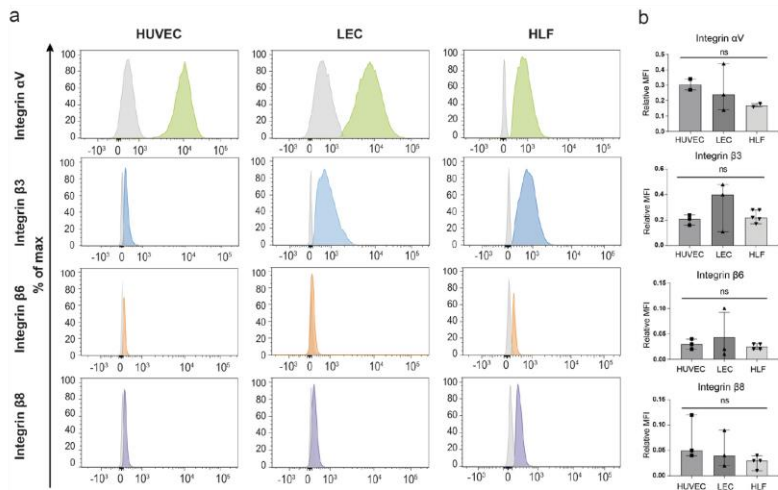
Figure A2. Evaluation of GARP integrins partners in HUVEC, LEC, and HLF cells cultured in basal condition. (**a**) Flow cytometric analyses were conducted to evaluate the expression of αV (green), β3 (blue), β6 (orange), and β8 (purple) integrins in the different cells. The isotype control is depicted in grey, and positive signals for each integrin are shown in color (described above) as a percentage of the maximum. (**b**) The relative MFI is represented with a bar graph for each integrin shown on the left panel; n is at least equal to 4 (n $\geq$ 4, means $\pm$ SD, n.s, no significance, determined by one−way ANOVA).
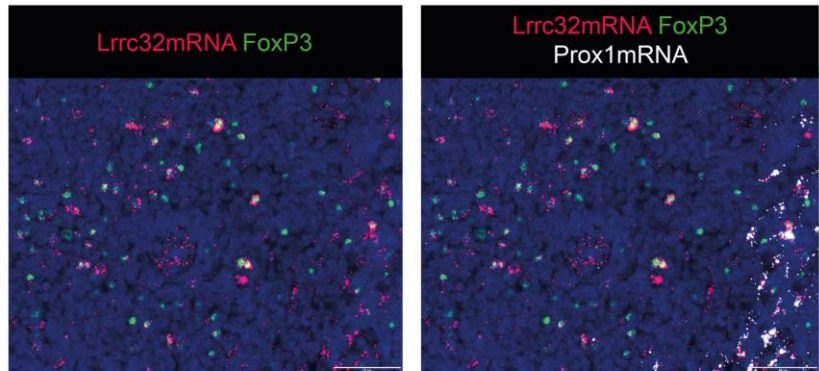
Figure A3. Lrrc32mRNA (Garp) and Prox1mRNA expression by RNAscope coupled with FoxP3 immunostaining as a control in Tregs cells. Scale bar = 50 µm.
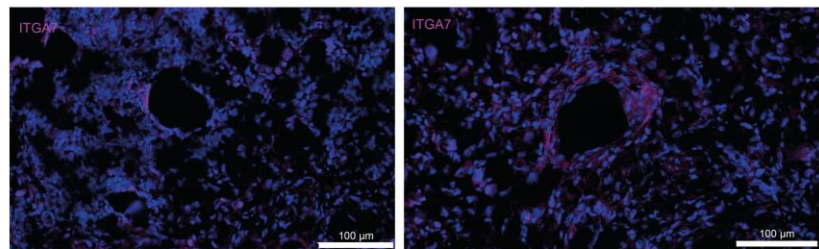
Figure A4. Immunostaining ITGA7 (pink) in human LN samples. Scale bar = 100 µm.

References

1. Chatterjee, G.; Pai, T.; Hardiman, T.; Avery-Kiejda, K.; Scott, R.J.; Spencer, J.; Pinder, S.E.; Grigoriadis, A. Molecular Patterns of Cancer Colonisation in Lymph Nodes of Breast Cancer Patients. *Breast Cancer Res.* **2018**, *20*, 143. [CrossRef] [PubMed]
2. Balsat, C.; Blacher, S.; Herfs, M.; Van de Velde, M.; Signolle, N.; Sauthier, P.; Pottier, C.; Gofflot, S.; De Cuypere, M.; Delvenne, P.; et al. A Specific Immune and Lymphatic Profile Characterizes the Pre-Metastatic State of the Sentinel Lymph Node in Patients with Early Cervical Cancer. *Oncoimmunology* **2017**, *6*, e1265718. [CrossRef] [PubMed]
3. Wakisaka, N.; Hasegawa, Y.; Yoshimoto, S.; Miura, K.; Shiotani, A.; Yokoyama, J.; Sugasawa, M.; Moriyama-Kita, M.; Endo, K.; Yoshizaki, T. Primary Tumor-Secreted Lymphangiogenic Factors Induce Pre-Metastatic Lymphvascular Niche Formation at Sentinel Lymph Nodes in Oral Squamous Cell Carcinoma. *PLoS ONE* **2015**, *10*, e0144056. [CrossRef] [PubMed]
4. Tammela, T.; Alitalo, K. Lymphangiogenesis: Molecular Mechanisms and Future Promise. *Cell* **2010**, *140*, 460–476. [CrossRef] [PubMed]
5. Maus, R.L.G.; Jakub, J.W.; Hieken, T.J.; Nevala, W.K.; Christensen, T.A.; Sutor, S.L.; Flotte, T.J.; Markovic, S.N. Identification of Novel, Immune-Mediating Extracellular Vesicles in Human Lymphatic Effluent Draining Primary Cutaneous Melanoma. *OncoImmunology* **2019**, *8*, e1667742. [CrossRef] [PubMed]
6. Cho, J.K.; Hyun, S.H.; Choi, N.; Kim, M.J.; Padera, T.P.; Choi, J.Y.; Jeong, H.S. Significance of Lymph Node Metastasis in Cancer Dissemination of Head and Neck Cancer. *Transl. Oncol.* **2015**, *8*, 119–125. [CrossRef] [PubMed]
7. Stacker, S.A.; Williams, S.P.; Karnezis, T.; Shayan, R.; Fox, S.B.; Achen, M.G. Lymphangiogenesis and Lymphatic Vessel Remodelling in Cancer. *Nat. Rev. Cancer* **2014**, *14*, 159–172. [CrossRef]
8. Brown, M.; Assen, F.P.; Leithner, A.; Abe, J.; Schachner, H.; Asfour, G.; Bago-Horvath, Z.; Stein, J.V.; Uhrin, P.; Sixt, M.; et al. Lymph Node Blood Vessels Provide Exit Routes for Metastatic Tumor Cell Dissemination in Mice. *Science* **2018**, *359*, 1408–1411. [CrossRef]
9. Padera, T.P.; Meijer, E.F.J.; Munn, L.L. The Lymphatic System in Disease Processes and Cancer Progression. *Annu. Rev. Biomed. Eng.* **2016**, *18*, 125–158. [CrossRef]
10. Sleeman, J.P. The Lymph Node Pre-Metastatic Niche. *J. Mol. Med.* **2015**, *93*, 1173–1184. [CrossRef]
11. Kaplan, R.N.; Riba, R.D.; Zacharoulis, S.; Bramley, A.H.; Vincent, L.; Costa, C.; MacDonald, D.D.; Jin, D.K.; Shido, K.; Kerns, S.A.; et al. VEGFR1-Positive Haematopoietic Bone Marrow Progenitors Initiate the Pre-Metastatic Niche. *Nature* **2005**, *438*, 820–827. [CrossRef] [PubMed]
12. Peinado, H.; Zhang, H.; Matei, I.R.; Costa-Silva, B.; Hoshino, A.; Rodrigues, G.; Psaila, B.; Kaplan, R.N.; Bromberg, J.F.; Kang, Y.; et al. Pre-Metastatic Niches: Organ-Specific Homes for Metastases. *Nat. Rev. Cancer* **2017**, *17*, 302–317. [CrossRef] [PubMed]

13. Psaila, B.; Lyden, D. The Metastatic Niche: Adapting the Foreign Soil. *Nat. Rev. Cancer* **2009**, *9*, 285–293. [CrossRef] [PubMed]
14. Hirakawa, S.; Kodama, S.; Kunstfeld, R.; Kajiya, K.; Brown, L.F.; Detmar, M. VEGF-A Induces Tumor and Sentinel Lymph Node Lymphangiogenesis and Promotes Lymphatic Metastasis. *J. Exp. Med.* **2005**, *201*, 1089–1099. [CrossRef] [PubMed]
15. Hirakawa, S.; Brown, L.F.; Kodama, S.; Paavonen, K.; Alitalo, K.; Detmar, M. VEGF-C–Induced Lymphangiogenesis in Sentinel Lymph Nodes Promotes Tumor Metastasis to Distant Sites. *Blood* **2007**, *109*, 1010–1017. [CrossRef] [PubMed]
16. Gillot, L.; Lebeau, A.; Baudin, L.; Pottier, C.; Louis, T.; Durré, T.; Longuespée, R.; Mazzucchelli, G.; Nizet, C.; Blacher, S.; et al. Periostin in Lymph Node Pre-Metastatic Niches Governs Lymphatic Endothelial Cell Functions and Metastatic Colonization. *Cell. Mol. Life Sci.* **2022**, *79*, 295. [CrossRef] [PubMed]
17. De Streel, G.; Lucas, S. Targeting Immunosuppression by TGF-B1 for Cancer Immunotherapy. *Biochem. Pharmacol.* **2021**, *192*, 114697. [CrossRef]
18. Travis, M.A.; Sheppard, D. TGF-β Activation and Function in Immunity. *Annu. Rev. Immunol.* **2014**, *32*, 51–82. [CrossRef]
19. Liénart, S.; Merceron, R.; Vanderaa, C.; Lambert, F.; Colau, D.; Stockis, J.; Van Der Woning, B.; De Haard, H.; Saunders, M.; Coulie, P.G.; et al. Structural Basis of Latent TGF-B1 Presentation and Activation by GARP on Human Regulatory T Cells. *Science* **2018**, *362*, 952–956. [CrossRef]
20. Cuende, J.; Liénart, S.; Dedobbeleer, O.; Van Der Woning, B.; De Boeck, G.; Stockis, J.; Huygens, C.; Colau, D.; Somja, J.; Delvenne, P.; et al. Monoclonal Antibodies against GARP/TGF-B1 Complexes Inhibit the Immunosuppressive Activity of Human Regulatory T Cells In Vivo. *Sci. Transl. Med.* **2015**, *7*, 284ra56. [CrossRef]
21. Zimmer, N.; Trzeciak, E.R.; Graefen, B.; Satoh, K.; Tuettenberg, A. GARP as a Therapeutic Target for the Modulation of Regulatory T Cells in Cancer and Autoimmunity. *Front. Immunol.* **2022**, *13*, 928450. [CrossRef] [PubMed]
22. Tran, D.Q.; Andersson, J.; Wang, R.; Ramsey, H.; Unutmaz, D.; Shevach, E.M. GARP (LRRC32) Is Essential for the Surface Expression of Latent TGF-Beta on Platelets and Activated FOXP3+ Regulatory T Cells. *Proc. Natl. Acad. Sci. USA* **2009**, *106*, 13445–13450. [CrossRef] [PubMed]
23. Dedobbeleer, O.; Stockis, J.; Van Der Woning, B.; Coulie, P.G.; Lucas, S. Cutting Edge: Active TGF-B1 Released from GARP/TGF-B1 Complexes on the Surface of Stimulated Human B Lymphocytes Increases Class-Switch Recombination and Production of IgA. *J. Immunol.* **2017**, *199*, 391–396. [CrossRef] [PubMed]
24. Zhang, X.; Sharma, P.; Maschmeyer, P.; Hu, Y.; Lou, M.; Kim, J.; Fujii, H.; Unutmaz, D.; Schwabe, R.F.; Winau, F. GARP on Hepatic Stellate Cells Is Essential for the Development of Liver Fibrosis. *J. Hepatol.* **2023**, *79*, 1214–1225. [CrossRef] [PubMed]
25. Bertrand, C.; Van Meerbeeck, P.; De Streel, G.; Vaherto-Bleeckx, N.; Benhaddi, F.; Rouaud, L.; Noël, A.; Coulie, P.G.; Van Baren, N.; Lucas, S. Combined Blockade of GARP:TGF-B1 and PD-1 Increases Infiltration of T Cells and Density of Pericyte-Covered GARP+ Blood Vessels in Mouse MC38 Tumors. *Front. Immunol.* **2021**, *12*, 704050. [CrossRef] [PubMed]
26. Vermeersch, E.; Denorme, F.; Maes, W.; De Meyer, S.F.; Vanhoorelbeke, K.; Edwards, J.; Shevach, E.M.; Unutmaz, D.; Fujii, H.; Deckmyn, H.; et al. The Role of Platelet and Endothelial GARP in Thrombosis and Hemostasis. *PLoS ONE* **2017**, *12*, e0173329. [CrossRef] [PubMed]
27. Gillot, L.; Baudin, L.; Rouaud, L.; Kridelka, F.; Noël, A. The Pre-Metastatic Niche in Lymph Nodes: Formation and Characteristics. *Cell. Mol. Life Sci.* **2021**, *78*, 5987–6002. [CrossRef]
28. Miyasaka, M.; Hata, E.; Tohya, K.; Hayasaka, H. Lymphocyte Recirculation. In *Encyclopedia of Immunobiology*; Elsevier: Amsterdam, The Netherlands, 2016; pp. 486–492. ISBN 978-0-08-092152-5.
29. Acton, S.E.; Onder, L.; Novkovic, M.; Martinez, V.G.; Ludewig, B. Communication, Construction, and Fluid Control: Lymphoid Organ Fibroblastic Reticular Cell and Conduit Networks. *Trends Immunol.* **2021**, *42*, 782–794. [CrossRef]
30. Rodda, L.B.; Lu, E.; Bennett, M.L.; Sokol, C.L.; Wang, X.; Luther, S.A.; Barres, B.A.; Luster, A.D.; Ye, C.J.; Cyster, J.G. Single-Cell RNA Sequencing of Lymph Node Stromal Cells Reveals Niche-Associated Heterogeneity. *Immunity* **2018**, *48*, 1014–1028.e6. [CrossRef]
31. Abe, Y.; Sakata-Yanagimoto, M.; Fujisawa, M.; Miyoshi, H.; Suehara, Y.; Hattori, K.; Kusakabe, M.; Sakamoto, T.; Nishikii, H.; Nguyen, T.B.; et al. A Single-Cell Atlas of Non-Haematopoietic Cells in Human Lymph Nodes and Lymphoma Reveals a Landscape of Stromal Remodelling. *Nat. Cell Biol.* **2022**, *24*, 565–578. [CrossRef]
32. Takeda, A.; Hollmén, M.; Dermadi, D.; Pan, J.; Brulois, K.F.; Kaukonen, R.; Lönnberg, T.; Boström, P.; Koskivuo, I.; Irjala, H.; et al. Single-Cell Survey of Human Lymphatics Unveils Marked Endothelial Cell Heterogeneity and Mechanisms of Homing for Neutrophils. *Immunity* **2019**, *51*, 561–572.e5. [CrossRef] [PubMed]
33. Xiang, M.; Grosso, R.A.; Takeda, A.; Pan, J.; Bekkhus, T.; Brulois, K.; Dermadi, D.; Nordling, S.; Vanlandewijck, M.; Jalkanen, S.; et al. A Single-Cell Transcriptional Roadmap of the Mouse and Human Lymph Node Lymphatic Vasculature. *Front. Cardiovasc. Med.* **2020**, *7*, 52. [CrossRef] [PubMed]
34. Fujimoto, N.; He, Y.; D'Addio, M.; Tacconi, C.; Detmar, M.; Dieterich, L.C. Single-Cell Mapping Reveals New Markers and Functions of Lymphatic Endothelial Cells in Lymph Nodes. *PLoS Biol.* **2020**, *18*, e3000704. [CrossRef] [PubMed]
35. Li, L.; Shirkey, M.W.; Zhang, T.; Piao, W.; Li, X.; Zhao, J.; Mei, Z.; Guo, S.; Saxena, V.; Kensiski, A.; et al. Lymph Node Fibroblastic Reticular Cells Preserve a Tolerogenic Niche in Allograft Transplantation through Laminin A4. *J. Clin. Investig.* **2022**, *132*, e156994. [CrossRef] [PubMed]
36. Stockis, J.; Colau, D.; Coulie, P.G.; Lucas, S. Membrane Protein GARP Is a Receptor for Latent TGF-β on the Surface of Activated Human Treg: Cellular Immune Response. *Eur. J. Immunol.* **2009**, *39*, 3315–3322. [CrossRef] [PubMed]

37. Bankhead, P.; Loughrey, M.B.; Fernández, J.A.; Dombrowski, Y.; McArt, D.G.; Dunne, P.D.; McQuaid, S.; Gray, R.T.; Murray, L.J.; Coleman, H.G.; et al. QuPath: Open Source Software for Digital Pathology Image Analysis. *Sci. Rep.* **2017**, *7*, 16878. [CrossRef] [PubMed]

38. Chang, J.E.; Turley, S.J. Stromal Infrastructure of the Lymph Node and Coordination of Immunity. *Trends Immunol.* **2015**, *36*, 30–39. [CrossRef]

39. Van De Velde, M.; García-Caballero, M.; Durré, T.; Kridelka, F.; Noël, A. Ear Sponge Assay: A Method to Investigate Angiogenesis and Lymphangiogenesis in Mice. In *Proteases and Cancer*; Cal, S., Obaya, A.J., Eds.; Methods in Molecular Biology; Springer: New York, NY, USA, 2018; Volume 1731, pp. 223–233. ISBN 978-1-4939-7594-5.

40. De Streel, G.; Bertrand, C.; Chalon, N.; Liénart, S.; Bricard, O.; Lecomte, S.; Devreux, J.; Gaignage, M.; De Boeck, G.; Mariën, L.; et al. Selective Inhibition of TGF-B1 Produced by GARP-Expressing Tregs Overcomes Resistance to PD-1/PD-L1 Blockade in Cancer. *Nat. Commun.* **2020**, *11*, 4545. [CrossRef]

41. Lahimchi, M.R.; Eslami, M.; Yousefi, B. New Insight into GARP Striking Role in Cancer Progression: Application for Cancer Therapy. *Med. Oncol.* **2022**, *40*, 33. [CrossRef]

42. Jalkanen, S.; Salmi, M. Lymphatic Endothelial Cells of the Lymph Node. *Nat. Rev. Immunol.* **2020**, *20*, 566–578. [CrossRef]

43. Gerli, M.F.M.; Moyle, L.A.; Benedetti, S.; Ferrari, G.; Ucuncu, E.; Ragazzi, M.; Constantinou, C.; Louca, I.; Sakai, H.; Ala, P.; et al. Combined Notch and PDGF Signaling Enhances Migration and Expression of Stem Cell Markers While Inducing Perivascular Cell Features in Muscle Satellite Cells. *Stem Cell Rep.* **2019**, *12*, 461–473. [CrossRef] [PubMed]

44. Flintoff-Dye, N.L.; Welser, J.; Rooney, J.; Scowen, P.; Tamowski, S.; Hatton, W.; Burkin, D.J. Role for the A7β1 Integrin in Vascular Development and Integrity. *Dev. Dyn.* **2005**, *234*, 11–21. [CrossRef] [PubMed]

45. Hahn, S.A.; Stahl, H.F.; Becker, C.; Correll, A.; Schneider, F.-J.; Tuettenberg, A.; Jonuleit, H. Soluble GARP Has Potent Antiinflammatory and Immunomodulatory Impact on Human CD4+ T Cells. *Blood* **2013**, *122*, 1182–1191. [CrossRef] [PubMed]

46. Wang, R.; Zhu, J.; Dong, X.; Shi, M.; Lu, C.; Springer, T.A. GARP Regulates the Bioavailability and Activation of TGFβ. *Mol. Biol. Cell* **2012**, *23*, 1129–1139. [CrossRef] [PubMed]

47. Metelli, A.; Wu, B.X.; Riesenberg, B.; Guglietta, S.; Huck, J.D.; Mills, C.; Li, A.; Rachidi, S.; Krieg, C.; Rubinstein, M.P.; et al. Thrombin Contributes to Cancer Immune Evasion via Proteolysis of Platelet-Bound GARP to Activate LTGF-β. *Sci. Transl. Med.* **2020**, *12*, eaay4860. [CrossRef] [PubMed]

48. Lecomte, S.; Devreux, J.; de Streel, G.; van Baren, N.; Havelange, V.; Schröder, D.; Vaherto, N.; Vanhaver, C.; Vanderaa, C.; Dupuis, N.; et al. Therapeutic Activity of GARP:TGF-B1 Blockade in Murine Primary Myelofibrosis. *Blood* **2023**, *141*, 490–502. [CrossRef] [PubMed]

49. Wallace, C.H.; Wu, B.X.; Salem, M.; Ansa-Addo, E.A.; Metelli, A.; Sun, S.; Gilkeson, G.; Shlomchik, M.J.; Liu, B.; Li, Z. B Lymphocytes Confer Immune Tolerance via Cell Surface GARP-TGF-β Complex. *JCI Insight* **2018**, *3*, e99863. [CrossRef]

50. Carrillo-Gálvez, A.B.; Quintero, J.E.; Rodríguez, R.; Menéndez, S.T.; Victoria González, M.; Blanco-Lorenzo, V.; Allonca, E.; De Araújo Farias, V.; González-Correa, J.E.; Erill-Sagalés, N.; et al. GARP Promotes the Proliferation and Therapeutic Resistance of Bone Sarcoma Cancer Cells through the Activation of TGF-β. *Cell Death Dis.* **2020**, *11*, 985. [CrossRef]

Supplementary data - Spatial Distribution of Non-Immune Cells Expressing Glycoprotein A Repetitions Predominant in Human and Murine Metastatic Lymph Nodes (Rouaud L., Baudin L., *et al*. Cancers 2023)
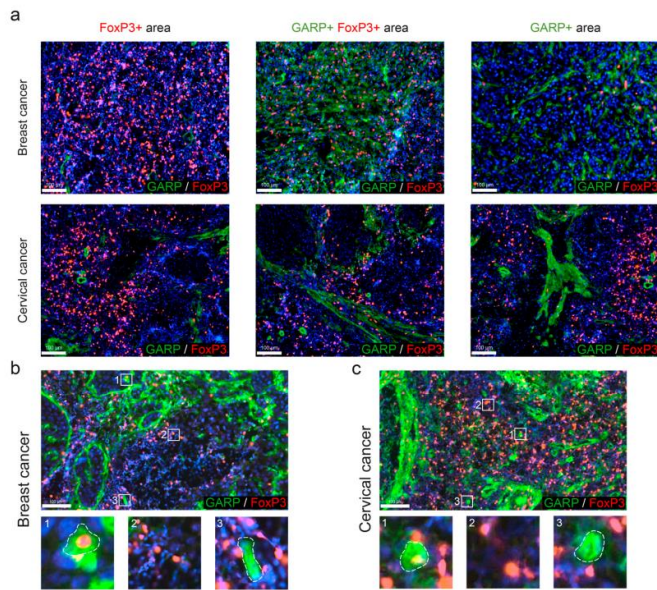
Figure S1. Multiplex immunofluorescence identifies GARP expression by Tregs and non-Tregs in human LN. (a) Dual-plex immunofluorescence staining of GARP (in green), FOXP3 (in red), and nuclei (DAPI, in blue) on MLN+ from patients with breast cancer or cervical cancer. (b, c) Focus on FoxP3/GARP pattern, scale bar = 100 μm and higher magnification of (1) GARP+/FOXP3 cells, (2) GARP-/FOXP3+ cells, and (3) GARP+/FOXP3- cells in (b) breast cancer or (c) cervical cancer.

2 GARP-dependent TGF-β1 activation in blood, lymphatic and fibroblast cells in vitro and in murine (pre)-metastatic niche

Question 2: Does the production of GARP protein allow the secretion of active TGF-β1 in non-immune cells?

2.1   Introduction

Our data presented in Part I revealed that besides the prominent expression of GARP by Tregs[280], GARP is also produced by other non-immune cell types in the LN of humans and mice at a metastatic stage. We provided the mapping of GARP on other non-immune cells including BECs forming blood vessels, HEVs, αSMA+ fibroblast cells in the ECM, around lymphatic vessels[348]. Whether these non-immune cells contribute to TGF-β1 activation and the anti-tumoral immune response remains to be determined.

This part of my thesis aimed to determine whether these cells expressing GARP could contribute to the secretion of active TGF-β1. Our in vitro study was first carried out to identify the contributors and partners of TGF-β1 activation in BECs and LECs, as well as in fibroblasts. Primary cells were used as in Part I. Through western blot analyses, immuno-histological staining and reporting cells TMLECs, we searched for the presence of active TGF-β1. If these primary cells studied in vitro show active TGF-β1 secretion, we could then hypothesize that these cell populations contribute to the establishment of an immunosuppressive environment. Thus, their secretion of active TGF-β1 could contribute to the escape of the immune system at the SCS level, at the stroma level or via the exit constituted by HEVs.

2.2   Materials and methods

a.   In Vitro Cell Culture

We used primary human dermal lymphatic microvascular endothelial cells (HMVEC-dLyAd, CC-2810, Lonza, Verviers, Belgium) and human umbilical vein endothelial cells (CC-2519A, Lonza, Verviers, Belgium), herein referred to as LECs and HUVEC, respectively. These cells were cultured as a monolayer in EGM2-MV medium (complete medium) (CC-3202 for LECs and CC-3162 for HUVEC, Lonza, Verviers, Belgium) until confluence. Primary human lymphatic fibroblasts (HLFs from ScienCell, #2530, Carlsbad,

CA, USA) were cultured in a complete fibroblast medium (FM, Cat. #2301, ScienCell) until confluence was achieved, according to the manufacturer's instructions. TMLEC cells were cultured in DMEM medium containing 10 % FBS and 1% of penicillin-streptomycin at 37°C with 5%CO_2. TMLEC cells were supplied by the team of Sophie Lucas (de Duve Institute, UCLouvain, Brussel, Belgium).

   b.   *Measure of active TGF-β1 using TMLEC reporting cells and recombinant TGF-β1*

TMLEC cells are transformed mink lung epithelial cells stably transfected with a cDNA construction containing a truncated and functional human PAI-1 promotor fused with the gene of luciferase. This model is based on the TGF-β1 pathway known to activate PAI-1[353]. The TMLEC cells express luciferase in response to active TGF-β1 and have been described as robust in measuring TGF-β1 activation[354,355]. TMLECs cells were stimulated with human recombinant TGF-β1 (#11409-BH, R&D Systems) at 5000 pg/mL as positive control or cultured with cells of interest. After the culture of TMLEC in a 96-well plate for 6 hours, with or without cells of interest for the desired time, the luciferase enzyme was released using cell lysis kit Bright-Glo (Bright-Glo™ Luciferase Assay System – E2650, Promega), including the luciferase substrate or luciferin and the luminescence was measured by a plate reader (**Fig. 20**).
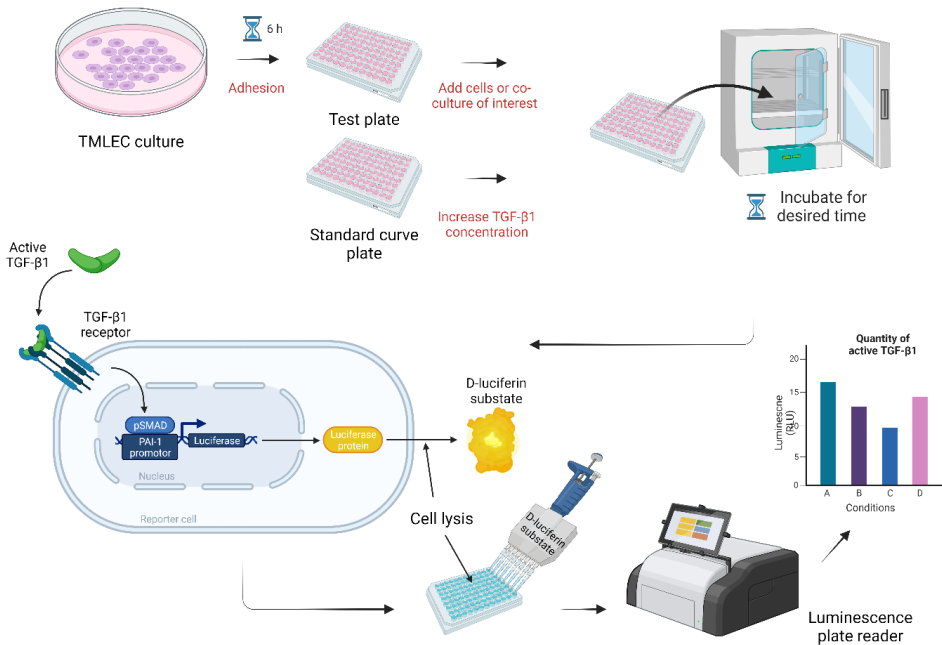
Figure 20. Explanatory protocol for measuring luminescence resulting from the release of active TGF-β1 using TMLEC reporter cells
(Description in the text)

c. Blocking antibodies

The blocking antibody 1D11.16.8 (#BE0057, InVivoMAb antimouse / human / rat / monkey/ hamster / canine / bovine TGF-β) was used in vitro and in vivo to block the action of all TGF-β isoformes.To block the complex GARP:TGF-β1, the clone MHG-8 was used in vitro on human primary cells, and clone 58A2 was used for in vivo experiments (all antibodies against the GARP:TGF-β1 complex were provided by the team of Sophie Lucas).

d. Western Blot

Cells were lysed with cell lysis buffer 1x composed of 20 mM Tris-HCl pH 7.5, 150 mM NaCl, 1 mM Na2EDTA, 1 mM EGTA, 1% Triton, 2.5 mM sodium pyrophosphate, 1 mM β-glycerophosphate, 1 mM Na3VO4, 1 µg/mL leupeptin (#9803, Cell Signaling, Danvers, MA, USA), and 1× protease/phosphatase inhibitor cocktail (Complete and phosSTOP, Roche, Indianapolis, IN, USA). Lysate samples were separated on acrylamide gels (10%) in a reducing condition with SDS at 20 µg/well and then transferred onto PVDF

transfer membranes (88518, ThermoScientific, Waltham, MA, USA). Membranes were probed by overnight incubation at 4 °C with the indicated antibodies followed by 1 h incubation at room temperature with horseradish peroxidase-coupled secondary antibody 1/2000 (Anti-mouse 7076 or anti-Rabbit 7074, Cell Signaling, Danvers, MA, USA) and enhanced chemiluminescent substrate (NEL104001EA, PerkinElmer, Waltham, MA, USA) using an Amersham ImageQuant 800 (GE Healthcare, Chicago, IL, USA). The following antibodies were used: GARP (1/1000; LRRC32 monoclonal antibody, Plato-1, ALX-804-867-C100, Enzo Life Sciences, Farmingdale, NY, USA), pSMAD2 (1/1000, #3108, Cell Signaling), pSMAD3 (1/1000, #9520, Cell Signaling), SMAD2 (#3122, Cell Signaling), SMAD3 (1/1000, #9523, Cell Signaling) and GAPDH (1/10,000; MAB 374, Millipore, Burlington, MA, USA).

e. *Ear-sponge assay model*

C57Bl6 female mice (6 to 8 weeks old) were used throughout this study. The animals were maintained under a 12 h light–dark cycle with free access to food and water. Gelatin sponges were incubated with tumor cells (2×10^5 B16F10 cells/sponge) or control medium (serum-free DMEM without tumor cells) for 30 min in serum-free-DMEM, embedded with collagen, and implanted into mouse ears as previously described [346,356]. Bioluminescence was detected in animals bearing ear sponges soaked with luciferase-expressing cells using the in vivo Imaging System IVIS 200 (Xenogen Corp.; Alameda, CA, USA). At the end of the experiment, the sponges and cervical LNs were harvested, incubated in 4% formol (11699408, VWR, Leuven, Belgium) for 16 h, dehydrated in ethanol, and fixed in paraffin (X881.2, Leica, Frankfurt, Germany).

2.3 Results

a. Study of LEC and HLF responses to the TGF-β1 stimulation

We first demonstrated the presence of GARP and integrins that can contribute to
the release of active TGF-β1 from the cell surface, by flow cytometry and western blot
analyses. We found that the primary cells used (LECs, HUVECs, and HLFs) expressed αVβ6
and αVβ8 integrins at their surface, two important GARP partners involved in TGF-β1
activation (**Fig. 21, Fig. A1 from part I**)[348].
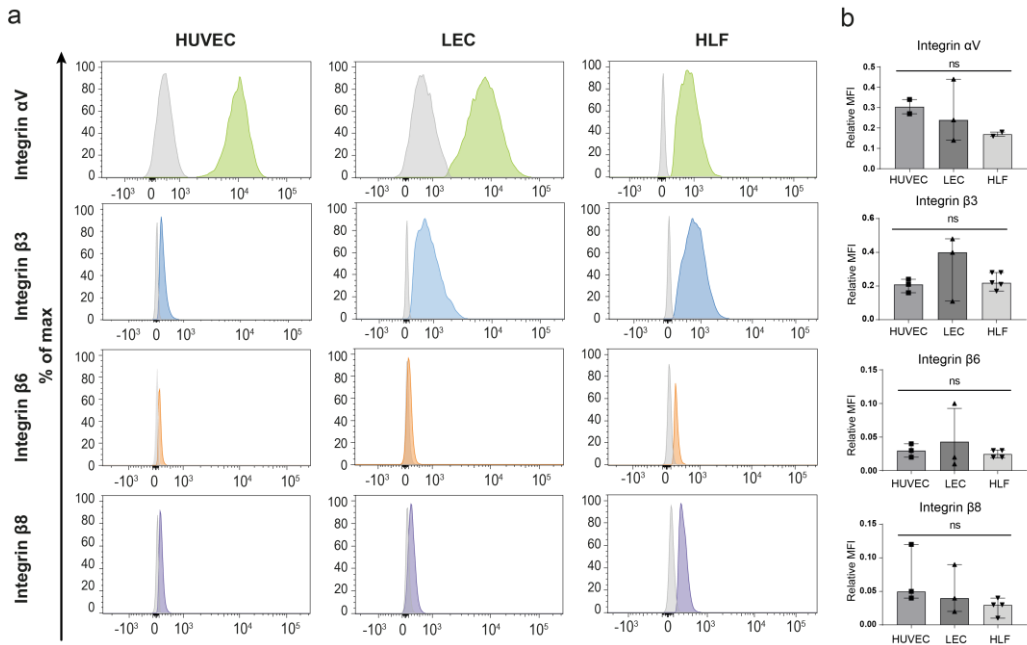
**Figure 21. Evaluation of GARP integrins partners in HUVEC, LEC, and HLF cells cultured in basal
condition**
(a) Flow cytometric analyses were conducted to evaluate the expression of αV (green), β3 (blue),
β6 (orange), and β8 (purple) integrins in the different cells. The isotype control is depicted in grey,
and positive signals for each integrin are shown in color (described above) as a percentage of the
maximum. (b) The relative MFI is represented with a bar graph for each integrin shown on the left
panel; n is at least equal to 4 (n ≥ 4, means ± SD, n.s, no significance, determined by one–way
ANOVA). (Figure A1 from the article in part I)

For the remainder of our study, HUVECs were no longer used, as the work carried
out by Charlotte Bertrand of Sophie Lucas' team showed no secretion of active TGF-β1

by these cells. Western blot analyses were conducted on LECs and HLFs to check whether these cells can respond to TGF-β1 stimulation (**Fig. 22**). The analyses were focused on the phosphorylation of two SMADs, SMAD2 and SMAD3, which were detected through western blot. Using recombinant TGF-β1 to stimulate both LECs and HLFs, we showed that both cell types responded to the stimulation. Furthermore, using a TGF-β blocking antibody (clone 1D11) significantly decreased the amount of phosphorylated SMAD2 and SMAD3 (pSMAD2/3) and thus the activation of the pathway. These data indicate that fibroblasts and LECs express two integrin partners of GARP and can respond to TGF-β1 stimulation.
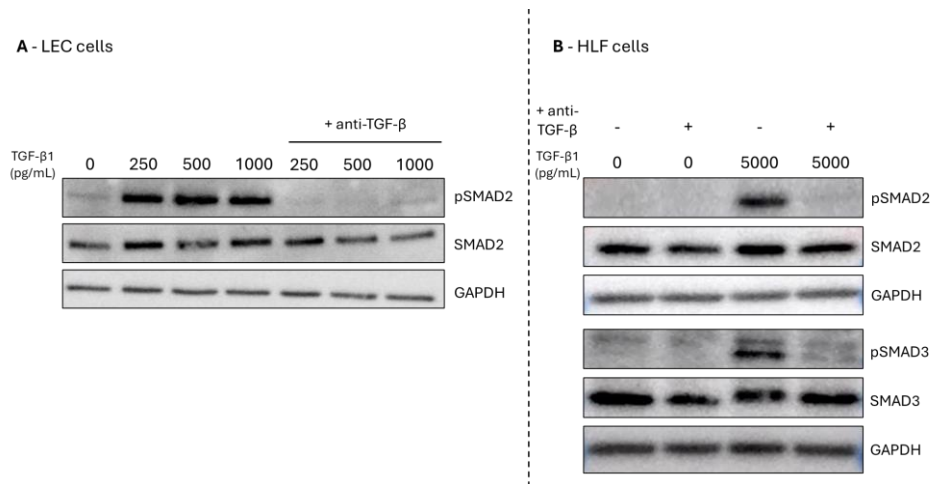
Figure 22. Evaluation of pSMAD2/3 in LEC and HLF cells cultured with or without recombinant TGF-β1
Western blot analysis of pSMAD2 was performed on LECs cells after stimulation with recombinant TGF-β1 at 250 to 1000 pg/mL or pSMAD2/3 on HLFs cells after stimulation with recombinant TGF-β1 at 5000 pg/mL with or without the presence of an anti-TGF-β antibody (clone 1D11).

b. Analysis of the release of active TGF-β1 by HLF and LEC cells in monoculture and co-culture

First, we cultured LEC, HUVEC, and HLF cells alone in the presence of TMLEC reporter cells. In this assay, we tested whether these primary cells alone could secrete active TGF-β1. This technique proved very specific for TGF-β1 by adding recombinant TGF-β1 to the TMLECs alone, where a luminescence of approximately 1000 RLU was detected

compared with unstimulated cells. In addition, the use of the anti-TGF-β blocking antibody 1D11 results in a decrease in luminescence to a level without stimulation. Each cell type used alone and confronted with reporter cells failed to activate TGF-β1, as luminescence was identical to that detected without TGF-β1 stimulation. We also observed the same result using a GARP-blocking antibody (MHG-8) known to block the release of active TGF-β1 in vitro in a GARP-dependent manner. The fact that we do not observe the presence of active TGF-β1 using cells alone in vitro might suggest that a necessary partner in this activation may be missing (**Fig. 23**).
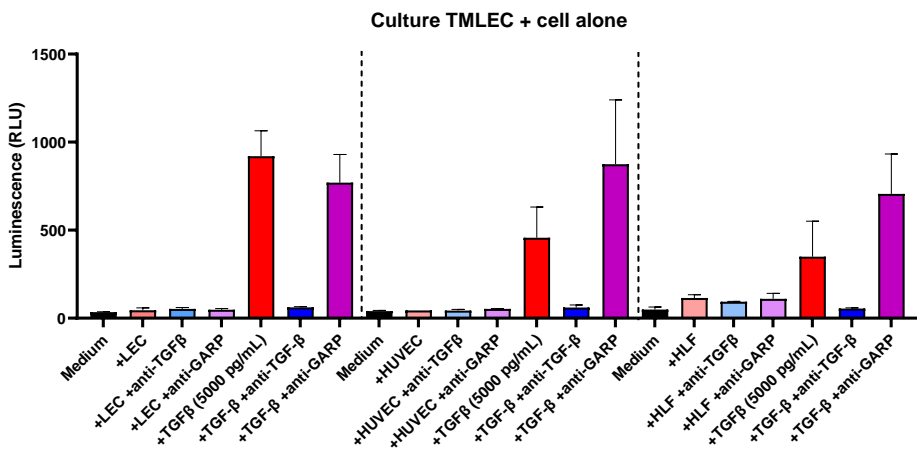
Figure 23. Culture of primary cells with the TMLEC reporting cells
Human LEC, HUVEC, and HLF were co-cultured with reporter TMLEC alone, stimulated by recombinant TGF-β1 (5000pg/mL) in the presence or absence of anti-TGF-β1 (1D11) or anti-GARP (MHG-8) antibody. After 24 hours, luciferase activity is assessed by adding Bright-Glo, and the luminescence signal is quantified using a luminescence plate reader. Each condition was tested in triplicate. Bars represent the mean. Error bars represent standard deviation (n=2).

We postulated that the missing partners could be 1) another cell type expressing the integrins that could contribute to TGF-β1 activation in a paracrine manner or 2) an extracellular matrix protein that could control GARP or integrin conformation at the cell surface. (**Fig. 24**).
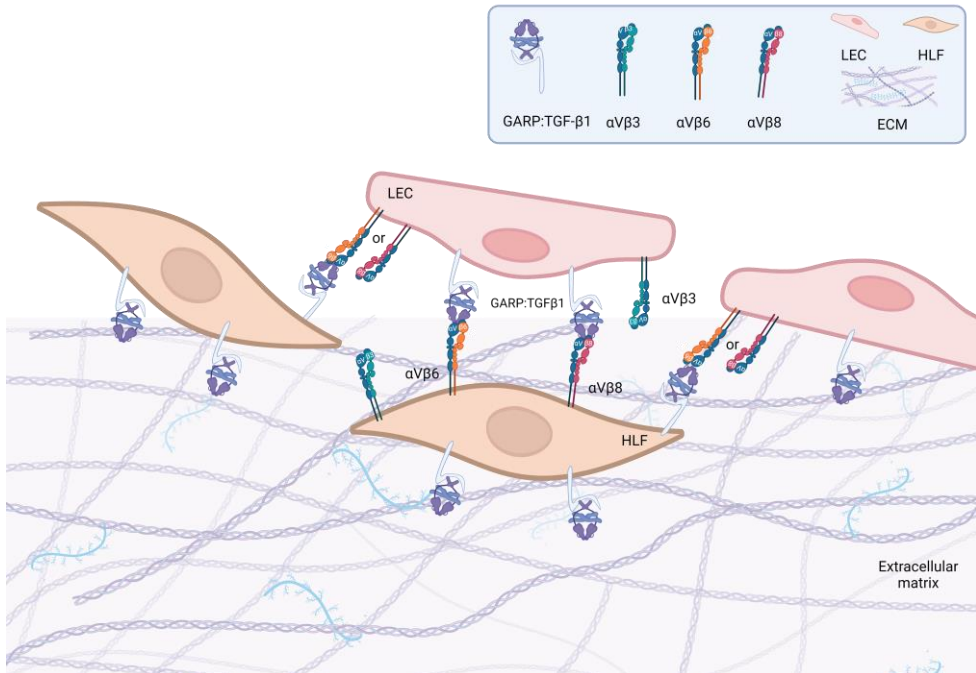
Figure 24. Working hypothesis of the interaction between LEC and HLF cells or the extracellular matrix components
Representation of the expression of GARP at the surface of HLF and LECs, and the possible cooperation between them. We postulate that interaction between both these cells can contribute to the release of TGF-β from GARP-expressing cells.

We conducted co-culture assays by combining LECs and HLFs in the presence of reporting cells TMLECs. In this test, an anti-TGF-β antibody decreased the positive control from 4200 to 1500 RLU in luminescence. While a slight luminescence was detected in the co-culture condition between LEC and HLF, it was not inhibited by anti-TGF-β or anti-GARP (MHG-8). These assays did not reveal any collaboration between the two cell types in TGF-β1 activation (**Fig. 25**). So far, we have not tested the combination of HUVECs and HLFs, despite a possible interaction given their production of GARP and the necessary integrin partners. It would be worth performing co-cultures between these two cell types with TMLECs to evaluate active TGF-β or no active TGF-β and confirm the results of Charlotte Bertrand on HUVECs.

tMLEC test (co-culture LEC/HLF)
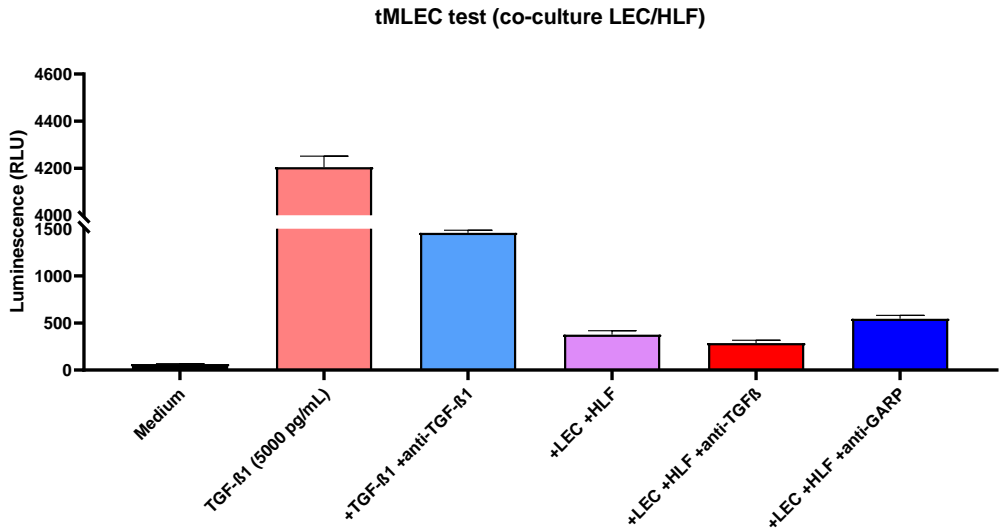
Figure 25. Co-cultures between LEC and HLF is not able to activate TGF-β1
Human LEC and HLF were co-cultured with reporter TMLEC, in the presence or absence of anti-TGF-β1 (1D11) or anti-GARP (MHG-8) antibody. After 24 hours, luciferase activity is assessed by the addition of Bright-Glo, and the luminescence signal is quantified using a luminescence plate reader. Each condition was tested in triplicate. Bars represent the mean. Error bars represent standard deviation (n=2).

We next addressed the possibility that ECM components could play a role in TGF-β1 activation and the modulation of GARP/TGF-β1 and/or integrin interaction at the cell surface. Different tests were carried out using two different types of coating: collagen I and periostin. Collagen I is found in the fibrous meshwork of LNs, as well as periostin. In addition, the periostin has been demonstrated in our laboratory for its involvement in the LN remodeling[357] (**Annex 2**). LEC or HLF cells were grown in the presence of both TMLEC and Coll I or periostin coating (**Fig. 26**). The monoculture of LEC and HLF led to similar results with or without collagen coating. Moreover, POSTN appeared to block the action of TGF-β1, the latter possibly being trapped by periostin. Thus, these two matrix components failed to modulate TGF-β1 activation by LEC or HLF.

RESULTS

tMLEC (LEC with coating)

tMLEC (HLF with coating)
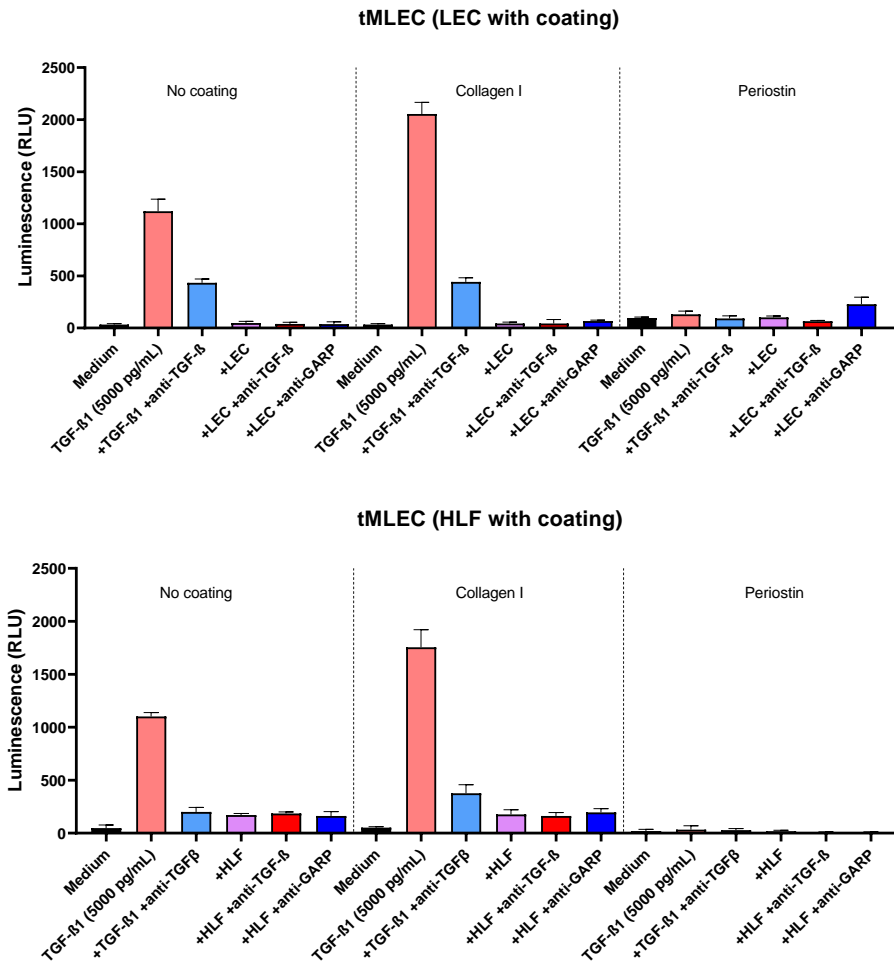
Figure 26. Human primary cells LEC, HUVEC and HLF are not able to activate the TGF-β1 in the presence of POSTN or Collagen I
Human LEC, HUVEC and HLF were co-cultured with reporter TMLEC, in the presence or absence of anti-TGF-β1 (1D11) or anti-GARP (MHG-8) antibody, on a substrate coated or not with periostin or Coll I. After 24 hours, luciferase activity was assessed by the addition of Bright-Glo, and the luminescence signal was quantified by using a luminescence plate reader. Each condition was tested in triplicate. Bars represent the mean. Error bars represent standard deviation (n=2).

c. Study of SMAD2 and SMAD3 phosphorylation resulting from the TGF-β1 pathway activation

Next, we attempted to detect TGF-β1 pathway activation through the phosphorylation of downstream effectors such as SMAD2 and SMAD3. Western blot analyses were performed on co-cultures. HLF cells were cultured for 24 hours, and then

LEC cells were seeded on them for 2 hours (**Fig. 27**). Despite several attempts, in these co-culture conditions, we observed a weak presence of pSMAD2/3 in a non-reproducible manner. Recombinant human TGF-β1 was used as a positive control.
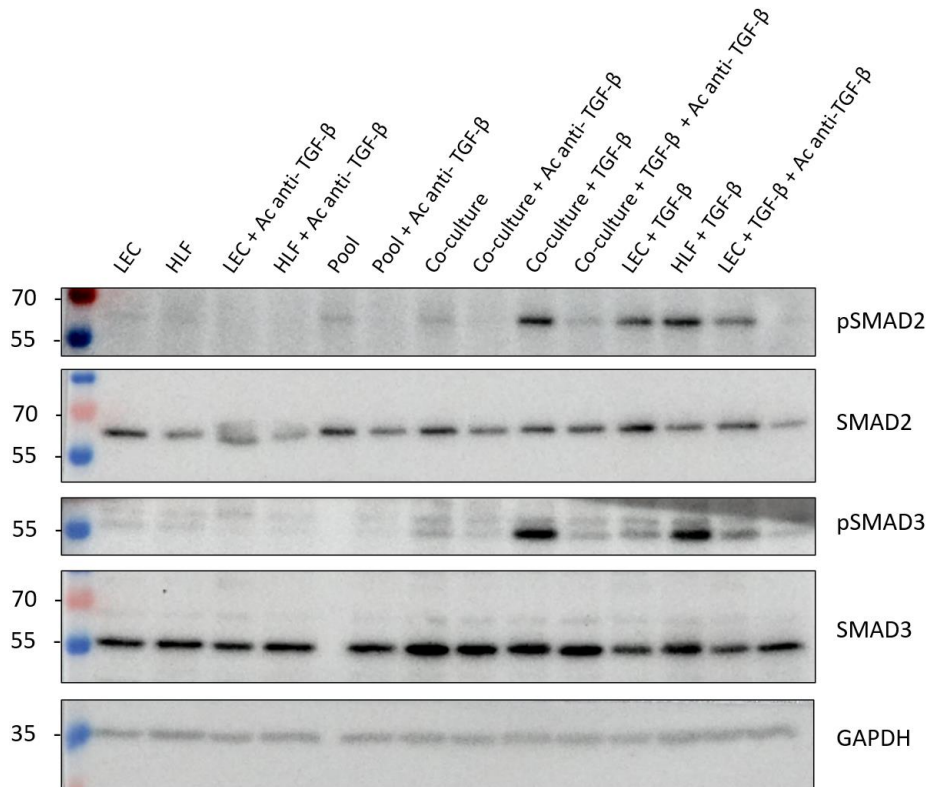
Figure 27. TGF-β signaling activity.
Western blot of pSMAD2/3 on co-culture between HLF and LEC (n=6)
Western Blot analysis of phospho-SMAD2 and phospho-SMAD3 on co-culture between HLF and LEC cells. The total amount of Smad2/Smad3 and GAPDH were taken as loading control.

It should be noted that the pSMAD2/3 pathway is not the unique pathway activated in endothelial cells with TGF-β1. Indeed, pSMAD1/5/8 could be involved in endothelial cells[298,299]. Therefore, experiments should be repeated with an antibody to reveal the phosphorylation of SMAD1/5/8 by western blot. (**Fig. 28**).

RESULTS

Part-3 DISCUSSION and PERSPECTIVES

Discussion and perspectives

GARP plays a role in maintaining the immune system homeostasis by regulating the availability of latent TGF-β1 and modulating its activation[358]. GARP particularly mediates TGF-β1 activation by Tregs in tumor-bearing mice. These findings underscore the significance of GARP in immune regulation and highlight its potential as a therapeutic target. A neutralizing anti-GARP:TGF-β1 mAb has been generated and blocks the release of TGF-β1. Interestingly, this antibody is able to induce the regression of tumors resistant to anti-PD-1 immunotherapy[283]. Previous work by Bertrand et *al*. showed tumor rejection using the combination of GARP:TGF-β1/PD-1 blockade. Of note, the observed effects of this anti-GARP:TGF-β1 mAb, in MC38 tumor-bearing mice, required the presence of the complex on Tregs, but not on platelets[283] (**Annex 1**[352]). These data further underline the importance of Treg-derived GARP:TGF-β1 complex in cancer-related immune suppression. Clinical trials in patients with locally advanced or metastatic solid tumors are currently tested (NCT03821935 and NCT05822752).

GARP overexpression has been observed in various types of primary tumors, including breast cancer, lung cancer, melanoma, bone sarcoma, gastric, and colon cancer[359,360]. These studies were primarily focused on Treg-derived GARP function in primary tumors. Despite strong interest in this protein, few studies have been carried out on LN. The originality of our work is to focus on non-immune cells in tumor-draining LN, which represents the first site of metastatic dissemination for a large range of cancers. In **Part I** of the results, we identified a panel of non-immune cells expressing GARP, including fibroblastic and endothelial cells. We aimed to identify and localize these non-immune cells that could secrete the GARP protein and, by extension, the complex GARP:TGF-β1 in humans and mice LNs. By combining complementary methodologies including cytometry, western blot, *in situ* hybridization and immunostaining, we mapped the spatial distribution of the GARP protein within human LNs and its RNA expression within murine LNs. Notably, GARP was present in blood vessels, surrounding lymphatic vessels, within αSMA+ fibroblasts, and in the ECM. Most remarkably, GARP was identified within endothelial cells that form the SCS and HEVs, which are vascular structures at the

interface between LNs and afferent lymphatic or blood vessels. In addition, perivascular cells and fibroblasts in the stroma were shown to express GARP.

1. What would be the relevance of GARP expression in endothelial cells?

The presence of GARP in LECs within the SCS suggests a potential role in modulating lymphocyte trafficking and creating immunosuppressive barriers in LN[232]. Thus, GARP-producing LECs in the SCS could participate in the creation of an immunosuppressive landscape at LN entry. Sc-RNASeq dataset analyses in mice revealed that ceiling and floor LECs strongly express Lrrc32 mRNA[348]. In humans, GARP was detected around lymphatic vessels, suggesting a potential role in forming a "protective shield" toward immune cell attack around these vessels. Nevertheless, a higher number of clinical samples, in different cancer types, would be necessary to confirm and strengthen our observations.

GARP expression by LECs underlines the multifunctionality of these poorly known cells in cancer. While LECs have been considered mainly as building blocks of lymphatic vessel walls, additional roles recently emerged. LECs play an important role in the regulation of immunity and antigen distribution in many diseases, including cancers[132]. LECs have also been shown to secrete potent pro-inflammatory cytokines such as IL-6[361]. Tumor-exposed LECs play a crucial role in promoting primary tumor growth. According to a recent study, performed by Van de Velde and Ebroin et al.[361] when exposed to tumor, LEC cells, undergo morphological and molecular changes that enhance cancer cell invasion in 3D cultures and tumor cell proliferation *in vivo*. One of the most modulated molecules in tumor-exposed LECs was IL6, produced in negligible quantities by unexposed LECs. Notably, the mitogenic effect of tumor-exposed LECs on tumor cells was abrogated *in vivo* by a neutralizing anti-human IL6 antibody. These results suggest that tumor-exposed LECs can exert "fibroblast-like properties" and contribute in a paracrine manner to the control of tumor cell properties. This discovery, combined with

our findings, provides a new paradigm in which LECs should be considered as key stromal determinants in tumor progression[361]. In this context, the production of GARP by LECs extends the role of these cells in immunosuppression with a putative effect on TGF-β1 activation, which however remains to be demonstrated, as discussed below.

Different subtypes of LEC have been recently identified through Sc-RNAseq analyses, both in human and mouse LNs[134,362]. The different LEC subtypes are known for expressing PROX1, a transcription factor. Other markers are now used for a sub-classification of LECs that includes at least: LECs of the valves (vLECs, *FOXC2*+, *CLDN11*+), subscapular sinus located at the floor (fLECS, *CCL20*+), or the ceiling (cLECs, *ACKR4*+), the paracortical sinuses (PTX3-LEC, *PTX3*+) and the medullary sinuses (MARCO-LECs, *MARCO*+)[133]. It would be interesting to determine the exact location of GARP in those different LEC sub-populations. Despite different attempts using antibodies raised against MARCO and ACKR4, we failed to detect GARP in the corresponding LEC populations. Further studies are required to characterize the different GARP-producing LECs in the whole LNs more precisely.

HEV vessels serve as specialized structures that enable the entry of circulating lymphocytes into LNs, a crucial process in immune surveillance. They contribute to the recruitment of naive CD62L+ lymphocytes[261]. They contribute to tissue inflammation in chronic inflammatory diseases such as, rheumatoid arthritis, Crohn's disease, atopic dermatitis, psoriasis and asthma. In cancers, HEV could have a beneficial effect by facilitating the entry of lymphocytes into solid tumors [363]. However, HEVs undergo changes in tumor-draining LNs that could modify their functions[40]. We here provide the first evidence that HEVs express GARP, both in our mouse and human analyses.

A better understanding of GARP implication in endothelial cells would potentially help to understand how tumor cells can survive and progress in the hostile environment of the LN.

2. What could be the function of GARP expression in fibroblastic cells and its association to the ECM?

Our data highlighted a surprising expression of GARP by fibroblasts, as well as a strong labeling in the associated ECM, both in human and mouse samples. Noteworthy, the antibody used could potentially recognize a cleaved and soluble form of GARP referred to as sGARP. It can be derived from various cellular sources such as activated Tregs, activated platelets and cancer cells [364]. Its capability to enhance the activation of latent TGF-β has been reported in autoimmune diseases and cancer contexts[365]. This soluble form of GARP can modulate immune responses by suppressing the proliferation and cytokine production of effector T cells (Teff), while inducing the differentiation of naive T cells into Tregs. Additionally, it promotes a tumor-associated "M2-like" macrophage phenotype [364]. sGARP also contributes to the endothelial to mesenchymal (EMT) process, enhancing tumor cell proliferation and migration capacities, further implicating its role in tumor progression and metastasis[366]. The mechanism underlying sGARP-mediated effects partially involves the TGF-β signaling pathway, as evidenced by the phosphorylation of Smad2/3 in sGARP-treated naive CD4+ T cells. However, inhibition of TGF-β signaling only partially attenuates sGARP effects, suggesting the involvement of additional signaling pathways[364]. One can postulate that the proteolytic degradation of ECM components during cell migration[367] can induce the release of sGARP and thereby influence the immune landscape within the LN. Further studies are required to validate or invalidate this hypothesis.

3. Do non-immune cells expressing GARP contribute to TGF-β1 activation in LN?

The identification of GARP expression by non-immune cell populations suggests their contribution to the creation and maintenance of an immunosuppressive TME by modulating TGF-β1 activation. However, the capacity of these cells to activate TGF-β1 in

a GARP-dependent manner remains to be established. We then conducted *in vitro* studies with the aim to determine whether GARP protein expressed by fibroblasts and endothelial cells can generate active TGF-β1. Our initial step involved the demonstration of the presence of GARP at the surface of LEC, HUVEC and HLF. Cytometry analyses also revealed the presence of the integrins αVβ6 and αVβ8, which can contribute to TGF-β1 release from the complex GARP: TGF-β. The expression of all those molecular determinants by the different cell types tested suggests their capacity to activate TGF-β1 via GARP. Moreover, stimulation of LECs and HLFs with human recombinant TGF-β1 demonstrated their responsiveness to this cytokine, as assessed by SMAD2 and SMAD3 phosphorylation, as part of the canonical TGF-β1 pathway. Despite multiple attempts, we did not detect *in vitro* the production of active TGF-β1 from LECs or fibroblastic cells, by western blot analyses. Our efforts also fell short in demonstrating the secretion of active TGF-β1 by using TMLEC reporter cells in the presence of LECs, HLFs ("mono-culture"), or both LECs and HLF ("co-culture"). Importantly, SMAD1/5/8 phosphorylation are worth considering for future analysis. Indeed, in endothelial cells, these SMADs are implicated in TGF-β1 activation through the participation of the co-receptor ALK1. It would be interesting to further investigate this pathway in the LEC/HLF crosstalk and the release of active TGF-β1. An alternative and unexplored approach in our study involves the use of wells directly coated with αVβ8 integrin as proposed by Seed and Nishimura (**Fig. 34**)[368]. This method offers a potential solution to address the question of whether active TGF-β1 can be released from the GARP:TGF-β1 complex present in these different human primary cells (i.e., LECs, HUVECs, and HLFs). In this experiment, we could measure the release of TGF-β1 from primary cell cultures or cells that would have been isolated using FACS.
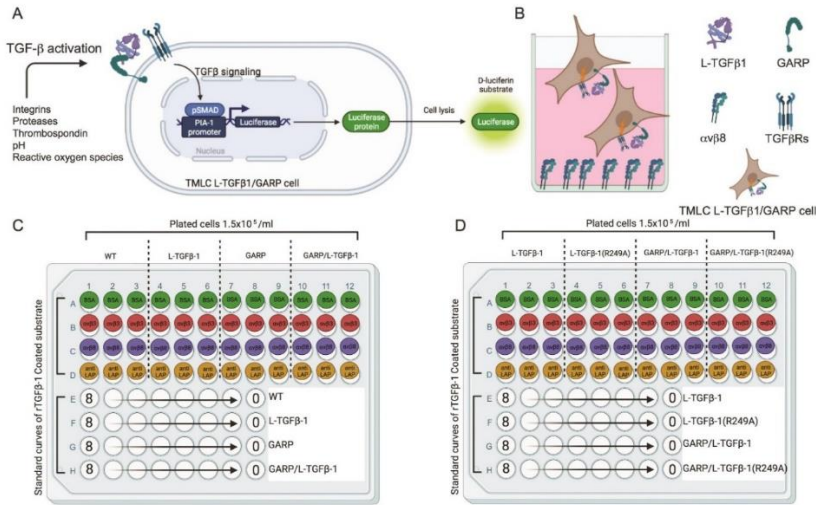
Figure 28. Assay design to assess the ability of recombinant αvβ8 ectodomain for promoting cell intrinsic TGF-β1 signaling, from both releasable and non-releasable forms of L-TGF-β1
(**A**) Cartoon depiction of TMLC TGF-β reporting cells (Abe et al., 1994). TGF-β. Downstream of TGF-β signaling, pSMAD drives the expression of luciferase, and TGF-β signaling can be reported following cell lysis and assessment of luciferase activity using luciferase assay buffer (containing the luciferin substrate). (**B**) Culture of TMLEC/cells expressing GARP with the presence of immobilized αvβ8 ectodomain. (**C**) An assay format was used to evaluate whether αvβ8 can activate TGF-β1 in cells. Negative controls were immobilized alongside αvβ8 ectodomain and TMLC cells were plated onto various substrates for comparison. (**D**) The assay assesses αvβ8's ability to promote cell intrinsic TGF-β signaling of non-releasable TGF-β. Controls of TMLC L-TGF-β1 alone, TMLC L-TGF-β1(R249A) alone, and TMLC L-TGF-β1/GARP were included. A standard curve of each cell type treated with known concentrations of recombinant human TGF-β1 was used to normalize TGFβ responsiveness between cell lines. Data was presented as concentration (ng/mL) of TGF-β1 signaling.

4. Can GARP be used as a biomarker in LN?

GARP protein expression has been observed in various types of cancer, including melanoma and oral squamous cell carcinoma. In melanoma, increased GARP expression has been associated with disease progression[360]. Similarly, in oral cancer, GARP expression may play a role in regulating tumor immunosuppression, thereby promoting cancer progression[359]. These observations performed in primary tumors suggest that GARP could serve as a potential biomarker for these types of cancer. It is also viewed as

a promising therapeutic target and clinical trials are ongoing (NCT03821935 and NCT05822752). Our study suggests the interest also to consider GARP expression in the LNs of cancerous patients. We here focused on LNs derived from patients with breast and cervical cancer. It would be most interesting to extend our study to other cancers using the lymphatic system to disseminate (for instance, melanoma, pancreatic, head, and neck cancers). Our study paves the way for future investigations on GARP production as a prognostic and/or predictive marker for LN and distant metastases.

Conclusion

The identification of non-immune cell populations expressing GARP and secreting GARP:TGF-β1 in LN opens new perspectives. Our research has brought attention to new cell populations producing GARP mRNA and protein, in human and mouse LNs. We have identified and mapped non-immune cell populations that express GARP in tumor draining LNs. Provided that they can activate TGF-β1, these cells could play a significant role in establishing an immunosuppressive landscape in metastatic LNs. Therefore, these cells, along with Tregs, should be considered as targets of the anti-blocking antibodies used in clinical trials. Their role in TGF-β1 activation and likely to other yet unknown biological functions remain to be established.
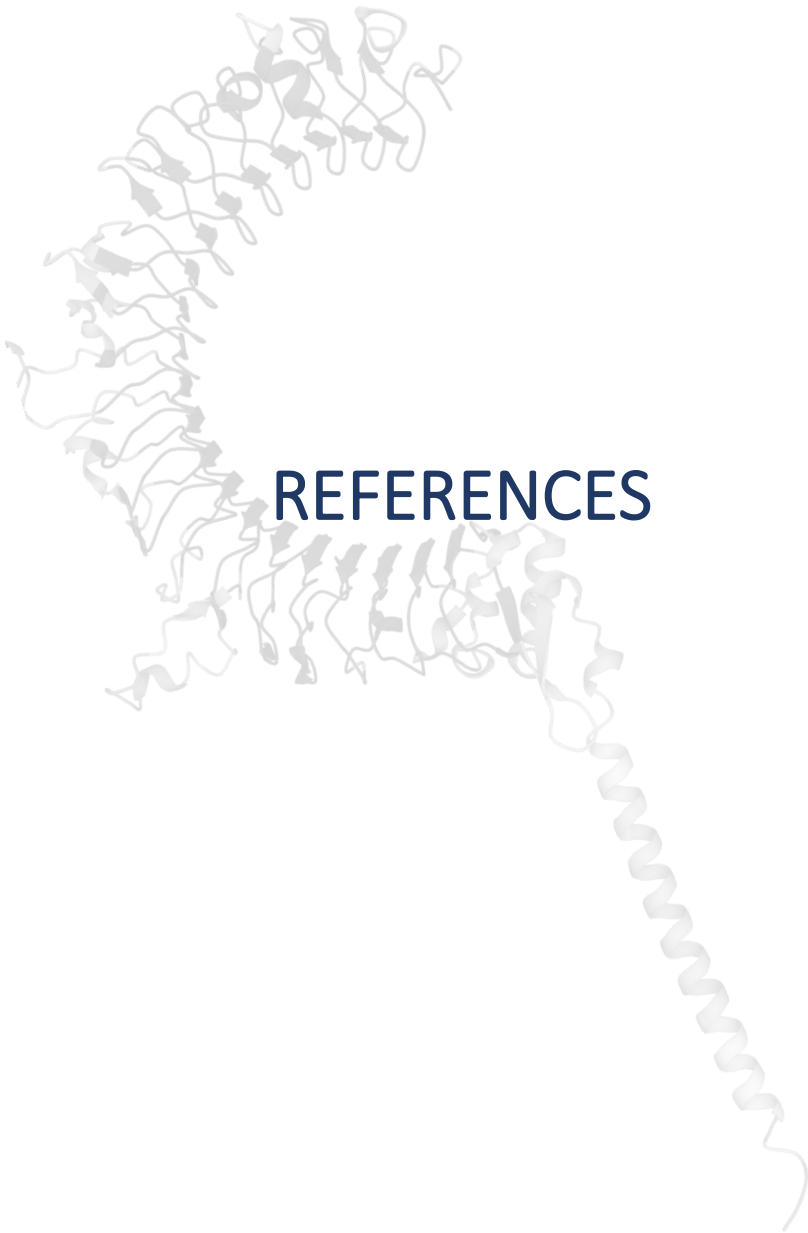
REFERENCES

References

1.   Mukherjee, S. Cancer, Our Genes, And The Anxiety Of Risk-Based Medicine. *Health Aff. (Millwood)* **37**, 817–820 (2018).

2.   Hanahan, D. & Weinberg, R. A. Hallmarks of Cancer: The Next Generation. *Cell* **144**, 646–674 (2011).

3.   Vogelstein, B. *et al.* Genetic alterations during colorectal-tumor development. *N. Engl. J. Med.* **319**, 525–532 (1988).

4.   Hanahan, D. Hallmarks of Cancer: New Dimensions. *Cancer Discov.* **12**, 31–46 (2022).

5.   Nowell, P. C. The clonal evolution of tumor cell populations. *Science* **194**, 23–28 (1976).

6.   McGranahan, N. & Swanton, C. Clonal Heterogeneity and Tumor Evolution: Past, Present, and the Future. *Cell* **168**, 613–628 (2017).

7.   Strasser, A. & Vaux, D. L. Cell Death in the Origin and Treatment of Cancer. *Mol. Cell* **78**, 1045–1054 (2020).

8.   Martin, G. S. Cell signaling and cancer. *Cancer Cell* **4**, 167–174 (2003).

9.   Kerr, J. F. R., Wyllie, A. H. & Currie, A. R. Apoptosis: A Basic Biological Phenomenon with Wideranging Implications in Tissue Kinetics. *Br. J. Cancer* **26**, 239–257 (1972).

10.   Fan, X. Q. & Guo, Y. J. Apoptosis in oncology. *Cell Res.* **11**, 1–7 (2001).

11.   Vaux, D. L., Cory, S. & Adams, J. M. Bcl-2 gene promotes haemopoietic cell survival and cooperates with c-myc to immortalize pre-B cells. *Nature* **335**, 440–442 (1988).

12.   Adams, J. M. & Cory, S. The Bcl-2 apoptotic switch in cancer development and therapy. *Oncogene* **26**, 1324–1337 (2007).

13.   Vogelstein, B. & Kinzler, K. W. p53 function and dysfunction. *Cell* **70**, 523–526 (1992).

14.   Levine, A. J. p53, the Cellular Gatekeeper for Growth and Division. *Cell* **88**, 323–331 (1997).

15.   Kalkat, M. *et al.* MYC Deregulation in Primary Human Cancers. *Genes* **8**, 151 (2017).

REFERENCES

16. Weinberg, R. A. The retinoblastoma protein and cell cycle control. *Cell* **81**, 323–330 (1995).

17. Kim, B. N. *et al.* TGF-β induced EMT and stemness characteristics are associated with epigenetic regulation in lung cancer. *Sci. Rep.* **10**, 10597 (2020).

18. Leal-Esteban, L. C. & Fajas, L. Cell cycle regulators in cancer cell metabolism. *Biochim. Biophys. Acta BBA - Mol. Basis Dis.* **1866**, 165715 (2020).

19. Cheng, N., Chytil, A., Shyr, Y., Joly, A. & Moses, H. L. Transforming Growth Factor-β Signaling–Deficient Fibroblasts Enhance Hepatocyte Growth Factor Signaling in Mammary Carcinoma Cells to Promote Scattering and Invasion. *Mol. Cancer Res.* **6**, 1521–1533 (2008).

20. Bhowmick, N. A., Neilson, E. G. & Moses, H. L. Stromal fibroblasts in cancer initiation and progression. *Nature* **432**, 332–337 (2004).

21. Werner, S. & Grose, R. Regulation of Wound Healing by Growth Factors and Cytokines. *Physiol. Rev.* **83**, 835–870 (2003).

22. Aaronson, S. A. Growth Factors and Cancer. *Science* **254**, 1146–1153 (1991).

23. Lukashev, M. ECM signalling: orchestrating cell behaviour and misbehaviour. *Trends Cell Biol.* **8**, 437–441 (1998).

24. Giancotti, F. G. & Ruoslahti, E. Integrin Signaling. *Science* **285**, 1028–1033 (1999).

25. Davies, M. A. & Samuels, Y. Analysis of the genome to personalize therapy for melanoma. *Oncogene* **29**, 5545–5555 (2010).

26. Toomey, S. *et al.* Impact of somatic PI3K pathway and ERBB family mutations on pathological complete response (pCR) in HER2-positive breast cancer patients who received neoadjuvant HER2-targeted therapies. *Breast Cancer Res.* **19**, 87 (2017).

27. Bryan, T. M. & Cech, T. R. Telomerase and the maintenance of chromosome ends. *Curr. Opin. Cell Biol.* **11**, 318–324 (1999).

28. Armanios, M. The Role of Telomeres in Human Disease. *Annu. Rev. Genomics Hum. Genet.* **23**, 363–381 (2022).

29. Greenberg, R. A. *et al.* Short Dysfunctional Telomeres Impair Tumorigenesis in the INK4aΔ2/3 Cancer-Prone Mouse. *Cell* **97**, 515–525 (1999).

30. Lowe, S. W., Cepero, E. & Evan, G. Intrinsic tumour suppression. *Nature* **432**, 307–315 (2004).

REFERENCES

31. Artandi, S. E. & DePinho, R. A. Telomeres and telomerase in cancer. *Carcinogenesis* **31**, 9–18 (2010).

32. Augsten, M. Cancer-associated fibroblasts as another polarized cell type of the tumor microenvironment. *Front. Oncol.* **4**, 62 (2014).

33. Mantovani, A., Allavena, P., Sica, A. & Balkwill, F. Cancer-related inflammation. *Nature* **454**, 436–444 (2008).

34. Lu, P., Weaver, V. M. & Werb, Z. The extracellular matrix: a dynamic niche in cancer progression. *J. Cell Biol.* **196**, 395–406 (2012).

35. Veikkola, T. & Alitalo, K. VEGFs, receptors and angiogenesis. *Semin. Cancer Biol.* **9**, 211–220 (1999).

36. Carmeliet, P. VEGF as a Key Mediator of Angiogenesis in Cancer. *Oncology* **69**, 4–10 (2005).

37. Kazerounian, S., Yee, K. O. & Lawler, J. Thrombospondins: from structure to therapeutics: Thrombospondins in cancer. *Cell. Mol. Life Sci.* **65**, 700–712 (2008).

38. Ansari, M. J. *et al.* Cancer combination therapies by angiogenesis inhibitors; a comprehensive review. *Cell Commun. Signal.* **20**, 49 (2022).

39. Raza, A., Franklin, M. J. & Dudek, A. Z. Pericytes and vessel maturation during tumor angiogenesis and metastasis. *Am. J. Hematol.* **85**, 593–598 (2010).

40. Bergers, G. & Song, S. The role of pericytes in blood-vessel formation and maintenance. *Neuro-Oncol.* **7**, 452–464 (2005).

41. Langley, R. R. & Fidler, I. J. Tumor cell-organ microenvironment interactions in the pathogenesis of cancer metastasis. *Endocr. Rev.* **28**, 297–321 (2007).

42. Sporn, M. B. The war on cancer. *The Lancet* **347**, 1377–1381 (1996).

43. Balzer, E. M. & Konstantopoulos, K. Intercellular adhesion: mechanisms for growth and metastasis of epithelial cancers. *WIREs Syst. Biol. Med.* **4**, 171–181 (2012).

44. Perl, A.-K., Wilgenbus, P., Dahl, U., Semb, H. & Christofori, G. A causal role for E-cadherin in the transition from adenoma to carcinoma. *Nature* **392**, 190–193 (1998).

45. Martin, C. E. & List, K. Cell-surface anchored serine proteases in cancer progression and metastasis. *Cancer Metastasis Rev.* **38**, 357–387 (2019).

REFERENCES

46. Werb, Z. ECM and Cell Surface Proteolysis: Regulating Cellular Ecology. *Cell* **91**, 439–442 (1997).

47. Graham, T. A. & Shibata, D. Navigating the path to distant metastasis. *Nat. Genet.* **52**, 642–643 (2020).

48. Müller, A. *et al.* Involvement of chemokine receptors in breast cancer metastasis. *Nature* **410**, 50–56 (2001).

49. Majidpoor, J. & Mortezaee, K. Steps in metastasis: an updated review. *Med. Oncol.* **38**, 3 (2021).

50. Laudato, S., Aparicio, A. & Giancotti, F. G. Clonal Evolution and Epithelial Plasticity in the Emergence of AR-Independent Prostate Carcinoma. *Trends Cancer* **5**, 440–455 (2019).

51. Birkbak, N. J. & McGranahan, N. Cancer Genome Evolutionary Trajectories in Metastasis. *Cancer Cell* **37**, 8–19 (2020).

52. Strilic, B. & Offermanns, S. Intravascular Survival and Extravasation of Tumor Cells. *Cancer Cell* **32**, 282–293 (2017).

53. Sennino, B. & McDonald, D. M. Controlling escape from angiogenesis inhibitors. *Nat. Rev. Cancer* **12**, 699–709 (2012).

54. Dhamija, S. & Diederichs, S. From junk to master regulators of invasion: lncRNA functions in migration, EMT and metastasis. *Int. J. Cancer* **139**, 269–280 (2016).

55. Tong, L. *et al.* Proteasome-dependent degradation of Smad7 is critical for lung cancer metastasis. *Cell Death Differ.* **27**, 1795–1806 (2020).

56. Padmanaban, V. *et al.* E-cadherin is required for metastasis in multiple models of breast cancer. *Nature* **573**, 439–444 (2019).

57. Hu, X. *et al.* The RNA-binding protein AKAP8 suppresses tumor metastasis by antagonizing EMT-associated alternative splicing. *Nat. Commun.* **11**, 486 (2020).

58. Pradip, D., Jennifer, A. & Nandini, D. Cancer-Associated Fibroblasts in Conversation with Tumor Cells in Endometrial Cancers: A Partner in Crime. *Int. J. Mol. Sci.* **22**, 9121 (2021).

59. Labernadie, A. *et al.* A mechanically active heterotypic E-cadherin/N-cadherin adhesion enables fibroblasts to drive cancer cell invasion. *Nat. Cell Biol.* **19**, 224–237 (2017).

REFERENCES

60. Radisky, D. C., Kenny, P. A. & Bissell, M. J. Fibrosis and Cancer: Do Myofibroblasts Come Also From Epithelial Cells Via EMT? *J. Cell. Biochem.* **101**, 830–839 (2007).

61. Anderson, R. L. *et al.* A framework for the development of effective anti-metastatic agents. *Nat. Rev. Clin. Oncol.* **16**, 185–204 (2019).

62. Sanchez, L. R. *et al.* The emerging roles of macrophages in cancer metastasis and response to chemotherapy. *J. Leukoc. Biol.* **106**, 259–274 (2019).

63. Cassetta, L. & Pollard, J. W. Targeting macrophages: therapeutic approaches in cancer. *Nat. Rev. Drug Discov.* **17**, 887–904 (2018).

64. Erdogan, B. & Webb, D. J. Cancer-associated fibroblasts modulate growth factor signaling and extracellular matrix remodeling to regulate tumor metastasis. *Biochem. Soc. Trans.* **45**, 229–236 (2017).

65. Yang, L. & Zhang, Y. Tumor-associated macrophages: from basic research to clinical application. *J. Hematol. Oncol.J Hematol Oncol* **10**, 58 (2017).

66. Chen, X. & Song, E. Turning foes to friends: targeting cancer-associated fibroblasts. *Nat. Rev. Drug Discov.* **18**, 99–115 (2019).

67. Su, S.-C. *et al.* Cancer metastasis: Mechanisms of inhibition by melatonin. *J. Pineal Res.* **62**, e12370 (2017).

68. Mollinedo, F. Neutrophil Degranulation, Plasticity, and Cancer Metastasis. *Trends Immunol.* **40**, 228–242 (2019).

69. Primac, I. *et al.* Stromal integrin α11 regulates PDGFR-β signaling and promotes breast cancer progression. *J. Clin. Invest.* **129**, 4609–4628 (2019).

70. Lo, H. C. *et al.* Resistance to natural killer cell immunosurveillance confers a selective advantage to polyclonal metastasis. *Nat. Cancer* **1**, 709–722 (2020).

71. Headley, M. B. *et al.* Visualization of immediate immune responses to pioneer metastatic cells in the lung. *Nature* **531**, 513–517 (2016).

72. Follain, G. *et al.* Fluids and their mechanics in tumour transit: shaping metastasis. *Nat. Rev. Cancer* **20**, 107–124 (2020).

73. Wheeler, L. J. *et al.* Multi-Omic Approaches Identify Metabolic and Autophagy Regulators Important in Ovarian Cancer Dissemination. *iScience* **19**, 474–491 (2019).

REFERENCES

74. Najafi, M., Ahmadi, A. & Mortezaee, K. Extracellular-signal-regulated kinase/mitogen-activated protein kinase signaling as a target for cancer therapy: an updated review. *Cell Biol. Int.* **43**, 1206–1222 (2019).

75. Bersini, S. *et al.* A combined microfluidic-transcriptomic approach to characterize the extravasation potential of cancer cells. *Oncotarget* **9**, 36110–36125 (2018).

76. Osmani, N. *et al.* Metastatic Tumor Cells Exploit Their Adhesion Repertoire to Counteract Shear Forces during Intravascular Arrest. *Cell Rep.* **28**, 2491-2500.e5 (2019).

77. Osmani, N. *et al.* Intravascular Arrest of Circulating Tumor Cells is a Two-Step Process Exploiting Their Adhesion Repertoire. SSRN Scholarly Paper at https://doi.org/10.2139/ssrn.3272239 (2018).

78. Leong, H. S. *et al.* Invadopodia are required for cancer cell extravasation and are a therapeutic target for metastasis. *Cell Rep.* **8**, 1558–1570 (2014).

79. Steinbichler, T. B., Dudás, J., Riechelmann, H. & Skvortsova, I.-I. The role of exosomes in cancer metastasis. *Semin. Cancer Biol.* **44**, 170–181 (2017).

80. Gau, D. M., Chakraborty, S., Boone, D., Wells, A. & Roy, P. Abstract LB-043: MRTF|Profilin is an important signaling axis for metastatic outgrowth of triple negative breast cancer cells. *Cancer Res.* **79**, LB-043 (2019).

81. La Belle Flynn, A. *et al.* Autophagy inhibition elicits emergence from metastatic dormancy by inducing and stabilizing Pfkfb3 expression. *Nat. Commun.* **10**, 3668 (2019).

82. Guereño, M. *et al.* Glypican-3 (GPC3) inhibits metastasis development promoting dormancy in breast cancer cells by p38 MAPK pathway activation. *Eur. J. Cell Biol.* **99**, 151096 (2020).

83. Brown, M. *et al.* Lymph node blood vessels provide exit routes for metastatic tumor cell dissemination in mice. *Science* **359**, 1408–1411 (2018).

84. Pereira, E. R. *et al.* Lymph node metastases can invade local blood vessels, exit the node, and colonize distant organs in mice. *Science* **359**, 1403–1407 (2018).

85. Tammela, T. & Alitalo, K. Lymphangiogenesis: Molecular Mechanisms and Future Promise. *Cell* **140**, 460–476 (2010).

REFERENCES

86. Aspelund, A., Robciuc, M. R., Karaman, S., Makinen, T. & Alitalo, K. Lymphatic System in Cardiovascular Medicine. *Circ. Res.* **118**, 515–530 (2016).

87. Vaahtomeri, K., Karaman, S., Mäkinen, T. & Alitalo, K. Lymphangiogenesis guidance by paracrine and pericellular factors. *Genes Dev.* **31**, 1615–1634 (2017).

88. Breslin, J. W. *et al.* Lymphatic Vessel Network Structure and Physiology. in *Comprehensive Physiology* (ed. Prakash, Y. S.) 207–299 (Wiley, 2018). doi:10.1002/cphy.c180015.

89. Choi, I., Lee, S. & Hong, Y.-K. The New Era of the Lymphatic System: No Longer Secondary to the Blood Vascular System. *Cold Spring Harb. Perspect. Med.* **2**, a006445–a006445 (2012).

90. Uddin, N. & Rutar, M. Ocular Lymphatic and Glymphatic Systems: Implications for Retinal Health and Disease. *Int. J. Mol. Sci.* **23**, 10139 (2022).

91. Yankova, G., Bogomyakova, O. & Tulupov, A. The glymphatic system and meningeal lymphatics of the brain: new understanding of brain clearance. *Rev. Neurosci.* **32**, 693–705 (2021).

92. González-Loyola, A. & Petrova, T. V. Development and aging of the lymphatic vascular system. *Adv. Drug Deliv. Rev.* **169**, 63–78 (2021).

93. Podgrabinska, S. *et al.* Molecular characterization of lymphatic endothelial cells. *Proc. Natl. Acad. Sci.* **99**, 16069–16074 (2002).

94. Baluk, P. *et al.* Functionally specialized junctions between endothelial cells of lymphatic vessels. *J. Exp. Med.* **204**, 2349–2362 (2007).

95. Danussi, C. *et al. Emilin1* Deficiency Causes Structural and Functional Defects of Lymphatic Vasculature. *Mol. Cell. Biol.* **28**, 4026–4039 (2008).

96. Paupert, J., Sounni, N. E. & Noël, A. Lymphangiogenesis in post-natal tissue remodeling: Lymphatic endothelial cell connection with its environment. *Mol. Aspects Med.* **32**, 146–158 (2011).

97. Petrova, T. V. *et al.* Defective valves and abnormal mural cell recruitment underlie lymphatic vascular failure in lymphedema distichiasis. *Nat. Med.* **10**, 974–981 (2004).

98. Dieterich, L. C., Tacconi, C., Ducoli, L. & Detmar, M. Lymphatic vessels in cancer. *Physiol. Rev.* **102**, 1837–1879 (2022).

REFERENCES

99. Pflicke, H. & Sixt, M. Preformed portals facilitate dendritic cell entry into afferent lymphatic vessels. *J. Exp. Med.* **206**, 2925–2935 (2009).

100. Gerli, R., Solito, R., Weber, E. & Aglianó, M. Specific adhesion molecules bind anchoring filaments and endothelial cells in human skin initial lymphatics. *Lymphology* **33**, 148–157 (2000).

101. Sakai, L. Y., Keene, D. R., Morris, N. P. & Burgeson, R. E. Type VII collagen is a major structural component of anchoring fibrils. *J. Cell Biol.* **103**, 1577–1586 (1986).

102. Keene, D. R., Sakai, L. Y., Lunstrum, G. P., Morris, N. P. & Burgeson, R. E. Type VII collagen forms an extended network of anchoring fibrils. *J. Cell Biol.* **104**, 611–621 (1987).

103. Danussi, C. *et al.* EMILIN1/α9β1 Integrin Interaction Is Crucial in Lymphatic Valve Formation and Maintenance. *Mol. Cell. Biol.* **33**, 4381–4394 (2013).

104. Capuano, A. *et al.* Integrin binding site within the gC1q domain orchestrates EMILIN-1-induced lymphangiogenesis. *Matrix Biol.* **81**, 34–49 (2019).

105. Bazigou, E. & Makinen, T. Flow control in our vessels: vascular valves make sure there is no way back. *Cell. Mol. Life Sci.* **70**, 1055–1066 (2013).

106. Card, C. M., Yu, S. S. & Swartz, M. A. Emerging roles of lymphatic endothelium in regulating adaptive immunity. *J. Clin. Invest.* **124**, 943–952 (2014).

107. Grant, S. M., Lou, M., Yao, L., Germain, R. N. & Radtke, A. J. The lymph node at a glance – how spatial organization optimizes the immune response. *J. Cell Sci.* **133**, jcs241828 (2020).

108. Waithman, J., Moffat, J. M., Patterson, N. L., Van Beek, A. E. & Mintern, J. D. Antigen Presentation. in *Reference Module in Biomedical Sciences* B9780128012383001185 (Elsevier, 2014). doi:10.1016/B978-0-12-801238-3.00118-5.

109. Cherrier, M. & Eberl, G. The development of LTi cells. *Curr. Opin. Immunol.* **24**, 178–183 (2012).

110. van de Pavert, S. A. & Mebius, R. E. New insights into the development of lymphoid tissues. *Nat. Rev. Immunol.* **10**, 664–674 (2010).

REFERENCES

111. van de Pavert, S. A. *et al.* Chemokine CXCL13 is essential for lymph node initiation and is induced by retinoic acid and neuronal stimulation. *Nat. Immunol.* **10**, 1193–1199 (2009).

112. Randall, T. D., Carragher, D. M. & Rangel-Moreno, J. Development of Secondary Lymphoid Organs. *Annu. Rev. Immunol.* **26**, 627–650 (2008).

113. Antonioli, L. *et al.* Ectopic Lymphoid Organs and Immune-Mediated Diseases: Molecular Basis for Pharmacological Approaches. *Trends Mol. Med.* **26**, 1021–1033 (2020).

114. Bovay, E. *et al.* Multiple roles of lymphatic vessels in peripheral lymph node development. *J. Exp. Med.* **215**, 2760–2777 (2018).

115. Onder, L. & Ludewig, B. A Fresh View on Lymph Node Organogenesis. *Trends Immunol.* **39**, 775–787 (2018).

116. Jalkanen, S. & Salmi, M. Lymphatic endothelial cells of the lymph node. *Nat. Rev. Immunol.* (2020) doi:10.1038/s41577-020-0281-x.

117. Fletcher, A. L., Acton, S. E. & Knoblich, K. Lymph node fibroblastic reticular cells in health and disease. *Nat. Rev. Immunol.* **15**, 350–361 (2015).

118. Martinez, V. G. *et al.* Fibroblastic Reticular Cells Control Conduit Matrix Deposition during Lymph Node Expansion. *Cell Rep.* **29**, 2810-2822.e5 (2019).

119. Roozendaal, R. *et al.* Conduits Mediate Transport of Low-Molecular-Weight Antigen to Lymph Node Follicles. *Immunity* **30**, 264–276 (2009).

120. Sobocinski, G. P. *et al.* Ultrastructural localization of extracellular matrix proteins of the lymph node cortex: Evidence supporting the reticular network as a pathway for lymphocyte migration. *BMC Immunol.* **11**, 42 (2010).

121. Schiavinato, A., Przyklenk, M., Kobbe, B., Paulsson, M. & Wagener, R. Collagen type VI is the antigen recognized by the ER-TR7 antibody. *Eur. J. Immunol.* **51**, 2345–2347 (2021).

122. Rodda, L. B. *et al.* Single-Cell RNA Sequencing of Lymph Node Stromal Cells Reveals Niche-Associated Heterogeneity. *Immunity* **48**, 1014-1028.e6 (2018).

123. Harlé, G., Kowalski, C., Garnier, L. & Hugues, S. Lymph Node Stromal Cells: Mapmakers of T Cell Immunity. *Int. J. Mol. Sci.* **21**, 7785 (2020).

REFERENCES

124. Reynoso, G. V. *et al.* Lymph node conduits transport virions for rapid T cell activation. *Nat. Immunol.* **20**, 602–612 (2019).

125. Gillot, L., Baudin, L., Rouaud, L., Kridelka, F. & Noël, A. The pre-metastatic niche in lymph nodes: formation and characteristics. *Cell. Mol. Life Sci.* **78**, 5987–6002 (2021).

126. Girard, J.-P., Moussion, C. & Förster, R. HEVs, lymphatics and homeostatic immune cell trafficking in lymph nodes. *Nat. Rev. Immunol.* **12**, 762–773 (2012).

127. Gray, E. E. & Cyster, J. G. Lymph Node Macrophages. *J. Innate Immun.* **4**, 424–436 (2012).

128. Bellomo, A., Gentek, R., Bajénoff, M. & Baratin, M. Lymph node macrophages: Scavengers, immune sentinels and trophic effectors. *Cell. Immunol.* **330**, 168–174 (2018).

129. Petrova, T. V. & Koh, G. Y. Organ-specific lymphatic vasculature: From development to pathophysiology. *J. Exp. Med.* **215**, 35–49 (2018).

130. Ulvmar, M. H. & Mäkinen, T. Heterogeneity in the lymphatic vascular system and its origin. *Cardiovasc. Res.* **111**, 310–321 (2016).

131. Iftakhar-E-Khuda, I. *et al.* Gene-expression profiling of different arms of lymphatic vasculature identifies candidates for manipulation of cell traffic. *Proc. Natl. Acad. Sci.* **113**, 10643–10648 (2016).

132. Fujimoto, N. *et al.* Single-cell mapping reveals new markers and functions of lymphatic endothelial cells in lymph nodes. *PLOS Biol.* **18**, e3000704 (2020).

133. Xiang, M. *et al.* A Single-Cell Transcriptional Roadmap of the Mouse and Human Lymph Node Lymphatic Vasculature. *Front. Cardiovasc. Med.* **7**, 52 (2020).

134. Takeda, A. *et al.* Single-Cell Survey of Human Lymphatics Unveils Marked Endothelial Cell Heterogeneity and Mechanisms of Homing for Neutrophils. *Immunity* **51**, 561-572.e5 (2019).

135. Cohen, J. N. *et al.* Tolerogenic Properties of Lymphatic Endothelial Cells Are Controlled by the Lymph Node Microenvironment. *PLoS ONE* **9**, e87740 (2014).

136. Ulvmar, M. H. *et al.* The atypical chemokine receptor CCRL1 shapes functional CCL21 gradients in lymph nodes. *Nat. Immunol.* **15**, 623–630 (2014).

REFERENCES

137. Cochran, A. J. *et al.* Tumour–induced immune modulation of sentinel lymph nodes. *Nat. Rev. Immunol.* **6**, 659–670 (2006).

138. Padera, T. P., Meijer, E. F. J. & Munn, L. L. The Lymphatic System in Disease Processes and Cancer Progression. *Annu. Rev. Biomed. Eng.* **18**, 125–158 (2016).

139. Ager, A. High Endothelial Venules and Other Blood Vessels: Critical Regulators of Lymphoid Organ Development and Function. *Front. Immunol.* **8**, (2017).

140. Pawlak, J. B. & Caron, K. M. Lymphatic Programing and Specialization in Hybrid Vessels. *Front. Physiol.* **11**, 114 (2020).

141. Förster, R., Davalos-Misslitz, A. C. & Rot, A. CCR7 and its ligands: balancing immunity and tolerance. *Nat. Rev. Immunol.* **8**, 362–371 (2008).

142. Arroz-Madeira, S., Bekkhus, T., Ulvmar, M. H. & Petrova, T. V. Lessons of Vascular Specialization From Secondary Lymphoid Organ Lymphatic Endothelial Cells. *Circ. Res.* **132**, 1203–1225 (2023).

143. Sabine, A. *et al.* Mechanotransduction, PROX1, and FOXC2 cooperate to control connexin37 and calcineurin during lymphatic-valve formation. *Dev. Cell* **22**, 430–445 (2012).

144. Sabine, A. *et al.* FOXC2 and fluid shear stress stabilize postnatal lymphatic vasculature. *J. Clin. Invest.* **125**, 3861–3877 (2015).

145. Huang, S. *et al.* Lymph nodes are innervated by a unique population of sensory neurons with immunomodulatory potential. *Cell* **184**, 441-459.e25 (2021).

146. Camara, A. *et al.* Lymph Node Mesenchymal and Endothelial Stromal Cells Cooperate via the RANK-RANKL Cytokine Axis to Shape the Sinusoidal Macrophage Niche. *Immunity* **50**, 1467-1481.e6 (2019).

147. Mondor, I. *et al.* Lymphatic Endothelial Cells Are Essential Components of the Subcapsular Sinus Macrophage Niche. *Immunity* **50**, 1453-1466.e4 (2019).

148. D'Addio, M. *et al.* Sialoglycans on lymphatic endothelial cells augment interactions with Siglec-1 (CD169) of lymph node macrophages. *FASEB J. Off. Publ. Fed. Am. Soc. Exp. Biol.* **35**, e22017 (2021).

149. Tewalt, E. F. *et al.* Lymphatic endothelial cells induce tolerance via PD-L1 and lack of costimulation leading to high-level PD-1 expression on CD8 T cells. *Blood* **120**, 4772–4782 (2012).

REFERENCES

150. Hirosue, S. *et al.* Steady-State Antigen Scavenging, Cross-Presentation, and CD8+ T Cell Priming: A New Role for Lymphatic Endothelial Cells. *J. Immunol. Author Choice* **192**, 5002–5011 (2014).

151. Kedl, R. M. & Tamburini, B. A. Antigen archiving by lymph node stroma: A novel function for the lymphatic endothelium. *Eur. J. Immunol.* **45**, 2721–2729 (2015).

152. Tamburini, B. A., Burchill, M. A. & Kedl, R. M. Antigen capture and archiving by lymphatic endothelial cells following vaccination or viral infection. *Nat. Commun.* **5**, 3989 (2014).

153. Pham, T. H. M. *et al.* Lymphatic endothelial cell sphingosine kinase activity is required for lymphocyte egress and lymphatic patterning. *J. Exp. Med.* **207**, 17–27 (2010).

154. Carpentier, K. S. *et al.* MARCO+ lymphatic endothelial cells sequester arthritogenic alphaviruses to limit viremia and viral dissemination. *EMBO J.* **40**, e108966 (2021).

155. Hynes, R. O. & Naba, A. Overview of the matrisome-An inventory of extracellular matrix constituents and functions. *Cold Spring Harb. Perspect. Biol.* **4**, a004903–a004903 (2012).

156. Bourgot, I., Primac, I., Louis, T., Noël, A. & Maquoi, E. Reciprocal Interplay Between Fibrillar Collagens and Collagen-Binding Integrins: Implications in Cancer Progression and Metastasis. *Front. Oncol.* **10**, 1–28 (2020).

157. Sixt, M. *et al.* The conduit system transports soluble antigens from the afferent lymph to resident dendritic cells in the T cell area of the lymph node. *Immunity* **22**, 19–29 (2005).

158. Robertson, I. B., Horiguchi, M., Zilberberg, L., Dabovic, B. & Rifkin, D. B. Latent TGF-β-binding proteins. 44–53 (2016) doi:10.1016/j.matbio.2015.05.005.

159. Paolillo, M. & Schinelli, S. Extracellular matrix alterations in metastatic processes. *Int. J. Mol. Sci.* **20**, 4947 (2019).

160. Martinez, V. G. *et al.* Fibroblastic Reticular Cells Control Conduit Matrix Deposition during Lymph Node Expansion. *Cell Rep.* **29**, 2810-2822.e5 (2019).

161. Malhotra, D. *et al.* Transcriptional profiling of stroma from inflamed and resting lymph nodes defines immunological hallmarks. *Nat. Immunol.* **13**, 499–510 (2012).

REFERENCES

162. Hamidi, H. & Ivaska, J. Every step of the way: integrins in cancer progression and metastasis. *Nat. Rev. Cancer* 1–16 (2018) doi:10.1038/s41568-018-0038-z.

163. González-González, L. & Alonso, J. Periostin: A matricellular protein with multiple functions in cancer development and progression. *Front. Oncol.* **8**, 1–15 (2018).

164. Yokosaki, Y., Monis, H., Ghen, J. & Sheppard, D. Differential effects of the integrins α9β1, αvβ3, and αvβ6 on cell proliferative responses to tenascin. Roles of the β subunit extracellular and cytoplasmic domains. *J. Biol. Chem.* **271**, 24144–24150 (1996).

165. Natale, G., Stouthandel, M. E. J., Van Hoof, T. & Bocci, G. The Lymphatic System in Breast Cancer: Anatomical and Molecular Approaches. *Medicina (Mex.)* **57**, 1272 (2021).

166. Tasdogan, A. *et al.* Metabolic heterogeneity confers differences in melanoma metastatic potential. *Nature* **577**, 115–120 (2020).

167. Wakisaka, N. *et al.* Primary tumor-secreted lymphangiogenic factors induce pre-metastatic lymphvascular niche formation at sentinel lymph nodes in oral squamous cell carcinoma. *PLoS ONE* **10**, 1–14 (2015).

168. Shen, C.-N. *et al.* Lymphatic vessel remodeling and invasion in pancreatic cancer progression. *EBioMedicine* **47**, 98–113 (2019).

169. Balsat, C. *et al.* A specific immune and lymphatic profile characterizes the pre-metastatic state of the sentinel lymph node in patients with early cervical cancer. *Oncoimmunology* **6**, (2017).

170. Cho, J. K. *et al.* Significance of lymph node metastasis in cancer dissemination of head and neck cancer. *Transl. Oncol.* **8**, 119–125 (2015).

171. Massagué, J. & Obenauf, A. C. Metastatic colonization by circulating tumour cells. *Nature* **529**, 298–306 (2016).

172. Paupert, J., Van De Velde, M., Kridelka, F. & Noël, A. Tumor Angiogenesis and Lymphangiogenesis: Microenvironmental Soil for Tumor Progression and Metastatic Dissemination. in *Molecular Mechanisms of Angiogenesis: From Ontogenesis to Oncogenesis* (eds. Feige, J.-J., Pagès, G. & Soncin, F.) 283–306 (Springer, Paris, 2014). doi:10.1007/978-2-8178-0466-8_13.

REFERENCES

173. Karaman, S. & Detmar, M. Mechanisms of lymphatic metastasis. *J. Clin. Invest.* **124**, 922–928 (2014).

174. Shayan, R. *et al.* Lymphatic vessel density in primary melanomas predicts sentinel lymph node status and risk of metastasis. *Histopathology* **61**, 702–710 (2012).

175. Wang, J. *et al.* Lymphatic microvessel density and vascular endothelial growth factor-C and -D as prognostic factors in breast cancer: a systematic review and meta-analysis of the literature. *Mol. Biol. Rep.* **39**, 11153–11165 (2012).

176. Karpanen, T. & Alitalo, K. Molecular biology and pathology of lymphangiogenesis. *Annu. Rev. Pathol.* **3**, 367–397 (2008).

177. Papetti, M. & Herman, I. M. Mechanisms of normal and tumor-derived angiogenesis. *Am. J. Physiol. Cell Physiol.* **282**, C947-970 (2002).

178. Sato, M. *et al.* Microvessel area of immature vessels is a prognostic factor in renal cell carcinoma. *Int. J. Urol. Off. J. Jpn. Urol. Assoc.* **21**, 130–134 (2014).

179. Ren, J. *et al.* Relations between GPR4 expression, microvascular density (MVD) and clinical pathological characteristics of patients with epithelial ovarian carcinoma (EOC). *Curr. Pharm. Des.* **20**, 1904–1916 (2014).

180. Stacker, S. A. *et al.* Lymphangiogenesis and lymphatic vessel remodelling in cancer. *Nat. Rev. Cancer* **14**, 159–172 (2014).

181. Sleeman, J. P. The lymph node pre-metastatic niche. *J. Mol. Med.* **93**, 1173–1184 (2015).

182. Christiansen, A. & Detmar, M. Lymphangiogenesis and Cancer. *Genes Cancer* **2**, 1146–1158 (2011).

183. Jain, R. K. Normalization of tumor vasculature: an emerging concept in antiangiogenic therapy. *Science* **307**, 58–62 (2005).

184. Mendoza, E. & Schmid-Schönbein, G. W. A model for mechanics of primary lymphatic valves. *J. Biomech. Eng.* **125**, 407–414 (2003).

185. Hoshida, T. *et al.* Imaging steps of lymphatic metastasis reveals that vascular endothelial growth factor-C increases metastasis by increasing delivery of cancer cells to lymph nodes: therapeutic implications. *Cancer Res.* **66**, 8065–8075 (2006).

REFERENCES

186. Hirakawa, S. *et al.* VEGF-A induces tumor and sentinel lymph node lymphangiogenesis and promotes lymphatic metastasis. *J. Exp. Med.* **201**, 1089–1099 (2005).

187. Hirakawa, S. *et al.* VEGF-C–induced lymphangiogenesis in sentinel lymph nodes promotes tumor metastasis to distant sites. *Blood* **109**, 1010–1017 (2007).

188. Harrell, M. I., Iritani, B. M. & Ruddell, A. Tumor-induced sentinel lymph node lymphangiogenesis and increased lymph flow precede melanoma metastasis. *Am. J. Pathol.* **170**, 774–786 (2007).

189. Qian, C.-N. *et al.* Preparing the "Soil": The Primary Tumor Induces Vasculature Reorganization in the Sentinel Lymph Node before the Arrival of Metastatic Cancer Cells. *Cancer Res.* **66**, 10365–10376 (2006).

190. Strauss, L., Volland, D., Kunkel, M. & Reichert, T. E. Dual role of VEGF family members in the pathogenesis of head and neck cancer (HNSCC): possible link between angiogenesis and immune tolerance. *Med. Sci. Monit. Int. Med. J. Exp. Clin. Res.* **11**, BR280-292 (2005).

191. Lukacs-Kornek, V. *et al.* Regulated release of nitric oxide by nonhematopoietic stroma controls expansion of the activated T cell pool in lymph nodes. *Nat. Immunol.* **12**, 1096–1104 (2011).

192. Taube, J. M. *et al.* Colocalization of inflammatory response with B7-h1 expression in human melanocytic lesions supports an adaptive resistance mechanism of immune escape. *Sci. Transl. Med.* **4**, 127ra37 (2012).

193. Topalian, S. L., Drake, C. G. & Pardoll, D. M. Targeting the PD-1/B7-H1(PD-L1) pathway to activate anti-tumor immunity. *Curr. Opin. Immunol.* **24**, 207–212 (2012).

194. Valastyan, S. & Weinberg, R. A. Tumor metastasis: molecular insights and evolving paradigms. *Cell* **147**, 275–292 (2011).

195. Langley, R. R. & Fidler, I. J. The seed and soil hypothesis revisited—The role of tumor-stroma interactions in metastasis to different organs. *Int. J. Cancer* **128**, 2527–2535 (2011).

196. Kaplan, R. N. *et al.* VEGFR1-positive haematopoietic bone marrow progenitors initiate the pre-metastatic niche. *Nature* **438**, 820–827 (2005).

REFERENCES

197. Deasy, S. K. & Erez, N. A glitch in the matrix: organ-specific matrisomes in metastatic niches. *Trends Cell Biol.* **32**, 110–123 (2022).

198. Cucanic, O., Farnsworth, R. H. & Stacker, S. A. The cellular and molecular mediators of metastasis to the lung. *Growth Factors* **40**, 119–152 (2022).

199. Psaila, B. & Lyden, D. The metastatic niche: Adapting the foreign soil. *Nat. Rev. Cancer* **9**, 285–293 (2009).

200. Padera, T. P., Meijer, E. F. J. & Munn, L. L. The Lymphatic System in Disease Processes and Cancer Progression. *Annu. Rev. Biomed. Eng.* **18**, 125–158 (2016).

201. Maru, Y. The lung metastatic niche. *J. Mol. Med.* **93**, 1185–1192 (2015).

202. Houg, D. S. & Bijlsma, M. F. The hepatic pre-metastatic niche in pancreatic ductal adenocarcinoma. *Mol. Cancer* **17**, 95 (2018).

203. Ren, G., Esposito, M. & Kang, Y. Bone metastasis and the metastatic niche. *J. Mol. Med.* **93**, 1203–1212 (2015).

204. Hirakawa, S. *et al.* VEGF-A induces tumor and sentinel lymph node lymphangiogenesis and promotes lymphatic metastasis. *J. Exp. Med.* **201**, 1089–1099 (2005).

205. Hirakawa, S. *et al.* VEGF-C-induced lymphangiogenesis in sentinel lymph nodes promotes tumor metastasis to distant sites. *Blood* **109**, 1010–1017 (2007).

206. Farnsworth, R. H., Lackmann, M., Achen, M. G. & Stacker, S. A. Vascular remodeling in cancer. *Oncogene* **33**, 3496–3505 (2014).

207. Piao, Y. J., Kim, H. S., Hwang, E. H., Woo, J. & Zhang, M. Breast cancer cell-derived exosomes and macrophage polarization are associated with lymph node metastasis. *Oncotarget* **9**, 7398–7410 (2018).

208. Tickner, J. A., Urquhart, A. J., Stephenson, S. A., Richard, D. J. & O'Byrne, K. J. Functions and therapeutic roles of exosomes in cancer. *Front. Oncol.* **4**, 1–8 (2014).

209. Plebanek, M. P. *et al.* Pre-metastatic cancer exosomes induce immune surveillance by patrolling monocytes at the metastatic niche. *Nat. Commun.* **8**, 1319 (2017).

210. Hood, J. L., San Roman, S. & Wickline, S. A. Exosomes released by melanoma cells prepare sentinel lymph nodes for tumor metastasis. *Cancer Res.* **71**, 3792–3801 (2011).

REFERENCES

211. Zhou, W. *et al.* Cancer-secreted miR-105 destroys vascular endothelial barriers to promote metastasis. *Cancer Cell* **25**, 501–515 (2014).

212. Zeng, Z. *et al.* Cancer-derived exosomal miR-25-3p promotes pre-metastatic niche formation by inducing vascular permeability and angiogenesis. *Nat. Commun.* **9**, 5395 (2018).

213. Maus, R. L. G. *et al.* Identification of novel, immune-mediating extracellular vesicles in human lymphatic effluent draining primary cutaneous melanoma. *OncoImmunology* **8**, 1–10 (2019).

214. Dieterich, L. C. Mechanisms of extracellular vesicle-mediated immune evasion in melanoma. *Front. Immunol.* **13**, (2022).

215. Broggi, M. A. S. *et al.* Tumor-associated factors are enriched in lymphatic exudate compared to plasma in metastatic melanoma patients. *J. Exp. Med.* **216**, 1091–1107 (2019).

216. Mäkinen, T. *et al.* Inhibition of lymphangiogenesis with resulting lymphedema in transgenic mice expressing soluble VEGF receptor-3. *Nat. Med.* **7**, 199–205 (2001).

217. García-Silva, S. *et al.* Use of extracellular vesicles from lymphatic drainage as surrogate markers of melanoma progression and BRAFV600E mutation. *J. Exp. Med.* **216**, 1061–1070 (2019).

218. Nogués, L., Benito-Martin, A., Hergueta-Redondo, M. & Peinado, H. The influence of tumour-derived extracellular vesicles on local and distal metastatic dissemination. *Mol. Aspects Med.* **60**, 15–26 (2018).

219. Theodoraki, M.-N., Yerneni, S. S., Hoffmann, T. K., Gooding, W. E. & Whiteside, T. L. Clinical Significance of PD-L1+ Exosomes in Plasma of Head and Neck Cancer Patients. *Clin. Cancer Res.* **24**, 896–905 (2018).

220. Sleeman, J. P. The lymph node pre-metastatic niche. *J. Mol. Med.* **93**, 1173–1184 (2015).

221. Chen, J.-Y. *et al.* Cancer-Derived VEGF-C Increases Chemokine Production in Lymphatic Endothelial Cells to Promote CXCR2-Dependent Cancer Invasion and MDSC Recruitment. *Cancers* **11**, 1120 (2019).

222. Kitamura, T., Qian, B.-Z. & Pollard, J. W. Immune cell promotion of metastasis. *Nat. Rev. Immunol.* **15**, 73–86 (2015).

REFERENCES

223. Schaller, J. & Agudo, J. Metastatic Colonization: Escaping Immune Surveillance. *Cancers* **12**, 3385 (2020).

224. Watanabe, S. *et al.* Tumor-Induced CD11b+Gr-1+ Myeloid Cells Suppress T Cell Sensitization in Tumor-Draining Lymph Nodes1. *J. Immunol.* **181**, 3291–3300 (2008).

225. Alicea-Torres, K. & Gabrilovich, D. I. Biology of Myeloid-Derived Suppressor Cells. in *Oncoimmunology: A Practical Guide for Cancer Immunotherapy* (eds. Zitvogel, L. & Kroemer, G.) 181–197 (Springer International Publishing, Cham, 2018). doi:10.1007/978-3-319-62431-0_10.

226. Vetsika, E.-K., Koukos, A. & Kotsakis, A. Myeloid-Derived Suppressor Cells: Major Figures that Shape the Immunosuppressive and Angiogenic Network in Cancer. *Cells* **8**, 1647 (2019).

227. Cochran, A. J., Huang, R.-R., Su, A., Itakura, E. & Wen, D.-R. Is Sentinel Node Susceptibility to Metastases Related to Nodal Immune Modulation? *Cancer J.* **21**, 39 (2015).

228. Lee, J. H. *et al.* Quantitative analysis of melanoma-induced cytokine-mediated immunosuppression in melanoma sentinel nodes. *Clin. Cancer Res. Off. J. Am. Assoc. Cancer Res.* **11**, 107–112 (2005).

229. Baratin, M. *et al.* T Cell Zone Resident Macrophages Silently Dispose of Apoptotic Cells in the Lymph Node. *Immunity* **47**, 349-362.e5 (2017).

230. Asano, K. *et al.* CD169-Positive Macrophages Dominate Antitumor Immunity by Crosspresenting Dead Cell-Associated Antigens. *Immunity* **34**, 85–95 (2011).

231. Strömvall, K., Sundkvist, K., Ljungberg, B., Halin Bergström, S. & Bergh, A. Reduced number of CD169+ macrophages in pre-metastatic regional lymph nodes is associated with subsequent metastatic disease in an animal model and with poor outcome in prostate cancer patients. *The Prostate* **77**, 1468–1477 (2017).

232. Pucci, F. *et al.* SCS macrophages suppress melanoma by restricting tumor-derived vesicle–B cell interactions. *Science* **352**, 242–246 (2016).

233. Gu, Y. *et al.* Tumor-educated B cells selectively promote breast cancer lymph node metastasis by HSPA4-targeting IgG. *Nat. Med.* **25**, 312–322 (2019).

REFERENCES

234. Liu, Y. & Cao, X. Immunosuppressive cells in tumor immune escape and metastasis. *J. Mol. Med.* **94**, 509–522 (2016).

235. Liu, Y. & Cao, X. Characteristics and Significance of the Pre-metastatic Niche. *Cancer Cell* **30**, 668–681 (2016).

236. J. Rouhani, S. Regulation of T-cell Tolerance by Lymphatic Endothelial Cells. *J. Clin. Cell. Immunol.* **05**, (2014).

237. Habenicht, L. M., Kirschbaum, S. B., Furuya, M., Harrell, M. I. & Ruddell, A. Tumor Regulation of Lymph Node Lymphatic Sinus Growth and Lymph Flow in Mice and in Humans. *Yale J. Biol. Med.* **90**, 403–415 (2017).

238. Petrova, T. V. & Koh, G. Y. Biological functions of lymphatic vessels. *Science* **369**, eaax4063 (2020).

239. Lund, A. W. *et al.* VEGF-C Promotes Immune Tolerance in B16 Melanomas and Cross-Presentation of Tumor Antigen by Lymph Node Lymphatics. *Cell Rep.* **1**, 191–199 (2012).

240. Pal, S. K. *et al.* Clinical and Translational Assessment of VEGFR1 as a Mediator of the Premetastatic Niche in High-Risk Localized Prostate Cancer. *Mol. Cancer Ther.* **14**, 2896–2900 (2015).

241. Fujita, S., Sumi, M., Tatsukawa, E., Nagano, K. & Katase, N. Expressions of extracellular matrix-remodeling factors in lymph nodes from oral cancer patients. *Oral Dis.* **26**, 1424–1431 (2020).

242. Chung, M. K. *et al.* Lymphatic Vessels and High Endothelial Venules are Increased in the Sentinel Lymph Nodes of Patients with Oral Squamous Cell Carcinoma Before the Arrival of Tumor Cells. *Ann. Surg. Oncol.* **19**, 1595–1601 (2012).

243. Bekkhus, T. *et al.* Remodeling of the Lymph Node High Endothelial Venules Reflects Tumor Invasiveness in Breast Cancer and is Associated with Dysregulation of Perivascular Stromal Cells. *Cancers* **13**, 211 (2021).

244. du Bois, H., Heim, T. A. & Lund, A. W. Tumor-draining lymph nodes: At the crossroads of metastasis and immunity. *Sci. Immunol.* **6**, eabg3551 (2021).

245. Acton, S. E. *et al.* Podoplanin-Rich Stromal Networks Induce Dendritic Cell Motility via Activation of the C-type Lectin Receptor CLEC-2. *Immunity* **37**, 276–289 (2012).

REFERENCES

246. He, M. *et al.* Role of lymphatic endothelial cells in the tumor microenvironment—a narrative review of recent advances. *Transl. Lung Cancer Res.* **10**, 2252–2277 (2021).

247. Milutinovic, S., Abe, J., Godkin, A., Stein, J. V. & Gallimore, A. The Dual Role of High Endothelial Venules in Cancer Progression versus Immunity. *Trends Cancer* **7**, 214–225 (2021).

248. Riedel, A., Shorthouse, D., Haas, L., Hall, B. A. & Shields, J. Tumor-induced stromal reprogramming drives lymph node transformation. *Nat. Immunol.* **17**, 1118–1127 (2016).

249. Jeong, H.-S. *et al.* Investigation of the Lack of Angiogenesis in the Formation of Lymph Node Metastases. *JNCI J. Natl. Cancer Inst.* **107**, djv155 (2015).

250. Lucas, E. D. *et al.* Type 1 IFN and PD-L1 Coordinate Lymphatic Endothelial Cell Expansion and Contraction during an Inflammatory Immune Response. *J. Immunol.* **201**, 1735–1747 (2018).

251. Cochran, A. J., Wen, D. R. & Morton, D. L. Occult tumor cells in the lymph nodes of patients with pathological stage I malignant melanoma. An immunohistological study. *Am. J. Surg. Pathol.* **12**, 612–618 (1988).

252. Tacconi, C. *et al.* CD169+ lymph node macrophages have protective functions in mouse breast cancer metastasis. *Cell Rep.* **35**, (2021).

253. Ulvmar, M. H. *et al.* The atypical chemokine receptor CCRL1 shapes functional CCL21 gradients in lymph nodes. *Nat. Immunol.* **15**, 623–630 (2014).

254. Emmett, M. S., Lanati, S., Dunn, D. B. a., Stone, O. A. & Bates, D. O. CCR7 Mediates Directed Growth of Melanomas Towards Lymphatics. *Microcirculation* **18**, 172–182 (2011).

255. Ogawa, F. *et al.* Prostanoid induces premetastatic niche in regional lymph nodes. *J. Clin. Invest.* **124**, 4882–4894 (2014).

256. Pul, K. M. van *et al.* Selectively hampered activation of lymph node-resident dendritic cells precedes profound T cell suppression and metastatic spread in the breast cancer sentinel lymph node. *J. Immunother. Cancer* **7**, 133 (2019).

257. Núñez, N. G. *et al.* Tumor invasion in draining lymph nodes is associated with Treg accumulation in breast cancer patients. *Nat. Commun.* **11**, 3272 (2020).

REFERENCES

258. Deng, L. *et al.* Accumulation of Foxp3+ T Regulatory Cells in Draining Lymph Nodes Correlates with Disease Progression and Immune Suppression in Colorectal Cancer Patients. *Clin. Cancer Res.* **16**, 4105–4112 (2010).

259. Allen, B. M. *et al.* Systemic dysfunction and plasticity of the immune macroenvironment in cancer models. *Nat. Med.* **26**, 1125–1134 (2020).

260. Chen, M.-L. *et al.* Regulatory T cells suppress tumor-specific CD8 T cell cytotoxicity through TGF-β signals in vivo. *Proc. Natl. Acad. Sci.* **102**, 419–424 (2005).

261. Bekkhus, T. *et al.* Remodeling of the Lymph Node High Endothelial Venules Reflects Tumor Invasiveness in Breast Cancer and is Associated with Dysregulation of Perivascular Stromal Cells. *Cancers* **13**, 211 (2021).

262. Kubiczkova, L., Sedlarikova, L., Hajek, R. & Sevcikova, S. TGF-β – an excellent servant but a bad master. *J. Transl. Med.* **10**, 183 (2012).

263. Moses, H. L., Roberts, A. B. & Derynck, R. The discovery and early days of TGF-b: A historical perspective. *Cold Spring Harb. Perspect. Biol.* **8**, (2016).

264. Tzavlaki, K. & Moustakas, A. TGF-β Signaling. *Biomolecules* **10**, 487 (2020).

265. David, C. J. & Massagué, J. Contextual determinants of TGFβ action in development, immunity and cancer. *Nat. Rev. Mol. Cell Biol.* **19**, 419–435 (2018).

266. Morikawa, M., Derynck, R. & Miyazono, K. TGF- β and the TGF-β family: Context-dependent roles in cell and tissue physiology. *Cold Spring Harb. Perspect. Biol.* **8**, (2016).

267. Kreidl, E., Öztürk, D., Metzner, T., Berger, W. & Grusch, M. Activins and follistatins: Emerging roles in liver physiology and cancer. *World J. Hepatol.* **1**, 17–27 (2009).

268. Peng, J. *et al.* Growth differentiation factor 9:bone morphogenetic protein 15 heterodimers are potent regulators of ovarian functions. *Proc. Natl. Acad. Sci.* **110**, E776–E785 (2013).

269. Valera, E., Isaacs, M. J., Kawakami, Y., Belmonte, J. C. I. & Choe, S. BMP-2/6 Heterodimer Is More Effective than BMP-2 or BMP-6 Homodimers as Inductor of Differentiation of Human Embryonic Stem Cells. *PLOS ONE* **5**, e11167 (2010).

270. Huang, T., Schor, S. L. & Hinck, A. P. Biological Activity Differences between TGF-β1 and TGF-β3 Correlate with Differences in the Rigidity and Arrangement of Their Component Monomers. *Biochemistry* **53**, 5737–5749 (2014).

REFERENCES

271. Kaartinen, V. *et al.* Abnormal lung development and cleft palate in mice lacking TGF–β3 indicates defects of epithelial–mesenchymal interaction. *Nat. Genet.* **11**, 415–421 (1995).

272. Sanford, L. P. *et al.* TGFbeta2 knockout mice have multiple developmental defects that are non-overlapping with other TGFbeta knockout phenotypes. *Dev. Camb. Engl.* **124**, 2659–2670 (1997).

273. Hinck, A. P., Mueller, T. D. & Springer, T. A. Structural Biology and Evolution of the TGF-β Family. *Cold Spring Harb. Perspect. Biol.* **8**, a022103 (2016).

274. De Streel, G. & Lucas, S. Targeting immunosuppression by TGF-β1 for cancer immunotherapy. *Biochem. Pharmacol.* **192**, 114697 (2021).

275. Travis, M. A. & Sheppard, D. TGF-β Activation and Function in Immunity. *Annu. Rev. Immunol.* **32**, 51–82 (2014).

276. Duan, Z. *et al.* Specificity of TGF-β1 signal designated by LRRC33 and integrin αVβ8. *Nat. Commun.* **13**, 4988 (2022).

277. Robertson, I. B. & Rifkin, D. B. Unchaining the beast; insights from structural and evolutionary studies on TGFβ secretion, sequestration, and activation. *Cytokine Growth Factor Rev.* **24**, 355–372 (2013).

278. Godwin, A. R. F. *et al.* The role of fibrillin and microfibril binding proteins in elastin and elastic fibre assembly. *Matrix Biol.* **84**, 17–30 (2019).

279. Liénart, S. *et al.* Structural basis of latent TGF-β1 presentation and activation by GARP on human regulatory T cells. *Science* **362**, 952–956 (2018).

280. Stockis, J., Colau, D., Coulie, P. G. & Lucas, S. Membrane protein GARP is a receptor for latent TGF-β on the surface of activated human Treg: Cellular immune response. *Eur. J. Immunol.* **39**, 3315–3322 (2009).

281. Tran, D. Q. *et al.* GARP (LRRC32) is essential for the surface expression of latent TGF-beta on platelets and activated FOXP3+ regulatory T cells. *Proc. Natl. Acad. Sci. U. S. A.* **106**, 13445–13450 (2009).

282. Dedobbeleer, O., Stockis, J., Van Der Woning, B., Coulie, P. G. & Lucas, S. Cutting Edge: Active TGF-β1 Released from GARP/TGF-β1 Complexes on the Surface of Stimulated Human B Lymphocytes Increases Class-Switch Recombination and Production of IgA. *J. Immunol.* **199**, 391–396 (2017).

REFERENCES

283. De Streel, G. *et al.* Selective inhibition of TGF-β1 produced by GARP-expressing Tregs overcomes resistance to PD-1/PD-L1 blockade in cancer. *Nat. Commun.* **11**, 4545 (2020).

284. Vermeersch, E. *et al.* The role of platelet and endothelial GARP in thrombosis and hemostasis. *PloS One* **12**, e0173329 (2017).

285. Cuende, J. *et al.* Monoclonal antibodies against GARP/TGF-β1 complexes inhibit the immunosuppressive activity of human regulatory T cells in vivo. *Sci. Transl. Med.* **7**, (2015).

286. Barbet, R., Peiffer, I., Hatzfeld, A., Charbord, P. & Hatzfeld, J. A. Comparison of Gene Expression in Human Embryonic Stem Cells, hESC-Derived Mesenchymal Stem Cells and Human Mesenchymal Stem Cells. *Stem Cells Int.* **2011**, 368192 (2011).

287. Carrillo-Galvez, A. B. *et al.* Mesenchymal stromal cells express GARP/LRRC32 on their surface: effects on their biology and immunomodulatory capacity. *Stem Cells Dayt. Ohio* **33**, 183–195 (2015).

288. Li, Y. *et al.* Hepatic Stellate Cells Inhibit T Cells through Active TGF-β1 from a Cell Surface-Bound Latent TGF-β1/GARP Complex. *J. Immunol. Baltim. Md 1950* **195**, 2648–2656 (2015).

289. Qin, Y. *et al.* A Milieu Molecule for TGF-β Required for Microglia Function in the Nervous System. *Cell* **174**, 156-171.e16 (2018).

290. Derynck, R. & Budi, E. H. Specificity, versatility, and control of TGF-β family signaling. *Sci. Signal.* **12**, eaav5183 (2019).

291. Xie, F., Ling, L., van Dam, H., Zhou, F. & Zhang, L. TGF-β signaling in cancer metastasis. *Acta Biochim. Biophys. Sin.* **50**, 121–132 (2018).

292. Miyazawa, K. & Miyazono, K. Regulation of TGF-β Family Signaling by Inhibitory Smads. *Cold Spring Harb. Perspect. Biol.* **9**, a022095 (2017).

293. Stockis, J., Dedobbeleer, O. & Lucas, S. Role of GARP in the activation of latent TGF-β1. *Mol. Biosyst.* **13**, 1925–1935 (2017).

294. Lodyga, M. & Hinz, B. TGF-β1 - A truly transforming growth factor in fibrosis and immunity. *Semin. Cell Dev. Biol.* **101**, 123–139 (2020).

REFERENCES

295. Robertson, I. B. *et al.* Latent TGF-β-binding proteins. *Matrix Biol. J. Int. Soc. Matrix Biol.* **47**, 44–53 (2015).

296. Guerrero, P. A. & McCarty, J. H. TGF-β Activation and Signaling in Angiogenesis. in *Physiologic and Pathologic Angiogenesis - Signaling Mechanisms and Targeted Therapy* (eds. Simionescu, D. & Simionescu, A.) (InTech, 2017). doi:10.5772/66405.

297. Xie, F., Zhang, Z., van Dam, H., Zhang, L. & Zhou, F. Regulation of TGF-β Superfamily Signaling by SMAD Mono-Ubiquitination. *Cells* **3**, 981–993 (2014).

298. Nickel, J., Ten Dijke, P. & Mueller, T. D. TGF-β family co-receptor function and signaling. *Acta Biochim. Biophys. Sin.* **50**, 12–36 (2018).

299. Bernabeu, C., Lopez-Novoa, J. M. & Quintanilla, M. The emerging role of TGF-β superfamily coreceptors in cancer. *Biochim. Biophys. Acta BBA - Mol. Basis Dis.* **1792**, 954–973 (2009).

300. Lee, M. K. *et al.* TGF-beta activates Erk MAP kinase signalling through direct phosphorylation of ShcA. *EMBO J.* **26**, 3957–3967 (2007).

301. Hawke, L. G., Mitchell, B. Z. & Ormiston, M. L. TGF-β and IL-15 Synergize through MAPK Pathways to Drive the Conversion of Human NK Cells to an Innate Lymphoid Cell 1-like Phenotype. *J. Immunol. Baltim. Md 1950* **204**, 3171–3181 (2020).

302. Zhang, Y. E. Non-Smad Signaling Pathways of the TGF-β Family. *Cold Spring Harb. Perspect. Biol.* **9**, a022129 (2017).

303. Xu, P., Lin, X. & Feng, X.-H. Posttranslational Regulation of Smads. *Cold Spring Harb. Perspect. Biol.* **8**, a022087 (2016).

304. Zhang, Y., Alexander, P. B. & Wang, X.-F. TGF-β Family Signaling in the Control of Cell Proliferation and Survival. *Cold Spring Harb. Perspect. Biol.* **9**, a022145 (2017).

305. Ollendorff, V., Szepetowski, P., Mattei, M. G., Gaudray, P. & Birnbaum, D. New gene in the homologous human 11q13-q14 and mouse 7F chromosomal regions. *Mamm. Genome Off. J. Int. Mamm. Genome Soc.* **2**, 195–200 (1992).

306. Roubin, R. *et al.* Structure and developmental expression of mouse Garp, a gene encoding a new leucine-rich repeat-containing protein. *Int. J. Dev. Biol.* **40**, 545–555 (1996).

REFERENCES

307. Ollendorff, V., Noguchi, T., deLapeyriere, O. & Birnbaum, D. The GARP gene encodes a new member of the family of leucine-rich repeat-containing proteins. *Cell Growth Differ. Mol. Biol. J. Am. Assoc. Cancer Res.* **5**, 213–219 (1994).

308. Probst-Kepper, M. *et al.* GARP: a key receptor controlling FOXP3 in human regulatory T cells. *J. Cell. Mol. Med.* **13**, 3343–3357 (2009).

309. Matsushima, N. *et al.* Comparative sequence analysis of leucine-rich repeats (LRRs) within vertebrate toll-like receptors. *BMC Genomics* **8**, 124 (2007).

310. Ng, A. C. Y. *et al.* Human leucine-rich repeat proteins: a genome-wide bioinformatic categorization and functional analysis in innate immunity. *Proc. Natl. Acad. Sci. U. S. A.* **108 Suppl 1**, 4631–4638 (2011).

311. Kobe, B. & Kajava, A. V. The leucine-rich repeat as a protein recognition motif. *Curr. Opin. Struct. Biol.* **11**, 725–732 (2001).

312. de Wit, J. & Ghosh, A. Control of neural circuit formation by leucine-rich repeat proteins. *Trends Neurosci.* **37**, 539–550 (2014).

313. Zhang, Y. *et al.* GP96 is a GARP chaperone and controls regulatory T cell functions. *J. Clin. Invest.* **125**, 859–869 (2015).

314. Wang, R. *et al.* GARP regulates the bioavailability and activation of TGFβ. *Mol. Biol. Cell* **23**, 1129–1139 (2012).

315. Sakaguchi, S. *et al.* Regulatory T Cells and Human Disease. *Annu. Rev. Immunol.* **38**, 541–566 (2020).

316. Hadaschik, E. N. *et al.* Regulatory T cell-deficient scurfy mice develop systemic autoimmune features resembling lupus-like disease. *Arthritis Res. Ther.* **17**, 35 (2015).

317. Fu, S. *et al.* TGF-beta induces Foxp3 + T-regulatory cells from CD4 + CD25 - precursors. *Am. J. Transplant. Off. J. Am. Soc. Transplant. Am. Soc. Transpl. Surg.* **4**, 1614–1627 (2004).

318. Batlle, E. & Massagué, J. Transforming Growth Factor-β Signaling in Immunity and Cancer. *Immunity* **50**, 924–940 (2019).

319. Wolfraim, L. A., Walz, T. M., James, Z., Fernandez, T. & Letterio, J. J. p21Cip1 and p27Kip1 act in synergy to alter the sensitivity of naive T cells to TGF-beta-mediated

G1 arrest through modulation of IL-2 responsiveness. *J. Immunol. Baltim. Md 1950* **173**, 3093–3102 (2004).

320. Stockis, J. *et al.* Blocking immunosuppression by human Tregs in vivo with antibodies targeting integrin αVβ8. *Proc. Natl. Acad. Sci.* **114**, (2017).

321. Wang, R. *et al.* Expression of GARP selectively identifies activated human FOXP3+ regulatory T cells. *Proc. Natl. Acad. Sci. U. S. A.* **106**, 13439–13444 (2009).

322. Hahn, S. A. *et al.* A key role of GARP in the immune suppressive tumor microenvironment. *Oncotarget* **7**, 42996–43009 (2016).

323. Lam, A. J., Uday, P., Gillies, J. K. & Levings, M. K. Helios is a marker, not a driver, of human Treg stability. *Eur. J. Immunol.* **52**, 75–84 (2022).

324. Kuhn, C., Rezende, R. M., M'Hamdi, H., da Cunha, A. P. & Weiner, H. L. IL-6 Inhibits Upregulation of Membrane-Bound TGF-β 1 on CD4+ T Cells and Blocking IL-6 Enhances Oral Tolerance. *J. Immunol. Baltim. Md 1950* **198**, 1202–1209 (2017).

325. Edwards, J. P. *et al.* Regulation of the expression of GARP/latent TGF-β1 complexes on mouse T cells and their role in regulatory T cell and Th17 differentiation. *J. Immunol. Baltim. Md 1950* **190**, 5506–5515 (2013).

326. Haupt, S., Söntgerath, V. S. A., Leipe, J., Schulze-Koops, H. & Skapenko, A. Methylation of an intragenic alternative promoter regulates transcription of GARP. *Biochim. Biophys. Acta* **1859**, 223–234 (2016).

327. Downs-Canner, S. *et al.* Suppressive IL-17A+Foxp3+ and ex-Th17 IL-17AnegFoxp3+ Treg cells are a source of tumour-associated Treg cells. *Nat. Commun.* **8**, 14649 (2017).

328. Pu, M. *et al.* Regulatory network of miRNA on its target: coordination between transcriptional and post-transcriptional regulation of gene expression. *Cell. Mol. Life Sci. CMLS* **76**, 441–451 (2019).

329. Liu, C., Li, N. & Liu, G. The Role of MicroRNAs in Regulatory T Cells. *J. Immunol. Res.* **2020**, e3232061 (2020).

330. Gauthy, E. *et al.* GARP is regulated by miRNAs and controls latent TGF-β1 production by human regulatory T cells. *PloS One* **8**, e76186 (2013).

REFERENCES

331. Jebbawi, F. *et al.* A microRNA profile of human CD8+ regulatory T cells and characterization of the effects of microRNAs on Treg cell-associated genes. *J. Transl. Med.* **12**, 218 (2014).

332. Yang, Z. *et al.* Absence of integrin-mediated TGFβ1 activation in vivo recapitulates the phenotype of TGFβ1-null mice. *J. Cell Biol.* **176**, 787–793 (2007).

333. Nieberler, M. *et al.* Exploring the Role of RGD-Recognizing Integrins in Cancer. *Cancers* **9**, 116 (2017).

334. Shi, M. *et al.* Latent TGF-β structure and activation. *Nature* **474**, 343–349 (2011).

335. Munger, J. S. *et al.* The integrin alpha v beta 6 binds and activates latent TGF beta 1: a mechanism for regulating pulmonary inflammation and fibrosis. *Cell* **96**, 319–328 (1999).

336. Dong, X. *et al.* Force interacts with macromolecular structure in activation of TGF-β. *Nature* **542**, 55–59 (2017).

337. Campbell, M. G. *et al.* Cryo-EM Reveals Integrin-Mediated TGF-β Activation without Release from Latent TGF-β. *Cell* **180**, 490-501.e16 (2020).

338. Zimmer, N., Trzeciak, E. R., Graefen, B., Satoh, K. & Tuettenberg, A. GARP as a Therapeutic Target for the Modulation of Regulatory T Cells in Cancer and Autoimmunity. *Front. Immunol.* **13**, 928450 (2022).

339. Manz, J. *et al.* Targeted Resequencing and Functional Testing Identifies Low-Frequency Missense Variants in the Gene Encoding GARP as Significant Contributors to Atopic Dermatitis Risk. *J. Invest. Dermatol.* **136**, 2380–2386 (2016).

340. Bonné-Tamir, B. *et al.* Usher syndrome in the Samaritans: strengths and limitations of using inbred isolated populations to identify genes causing recessive disorders. *Am. J. Phys. Anthropol.* **104**, 193–200 (1997).

341. Bekri, S. *et al.* Detailed map of a region commonly amplified at 11q13-->q14 in human breast carcinoma. *Cytogenet. Cell Genet.* **79**, 125–131 (1997).

342. Ahlemann, M. *et al.* Carcinoma-associated eIF3i overexpression facilitates mTOR-dependent growth transformation. *Mol. Carcinog.* **45**, 957–967 (2006).

343. Edwards, J., Krishna, N. S., Witton, C. J. & Bartlett, J. M. S. Gene amplifications associated with the development of hormone-resistant prostate cancer. *Clin. Cancer Res. Off. J. Am. Assoc. Cancer Res.* **9**, 5271–5281 (2003).

REFERENCES

344. Maire, G. *et al.* 11q13 alterations in two cases of hibernoma: large heterozygous deletions and rearrangement breakpoints near GARP in 11q13.5. *Genes. Chromosomes Cancer* **37**, 389–395 (2003).

345. Zimmer, N., Trzeciak, E. R., Graefen, B., Satoh, K. & Tuettenberg, A. GARP as a Therapeutic Target for the Modulation of Regulatory T Cells in Cancer and Autoimmunity. *Front. Immunol.* **13**, 928450 (2022).

346. Van De Velde, M., García-Caballero, M., Durré, T., Kridelka, F. & Noël, A. Ear Sponge Assay: A Method to Investigate Angiogenesis and Lymphangiogenesis in Mice. in *Proteases and Cancer* (eds. Cal, S. & Obaya, A. J.) vol. 1731 223–233 (Springer New York, New York, NY, 2018).

347. Zhao, B., Smith, G., Cai, J., Ma, A. & Boulton, M. Vascular endothelial growth factor C promotes survival of retinal vascular endothelial cells via vascular endothelial growth factor receptor-2. *Br. J. Ophthalmol.* **91**, 538–545 (2007).

348. Rouaud, L. *et al.* Spatial Distribution of Non-Immune Cells Expressing Glycoprotein A Repetitions Predominant in Human and Murine Metastatic Lymph Nodes. *Cancers* **15**, 5621 (2023).

349. Psaila, B. & Lyden, D. The metastatic niche: adapting the foreign soil. *Nat. Rev. Cancer* **9**, 285–293 (2009).

350. De Streel, G. & Lucas, S. Targeting immunosuppression by TGF-β1 for cancer immunotherapy. *Biochem. Pharmacol.* **192**, 114697 (2021).

351. Zhang, X. *et al.* GARP on hepatic stellate cells is essential for the development of liver fibrosis. *J. Hepatol.* **79**, 1214–1225 (2023).

352. Bertrand, C. *et al.* Combined Blockade of GARP:TGF-β1 and PD-1 Increases Infiltration of T Cells and Density of Pericyte-Covered GARP+ Blood Vessels in Mouse MC38 Tumors. *Front. Immunol.* **12**, 704050 (2021).

353. Abe, M. *et al.* An Assay for Transforming Growth Factor-β Using Cells Transfected with a Plasminogen Activator Inhibitor-1 Promoter-Luciferase Construct. *Anal. Biochem.* **216**, 276–284 (1994).

354. Samarakoon, R., Higgins, S. P., Higgins, C. E. & Higgins, P. J. TGF-β1-induced plasminogen activator inhibitor-1 expression in vascular smooth muscle cells

requires pp60c-src/EGFRY845 and Rho/ROCK signaling. *J. Mol. Cell. Cardiol.* **44**, 527–538 (2008).

355. Samarakoon, R., Higgins, C. E., Higgins, S. P., Kutz, S. M. & Higgins, P. J. Plasminogen activator inhibitor type-1 gene expression and induced migration in TGF-beta1-stimulated smooth muscle cells is pp60(c-src)/MEK-dependent. *J. Cell. Physiol.* **204**, 236–246 (2005).

356. García-Caballero, M. *et al.* Modeling pre-metastatic lymphvascular niche in the mouse ear sponge assay. *Sci. Rep.* **7**, 41494 (2017).

357. Gillot, L. *et al.* Periostin in lymph node pre-metastatic niches governs lymphatic endothelial cell functions and metastatic colonization. *Cell. Mol. Life Sci.* **79**, 295 (2022).

358. Metelli, A. *et al.* Immunoregulatory functions and the therapeutic implications of GARP-TGF-β in inflammation and cancer. *J. Hematol. Oncol.J Hematol Oncol* **11**, 24 (2018).

359. Lahimchi, M. R., Eslami, M. & Yousefi, B. New insight into GARP striking role in cancer progression: application for cancer therapy. *Med. Oncol.* **40**, 33 (2022).

360. Bouchard, A., Collin, B., Garrido, C., Bellaye, P.-S. & Kohli, E. GARP: A Key Target to Evaluate Tumor Immunosuppressive Microenvironment. *Biology* **10**, 836 (2021).

361. Van de Velde, M. *et al.* Tumor exposed-lymphatic endothelial cells promote primary tumor growth via IL6. *Cancer Lett.* **497**, 154–164 (2021).

362. Takeda, A., Salmi, M. & Jalkanen, S. Lymph node lymphatic endothelial cells as multifaceted gatekeepers in the immune system. *Trends Immunol.* **44**, 72–86 (2023).

363. Veerman, K., Tardiveau, C., Martins, F., Coudert, J. & Girard, J.-P. Single-Cell Analysis Reveals Heterogeneity of High Endothelial Venules and Different Regulation of Genes Controlling Lymphocyte Entry to Lymph Nodes. *Cell Rep.* **26**, 3116-3131.e5 (2019).

364. Hahn, S. A. *et al.* Soluble GARP has potent antiinflammatory and immunomodulatory impact on human CD4+ T cells. *Blood* **122**, 1182–1191 (2013).

365. Fridrich, S. *et al.* How Soluble GARP Enhances TGFβ Activation. *PLOS ONE* **11**, e0153290 (2016).

REFERENCES

366. Metelli, A. *et al.* Surface Expression of TGFβ Docking Receptor GARP Promotes Oncogenesis and Immune Tolerance in Breast Cancer. *Cancer Res.* **76**, 7106–7117 (2016).

367. Bejarano, L., Jordāo, M. J. C. & Joyce, J. A. Therapeutic Targeting of the Tumor Microenvironment. *Cancer Discov.* **11**, 933–959 (2021).

368. Seed, R. I. & Nishimura, S. L. Measurement of Cell Intrinsic TGF-β Activation Mediated by the Integrin αvβ8. *Bio-Protoc.* **12**, e4385 (2022).
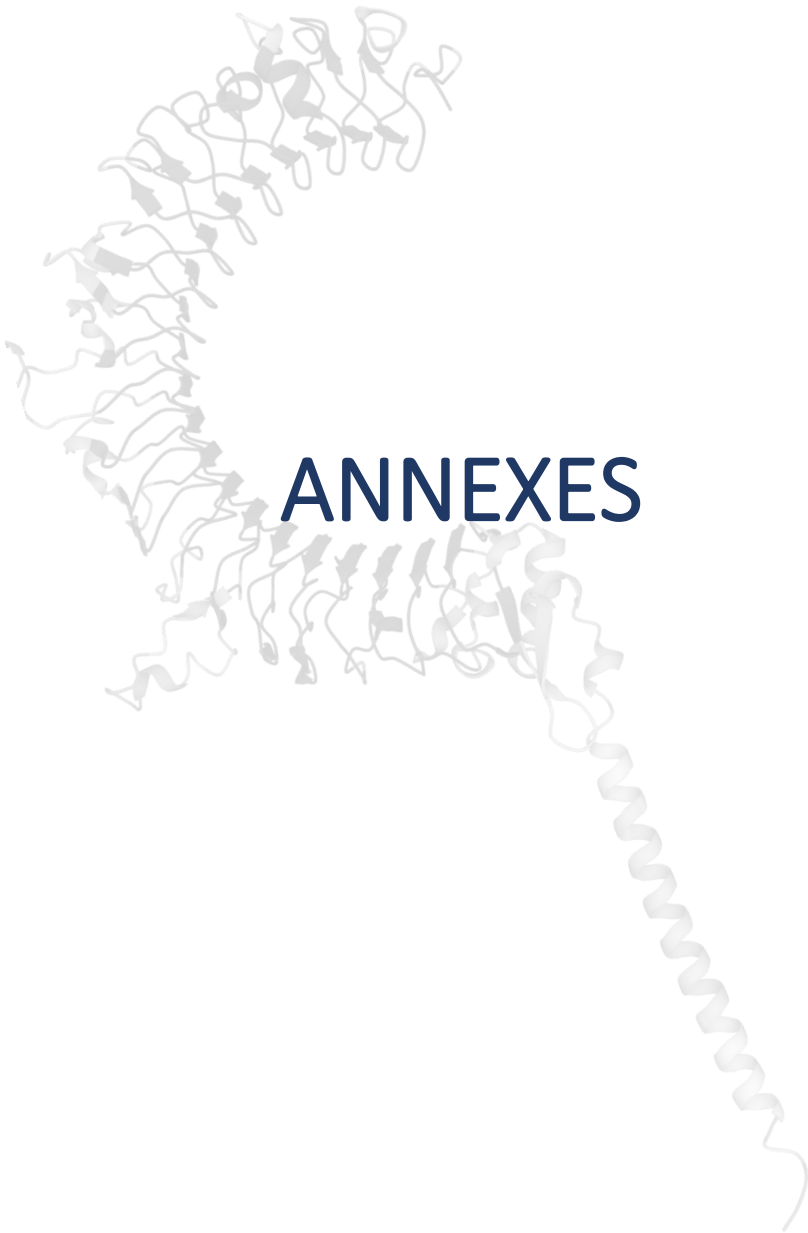
ANNEXES

Annex n°1: Combined Blockade of GARP:TGF-β1 and PD-1 Increases Infiltration of T Cells and Density of Pericyte-Covered GARP+ Blood Vessels in Mouse MC38 Tumors

Charlotte Bertrand, Pierre Van Meerbeeck, Grégoire de Streel, Noora Vaherto-Bleeckx, Fatima Benhaddi, **Loïc Rouaud**, Agnès Noël, Pierre G. Coulie, Nicolas van Baren and Sophie Lucas.

Combined Blockade of GARP:TGF-β1 and PD-1 Increases Infiltration of T Cells and Density of Pericyte-Covered GARP⁺ Blood Vessels in Mouse MC38 Tumors

Charlotte Bertrand[1], Pierre Van Meerbeeck[1], Grégoire de Streel[1], Noora Vaherto-Bleeckx[1], Fatima Benhaddi[1], Loïc Rouaud[2], Agnès Noël[2], Pierre G. Coulie[1], Nicolas van Baren[1] and Sophie Lucas[1,3]*

[1] de Duve Institute, Université Catholique de Louvain, Brussels, Belgium, [2] GIGA-Cancer Research Center, University of Liège, Liège, Belgium, [3] Walloon Excellence in Life Sciences and Biotechnology (WELBIO), Wavre, Belgium

When combined with anti-PD-1, monoclonal antibodies (mAbs) against GARP:TGF-β1 complexes induced more frequent immune-mediated rejections of CT26 and MC38 murine tumors than anti-PD-1 alone. In both types of tumors, the activity of anti-GARP: TGF-β1 mAbs resulted from blocking active TGF-β1 production and immunosuppression by GARP-expressing regulatory T cells. In CT26 tumors, combined GARP:TGF-β1/PD-1 blockade did not augment the infiltration of T cells, but did increase the effector functions of already present anti-tumor T cells. Here we show that, in contrast, in MC38, combined GARP:TGF-β1/PD-1 blockade increased infiltration of T cells, as a result of increased extravasation of T cells from blood vessels. Unexpectedly, combined GARP:TGF-β1/PD-1 blockade also increased the density of GARP⁺ blood vessels covered by pericytes in MC38, but not in CT26 tumors. This appears to occur because anti-GARP:TGF-β1, by blocking TGF-β1 signals, favors the proliferation of and expression of adhesion molecules such as E-selectin by blood endothelial cells. The resulting densification of intratumoral blood vasculature probably contributes to increased T cell infiltration and to the therapeutic efficacy of GARP:TGF-β1/PD-1 blockade in MC38. We conclude from these distinct observations in MC38 and CT26, that the combined blockades of GARP: TGF-β1 and PD-1 can exert anti-tumor activity *via* multiple mechanisms, including the densification and normalization of intratumoral blood vasculature, the increase of T cell infiltration into the tumor and the increase of the effector functions of intratumoral tumor-specific T cells. This may prove important for the selection of cancer patients who could benefit from combined GARP:TGF-β1/PD-1 blockade in the clinics.

Keywords: GARP, TGF-β1, cancer immunotherapy, immunosuppression, immune checkpoint inhibition

ANNEXES

Bertrand et al.   Mechanisms of Combined GARP:TGF-β1/PD-1 Blockade

INTRODUCTION

TGF-β1 is a potent immunosuppressive cytokine produced by most cells in an inactive, latent form. In its latent form, the mature TGF-β1 dimer is non-covalently associated to the Latency Associated Peptide (LAP), which prevents receptor binding and signaling by the cytokine. Some cell types can activate latent TGF-β1 in response to various stimuli by releasing mature TGF-β1 from LAP, *via* cell-type specific mechanisms. Regulatory T cells (Tregs) stimulated through the T cell receptor (TCR) produce latent TGF-β1 covalently linked to transmembrane protein GARP. Presentation of GARP:(latent)TGF-β1 complexes, and the interaction with integrin αVβ8 on the surface of TCR-stimulated Tregs, leads to TGF-β1 activation and autocrine or short-distance paracrine TGF-β1 activity (1–4). In cancer patients, Tregs can exert detrimental immunosuppression and thus limit the efficacy of immunotherapy (5, 6).

We previously developed monoclonal antibodies (mAbs) that bind GARP:TGF-β1 complexes and block TGF-β1 activation and immunosuppression by human or mouse Tregs (4, 7, 8). Anti-GARP:TGF-β1 mAbs inhibited the immunosuppressive function of human Tregs in a xenogeneic model of graft-versus-host disease induced by the transfer of human PBMCs in NSG mice (7). More recently, we reported that anti-GARP:TGF-β1 combined with anti-PD-1 induced immune-mediated rejections of CT26 and MC38 tumors resistant to anti-PD-1 alone (8). Blocking TGF-β1 activation by GARP-expressing Tregs was sufficient for anti-GARP:TGF-β1 to overcome resistance to anti-PD-1 in these tumor models. Indeed, the anti-tumor activity of combined GARP:TGF-β1/PD-1 blockade: i) occurred without Treg depletion, ii) was observed using anti-GARP:TGF-β1 incapable of binding Fcγ receptors, and iii) was lost in MC38 tumor-bearing mice carrying a Treg-specific deletion of the *Garp* gene (8). In contrast, blocking TGF-β1 activation by GARP-expressing platelets was not required, as anti-tumor activity of combined GARP:TGF-β1/PD-1 blockade was conserved in MC38 tumor-bearing mice carrying a platelet-specific deletion of the *Garp* gene. Thus, in MC38, the predominant source of active TGF-β1 that needs to be blocked by anti-GARP:TGF-β1 to overcome resistance to anti-PD-1 are Tregs, but not platelets (8).

Further characterizing its mode of action, we observed that combined GARP:TGF-β1/PD-1 blockade increased the effector functions of anti-tumor CD8 T cells already present within CT26 tumors, without augmenting the immune cell infiltration (8). Together with our observation that GARP-expressing Tregs are found mostly in human melanoma metastases that are already infiltrated by activated T cells, this led us to suggest testing anti-GARP:TGF-β1 to overcome resistance to PD-1/PD-L1 blockade in patients with inflamed tumors.

Different modes of action were proposed to explain the anti-tumor activity of PD-1/PD-L1 blockade combined with mAbs that block latent TGF-β1 activation (9) or neutralize all three TGF-β1, β2 and β3 isoforms (10, 11). In these reports, infiltration of immune cells in tumors was increased as a consequence of either increased CD8 T cell entry from blood vessels (9), or reduced TGF-β1 signaling in stromal fibroblasts

with subsequent increased CD8 T cell penetration towards the center of tumors (10, 12). The variations in the mode of action could result from the different tumor models that were used in our laboratories, or from the different cellular sources of TGF-β activity that were blocked by the mAbs. While anti-GARP:TGF-β1 selectively blocks TGF-β1 released from GARP-expressing cells, other mAbs block TGF-β1 activation, or neutralize the activity of all three TGF-β isoforms, whatever their cellular source. It is noteworthy that in addition to Tregs, murine and human endothelial cells and platelets do also express surface GARP:TGF-β1 complexes. Anti-GARP:TGF-β1 mAbs could thus exert anti-tumor activities *via* multiple modes of action, by directly or indirectly targeting different cell types depending on the tumor microenvironment (2, 8, 13).

We thus resorted to determine if the anti-tumor activity of combined GARP:TGF-β1/PD-1 blockade could encompass other mechanisms than increasing the effector functions of anti-tumor CD8 T cells already present within tumors, as observed in CT26.

MATERIALS AND METHODS

Mice

BALB/c and C57BL/6 mice were bred at the SPF animal facility of the UCLouvain. The facility is controlled to maintain the temperature between 20 and 24°C; humidity rate between 40 and 65% and day–night cycles of 12 h–12 h. All animal studies were performed in accordance with national and institutional guidelines for animal care, under permit numbers 2015/UCL/MD/19 and 2019/UCL/MD/032 at the UCLouvain.

Antibodies

Anti-mouse GARP:TGF-β1 clone 58A2 was described previously (8). Batches of 58A2 under mIgG1 or mIgG2a DANA formats, and corresponding isotype controls (motavizumab) were kindly provided by Dr. Bas van der Woning (argenx BV). mIgG1 and mIgG2a DANA antibodies do not exert FcγR-dependent activities (8, 14). Anti-PD-1 clone RMP1-14 (mIgG2a FcSilent format) was purchased from Absolute Antibodies. Anti-active TGF-β1,2,3 clone 1D11 was purchased at BioXcell.

Cells

CT26 and MC38 colon carcinoma cell lines were maintained *in vitro* as a monolayer culture in Iscove's Modified Dulbecco Medium (CT26), or Roswell Park Memorial Institute Medium (MC38), supplemented with 10% fetal calf serum (FCS) and 10 mM Hepes, 1 mM sodium pyruvate and 0.1 mM non-essential amino acids, at 37°C in an atmosphere of 8% (CT26) or 5% (MC38) CO_2 in air. Murine tumor cells in exponential growth phase were harvested, washed in PBS, and resuspended in endotoxin-free Dulbecco's PBS (Millipore) prior to inoculation into mice.

Endothelial cell lines C166 and MS1 were purchased at ATCC or kindly provided by the group of Agnès Noël (ULiège, Belgium), respectively. Both were maintained *in vitro* as a monolayer culture in Dulbecco's Modified Eagle Medium

150

supplemented with 10% FCS, at 37°C in an atmosphere of 5% CO_2 in air.

Animal Experiments

On day 0, live CT26 cells (10^6 cells/mouse) or MC38 cells (1×10^6/mouse for mIF experiments or 1.5×10^6 cells/mouse for flow cytometry experiments) were injected *s.c.* into 7- to 8-week-old syngeneic mice. Large (D) and small (d) tumor diameters were measured with a caliper every 2 or 3 days starting on day 6. Tumor volumes were calculated as follows: $V = \pi \times D \times d^2/6$. On days indicated in the figure legends, mice received intraperitoneal (*i.p.*) injections of the following mAbs (250 μg of each), administered alone or combined as indicated in the figure legends: isotype control (motavizumab), anti-GARP:TGF-β1 (clone 58A2) and/or anti-PD-1 (clone RMP1-14 FcSilent). Anti-GARP:TGF-β1 injected in BALB/c or C57BL/6 mice were under mIgG2a DANA or mIgG1 formats, respectively (corresponding isotypes were used for the motavizumab control). All mice were sacrificed on day 13 or 14, and tumors were collected after sacrifice for further analyses.

Multiplexed Immunofluorescence on Mouse Tumor Sections

Immediately after collection, CT26 and MC38 tumors were fixed in formaldehyde (FA) 4% during 24 h, then embedded in paraffin using the Tissue-Tek VIP (Sakura). Formaldehyde-fixed paraffin-embedded (FFPE) tumors were cut in 5 μm-thick sections and mounted on a microscope slide. Slides were deparaffinized in subsequent baths of HistoClear and decreasing concentrations of ethanol. Antigen retrieval was performed in Tris–EDTA buffer (pH 9) with microwave treatment. Endogenous peroxidases were inactivated using a peroxidase block reagent (Enzo) for 15 min and sections were permeabilized and blocked with Tris Buffered Saline (TBS) supplemented with 0.1% Tween 20, 2% milk, 5% Bovine Serum Albumin (BSA), and 1% human Ig for 30 min. The following primary antibodies were used (incubation time was 90 min) for immunofluorescent staining on these sections, alone or in combination, as indicated in the figure legends: anti-CD3 (Abcam, clone SP7, diluted 1:500), anti-CD8 (Cell signaling, clone D4W2Z, diluted 1:400), anti-CD146 (Abcam, clone EPR3208, diluted 1:250), anti-PDGFRβ (Abcam, clone Y92, diluted 1:200). Ready-to-use EnVision+ System-HRP Labelled Polymer Anti-Rabbit (Dako) was used (60 min) as a secondary antibody for all antibodies cited above, followed by incubation with a Tyramide Reagent coupled either to Alexa Fluor 488, Alexa Fluor 555 or Alexa Fluor 647 (Thermo, diluted 1:200), prepared in a buffer containing 0.1 M boric acid, 3 M NaCl, 0.1% Tween 20 (pH 7.8) supplemented with 0.003% H_2O_2, for 10 min. After each staining, an additional step of heat-mediated antibody elution in citrate buffer (pH 6) was performed in a microwave oven. Counterstaining of nuclei was performed with Hoechst33258 reagent (1:1,000) for 5 min. Slides were mounted with Fluorescent Mounting Medium (Dako) and covered.

Another piece of tumor was frozen, embedded in OCT and cut in 7 μm-thick sections to perform staining, including GARP. Cryosections were fixed for 5 min in FA 4%. Endogenous

peroxidase blocking and permeabilization were performed, as described above. For GARP staining, clone YGIC86 (Thermo, diluted 1:80) was used as the primary antibody and the signal was amplified with ready-to-use ImPRESS HRP Goat Anti-Rat IgG (Vector) and a Tyramide Reagent, coupled to Alexa Fluor 555. Slides were counterstained and mounted as described previously.

Digital 3 or 4-color images of the stained tissue sections were acquired with a Pannoramic P250 Flash III scanner (3DHistech) equipped with a Plan-Apochromat 20×/N.A. 0.8× objective (Carl Zeiss) and with a Point Grey Grasshopper 5MP camera, using DAPI1, FITC, SpRed and Cy5 filter sets (Semrock).

Immunofluorescence Image Analysis

mIF images were analyzed with the Halo software (Indicalabs). The Cytonuclear FL module was used for the quantification of T cell densities as well as for the calculation of distances between the T cells to the tumor periphery (Dp), and to nearest neighbor endothelial cell. To calculate distances, we designed a dedicated R script that uses the position and phenotype of each event identified by Halo. For **Figure 2**, the tumor periphery was defined using the cells that are at the extremities of the tissue section, and the tumor center was calculated as centroid. A mean radius length was calculated for each section based on the lengths of all radiuses measured in the section (one radius represents the distance between the centroid and one DAPI[+] nucleus located on the tumor periphery). Five CT26 tumors were excluded from this analysis because their centroid were located outside of the tissue, due to their moon-like shape. The distance of each CD8 T cell to their closest endothelial cell was calculated using the nearest neighbor analysis. For quantification of blood vessels, the Object Quantification FL module of Halo was used, with each object corresponding to an individual blood vessel.

Flow Cytometry Analyses

On the day indicated in the figure legends, tumors were harvested and mechanically dissociated in the presence of enzymes (Collagenase I 100 mg/ml, Life Tech; Collagenase II 100 mg/ml, Life Tech; Dispase 1 mg/ml, Life Tech; and DNAse I 0.4 U/ml, Roche), using two cycles in the GentleMacs disruptor (Miltenyi) separated by 30 min of incubation at 37°C under continuous agitation. Tumor cell homogenates were clarified through 70 and 40 μm filters. Single cell suspensions were counted on a Luna® cell counter with a live-dead cell marker, then pelleted and resuspended in PBS containing 2 mM EDTA and 1% FCS for immediate staining, or in X-Vivo 10 medium (Invitrogen) to shortly incubate cells prior to staining.

Cells used for immediate staining were incubated with antibodies against surface markers (CD45, clone 30F-11; CD4, clone RM4-5; CD8a, clone 53-6.7) (Biolegend) in the presence of a viability dye (eBioscience) and anti-CD16/32 to block FcγRs. To identify MC38 tumor-specific T cells, cells were also incubated with an H2-K[b]-p15E (KSPWFTTL) pentamer coupled to APC (ProImmune). One million cells per tumor were kept for *ex vivo* incubation with Brefeldin A (Sigma, 5 μg/ml) to increase the accumulation of cytokines in the Golgi/endoplasmic reticulum. No stimulation reagents were

applied. Anti-CD107a mAb coupled to BV421 (clone 1D4B, Biolegend) was added to the mix. After 4 h of incubation at 37°C, cells were stained with antibodies against surface markers (CD45, CD4, CD8a) (Biolegend) in the presence of a viability dye (eBioscience) and an anti-CD16/32, fixed and permeabilized with the Cytofix/Cytoperm kit (BD Biosciences), then stained with antibodies against intracellular cytokines (IFNγ, clone XMG1.2; TNFα, clone MP6-XT22) (Biolegend) in the presence of additional anti-CD16/32.

C166 and MS1 cells were incubated with anti-CD16/32 antibody then stained with a biotinylated anti-GARP:TGF-β1 antibody (clone 58A2) and a streptavidin coupled to PE. Analyses were performed on a FACS LSRFortessa flow cytometer (DIVA, BD Biosciences) and data were computed using the FlowJo software (Tree Star).

RT-qPCR of Mouse Tissue Samples and Cell Lines

Mouse tumor fragments were collected and stored at −80°C until processing. After tissue disruption with the TissueLyser (Qiagen), total RNA was extracted using NucleoSpin Mini Columns (Macherey Nagel). RNA was reverse transcribed with Maxima First Strand cDNA Synthesis Kit (Thermofisher). For **Figure 6**, the MS1 cell line and splenocytes obtained from BALB/c mice were treated with recombinant TGF-β (rTGF-β) at 1 ng/ml for 24 h, then harvested and pelleted. RNA extraction and reverse transcription were performed as described above. qPCR were performed in the QuantStudio3 device (Thermofisher) in reaction volumes of 20 µl containing 0.025 U/µl of Takyon Master Mix (Eurogentec), 300 nM of each primers, 100 nM of Takyon probe, under either standard conditions (95°C for 3′; 45 cycles of 95°C for 10″ and 60°C for 30″) or fast conditions (95°C for 3′; 95°C for 3″ and 60°C for 30″) depending on amplicon size. The sequences of primers and probes are listed in **Table S1**.

Thymidine Incorporation Assay

C166 and MS1 endothelial cells (2,000 cells/well) were incubated in the presence of rTGF-β1, for the duration indicated in the figure legends. One µCurie of [³H]-thymidine (³H-T) was added during the last 24 h of culture. On the day of revelation, cells were incubated with trypsin and aspirated on a 96-filter plate (Unifilter GF/C) using a harvester (Packard Filtermate 196). The plate was washed several times with water. Radioactivity was measured by a scintillation counter (Packard Microplate Scintillation Counter), which calculates the counts per minute (cpm).

Statistical Analyses

All statistical analyses were performed using the JMP®Pro 15 software. Comparisons of measurements taken at a single time point were performed using a two-tailed, non-paired, non-parametric Wilcoxon test. *Post-hoc* Tukey's test was performed to adjust for multiple comparisons. The number of experiments and the number of mice (n) in the various experimental groups are indicated in the corresponding figure legend.

RESULTS

Combined GARP:TGF-β1/PD-1 Blockade Increases Infiltration of T Cells in MC38 but Not in CT26 Tumors

To compare the mechanism of action of combined GARP:TGF-β1/PD-1 blockade in two mouse tumor models, we injected MC38 or CT26 cells subcutaneously (*s.c.*) in syngeneic C57BL/6 or BALB/c mice, respectively. We then started intraperitoneal (*i.p.*) administrations of either isotype control, anti-GARP:TGF-β1 and/or anti-PD-1 mAbs after 6 days, when the tumors were well established in all mice. A total of three injections of single or combined mAbs were administered on days 6, 9 and 12, and tumors were collected on day 13. This time point was chosen based on our previous study, which showed that similar administration regimens significantly increased the frequency of complete, immune-mediated rejections of MC38 and CT26 tumors in mice treated with anti-GARP:TGF-β1 + anti-PD-1, as compared with anti-PD-1 alone. Notably, rejections occurred between days 15 and 40 in both MC38- and CT26-tumor bearing mice, leaving no sufficient tumor material for analyses after day 13 (8). Here on day 13, and as expected, volume and weight of tumors were already significantly reduced in mice treated with anti-GARP:TGF-β1 + anti-PD-1, or anti-PD-1 alone, as compared with controls (**Figure S1**).

We used digitalized multiplex immunofluorescence stainings (mIF) of formaldehyde-fixed paraffin-embedded (FFPE) sections to quantify T cell infiltration in the tumors (**Figures 1A, B**). In tumors from untreated mice, the proportion of CD3⁺ cells among DAPI⁺ nuclei was approximately 3-fold higher in MC38 (6.8% ± 0.4%; median ± interquartile range, or IQR) as compared with CT26 tumors (2.3% ± 1.4%) (**Figure 1B**). Consistent with our previous observations, administration of anti-GARP:TGF-β1 or anti-PD-1 alone did not significantly increase T cell infiltration in MC38 or CT26 tumors, and the anti-GARP:TGF-β1 + anti-PD-1 combination did not increase T cell infiltration in CT26 [**Figure 1B** and (8)]. However, the combination caused a significant 3-fold increase of the proportion of T cells infiltrating MC38 tumors in mice treated with the anti-GARP:TGF-β1 + anti-PD-1 combination (20.9% ± 7.5%) (**Figure 1B**). T cell infiltration was significantly higher with this combination than with the anti-PD-1 alone. Both CD8 and CD4 T cells contributed to the infiltration, but CD8 T cells more so (≈5-fold) than CD4 (≈2-fold). RT-qPCR for genes *Cd3e*, *Cd8b* and *Cd4* confirmed increased infiltration of total, CD8 and CD4 T cells in MC38 tumors after combined GARP:TGF-β1/PD-1 blockade (**Figure 1C**).

We observed with flow cytometry that the proportion of CD8 and CD4 T cells among MC38-infiltrating leukocytes (CD45⁺ cells) were not modified after GARP:TGF-β1/PD-1 blockade, indicating that the augmented T cell infiltration resulted from an increased infiltration of total leukocytes and not of a particular cell subset (**Figure S2A**). Lymphocytes directed against the tumor-specific antigen p15E were identified by staining with a fluorescent H2-K^b pentamer loaded with the p15E peptide (15). Their proportions among leukocytes (7.6% ± 4.9%) or CD8
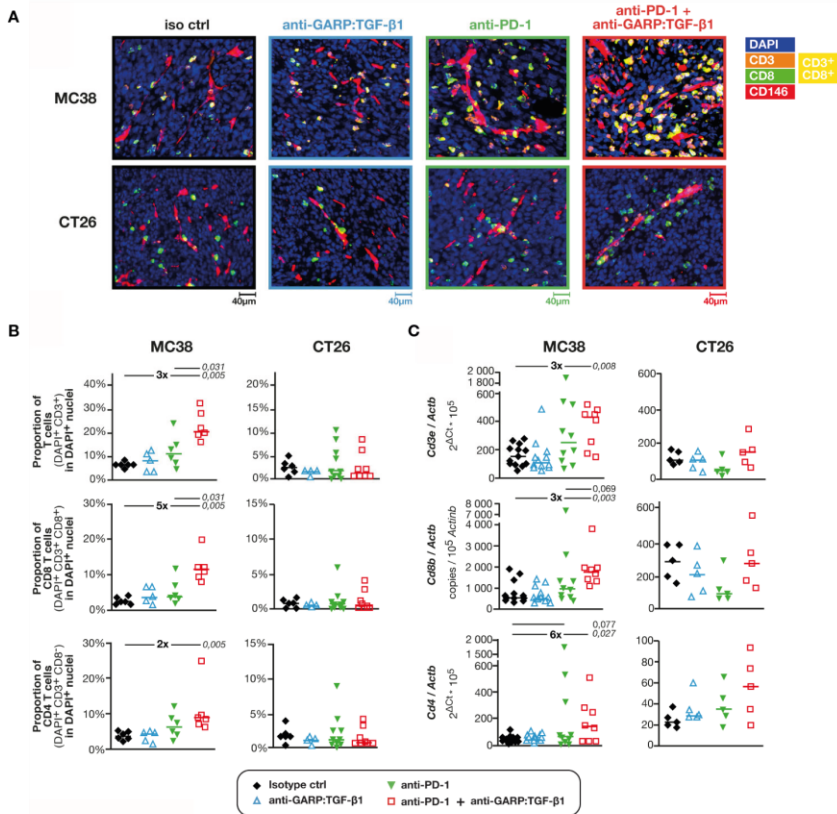
FIGURE 1 | Combined GARP:TGF-β1/PD-1 blockade increases infiltration of total, CD8 and CD4 T cells in MC38, but not in CT26 tumors. C57BL/6 or BALB/c mice were injected on day 0 with live MC38 or CT26 cells, respectively, and treated on days 6, 9 and 12 with anti-GARP:TGF-β1 (clone 58A2 mIgG1 in C57BL/6 mice; clone 58A2 mIgG2a DANA in BALB/c mice), anti-PD-1 (clone RMP1-14 mIgG2a FcSilent), a combination of both mAbs or the corresponding isotype controls. Tumors were collected on day 13 and fragments were analyzed by mIF and quantitative digital imaging or RT-qPCR. **(A)** Representative images of FFPE tumor sections stained with anti-CD3 antibody (orange), anti-CD8 antibody (green), anti-CD146 antibody (red) and Hoescht (DAPI, blue). CD8 T cells (CD3$^+$CD8$^+$) appear in yellow. **(B)** Proportions (%) of total, CD8 and CD4 T cells in DAPI$^+$ nuclei measured with Indicalabs Halo software. Results obtained in one experiment for MC38 (n = 5–6 mice/group) and pooled from two independent experiments for CT26 (n = 3–6 mice/group in each experiment). One tumor section analyzed per mouse. **(C)** Expression levels of *Cd3e*, *Cd8* and *Cd4* mRNA relative to housekeeping gene *Actb* in MC38 and CT26 samples. Samples from two independent experiments for MC38 (n = 4–7 mice/group in each experiment) and one experiment for CT26 (n = 5/group). Samples from the second MC38 experiment shown in c were also analyzed in **Figure S2** by flow cytometry. Data points represent values in individual mice. Horizontal bars: median per group. P values <0.05, calculated with a two-sided Wilcoxon test, are indicated in italics. Numbers in bold: fold-change between the indicated groups.

T cells (19.1% ± 11.6%) did not differ between the untreated or treated MC38 tumors (**Figure S2A**). We also did not find differences between the proportions of CD8 T cells or tumor-specific CD8 T cells that produced IFNγ and/or TNFα, or expressed the surface marker of degranulation CD107a (**Figures S2B**). The only difference was the proportions of CD4 T cells producing IFNγ, increased after combined GARP:TGF-β1/PD-1 blockade as compared with PD-1 blockade alone or controls (**Figure S2B**). RT-qPCR analyses confirmed these observations (**Figure S2C**).

We conclude that in MC38 tumors, the combined GARP:TGF-β1/PD-1 blockade increases the infiltration of T cells,

including activated tumor-specific CD8 T cells. This contrasts with our previously published observations in CT26, where combined GARP:TGF-β1/PD-1 blockade did not increase T cell infiltration, but did augment the effector functions of the anti-tumor T cells that were already present in the tumors (8).

Combined GARP:TGF-β1/PD-1 Blockade Does Not Increase the Proliferation or Penetration of Tumor-Infiltrating CD8 T Cells in MC38 or CT26 Tumors

The increased T cell infiltration into MC38 following GARP:TGF-β1 blockade could result from a local T cell

153

proliferation within MC38, but not CT26 tumors. However, we observed no change in levels of Ki-67 in CD8 T cells or in the proportion of proliferating Ki-67^{+} cells among CD8 T cells in any treatment group in MC38 or CT26 tumors (**Figures S3A, B**).

Increased T cell infiltration could also result from an increased penetration of T cells from the periphery towards the center of MC38 tumors, as shown in EMT6 treated with a combination of anti-active TGF-β1, β2 and β3 (clone 1D11) and anti-PD-L1 (clone 6E11) (10). We measured the distance separating each CD8 T cell from the closest point on the tumor periphery in MC38 and CT26 FFPE sections, stained by mIF (**Figure 2A**), then examined the distribution of all CD8 T cells at various distances from the periphery relative to mean radius length (**Figure 2B**). In control MC38 tumors, the vast majority of CD8 T cells were closer to the tumor periphery than its center (79% of CD8 T cells at <50% mean radius length). Treatment with anti-GARP:TGF-β1, combined or not with anti-PD-1, did not modify this distribution (**Figure 2B**). In control CT26, a majority of CD8 T cells were even closer to the periphery (89% CD8 T cells at <30% mean radius length), but here also, their distribution was not modified by any treatment (**Figure 2B**).

Combined GARP:TGF-β1/PD-1 Blockade Increases Entry of T Cells *via* Intratumoral Vessels in MC38

We then examined whether combined GARP:TGF-β1/PD-1 blockade increased T cell entry *via* intratumoral blood vessels, as reported by Martin et al. for combined latent TGF-β1/PD-1 blockade in MBT-2 tumors (9). Here we used mIF and quantitative imaging of FFPE tumor sections, this time to measure distances between each CD8 T cell and the nearest blood endothelial cell (DAPI^{+}CD146^{+} cell, or BEC) and determine the distribution of all CD8 T cells at various distances from their nearest BEC (**Figure 2C**). In murine tissues, CD146 is expressed by blood but not lymphatic endothelial cells (16). In control MC38 tumors, the vast majority of CD8 T cells were <100 μm away from the nearest BEC, with 48% at <30 μm. In mice treated with anti-GARP:TGF-β1, anti-PD-1, or both, the proportions of CD8 T cells at <30 μm from the nearest BEC rose to 55, 61 or 69%, respectively. This suggests that increased infiltration of CD8 T cells in MC38 tumors, after combined GARP:TGF-β1/PD-1 blockade (**Figure 1**), results from increased entry of T cells *via* blood vessels, but that T cells do not migrate further in the tumor bed after extravasation. In control CT26 tumors, 75% of CD8 T cells were at <30 μm from the nearest BEC, and this proportion did not vary with any treatment (**Figure 2C**).
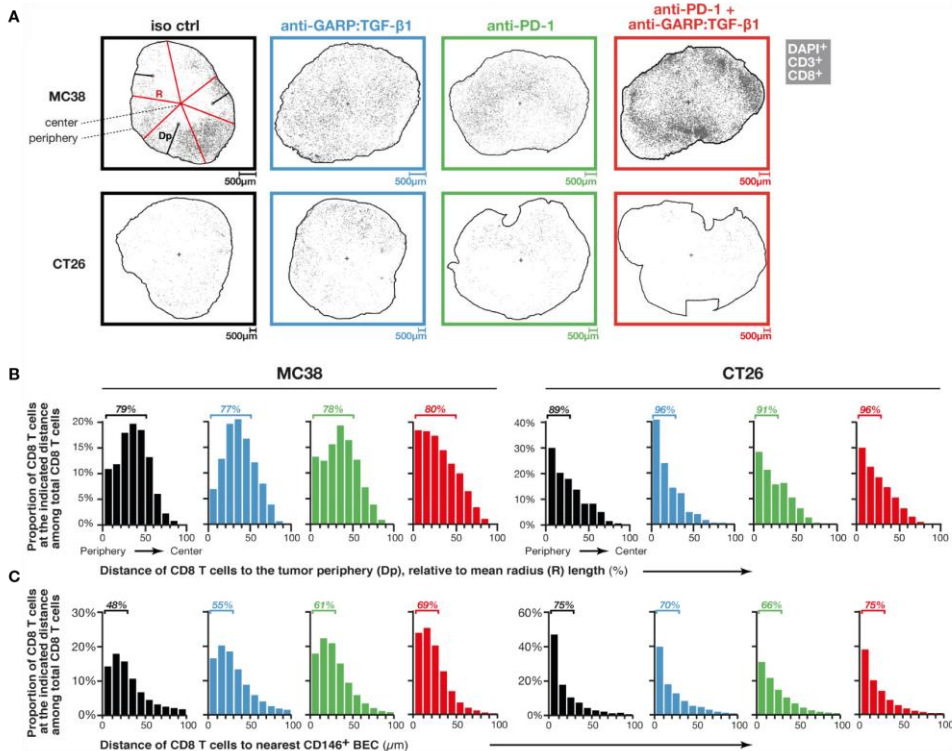
Combined GARP:TGF-β1/PD-1 Blockade Increases the Density of Blood Vessels Containing GARP[+] Endothelial Cells Covered by PDGFRβ[+] Pericytes in MC38, but Not in CT26 Tumors

Next, we examined if increased infiltration of T cells was associated with a higher density of blood vessels in MC38 tumors. Blood vessel-like objects (*i.e.* structures defined based on CD146^{+} surface segmentation) were identified and counted (**Figure 3A**). Median areas of blood vessels were similar in MC38 and CT26 tumors, regardless of treatment (**Figure S4**). Densities of blood vessel-like objects in control MC38 and CT26 tumors were also similar, with 161 ± 54 (median ± IQR) blood vessels per mm^2 in MC38, and 196 ± 132 in CT26 tumors (**Figure 3B**). Unexpectedly, we observed that combined GARP:TGF-β1/PD-1 blockade increased blood vessel density about 2-fold in MC38 (272 ± 91), but not in CT26 tumors (**Figure 3B**). Blood vessel densities correlated with proportions of tumor-infiltrating CD8 T cells in MC38, but not in CT26 tumors. Three of the four MC38 tumors with the highest CD8 T cell infiltration (>10% CD8 T cells in DAPI^{+} cells) and the highest blood vessel density (>250 vessels/mm^2) were from mice treated with anti-GARP: TGF-β1 + anti-PD-1 (**Figure 3C**). We counted a median of about 1.8 and 1.2 CD8 T cell in every 20 vessels of untreated MC38 and CT26 tumors, respectively, and this number increased 4-fold after combined GARP:TGF-β1/PD-1 blockade in MC38, but not in CT26 tumors (**Figure 3D**). Thus, increased T cell infiltration in MC38 tumors upon combined GARP:TGF-β1/PD-1 blockade results from both increased blood vessel density and increased CD8 T cell extravasation into the tumors.

Intratumoral blood vessels are often described as structurally abnormal, displaying loose cellular junctions, high number of fenestrations and discontinuous basement membrane, which can impair lymphocyte extravasation (17). To measure the functionality and stability of blood vessels, we used anti-PDGFRβ antibodies to identify blood vessels covered by pericytes (*i.e.* CD146^{+}PDGFRβ^{+} objects) (**Figure 4A**). We observed a 2-fold increase in the density of PDGFRβ^{+} blood vessels in MC38, but not in CT26 tumors, upon GARP:TGF-β1/PD-1 blockade as compared with controls or anti-PD-1 alone (**Figure 4B**). No increase in the density of PDGFRβ-negative blood vessels was observed in either MC38 or CT26 tumors, whatever the treatment (**Figure 4B**). Thus, increased blood vessel density in MC38 tumors after GARP:TGF-β1/PD-1 blockade can be attributed to an increased density of those vessels that are stabilized by pericytes, a parameter often taken as an indicator of blood vessel normalization in tumors (17).

GARP:TGF-β1 complexes are known to be expressed on endothelial cells (2, 8, 18). We therefore verified whether treatment with anti-GARP:TGF-β1 mAbs modified the densities and proportions of blood vessels containing GARP[+] BECs in frozen MC38 and CT26 tumors (**Figure 4C**), as GARP can be detected by mIF in frozen tissues only (8). In untreated tumors, 45.3% ± 6.2% (median ± IQR) of blood vessels contained GARP[+] BECs in MC38, versus 30.7% ± 7.7% in CT26 tumors. Combined GARP:TGF-β1/PD-1 blockade increased GARP[+] blood vessel density about 2-fold in MC38, but not in CT26 tumors (**Figure 4D**). Densities of GARP-negative blood vessels did not change in MC38 or CT26 tumors, whatever the treatment. In a follow up experiment, we co-stained frozen tumor sections for GARP and PDGFRβ. The two markers were frequently co-expressed in intratumoral blood vessels: whilst 63.8% ± 5.8% (median ± IQR) of GARP[+] blood vessels were also PDGFRβ[+] in MC38 tumors, only 13.6% ± 4.2% of GARP[-] vessels expressed PDGFRβ (**Figure S5**). We conclude that combined

FIGURE 2 | Combined GARP:TGF-β1/PD-1 blockade induces entry of T cells *via* intratumoral vessels rather than penetration from the tumor periphery. Sections of FFPE tumors from **Figures 1A, B** analyzed by mIF and quantitative digital imaging. Treatment groups are indicated in colored font on top (black: isotype control; blue: anti-GARP:TGF-β1; green: anti-PD-1; red: anti-PD-1 + anti-GARP:TGF-β1). **(A)** Digital representations generated by the Halo software of one representative tumor section per treatment group, with CD8 T cells (DAPI+CD3+CD8+) indicated as grey dots. The outer edge of the tumors (periphery) is delineated by a black line, and the position of the tumor center, calculated as a centroid, is depicted by a black cross. On one representative section (top left), the distance to the periphery (Dp) of a few CD8 T cells are illustrated by black lines, and a few radiuses (R) are depicted by red lines. A mean radius length was calculated for each section based on the lengths of all radiuses measured in the section (one radius represents the distance between the centroid and one DAPI+ nucleus located on the tumor periphery). **(B)** Distribution of Dp of CD8 T cells relative to mean radius length, *i.e.* proportion of CD8 T cells within all CD8 T cells in a given tumor section that are located at the indicated relative Dp (0–10%, 10–20%,...). Bars represent mean proportions in all sections analyzed in one treatment group. **(C)** Distribution of CD8 T cell distances to the nearest endothelial cell (DAPI+CD146+), as determined using nearest neighbor analysis. Bars represent mean proportions of CD8 T cells within all CD8 T cells in a given section that are located at the indicated distance (0–10 μm, 10–20 μm,...) from the nearest blood endothelial cell (BEC). Results from one experiment for MC38 (n = 5–6 mice/group) and pooled from two independent experiments for CT26 (n = 3–6 mice/group in each experiment). One tumor section analyzed per mouse.

GARP:TGF-β1/PD-1 blockade increased the density of GARP+ blood vessels covered by pericytes in MC38, but not in CT26 tumors.

Active TGF-β1 Inhibits the Proliferation of Murine GARP+ Endothelial Cells *In Vitro*

TGF-β1 exerts a cytostatic effect on many cell types. By blocking TGF-β1 activation on the surface of GARP+ endothelial cells, anti-GARP:TGF-β1 mAbs could increase endothelial cell proliferation and the formation of new GARP+PDGFRβ+ functional blood vessels in MC38 tumors. *In vitro* proliferation of MS1, an endothelial cell line which is derived from a pancreatic sarcoma and expressing surface GARP:TGF-β1 complexes (**Figure 5A**), was

inhibited by recombinant active TGF-β1 (rTGF-β1) in a dose-dependent manner (**Figure 5B**). Noteworthy, incubation with neutralizing anti-active TGF-β1,2,3 (clone 1D11) or blocking anti-GARP:TGF-β1 (clone 58A2) mAbs did not increase MS1 proliferation (**Figure S6**), indicating that they are not under the influence of autocrine TGF-β1 activity. This result indicates that in the absence of a stimulus or another cell type, MS1 endothelial cells are unable to activate the latent TGF-β1 presented by GARP on their surface. We also tested the effect of rTGF-β1 on another murine endothelial cell line, C166, which originates from yolk sac. We observed no inhibition of proliferation (**Figures 5A, B**).

The inhibition of MS1 proliferation by rTGF-β1 *in vitro* suggests that anti-GARP:TGF-β1 mAbs could favor the

FIGURE 3 | Combined GARP:TGF-β1/PD-1 blockade increases blood vessel density in MC38, but not in CT26 tumors. Sections of FFPE tumors from **Figures 1A, B** analyzed by mIF and quantitative digital imaging. **(A, B)** Representative images and quantification of immunostaining for CD146 (red) and DAPI (blue). Sections were analyzed with the Halo software to identify and quantify the number of blood vessel-like objects (*i.e.* CD146$^+$ objects) per mm^2 of section. Mean of two tumor sections per mouse. **(C)** Correlation between the proportion of CD8 T cells (**Figure 1B**) and the density of blood vessels. Linear regressions and corresponding coefficients of determination (R^2) are indicated. **(D)** Number of CD8 T cells colocalized with a blood vessel (*i.e.* DAPI$^+$CD3$^+$CD8$^+$CD146$^+$ events) per 20 blood vessels. Data points represent the values in individual mice. Horizontal bars: median per group. P values <0.05, calculated with a two-sided Wilcoxon test, are indicated in italics. Numbers in bold: fold-change between the indicated groups. Results from one experiment for MC38 (n = 5–6 mice/group), and pooled from two independent experiments for CT26 (n = 3–6 mice/group).

proliferation of GARP$^+$ endothelial cells *in vivo*, and consequently increase blood vessel densities in MC38 tumors.

Combined GARP:TGF-β1/PD-1 Blockade Increases Expression of E-Selectin by BECs in MC38, but Not in CT26 Tumors

TGF-β1 regulates expression of adhesion molecules in hematopoietic and endothelial cells (19–21). We measured the expression of genes encoding various adhesion molecules in MC38 and CT26 tumor samples from control and mAb-treated mice. No difference was observed for expression of *Vcam1* and *Icam1* relative to *Actb* in any treatment group as compared with controls (**Figure S7**). In contrast, expression of *Lfa1* and *Sell*, encoding adhesion molecules expressed on leukocytes, and that of *Sele*, encoding E-selectin expressed on BECs, were increased after combined GARP:TGF-β1/PD-1 blockade in MC38, but not in CT26 tumors (**Figure 6A** and **Figure S7**). We measured *Lfa1/Cd3e, Sell/Cd3e* and *Sele/Cd146* mRNA ratios, to normalize adhesion molecule expression to the abundance of CD3 T cells or CD146$^+$ BECs (**Figure 6A** and **Figure S7**). No significant difference in *Lfa1/Cd3e* or *Sell/Cd3e* ratios was observed in MC38 samples from control or mAb-treated mice. Thus, increased expression of these genes relative to

Actb after GARP:TGF-β1/PD-1 blockade in MC38 tumors is probably mostly due to increased T cell infiltration. This was different for expression of *Sele*: ratios of *Sele/Actb* and *Sele/Cd146* were significantly increased after combined GARP:TGF-β1/PD-1 blockade in MC38, but not in CT26 tumors. This suggests that increased *Sele* expression in MC38 tumors results not only from increased BEC densities but also from increased *Sele* mRNA levels per BEC. We verified whether exposure to rTGF-β1 regulates *Lfa1* or *Sele* expression by murine activated T cells or endothelial cells *in vitro*, respectively. rTGF-β1 marginally increased (1.3- to 1.5-fold) *Lfa1* expression by murine splenocytes stimulated or not with anti-CD3/CD28 beads (**Figure 6B**). In contrast, rTGF-β1 reduced *Sele* expression by more than 2-fold in MS1 endothelial cells (**Figure 6C**), confirming previous observations on HUVECs and murine lung, heart and liver endothelial cells (22, 23).

DISCUSSION

Altogether, our results suggest that combined GARP:TGF-β1/PD-1 blockade exerts anti-tumor activity in MC38 tumors by increasing the density of intratumoral GARP$^+$ blood vessels
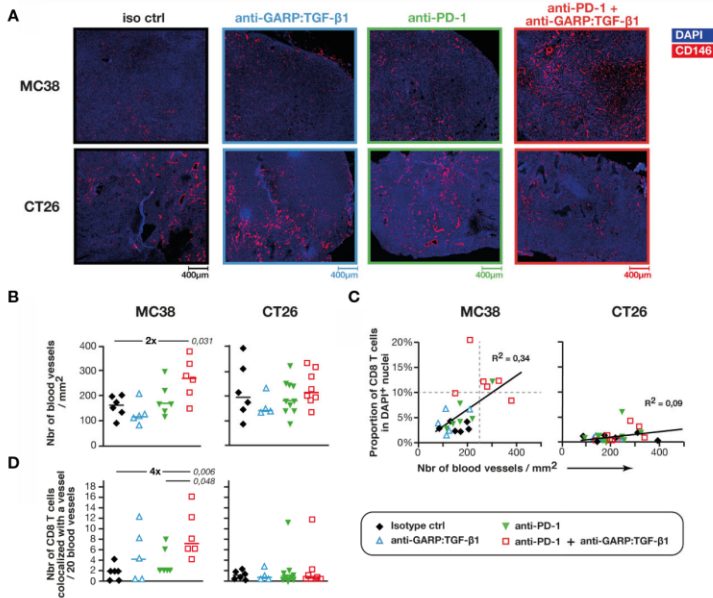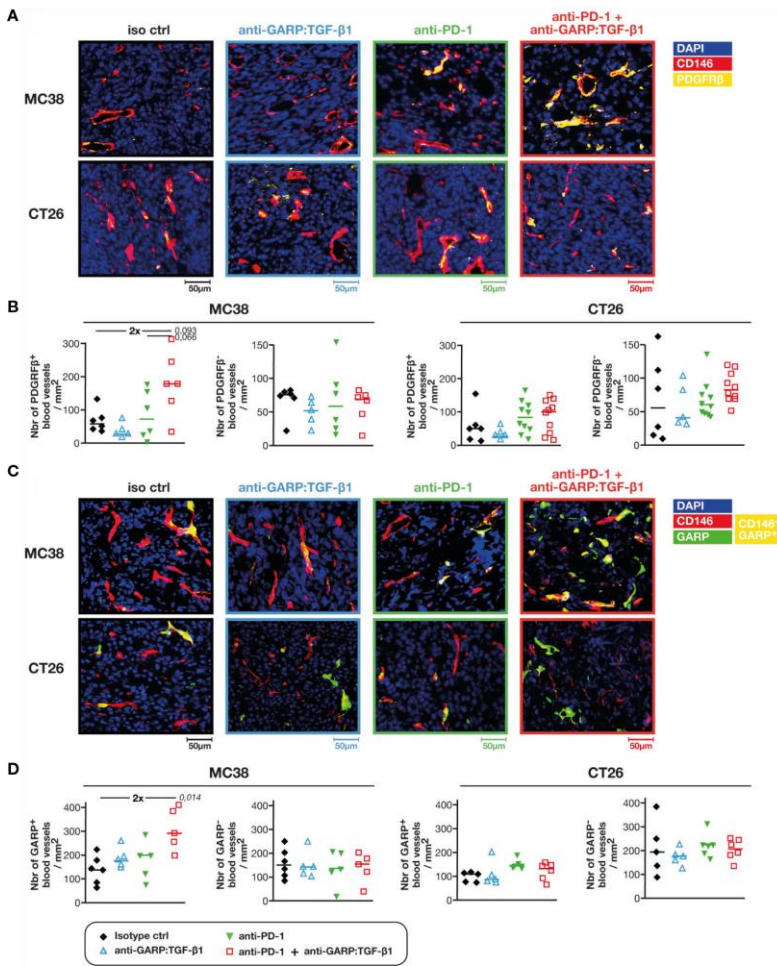
FIGURE 4 | Combined GARP:TGF-β1/PD-1 blockade increases the density of intratumoral GARP⁺ blood vessels covered by pericytes in MC38, but not in CT26 tumors. Additional FFPE and frozen tumor sections obtained from mice in **Figures 1A, B** were analyzed by mIF and quantitative digital imaging. **(A, B)** Representative images **(A)** and quantification **(B)** of PDGFRβ⁺ and PDGFRβ⁻ blood vessels (*i.e.* CD146⁺PDGFRβ⁺ and CD146⁺PDGFRβ⁻ objects) in FFPE tumor sections stained with anti-CD146 (red), anti-PDGFRβ (yellow) and Hoechst (DAPI, blue). **(C, D)** Representative images **(C)** and quantification **(D)** of GARP⁺ and GARP⁻ blood vessels (*i.e.* CD146⁺GARP⁺ and CD146⁺GARP⁻ objects) per mm² of frozen tumor sections stained with anti-CD146 (red), anti-GARP (green) and Hoechst (DAPI, blue). GARP⁺ vessels appear in yellow. Data points represent values in individual mice. Horizontal bars: median per group. P values <0.05 are indicated in italics (calculated with a two-sided Wilcoxon test). Numbers in bold: fold-change between the indicated groups. One tumor section analyzed per mouse.

covered by PDGFRβ⁺ pericytes, the expression of E-selectin by BECs, and the extravasation and infiltration of T cells, including activated anti-tumor CD8 T cells.

Because rTGF-β1 inhibited the proliferation of GARP⁺ endothelial cells *in vitro*, we propose that anti-GARP:TGF-β1 mAbs act by inhibiting TGF-β1-mediated endothelial cell cytostasis in MC38 tumors, thereby favoring BEC proliferation and densification of the intratumoral blood vasculature. Anti-PD-1 mAbs, alone or in combination with anti-CTLA-4, were previously shown to increase pericyte coverage of blood vessels

in mouse tumors, but these treatments did not increase, and even reduced intratumoral blood vessel densities (24–27). Combining anti-PD-1 with anti-GARP:TGF-β1 could therefore increase pericyte coverage of blood vessels as a result of PD-1 blockade, while also increasing BEC proliferation and blood vessel density as a result of GARP:TGF-β1 blockade. This would explain the densification of pericyte-covered blood vessels observed in MC38 tumors upon combined GARP:TGF-β1/PD-1 blockade. Increased density of pericyte-covered blood vessels is an indicator of tumor vasculature normalization, which could

FIGURE 5 | Recombinant TGF-β1 exerts a cytostatic effect on GARP⁺ endothelial cells *in vitro*. **(A)** Flow cytometry analyses of MS1 and C166 murine endothelial cell lines stained with anti-GARP:TGF-β1 antibody (clone 58A2) or isotype control. Histograms are gated on live single cells. Geom, geometric mean fluorescence intensity. **(B)** C166 and MS1 cells were seeded in presence or absence of rTGF-β1 (top: 1 ng/ml; bottom: indicated concentrations) and cultivated during 48, 72 or 96 h (top) or 96 h (bottom). Tritiated thymidine (³H-T) was added during the last 24 h of culture, and cells were collected to measure ³H-T incorporation as a read-out of proliferation. Data points represent means of triplicate wells. Results are representative of three independent experiments.

improve tumor perfusion (17, 28). Other approaches targeting the tumor vasculature to overcome resistance to PD-1/PD-L1 blockade were tested previously, *e.g.* with anti-VEGFR2 mAbs, which enhanced vascular normalization but did not increase blood vessel density in mouse models of breast and pancreatic cancer (29). Anti-GARP:TGF-β1 could represent a more efficient and safer alternative, densifying in addition to normalizing the blood vasculature by targeting GARP-expressing cells only.

The cellular source of the active TGF-β1 exerting cytostatic effects on BECs in MC38 tumors is not yet clearly identified. We observed that approximately half of tumor blood vessels in MC38 tumors contained endothelial cells expressing GARP:TGF-β1 on their surface. It would thus be tempting to speculate that anti-GARP:TGF-β1 improves the anti-tumor efficacy of anti-PD-1 by blocking TGF-β1 activation on the surface of GARP⁺ endothelial cells. However, we observed that *in vitro*, endothelial cells were not able to activate latent TGF-β1 presented by GARP on their surface. This suggests that an unidentified stimulus, or another cell type, may be required to allow TGF-β1 activation on the surface of endothelial cells *in vivo*. In T cells, the mere presence of surface GARP:TGF-β1 is not sufficient to induce TGF-β1 activation. TGF-β1 activation by Tregs requires TCR stimulation and interaction of GARP:TGF-β1 complexes with integrin αVβ8 (3). The situation might be similar for endothelial cells, which

would require an additional stimulus and/or the intervention of an αVβ8-expressing cell type to activate latent TGF-β1 presented by GARP on their surface *in vivo*. Tregs themselves, entering the tumor *via* blood vessels, represent interesting candidates. Indeed, we previously showed that the anti-tumor activity of combined GARP:TGF-β1/PD-1 blockade was lost in Treg-specific *Garp* knock-out mice bearing MC38 tumors, suggesting that targeting GARP-expressing Tregs is indispensable for anti-GARP:TGF-β1 to exert anti-tumor activity (8). It could thus very well be that the cellular source of the active TGF-β1 exerting cytostasis on BECs in MC38 tumors is the immunosuppressive Tregs. Considering that tumor-infiltrating T cells, which include Tregs, are more abundant in MC38 than in CT26 tumors, this could explain at least in part why GARP:TGF-β1 blockade increases the density of the tumor blood vasculature in MC38, but not in CT26 tumors.

Whichever the cellular source of TGF-β1 signals blocked by anti-GARP:TGF-β1, increased tumor perfusion will increase T cell influx in the MC38 tumor vasculature. We observed that expression of *Sele*, a gene encoding E-selectin and repressed by TGF-β1, was increased in MC38 tumors upon combined GARP:TGF-β1/PD-1 blockade. E-selectin on endothelial cells allows for the adhesion of activated leukocytes and facilitates their extravasation by slowing down their rolling on blood vessel walls. Therefore, anti-GARP:TGF-β1 mAbs, by blocking TGF-β1 activity and increasing *Sele* expression, could facilitate T cell extravasation and infiltration within MC38 tumors.

It is noteworthy that activated intratumoral T cells can themselves enhance vascular functionality by secreting TNFα, known to upregulate E-selectin on blood endothelial cells (23), and IFNγ, which induces expression of chemokines involved in pericyte recruitment (25, 30, 31). We observed a significant increase in *Ifng* mRNA levels and proportions of IFNγ-producing CD4 T cells in MC38 tumors after combined GARP:TGF-β1/PD-1 blockade. Thus, increased tumor blood vessel density and functionality induced by combined GARP:TGF-β1/PD-1 blockade could be further reinforced as a consequence of increased infiltration by activated T cells, in a positive feedback loop.

The mode of action of combined GARP:TGF-β1/PD-1 blockade in MC38 tumors contrasts with that previously described in CT26 tumors, in which it increased effector functions of already present anti-tumor CD8 T cells, without increasing T cell infiltration or blood vessel density. It is unclear why combined GARP:TGF-β1/PD-1 blockade did not densify the blood vasculature and increase T cell infiltration in CT26 tumors, and conversely, why it did not increase effector functions of tumor-infiltrating CD8 T cells in MC38 tumors. Whether different modes of action result from using different colon carcinoma cell lines (MC38 *vs* CT26) or different syngeneic mouse strains (C57BL/6 *vs* BALB/c, respectively) could be assessed by comparing the two tumor models in F1 mice. The proportion of blood vessels containing GARP⁺ BECs in CT26 tumors was lower as compared with MC38 tumors, perhaps contributing to the lack of effect of anti-GARP:TGF-β1 on the blood vasculature in these tumors. Nevertheless, combined GARP:TGF-β1/PD-1 blockade increased immune-mediated tumor rejections to a similar extent in CT26 and MC38 tumors (8),
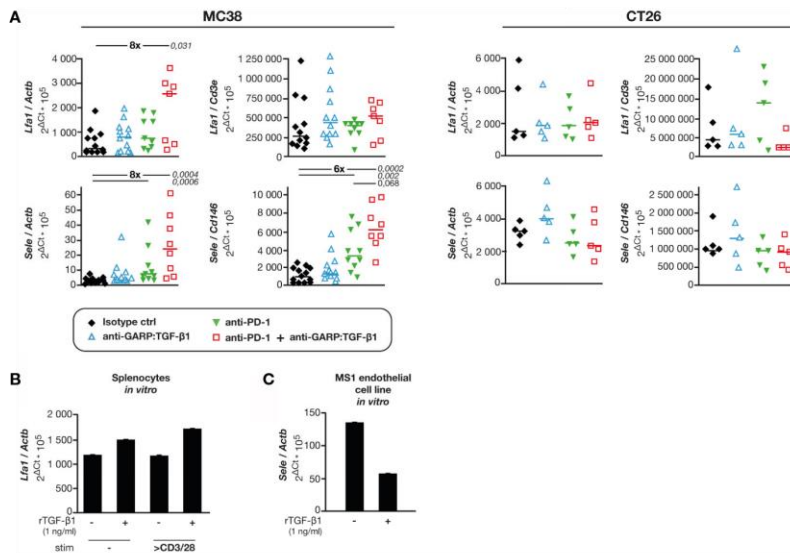
FIGURE 6 | Combined GARP:TGF-β1/PD-1 blockade increases expression of *Sele* and *Lfa1* in MC38, but not in CT26 tumors. Tumor samples shown in **Figure 1C** were analyzed by RT-qPCR. **(A)** mRNA levels of *Lfa1* and *Sele* relative to *Actb* (housekeeping gene), *Cd3e* (T-cell specific gene) or *Cd146* (endothelial cell-specific gene). Data points represent values in one mouse. Horizontal bars: median per group. P values <0.05, as calculated with a two-sided Wilcoxon test, are indicated in italics. Numbers in bold: fold-change between the indicated groups. **(B)** Expression of *Lfa1* in BALB/c splenocytes exposed to rTGF-β, in presence or absence of anti-CD3/CD28 beads during 24 h *in vitro*. Bars represent means (+SD) of duplicates. Results from one experiment. **(C)** Expression of *Sele* in C166 and MS1 cells exposed to rTGF-β during 24 h *in vitro*. Bars represent means (+SD) of duplicates. Results from one experiment.

indicating that both modes of action can significantly contribute to the anti-tumor activity of the combination.

Taken together, our results suggest that combined GARP:TGF-β1/PD-1 blockade can exert anti-tumor activity *via* multiple mechanisms, not only by increasing effector functions of anti-tumor T cells already present within tumors, but also by increasing tumor blood vessel density and infiltration by new anti-tumor T cells. Anti-GARP:TGF-β1 mAbs could thus be tested in the clinics to overcome resistance to PD-1/PD-L1 blockade in patients with a broad range of cancer types, including not only tumors already infiltrated by T cells, but also poorly vascularized tumors with low immune cell infiltration.

DATA AVAILABILITY STATEMENT

The original contributions presented in the study are included in the article/**Supplementary Material**. Further inquiries can be directed to the corresponding author.

ETHICS STATEMENT

The animal study was reviewed and approved by Comité d'Ethique pour l'Expérimentation Animale Secteur des Sciences de la Santé Université catholique de Louvain.

AUTHOR CONTRIBUTIONS

SL conceived the study. CB, PM, GS, AN, PC, NB, and SL analyzed the data. CB, PM, GS, NV-B, FB, and LR performed experiments. SL and CB wrote the manuscript. All authors contributed to the article and approved the submitted version.

FUNDING

SUPPLEMENTARY MATERIAL

The Supplementary Material for this article can be found online at: https://www.frontiersin.org/articles/10.3389/fimmu.2021.704050/full#supplementary-material

Supplementary Figure 1 | Combined GARP:TGF-β1/PD-1 blockade and anti-PD-1 alone reduce growth of MC38 and CT26 tumors. Volume and weight of tumors collected on day 13 for analyses shown in **Figures 1–4** and **Figure 6**. Data points represent values in individual mice. Horizontal bars: median per group. P values < 0.05, as calculated with a two-sided Wilcoxon test, are indicated by numbers in italics. Results from one experiment for MC38 (n=5-6 mice/group), and pooled from two independent experiments for CT26 (n=3-6 mice/group in each experiment).

Supplementary Figure 2 | CD8 T cells infiltrating MC38 tumors include activated anti-tumor T cells, but combined GARP:TGF-β1/PD-1 blockade does not increase their proportions or functions. MC38 tumors from mice treated as indicated in **Figure 1** were collected on day 13 to perform flow cytometry and RT-qPCR. **(A)** Proportions (%) of the indicated cell types among tumor infiltrating leukocytes (CD45⁺) or CD8 T cells (CD45⁺ CD8⁺). Results from one experiment (n=6-10 mice/group). **(B)** Proportions (%) of cells producing IFNγ, TNFα, and/or expressing surface CD107a among the indicated tumor-infiltrating cell subsets, obtained on unstimulated bulk processed tumors. Results from one experiment (n=6-10 mice/group). **(C)** Expression of *Ifng*, *Tnfa*, *Prf1* and *Gzmb* relative to *Actb* in MC38 tumors. Results from 2 independent experiments (n=4-7 mice/group in each experiment). Data points represent values in individual mice. Horizontal bars: median per group. P values < 0.05, as calculated with a two-sided Wilcoxon test are indicated in italics. Numbers in bold: fold-change between the indicated groups.

Supplementary Figure 3 | Combined GARP:TGF-β1/PD-1 blockade does not increase the proliferation of tumor infiltrating CD8 T cells in MC38 and CT26. MC38 tumors from mice treated as indicated in **Figure 1** were collected on day 13. CT26 tumors from mice treated as indicated in **Figure 1** (with the exception that antibodies were injected on days 6, 10 and 14) were collected on day 14. Tumors were dissociated and analyzed by flow cytometry. Results from one experiment for MC38 (n=5 mice/group) and one experiment for CT26 (n=4/group). **(A)** Percentage of Ki-67⁺ cells in live single CD8 T cells (CD45⁺CD8⁺ for MC38, and CD3⁺CD8⁺ for CT26). **(B)** Geometric

mean fluorescence intensity (geomean) for Ki-67 staining in live single Ki-67⁺ CD8 T cells. Data points represent values in one mouse. Horizontal bars: median per group.

Supplementary Figure 4 | Combined GARP:TGF-β1/PD-1 blockade does not modify mean area of blood vessels in MC38 and CT26 tumors. mIF and quantitative digital imaging of sections shown in **Figure 4**. Mean area of CD146⁺ objects in tumor sections (n=134 to 26 939 CD146⁺ objects per section). Data points represent the mean values of two tumor sections analyzed in individual mice. Horizontal bars: median per group.

Supplementary Figure 5 | A majority of GARP⁺ blood vessels also express PDGFRβ in MC38 tumors. Frozen MC38 tumor sections from mice shown in **Figures 1A, B** were used for mIF and quantitative imaging. **(A)** Representative image of a MC38 control tumor stained with anti-CD146 antibody (red), anti-PDGFRβ (yellow) and anti-GARP (green). Left: CD146 and PDGFRβ signals. Right: GARP and PDGFRβ signals on the same area. White arrow: CD146⁺PDGFRβ⁺GARP⁺ vessel (top images) or CD146⁺PDGFRβ⁺GARP⁻ vessel (bottom images). **(B)** Proportion (%) of PDGFRβ⁺ vessels in GARP⁻ or GARP⁺ blood vessels. Data points represent values for individual mice. Horizontal bars: median per group. P value < 0.05, as calculated with a two-sided Wilcoxon test, are indicated in italics. Number in bold: fold-change between the indicated groups. One tumor section analyzed per mouse.

Supplementary Figure 6 | C166 and MS1 endothelial cells do not activate TGF-β1 *in vitro* in absence of stimulus or another cell type. C166 and MS1 cells were used to perform a proliferation assay as described in **Figure 5B**. Incorporation of ³H-T was measured after 96 hours of culture in the presence of blocking anti-GARP:TGF-β1 (clone 58A2) or neutralizing anti-TGF-β1, β2, β3 (clone 1D11) mAbs. Bars indicate means (+ SD) for triplicate wells. Data representative of 3 independent experiments.

Supplementary Figure 7 | Combined GARP:TGF-β1/PD-1 blockade increases expression of *Sell* but not of *Icam1* and *Vcam1* in MC38 tumors. RT-qPCR analyses relative to **Figure 6A**. Graphs show the expression level of *Icam1*, *Vcam1* and *Sell* normalized by *Actb*, *Cd3e* or *Cd146*. Data points represent values measured in individual mice. Horizontal bars: median per group. Number in italics indicate P values < 0.05 as calculated with a two-sided Wilcoxon test, and numbers in bold indicate fold-changes between groups for selected comparisons.

Supplementary Table 1 | Primers and probes sequences.

REFERENCES

1. Stockis J, Colau D, Coulie PG, Lucas S. Membrane Protein GARP Is a Receptor for Latent TGF-β on the Surface of Activated Human Treg. *Eur J Immunol* (2009) 39(12):3315–22. doi: 10.1002/eji.200939684
2. Stockis J, Dedobbeleer O, Lucas S. Role of GARP in the Activation of Latent TGF-Beta1. *Mol Biosyst* (2017) 13(10):1925–35. doi: 10.1039/C7MB00251C
3. Stockis J, Lienart S, Colau D, Collignon A, Nishimura SL, Sheppard D, et al. Blocking immunosuppression by human Tregs In Vivo with antibodies targeting integrin alphaVbeta8. *Proc Natl Acad Sci U S A* (2017) 114(47): E10161–8. doi: 10.1073/pnas.1710680114
4. Liénart S, Merceron R, Vanderaa C, Lambert F, Colau D, Stockis J, et al. Structural Basis of Latent TGF-Beta1 Presentation and Activation by GARP on Human Regulatory T Cells. *Science* (2018) 362(6417):952–6. doi: 10.1126/science.aau2909
5. Tanaka A, Sakaguchi S. Regulatory T Cells in Cancer Immunotherapy. *Cell Res* (2017) 27(1):109–18. doi: 10.1038/cr.2016.151
6. Sakaguchi S, Mikami N, Wing JB, Tanaka A, Ichiyama K, Ohkura N. Regulatory T Cells and Human Disease. *Annu Rev Immunol* (2020) 38:541–66. doi: 10.1146/annurev-immunol-042718-041717
7. Cuende J, Lienart S, Dedobbeleer O, van der Woning B, De Boeck G, Stockis J, et al. Monoclonal Antibodies Against GARP/TGF-Beta1 Complexes Inhibit the Immunosuppressive Activity of Human Regulatory T Cells In Vivo. *Sci Transl Med* (2015) 7(284):284ra56. doi: 10.1126/scitranslmed.aaa1983
8. de Streel G, Bertrand C, Chalon N, Lienart S, Bricard O, Lecomte S, et al. Selective Inhibition of TGF-Beta1 Produced by GARP-Expressing Tregs Overcomes Resistance to PD-1/PD-L1 Blockade in Cancer. *Nat Commun* (2020) 11(1):4545. doi: 10.1038/s41467-020-17811-3
9. Martin CJ, Datta A, Littlefield C, Kalra A, Chapron C, Wawersik S, et al. Selective Inhibition of TGFbeta1 Activation Overcomes Primary Resistance to Checkpoint Blockade Therapy by Altering Tumor Immune Landscape. *Sci Transl Med* (2020) 12(536):eaay8456. doi: 10.1126/scitranslmed.aay8456
10. Mariathasan S, Turley SJ, Nickles D, Castiglioni A, Yuen K, Wang Y, et al. TGFbeta Attenuates Tumour Response to PD-L1 Blockade by Contributing to Exclusion of T Cells. *Nature* (2018) 554(7693):544–8. doi: 10.1038/nature25501
11. Dodagatta-Marri E, Meyer DS, Reeves MQ, Paniagua R, To MD, Binnewies M, et al. Alpha-PD-1 Therapy Elevates Treg/Th Balance and Increases Tumor Cell Psmad3 That are Both Targeted by Alpha-TGFbeta Antibody to Promote Durable Rejection and Immunity in Squamous Cell Carcinomas. *J Immunother Cancer* (2019) 7(1):62. doi: 10.1186/s40425-018-0493-9
12. Tauriello DVF, Palomo-Ponce S, Stork D, Berenguer-Llergo A, Badia-Ramentol J, Iglesias M, et al. TGFbeta Drives Immune Evasion in Genetically Reconstituted Colon Cancer Metastasis. *Nature* (2018) 554(7693):538–43. doi: 10.1038/nature25492
13. Metelli A, Wu BX, Fugle CW, Rachidi S, Sun S, Zhang Y, et al. Surface Expression of TGFbeta Docking Receptor GARP Promotes Oncogenesis and Immune Tolerance in Breast Cancer. *Cancer Res* (2016) 76(24):7106–17. doi: 10.1158/0008-5472.CAN-16-1456
14. Bruhns P. Properties of Mouse and Human IgG Receptors and Their Contribution to Disease Models. *Blood* (2012) 119(24):5640–9. doi: 10.1182/blood-2012-01-380121
15. Kershaw MH, Hsu C, Mondesire W, Parker LL, Wang G, Overwijk WW, et al. Immunization Against Endogenous Retroviral Tumor-Associated Antigens. *Cancer Res* (2001) 61(21):7920–4.
16. Schrage A, Loddenkemper C, Erben U, Lauer U, Hausdorf G, Jungblut PR, et al. Murine CD146 is Widely Expressed on Endothelial Cells and is

Recognized by the Monoclonal Antibody ME-9F1. *Histochem Cell Biol* (2008) 129(4):441–51. doi: 10.1007/s00418-008-0379-x

17. Zhao Y, Yu X, Li J. Manipulation of Immunevascular Crosstalk: New Strategies Towards Cancer Treatment. *Acta Pharm Sin B* (2020) 10 (11):2018–36. doi: 10.1016/j.apsb.2020.09.014

18. Vermeersch E, Denorme F, Maes W, De Meyer SF, Vanhoorelbeke K, Edwards J, et al. The Role of Platelet and Endothelial GARP in Thrombosis and Hemostasis. *PloS One* (2017) 12(3):e0173329. doi: 10.1371/journal.pone.0173329

19. Boutet M, Gauthier L, Leclerc M, Gros G, de Montpreville V, Theret N, et al. TGFbeta Signaling Intersects With CD103 Integrin Signaling to Promote T-Lymphocyte Accumulation and Antitumor Activity in the Lung Tumor Microenvironment. *Cancer Res* (2016) 76(7):1757–69. doi: 10.1158/0008-5472.CAN-15-1545

20. Bommireddy R, Saxena V, Ormsby I, Yin M, Boivin GP, Babcock GF, et al. TGF-Beta 1 Regulates Lymphocyte Homeostasis by Preventing Activation and Subsequent Apoptosis of Peripheral Lymphocytes. *J Immunol* (2003) 170 (9):4612–22. doi: 10.4049/jimmunol.170.9.4612

21. Bessa X, Elizalde JI, Mitjans F, Pinol V, Miquel R, Panes J, et al. Leukocyte Recruitment in Colon Cancer: Role of Cell Adhesion Molecules, Nitric Oxide, and Transforming Growth Factor Beta1. *Gastroenterology* (2002) 122 (4):1122–32. doi: 10.1053/gast.2002.32369

22. DiChiara MR, Kiely JM, Gimbrone MA Jr, Lee ME, Perrella MA, Topper JN. Inhibition of E-Selectin Gene Expression by Transforming Growth Factor Beta in Endothelial Cells Involves Coactivator Integration of Smad and Nuclear Factor kappaB-Mediated Signals. *J Exp Med* (2000) 192(5):695–704. doi: 10.1084/jem.192.5.695

23. Gamble JR, Khew-Goodall Y, Vadas MA. Transforming Growth Factor-Beta Inhibits E-Selectin Expression on Human Endothelial Cells. *J Immunol* (1993) 150(10):4494–503.

24. Zheng X, Fang Z, Liu X, Deng S, Zhou P, Wang X, et al. Increased Vessel Perfusion Predicts the Efficacy of Immune Checkpoint Blockade. *J Clin Invest* (2018) 128(5):2104–15. doi: 10.1172/JCI96582

25. Tian L, Goldstein A, Wang H, Ching H, Sun Kim I, Welte T, et al. Mutual Regulation of Tumour Vessel Normalization and Immunostimulatory Reprogramming. *Nature* (2017) 544(7649):250–4. doi: 10.1038/nature21724

26. Huang Y, Yuan J, Righi E, Kamoun WS, Ancukiewicz M, Nezivar J, et al. Vascular Normalizing Doses of Antiangiogenic Treatment Reprogram the Immunosuppressive Tumor Microenvironment and Enhance Immunotherapy. *Proc Natl Acad Sci U.S.A.* (2012) 109(43):17561–6. doi: 10.1073/pnas.1215397109

27. Shrimali RK, Yu Z, Theoret MR, Chinnasamy D, Restifo NP, Rosenberg SA. Antiangiogenic Agents can Increase Lymphocyte Infiltration Into Tumor and

Enhance the Effectiveness of Adoptive Immunotherapy of Cancer. *Cancer Res* (2010) 70(15):6171–80. doi: 10.1158/0008-5472.CAN-10-0153

28. Armulik A, Genove G, Betsholtz C. Pericytes: Developmental, Physiological, and Pathological Perspectives, Problems, and Promises. *Dev Cell* (2011) 21 (2):193–215. doi: 10.1016/j.devcel.2011.07.001

29. Allen E, Jabouille A, Rivera LB, Lodewijckx I, Missiaen R, Steri V, et al. Combined Antiangiogenic and Anti-PD-L1 Therapy Stimulates Tumor Immunity Through HEV Formation. *Sci Transl Med* (2017) 9(385): eaak9679. doi: 10.1126/scitranslmed.aak9679

30. Lee WS, Yang H, Chon HJ, Kim C. Combination of Anti-Angiogenic Therapy and Immune Checkpoint Blockade Normalizes Vascular-Immune Crosstalk to Potentiate Cancer Immunity. *Exp Mol Med* (2020) 52(9):1475–85. doi: 10.1038/s12276-020-00500-y

31. De Palma M, Jain RK. CD4(+) T Cell Activation and Vascular Normalization: Two Sides of the Same Coin? *Immunity* (2017) 46(5):773–5. doi: 10.1016/j.immuni.2017.04.015

Supplementary figures

Figure S1
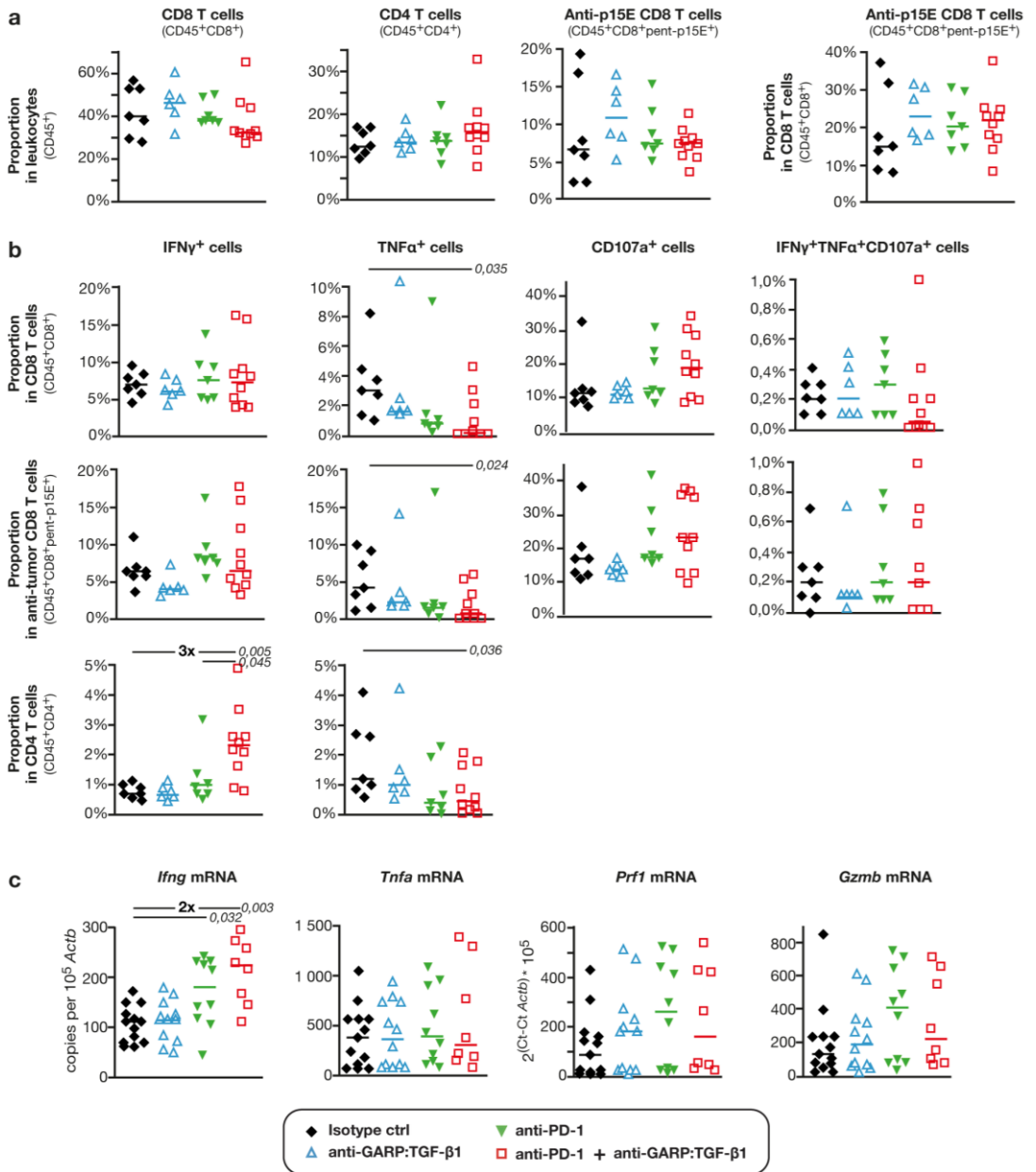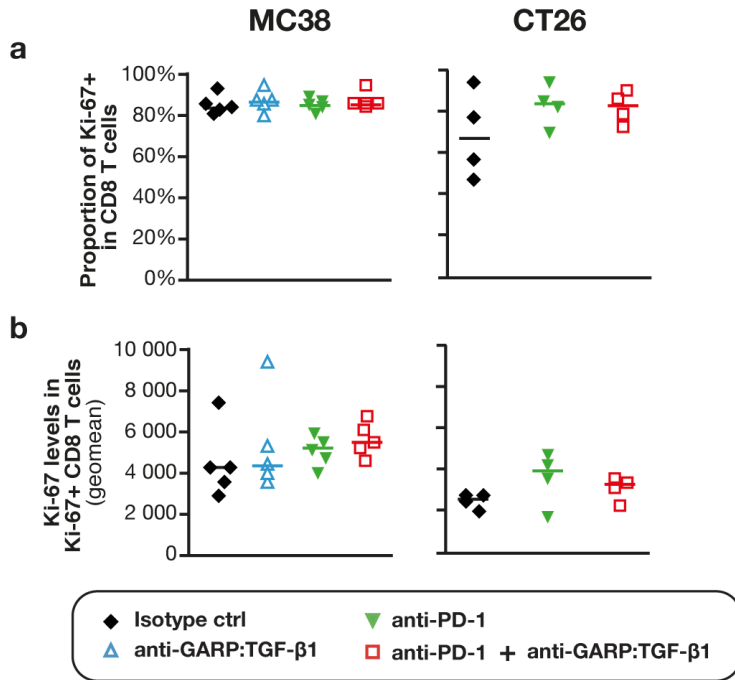
Figure S2

Figure S3
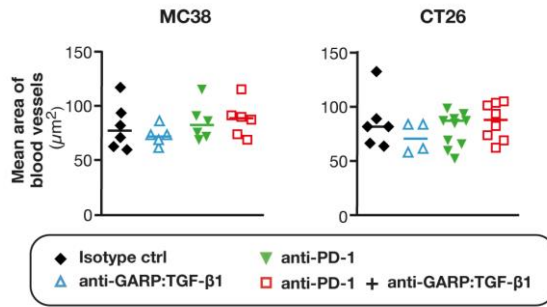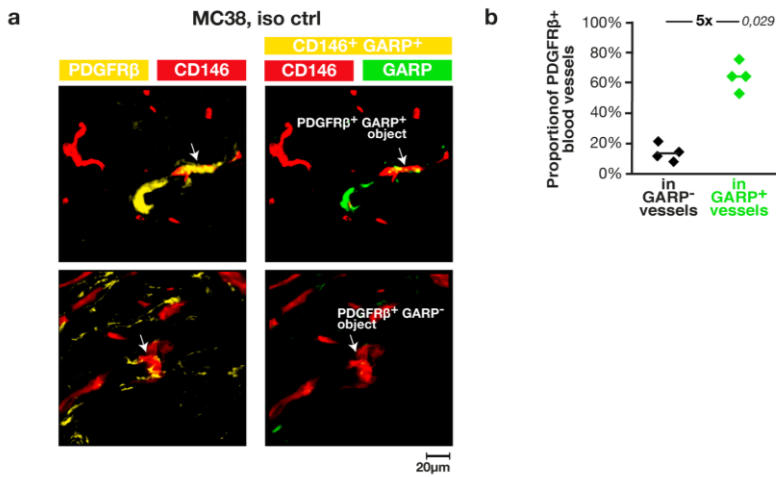
Figure S4

Figure S5
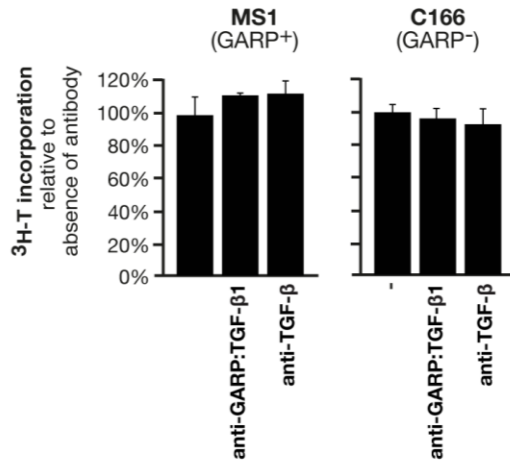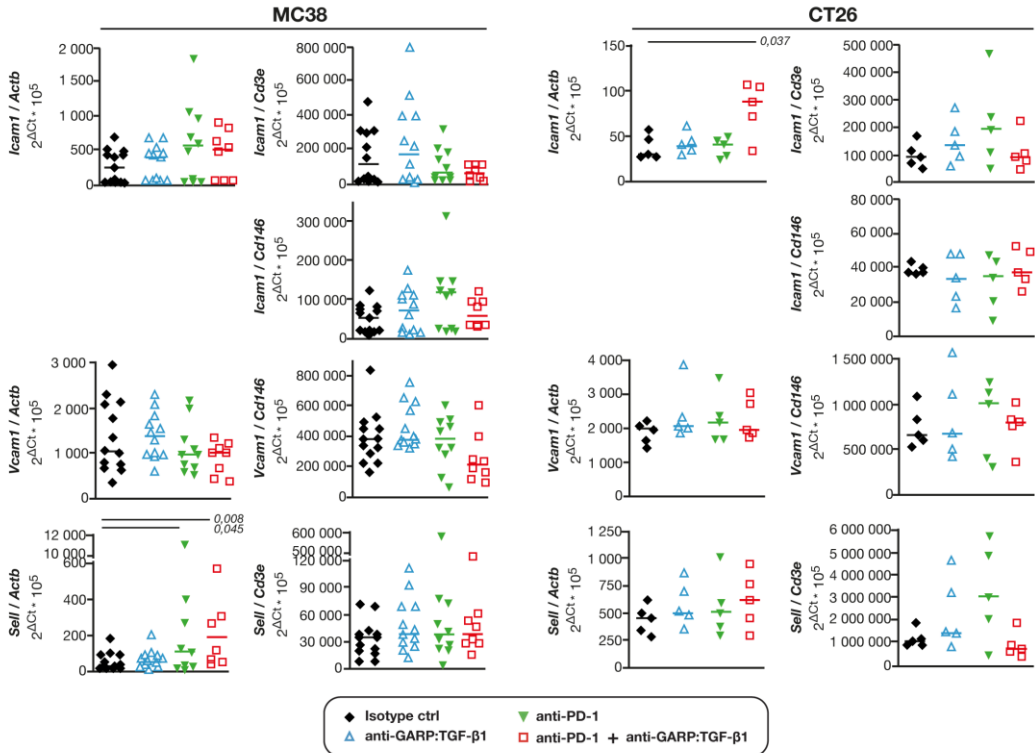
Figure S6

Figure S7

Supplementary Table 1. Primers sequences

Sequence (5' - 3')	Definition
TCAAGTGGCATAGATGTGGAAGAA	Forward primer in *mIfng* mRNA
TGGCTCTGCAGGATTTTCATG	Reverse primer in *mIfng* mRNA
TCACCATCCTTTTGCCAGTTCCTCCAG	Taqman probe in *mIfng* mRNA
AAGAGAGCAAGGACAACACTC	Forward primer in *mGzmb* mRNA
CATGTCCCCCGATGATCTC	Reverse primer in *mGzmb* mRNA
ACAAGGTCAGCAGTAGCAGGAGGA	Taqman probe in *mGzmb* mRNA
CAGTAGAGTGTCGCATGTACAG	Forward primer in *mPrf1* mRNA
GATGAGCCTGTGGTAAGCAT	Reverse primer *in mPrf1* mRNA
TCGCCTGGTACAAAAACCTCCACTC	Taqman probe in *mPrf1* mRNA
CATCTTCTCAAAATTCGAGTGACAA	Forward primer in *mTnfa* mRNA
GGGTTGTACCTTGTCTACTCCCA	Reverse primer in *mTnfa* mRNA
CACGTCGTAGCAAACCACCAAGTGGA	Taqman probe in *mTnfa* mRNA
ATAGGAAGGCCAAGGCCAAG	Forward primer in *mCd3e* mRNA
TTGCGGATGGGCTCATAGTC	Reverse primer in *mCd3e* mRNA
ACCCGAGGAACCGGTGCTGGT	Taqman probe in *mCd3e* mRNA
GTGGTTGATGTCCTTCCTACAA	Forward primer in *mCd8b* mRNA
TCCGCACACAGTAAAAGTAGAC	Reverse primer in *mCd8b* mRNA
AATGCCAGCAGAAGCAGGATGCAGACTA	Taqman probe in *mCd8b* mRNA
CGTGATAGCTGTGCTCTGAA	Forward primer in *mCd4* mRNA
GTTCTCTCCATGTCCAACCTAA	Reverse primer in *mCd4* mRNA
ACTGAGAGTGTCATGCCGAACCAG	Taqman probe in *mCd4* mRNA
GGTCCTTGCCTACTTGCTG	Forward primer in *mIcam1* mRNA
CTGTGCTTTGAGAACTGTGG	Reverse primer in *mIcam1* mRNA
CCGCTACCATCACCGTGTATTCGTT	Taqman probe in *mIcam1* mRNA
CCATCCTTTCTTGAGATTTCTTGC	Forward primer in *mSell* mRNA
CTTCATTCCTGTAGCCGTCAT	Reverse primer in *mSell* mRNA
TTAACCGCCTTGCCAGCCAAATG	Taqman probe in *mSell* mRNA
GTCCTTCCGACAGTTTCTCTC	Forward primer in *mLfa1* mRNA
GGAGTCATGGAGTGTGGTATC	Reverse primer in *mLfa1* mRNA
TCCCAATGTAGCCAGACTCACACC	Taqman probe in *mLfa1* mRNA
AGTTCATTTCCTGCTGTCTTCA	Forward primer in *mSele* mRNA
ATGTGCCTTCTTACAACGTCT	Reverse primer in *mSele* mRNA
CCACGATGCATTTGTGTTCCTGATTGTT	Taqman probe in *mSele* mRNA

Annex n°2: The pre-metastatic niche in lymph nodes: formation and characteristics

Lionel Gillot, Louis Baudin, **Loïc Rouaud**, Frédéric Kridellka, Agnès Noël

REVIEW

The pre-metastatic niche in lymph nodes: formation and characteristics

Lionel Gillot[1] · Louis Baudin[1] · Loïc Rouaud[1] · Frédéric Kridelka[2] · Agnès Noël[1]

Abstract

Lymph node metastasis is a crucial prognostic parameter in many different types of cancers and a gateway for further dissemination to distant organs. Prior to metastatic dissemination, the primary tumor prepares for the remodeling of the draining (sentinel) lymph node by secreting soluble factors or releasing extracellular vesicles that are transported by lymphatic vessels. These important changes occur before the appearance of the first metastatic cell and create what is known as a pre-metastatic niche giving rise to the subsequent survival and growth of metastatic cells. In this review, the lymph node structure, matrix composition and the emerging heterogeneity of cells forming it are described. Current knowledge of the major cellular and molecular processes associated with nodal pre-metastatic niche formation, including lymphangiogenesis, extracellular matrix remodeling, and immunosuppressive cell enlisting in lymph nodes are additionally summarized. Finally, future directions that research could possibly take and the clinical impact are discussed.

Keywords Lymph node · Pre-metastatic niche · Extracellular matrix · Lymphangiogenesis · Metastasis

Introduction

Many types of cancer, including melanoma, breast, oral, pancreatic and cervical cancers, disseminate through the lymphatic system [1–5]. In a large number of cases, lymph nodes (LNs) are relay the first metastases and the presence or absence of LN metastases is a crucial prognostic parameter for clinicians [6]. Indeed, the presence of tumor cells in the first draining LN, the so-called sentinel LN, is regarded as a predictor for poor patient outcome [7]. The expression of lymphangiogenic growth factors, high lymphatic vessel (LV) density, and high incidence of lymphovascular invasion are typically associated with LN metastases and poor patient outcome [8, 9]. Metastatic dissemination to LNs develops when tumor cells become detached from the primary neoplasm, enter an LV and are subsequently transported to the sentinel LN where they initially accumulate in the nodal subcapsular sinus (SCS). Within the LN, disseminated tumor cells may either be destroyed, pass through the LN and enter the efferent LV, or remain in the LN where they form a colony [10, 11]. It has been debated at length whether cancer cells in LNs can secondarily seed distant metastases and colonize in distant organs. LN metastases were either viewed as clinically inconsequential [12, 13] or had the potential to seed distant organs [14, 15]. Two elegant studies demonstrated the migration of metastatic cells from LNs to distant organs in pre-clinical models [16, 17]. These data provided a definitive proof-of-concept that metastatic cells in LNs can go on to seed distant organs. They also provide an indication that, when treating LN metastases, the aim should be, not only to obtain local control but also to prevent distant disease and, therefore, death. Nevertheless, there is still no explanation as to why some tumors tend to metastasize in

✉ Agnès Noël
agnes.noel@uliege.be

Lionel Gillot
lgillot@uliege.be

Louis Baudin
louis.baudin@uliege.be

Loïc Rouaud
loic.rouaud@uliege.be

Frédéric Kridelka
frederic.kridelka@chuliege.be

1   Laboratory of Tumor and Development Biology, GIGA-Cancer, Liege University, Avenue Hippocrate 13, 4000 Liege, Belgium

2   Department of Obstetrics and Gynecology, CHU of Liege, 4000 Liege, Belgium

Ⓐ Springer

LNs, while others intravasate directly into blood vessels and reach distal sites via the blood stream.

The concept of a pre-metastatic niche was first formulated by David Lyden and colleagues 15 years ago [18]. This pioneering study revealed that factors shed or secreted by tumor cells provide the microenvironment, within the organ, where metastases may later develop. These factors prepare the target organ to support the survival and proliferation of disseminating tumor cells. The main events in such a priming process include the secretion of pro-metastatic growth factors and chemokines/cytokines, as well as the release of extracellular vesicles (EVs) by the primary tumor. These primary tumor-derived factors induce the recruitment of specific cell types, an escalation in numbers of immunosuppressive cells and the remodeling of the extracellular matrix (ECM) in the pre-metastatic organ. These molecular and cellular changes create a unique microenvironment that will support subsequent metastatic growth [8, 10, 18–20]. Pre-metastatic niche formation has been described in detail for the lung [21], liver [22] and bone [23], with some specificities for each organ [24–26]. However, less is known about the pre-metastatic niche in LNs. Hirakawa et al. were the first to observe LN remodeling at a pre-metastatic stage in 2005 [27] and 2007 [28]. They proved that the vascular growth factors (VEGF-A and VEGF-C) are responsible for inducing lymphangiogenesis in sentinel LNs. Since then, a number of studies have elucidated a number of distinctive features of pre-metastatic LNs, including increased lymphangiogenesis and lymph flow, remodeling of high endothelial venules (HEVs), recruitment of myeloid cells and reduction of effector lymphocyte numbers and function[18, 28, 29]. This review will begin by describing the specific structure of LNs under physiological conditions to more clearly describe the tissue remodeling set in motion by the primary tumor. The latest findings on key components and mechanisms involved in pre-metastatic niche formation in LNs will also be summarized.

Cellular composition and compartmentalization in LNs under physiological conditions

The lymphatic system is a unidirectional, blind-ended vascular network, of not only lymphatic capillaries and larger collecting vessels, but also secondary lymphoid organs such as LNs. This vascular system is essential for maintaining fluid homeostasis, absorbing dietary lipids and transporting immune cells and soluble antigens from peripheral tissues towards LNs and the central circulatory system [30, 31].

LN development

LN formation during fetal development has been studied through the generation and phenotyping of various gene-deficient mice but is not yet fully understood [32–35]. However, what is known is that the interaction between lymphoid-tissue inducer (LTi) cells and lymphoid-tissue organizer (LTo) cells is crucial for LN development [36]. LTi cells arising in the fetal liver are attracted to LN development sites by a gradient of chemokines, including CXCL13, CCL19 and CCL21 [37]. In a mouse model, the loss of CXCR5, a receptor for CXCL13, prevented the formation of peripheral LNs [38], stromal LTo cells expressed lymphotoxin-β-receptor (LTβR), while LTi cells produced its ligand, lymphotoxin-$\alpha_1\beta_2$. This interaction between the two cell types induced an upregulation of adhesion molecules. For instance, vascular cell adhesion molecule 1 (VCAM-1) promoted the retention of hematopoietic cells in forming LNs [39]. LTβR signaling induced the secretion of VEGF-C by LTo cells, which could potentially attract lymphatic endothelial cells (LECs) into the developing organ. LECs surrounded LTi and LTo clusters and express CCL21, which further drew in LTi cells and activated LECs [40]. This activation was attributed to the expression of the receptor activator of NF-κB (RANK) by LECs. Accordingly, the ablation of RANK expression in LECs blocked LTi organization and LN formation [41]. Collecting lymphatic vessels are required for the transport of LTi cells, the formation of the LN capsule and SCS specialization in embryonic stages. Indeed, SCS specialization coincides with lymphatic vascular maturation. LECs of the LN lymphatic cup are organized in a double layer. LECs of the outer layer expressed FOXC2 (a marker for collecting vessels), whereas those of the inner layer expressed LYVE1, ITGA2B and MADCAM, specific markers of LECs lining the floor (fLEC). The genetic loss of FOXC2 in LECs from embryos is characterized by the absence of valves as a result of the suspension of collecting vessel development. In those mice, LN capsule formation was impaired, and SCS LECs failed to express ITGA2B. These results demonstrated that FOXC2 ensures collecting vessel maturation and capsule specialization [38].

LN organization

LNs are immune organs occupying strategic positions throughout the body. There is a complex network of lymphatic sinuses surrounding a highly organized parenchyma composed of reticular fibers, supporting immune cells, specialized blood vessels and fibroblastic reticular cells (FRCs). FRCs play a key role in B and T cell

compartmentalization in LNs and, together, represent between 20 and 50% of the non-hematopoietic component of them. These specialized cells express molecules commonly found in myofibroblasts, including desmin, vimentin, CD90, CD73, CD103, α-smooth muscle actin (αSMA) and the ERTR7 antigen [42]. FRCs form stellate cell–cell contacts, thereby creating a three-dimensional network along which leukocytes can migrate. They also produce fibroreticular fibers which are involved in molecular transportation and cell migration. Recently, heterogeneity of stromal cells has been identified in murine LNs [43]. In fact, a number of subsets were identified, including marginal reticular cells, which produce CXCL13 which has a key role in B cell homing and migration towards follicles

[44]. In the paracortex, two divergent subsets have been distinguished and express different levels of CCL19, a regulator of lymphocyte migration [43]. This organization provides an optimal environment for immune response induction and regulation[45]. The LN is divided into three areas: the cortex, paracortex and medulla (Fig. 1). The cortex contains follicular dendritic cells and B cells that are mainly associated with germinal follicles, where follicular dendritic cells present antigens to naïve B lymphocytes, leading to antibody production by activated B cells. An interfollicular zone is also present in the cortex and separates the germinal follicles. The paracortex is known as the T cell zone in which antigen-presenting dendritic cells (DCs) prime naïve T lymphocytes. The medulla contains a

Fig. 1 Lymph node (LN) organization. The LN is divided into three parts: the cortex (C), paracortex (PC) and medulla (M). A Dendritic cells (DCs) from all over the body arrive at the LN via afferent vessels and then migrate into the cortex (C). B B lymphocytes are located in germinal follicles and interact with follicular dendritic cells (FDCs). C T lymphocytes are in the paracortex to interact with DCs. D DCs migrate on reticular fibers to the high endothelial venules (HEVs), where they interact with naïve lymphocytes entering the LN from the HEV. Activated B and T lymphocytes crawl along the medullary sinus to leave the LN

🖄 Springer
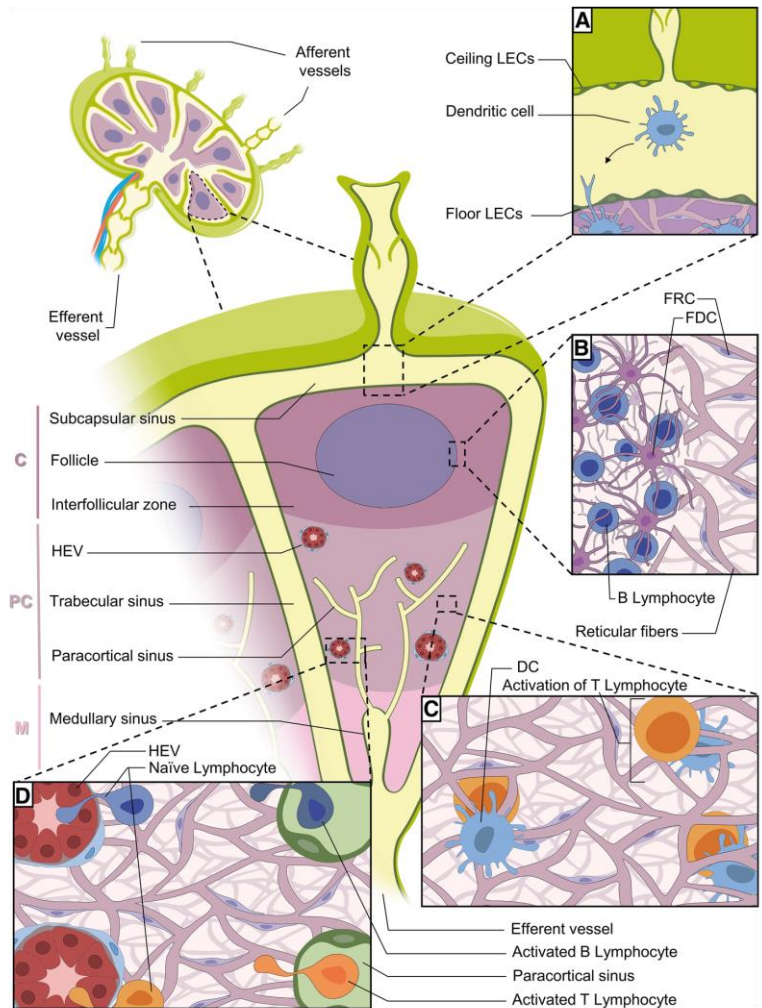
complex network of medullary sinuses (MS), which converge at the hilum into the efferent LVs [45, 46]. This region contains blood vessels, antibody-secreting B cells and macrophages, which express markers such as CD169, F4/80, MARCO and CD206 [47, 48].

Recent advances have identified intriguing LEC plasticity, heterogeneity and origin diversity [49, 50]. In LNs, different LEC subtypes have been identified in the different anatomical sites described above in both humans and mice [51–54]. Interestingly, SCS LECs and MS LECs display distinct features, including cellular organization, expression profiles, and roles [51]. Mouse SCS LECs produce macrophage scavenger receptors which are involved in the transmigration of lymphocytes entering LNs from peripheral tissues. MS LECs, which express high levels of PD-L1, can be said to contribute to the deletion of alloreactive CD8 + T cells [55]. In humans, however, an additional subset was identified in the MS and cortical sinuses which expressed the C-type lectin CD209, allowing the adhesion of neutrophils to the medulla. In addition, NT5E +, LYVE1 + and MFAP4 + are the LECs lining the ceiling of the medulla, whereas LECs from lymphatic capillaries express PDPN, LYVE1 and CCL21[54]. A first transcriptomic analysis from mouse LNs has revealed the existence of two intriguing LEC subsets in the SCS that further support a substantial degree of LEC specialization [51]. fLECs of the SCS secrete neutrophil chemoattractant CXCL1-CXCL5, and LECs lining the ceiling (cLECs) express CCRL1, a chemokine receptor, thereby creating a gradient favorable for DC migration [56]. In humans, these 2 LEC subsets can be distinguished by the expression of caveolin-1 (by cLECs), while fLECs express TNFRSF9 [54]. These data demonstrate a specific signature of LECs although this depends on where they are located within the LN.

The lymph enters the node via the afferent LVs, which pierce the capsule and drain into the space underneath, known as the SCS. The lymph contains lymphocytes, antigens and DCs that are scanned by macrophages when it arrives in the SCS [57]. It filters through the trabeculae, cortical sinuses and MS before leaving the LN via the efferent LV [58]. From the SCS, smaller antigens and soluble molecules can access the interfollicular zone and the paracortex via a tubular network composed of specialized reticular fibers deposited by FRCs [59]. These reticular fibers are made up of a collagen core surrounded by microfibrils and a basement membrane [58]. This highly organized and interconnected network of ECM components generates conduits, which rapidly transport soluble molecules deep into the LN parenchyma. These conduits form a real 3D pipeline-like system known to rapidly distribute lymphatic fluid, soluble molecules and antigens deep into the LN parenchyma [60, 61] and have also recently been found to transport even larger molecules, such as immunoglobulins or virions [62].

This mesh-like network is essentially present in the T cell zone but follicles remain sparse. It extends to the paracortex where the HEVs are located, creating a connection between the SCS and these specialized blood vessels [61]. This particular structural micro-anatomy where hematopoietic cells can circulate, survive, and interact, both together, and with their environment, allows the LN to carry out its task of an initial immune response site. During an immune response, FRCs produce CCL19/CCL21, which assists in the directional cell migration of naïve T cells, B cells and DCs expressing CCR7. During homeostasis and in the presence of infection, this chemokine gradient helps lymphocyte homing and mediates interactions between T cells and DCs [63]. The reticular fibers descend from fLECs towards the HEVs, which are post-capillary venules especially suitable for lymphocyte entry into the LN parenchyma [50]. They are surrounded by pericytes embedded in a thick basement membrane [64]. HEV endothelial cells have a cuboidal shape and express general endothelial markers (CD31, CD34, VE-cadherin and VEGFR-2), specific blood endothelial markers (von Willebrand factor and peripheral lymph node addressin (PNAd) and VEGFR1) [65].

The LN extracellular matrix

The ECM provides structural scaffolding and biochemical support for tissue function and mechanical integrity and regulates the availability of growth factors and cytokines. It is composed of a network of biochemically distinct components, including fibrous proteins, glycoproteins, proteoglycans and matricellular proteins [66]. Although it has always been described as a support structure for tissue architecture, it is, in fact, a highly dynamic compartment that regulates a large number of cell functions. An integral feature of the ECM is that it constantly remodels itself as ECM components are deposited, degraded, or modified by ECM-modifying enzymes such as matrix metalloproteinases (MMP) and lysyl oxidase (LOX). The ECM plays a crucial role, not only in the primary tumor [67] but also in the secondary site, particularly at a pre-metastatic stage [68, 69].

Collagen accounts for the largest number of ECM proteins, but its composition and structure vary across different tissue types [70]. For instance, the basement membrane surrounding endothelial cells mainly consists of collagen type IV, while the fibroreticular stroma is, for the most part, composed of fibrillar types I and III collagen embedded in a meshwork of fibrillin microfibers. In LNs, reticular fibers form the principal ECM fibers which support the lymphoid organ architecture. The reticular arrangement of those fibrils is particularly suited to forming conduits and they transport antigen and signaling molecules, as well as guiding migrating cells [71]. Reticular fibers begin at the SCS and extend to the MS. Fibrillin-1 and -2 are essential matricellular proteins

in the LN that connect collagen fibers and the basement membrane in tubular structures [71]. Fibrillins constitute the structural backbone of microfibrils, which are found in many elastic and non-elastic tissues where they carry out a diverse number of functions, including interactions with latent transforming growth factor-binding proteins (LTBP) described below [72].

In the majority of organs, fibroblasts are the main source of ECM components, including at least type I and III collagens, elastin, fibronectin, tenascin (TNC) and periostin (POSTN) [24]. In LNs, on the other hand, FRCs are the primary producers of ECM components [59]. Under physiological conditions, these cells produce fibrillar types I and III collagen, collagen type IV, laminin, fibronectin and TNC, which allow cell migration within the LN [59, 73]. A transcriptional analysis performed on murine LNs confirmed that FRCs expressed integrin subunits such as αV, α4, α5, α6, α9, β1, β3, and β5, enabling their adhesion to many ECM components [74]. For example, integrin α5β1 can bind to fibronectin, and αVβ3 interacts with fibronectin, vitronectin, fibrinogen, thrombospondin and POSTN [75, 76]. TNC can bind to numerous integrins, including α2β1 and ανβ3, but the TNC-integrin α9β1 interaction is considered to be of higher avidity [77].

Contribution of tumor-secreted EVs to the formation of the pre-metastatic LN niche

Extracellular vesicles (EVs), including exosomes, are released by a range of cells and contain proteins and nucleic acids but are produced in larger quantities by tumor cells than by normal cells [78, 79]. Metastatic cancers produce EVs that are able to prime a pre-metastatic niche. Cancer-derived EVs are thought to be involved in the suppression of innate immune responses through the mobilization of MDSCs and the activation of TAMs and neutrophils [80, 81]. However, the detailed mechanism through which EVs promote the pre-metastatic niche is not yet fully understood. miR-105 is expressed and secreted via EV by metastatic breast cancer cells and can be transferred to endothelial cells. Tumor-secreted miR-105 targets ZO-1, leading to increased vascular permeability and metastasis and has been detected in the blood of tumor-bearing mice in the pre-metastatic stage [82]. Recently, miR-25-3P has been shown to promote pre-metastatic niche formation by enhancing vascular permeability and angiogenesis. Tumor-secreted miR-25-3P can also be transferred to vascular endothelial cells where it targets KLF2 and KLF4. KLF2 inhibits VEGFR-2 promoter activity, and KLF4 regulates the integrity of the endothelial barrier [83]. A prospective study has recently revealed that lymphatic EVs from afferent LVs inhibit DC

maturation. Through a proteomic analysis performed on lymphatic exudates from patients with primary melanoma, a signature of 18 immune-modulating proteins was identified, including S100A9, a known inhibitor of DC maturation [5]. These data suggest that EVs present in draining lymphatics contain a panel of molecules capable of inducing pre-metastatic niche formation in melanoma patients. Broggi et al. compared lymphatic exudate contents from metastatic melanoma patients to the plasma from all patients [84]. They observed that lymphatic exudate was enriched in melanoma-associated proteins but with a fivefold increase in the numbers of EVs. The proteomic profile of EVs from patients undergoing lymphadenectomy with negative LNs was associated with pathways such as VEGF, integrin and cellular extravasation. On the other hand, in patients undergoing lymphadenectomy with positive LNs for tumor cells, upregulation of proliferation, cancer and cell death pathways was observed. Moreover, the expression of S100 was significantly higher in patients with positive LNs than in patients with non-metastatic LNs [84]. These data suggest that EVs from early or advanced melanoma express protein signatures that correlate with different stages of the metastatic process. Tumor-derived EVs were injected intradermally into transgenic mice lacking dermal lymphatics and were nearly undetectable in tissues compared to WT mice, suggesting that lymphatic vessels are actively involved in the transportation of EVs. Moreover, this demonstrated that LECs were the main stromal cells taking up EVs in the tumor-draining LNs [84]. Similar results were observed by Garcia-Silva et al. [85], who also observed that lymphatic exudate had a higher level of S100 protein than plasma. Interestingly, the BRAF^{V600E} mutation was detected in exudate-derived vesicles [85]. All these data suggest that exudate-derived EVs could represent a new prognostic tool for melanoma progression and for detecting melanoma mutations. Moreover, these data support the existence of a pre-metastatic niche and the role of LNs in tumor progression. Further details on EV implications in LN metastatic dissemination, can be found in a recent review [86].

Vascular remodeling in the pre-metastatic LN niche

Lymphangiogenesis and HEV remodeling are key events in the formation of the LN pre-metastatic niche. LN lymphangiogenesis is mainly driven by VEGF-A, VEGF-C, integrin and erythropoietin and correlates with increased systemic metastasis [8, 27, 28, 87, 88]. Lymphangiogenic factors such as VEGF-C are released in the primary tumor by cancer cells and stromal cells, among which macrophages are an important source [89]. VEGF-C stimulates LEC proliferation and migration, inducing the sprouting of LVs and

the enlargement of existing vessels, thereby increasing the potential surface of lymphatic contact with tumor cells [90]. Furthermore, the enlargement of collecting lymphatics due to LEC proliferation and structural remodeling of smooth muscle cells results in an enhanced flow rate and increases sentinel LN metastases [91]. Experimental studies have highlighted lymphovascular remodeling in sentinel LNs [27, 28]. Lymphatic remodeling, controlled by soluble factors drained from the primary tumor, within tumor-draining LNs was found to occur even before tumor cells were detected in the LN. It has been suggested that the expanded lymphatic network in LNs contribute to a pre-metastatic niche that promotes LN colonization by metastatic cells [90]. Pre-metastatic induction of lymphangiogenesis in LNs has already been described at length in experimental models. RNA sequencing analysis revealed an altered transcriptional profile of LECs issued from tumor-draining LNs compared to naïve LNs. Interestingly, one of the strongest upregulated genes was integrin αIIb [92], whose expression on a specific subset of LN LECs responsive to RANKL has previously been reported [93]. This integrin, which is upregulated in LECs issued from tumor-draining LNs, promotes LN LEC adhesion to fibrinogen. Another integrin, crucial for LN colonization by tumor cells, such as melanoma cells, is integrin α4. The activation of this integrin is increased by VEGF-C and the PI3Kα signaling pathway and promotes the expansion of the lymphatic endothelium in LNs. This activation also serves as an adhesive ligand that captures VCAM-1 + metastatic tumor cells, thereby promoting LN metastasis [87]. VCAM-1 is also upregulated in tumor-associated LECs and, importantly, increases lymphatic permeability by weakening lymphatic junctions through a mechanism triggered by its interaction with integrin α4β1 [94].

Single-cell RNA sequencing of LECs isolated from naïve murine LNs was performed by Fujimoto et al. [52]. Four subsets of LECs were identified, corresponding to distinct anatomical locations. cLECs were negative for LYVE1 and ITGA2B but positive for CCRL1 (chemokine receptors) and FLRT2, all of which play a role in cell–cell adhesion. Conversely, fLECs expressed LYVE1, ITGA2B and MADCAM but not CCRL1. The expression of genes coding for cell adhesion, such as MADCAM, ITGA2B and FLRT2, suggested that fLECs and cLECs could be the first LECs encountered by tumor cells, allowing LN colonization. Due to the expression of chemokines and chemokine receptors, fLECs and cLECs could also play a role in tumor cell migration [53], although there is currently no clear evidence for the implication of cLECs and fLECs in tumor progression. However, the increased ITGA2B expression in LN LECs during tumorigenesis suggests its involvement through mechanisms yet to be explained [92]. Two other LEC subsets were identified. The first, medullary LECs, defined by the expression of markers such as MRC1 and MARCO. The

second subset was cortex LECs expressed unique markers, including PTX3, ITIH5 and KCNJ8. In addition, a specific cortical LEC subtype implicated in rapid lymphocyte egress from LNs was identified [52]. In parallel, another study conducted on murine LN samples provided similar results but defined eight populations of LECs, including the four subsets described above and four new populations, including collecting valve LECs, a bridge population (between cLECs and fLECs) and transition zone LECs (tzLECs) [53]. It is worth noting that no specific gene markers of tzLECs were identified and only a variable expression of MADCAM, CCL20, MARCO and LYVE1. In this study, a clear distinction was made between medullary LECs by the expression of MARCO-LECs and CD274 + and PTX3-LECs (CD274-), but there was no distinction of cortex LECs [53]. Transcriptional profiling of LECs isolated from the LNs of mice bearing tumors has been reported by Commerford et al. [92]. Takeda and colleagues have recently conducted a single-cell sequencing analysis of non-sentinel LN LECs (distant from the tumor) collected from cancer patients [54]. In line with the mouse data, SCS cLECs, SCS fLECs and medullary sinus LECs were again distinguished. Two additional subsets were identified for lymphatic valves and capillary lymphatics. Blood endothelial cell heterogeneity in naïve murine LNs was also addressed. Eight different subtypes of blood endothelial cells from mouse LNs were identified with different gene expression. They included arterial ECs, two venous subsets, five capillary subsets, high endothelial cells (HECs) and non-HEC veins, and HECs express genes required for lymphocyte recruitment, such as Glycam1 and Chst4 [95]. Despite these important advances, there remains a need to discover how these lymphatic and blood endothelial subtypes contribute to the pre-metastatic LN niche.

The remodeling of HEVs in tumor-draining LNs is likely to impair the recruitment of naïve lymphocytes and the anti-tumor immune response and may also increase the supply of oxygen and nutrients to a growing metastatic lesion [8]. The features of these blood vessels can again be altered by the primary tumor, even before the appearance of metastases. These alterations are characterized by the dilation and flattening of the endothelium as well as a loss of functional molecules prior to colonization by tumor cells [29, 96, 97]. Bone morphogenetic protein-4 (BMP-4) expression is reduced in HEVs of tumor-draining LNs. This decrease in BMP-4 is implicated in HEV morphology by changing the shape of endothelial cells from a cuboidal to a flattened shape [98]. HEV remodeling further contributes to tumor-induced immunosuppression by interfering with lymphocyte trafficking. To study the role of HEVs in tumor dissemination, Brown et al. [16] developed a model of intra-lymphatic injection to directly add a number of fluorescent tumor cells into the LN SCS. To determine the importance of HEVs, the efferent LVs were ligated to avoid lymphatic

dissemination. Eleven days after injecting the tumor, mice developed lung metastases. Tumor cells became progressively associated with HEVs during tumor progression and frequently localized in their lumen. This experimental study provided evidence that HEVs represent an escape pathway for tumor cells to exit LNs and spread to distant organs using blood circulation [16, 17]. Structural and molecular remodeling of HEVs has been more recently observed in patients with breast cancer although not in healthy patients. This remodeling was associated with the dysregulation of CCL21 in perivascular FRCs, disturbing the migration of CCR7+ naïve lymphocytes in the LN parenchyma [99].

## Immunosuppressive microenvironment in pre-metastatic LNs

The LN is a dynamic organ subjected to important remodeling at histological, cellular and molecular levels under pathological conditions. In the context of cancer, it is believed that tumor antigens can induce an anti-tumoral response in LNs that initially restricts metastasis formation. Nevertheless, as tumors develop, immunomodulatory factors, drained from the tumor, prime an immunosuppressive response in the LNs that supports metastatic outgrowth (Fig. 2) [10]. Several immune cells, such as myeloid-derived suppressor cells (MDSCs), tumor-associated macrophages (TAMs), Tregs and immature DCs, all play a central role in tumor growth and metastasis and by accumulating in LNs can inhibit the anti-tumor immune activities of CD4, CD8 T cells and NK cells [100–102]. MDSCs are precursors of macrophages, DCs, granulocytes and myeloid cells and are key actors in eliciting immunosuppression. Myeloid differentiation and MDSC expansion are promoted by a variety of molecules, such as GM-CSF, M-CSF, IL-3, IL-6 and VEGF which are produced by tumor cells [103] and the mechanisms used to recruit MDSCs in tumor-draining and distant LNs are described[100, 103–107]. Immunosuppressive activity exerted by MDSCs involves several mechanisms acting on distinct targets through a consistent panel of molecules, including arginase 1, indoleamine-2,3-dioxygenase (IDO), NOS, ROS, peroxynitrite, TGF-β and IL-10 [108, 109]. IDO is an enzyme metabolizing tryptophan that can be expressed by a number of different cell types including DCs. IDO decreases the immune response of T cells and is likely to play a role in the establishment of an immunosuppressive microenvironment in LNs [110]. In fact, a correlation has already been established between the co-expression of IFN-γ and IL-10 and the expression of IDO in sentinel LNs [111]. The function and fate of MDSCs are dependent on their living environment. In lymphoid organs, high STAT3 activity prevents their differentiation into dendritic cells and macrophages and therefore induces their accumulation [112]. The principal target of MDSCs is the T lymphocyte compartment, a deficiency of which is associated with a poor prognosis [113] and targeting essential amino acids is an immunosuppressive strategy used by them [114]. Upregulation of arginase 1 activity leads to the depletion of L-arginine, which is essential for T cell proliferation [115]. MDSCs are also responsible for cysteine depletion and in the microenvironment this was found to impair T cell activation [116]. By secreting IDO, MDSCs also decrease the level of tryptophan, leading to T cell apoptosis via kynurenine generation [117]. The production of NO, which reacts with superoxide, promotes the production of peroxynitrite by MDSCs and this can cause nitration and nitrosylation of the T cell receptor, leading to T cell tolerance [118]. By nitrating chemokines such as CCL2, peroxynitrite also impairs T cell migration [119] although TGF-β and IL-10 represent the main immunosuppressive MDSC-derived factors owing to their ability to inhibit cytotoxic activity and T cell activation [108]. As a result of the expression of PD-L1 and FAS-L, binding the respective ligands PD-1 and FAS present at the T cell membrane, MDSCs also exert immunosuppressive activity through direct contact with T cells [120, 121] and can also induce the expansion of Tregs, another major immunosuppressive actor [122, 123]. These features highlight the dual role of recruited MDSCs in permissive microenvironment generation. Indeed, they are directly responsible for two synergic and complementary processes, immunosuppression and immunotolerance, which make them attractive therapeutic targets to overcome cancer immune escape strategies [124].

Together, these immune cells actively contribute to the formation of the pre-metastatic niche, necessary for LN colonization by metastatic cells that can eventually exit from the LN into the blood circulation [101, 125]. They modulate the local microenvironment by secreting inflammatory cytokines, growth factors, pro-angiogenic molecules and enzymes that remodel the matrix, such as LOX and MMPs [126].

Macrophages are present throughout the LN but are classified in different subtypes according to their location. A distinction is made between macrophages present in the SCS and MS from those residing in the LN parenchyma [47]. SCS macrophages are able to capture antigens from the lymph and transfer them to B cell follicles, but they appear poorly phagocytic. In contrast, CD209+ MS macrophages are more phagocytic and express F4/80. Both types are characterized by CD169 expression, a member of the sialic acid-binding lectin family. [48]. LECs play an important role in the maintenance of these macrophages via RANKL production and they are lost when there is RANKL deficiency [127]. LECs produce CSF-1 and this also plays a crucial role in the maintenance of the macrophages, as well as the MS macrophages [128]. An additional type of macrophage present in the LN

Fig. 2 Establishment of the lymph node (LN) pre-metastatic niche. Tumor-derived factors, including vascular endothelial growth factor (VEGF-A, VEGF-C and VEGF-D), extracellular vesicles, TGF-β and lysyl oxidase (LOX), induce an immunosuppressive microenvironment by recruiting macrophages, myeloid-derived suppressor cells (MDSCs) and regulatory T cells (Tregs). Proliferation of lymphatic endothelial cells (LECs) and fibroblastic reticular cells (FRCs) drives the production of LN factors such as chemokines (CCL19; CCL21; CXCL1, 2, 5, 8, and 12); TGF-β; matrix metalloproteinases (MMPs); indoleamine-2,3-dioxygenase (IDO); and nitric oxide (NO), which induce high endothelial venule (HEV) remodeling, stimulate lymphangiogenesis, and regulate tumor cells chemoattraction at metastatic stage
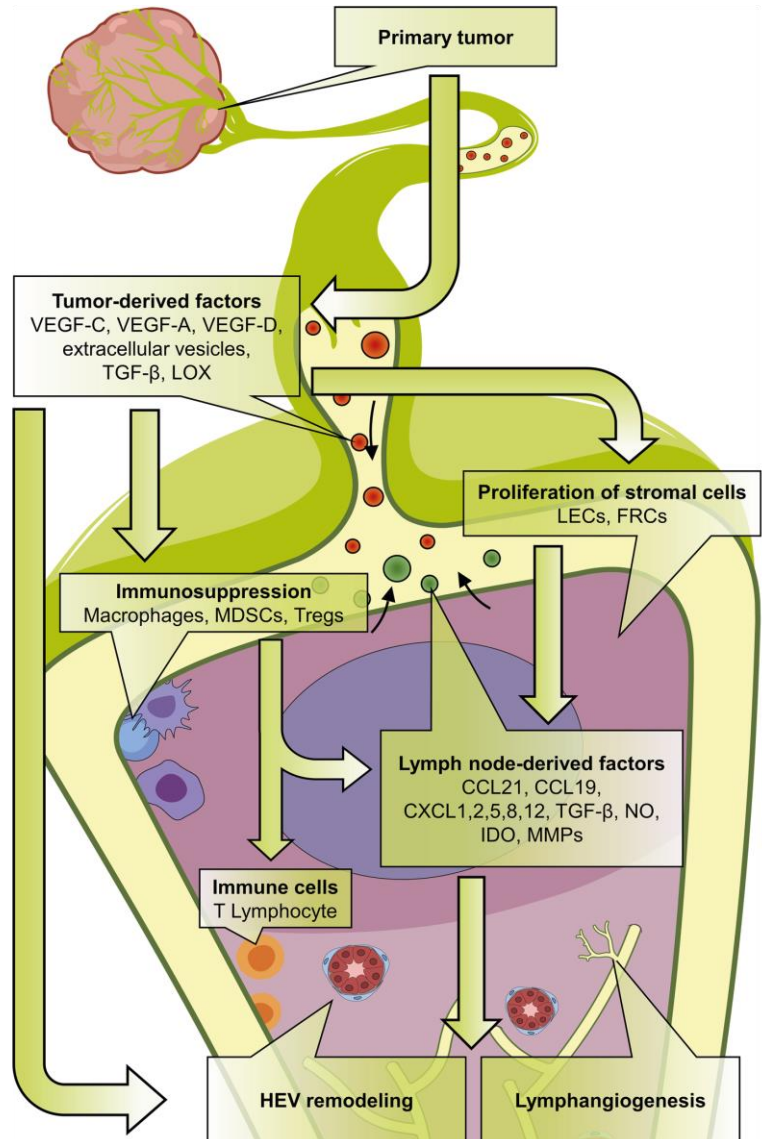
germinal center is tangible body macrophages, which have a particular role in the uptake of apoptotic cells within germinal centers [48]. Macrophages are also present in the parenchyma adjacent to the MS known as the medullary cords [47]. The last subset of parenchymal macrophages resides in the T cell zone. They express CD11c, CX3CR1, CD64 and MER proto-oncogene tyrosine kinase (MERTK) but test negative for CD169 and F4/80 [129]. Modifications in the CD169 + macrophage density have also been reported in pre-metastatic LNs. These macrophages capture tumor-derived

antigens in the SCS and transfer them to CD8 + T cells to elicit an anti-tumor response and can also capture EVs derived from tumor cells [86]. In a pre-clinical model, mice lacking CD169 + macrophages failed to induce anti-tumor immunity [130]. Reduced CD169 expression in pre-metastatic LNs is associated with subsequent metastatic disease and a poor outcome in several tumor types [131–134]. Tumor-derived EVs bind SCS CD169 + macrophages in tumor-draining LNs [135]. These macrophages are a major host cell type interacting with EVs in tumor-bearing

mice. 3D imaging of tumor-derived LNs with decreased CD169 + macrophages showed a higher penetration of EVs in the LN cortex. These data therefore suggest that SCS macrophages act as EV scavengers in an attempt to prevent cancer progression [135]. In humans, the presence of macrophages testing positive for HMB-45, a transmembrane glycoprotein expressed by melanomas, was localized near the LN capsule. LNs proved negative for tumor cells, suggesting that tumor-derived factors reach LNs in cancer progression, supporting the hypothesis of the pre-metastatic niche [135]. Prostaglandin E2 (PGE2) also plays an important role in the LN pre-metastatic niche and has been identified as an immunosuppressive molecule that increases the immunosuppressive potential of Tregs. PGE2 can also stimulate the expression of CXCL12 via the EP3 receptor, which increases the accumulation of CXCR4 + tumor cells and promotes the formation of the LN pre-metastatic niche [136].

Beyond the vessel wall lining functions described above, LECs can play a key role in immunosuppression, facilitating metastatic cell survival. LECs express inhibitory ligands such as PD-L1, which allows CD8 lymphocyte suppression or deletion [137]. LN LECs can also cross-present tumor antigens to promote CD4 suppression and produce immunosuppressive molecules such as nitric oxide, TGF-β, and IDO to promote an immunosuppressive nodal microenvironment [137–142]. It is known that both MHC class I and MHC class II are present in LN LECs [84, 143], and play an important part in immunotolerance and immune response. MHC I plays a crucial role in self-tolerance by presenting endogenous antigens to CD8 + T cells. Tumor-draining LN LECs were able to cross-present tumor antigens using MHC I and directly alter the CD8 + T cell response [9, 143, 144]. In addition, through acquiring MHC II from DCs, LECs were also shown to induce CD4 + T cell tolerance [145, 146]. fLECs can also be distinguished from other LEC subsets due to the expression of CD74 which is involved in the formation and transport of MHC class II antigen complexes [53].

The most striking TGF-β function is immunosuppression, of paramount importance in the context of cancer. Indeed, TGF-β is able to induce the expression of cell cycle regulators (p21 and p27), which inhibit the proliferation of naïve T lymphocytes [147]. TGF-β inhibits antigen presentation of DCs by suppressing the expression of major histocompatibility complex II [148] and promotes the differentiation of T cells in Tregs by triggering the expression of FOXP3 [149]. The emerging picture is that latent TGF-β could be activated through two different mechanisms, one involving LTBPs associated with the ECM and the other implicating transmembrane glycoprotein A repetitions predominant (GARP) [72, 150, 151]. Both mechanisms of TGF-β involve an integrin, binding to LAP to induce its mechanical deformation and the release of mature protein. The role of GARP has been mainly studied in Tregs, although it can be produced by non-immune cells such as endothelial cells and fibroblasts [152].

Under physiological conditions, TGF-β1 is the predominantly expressed isoform in immune cells, including immunosuppressive Tregs. Immunosuppression by the TGF-β1 pathway through Tregs avoids autoimmune reactions but contributes to tumor development [153]. Furthermore, myeloid cells such as TAMs, MDSCs and tumor-associated neutrophils also promote tumor progression by elaborating a pre-metastatic niche through an increased production of TGF-β [154].

The role of TGF-β in immunomodulation in LNs has been less well documented. Huang et al. demonstrated in a mouse model that Tregs secrete TGF-β1 in LNs [155], which in turn induces the expression of IL-17rb in 4T1 cells via the Smad2/3 signaling pathway boosting tumor malignancy [155]. Furthermore, the integrin-mediated regulation of TGF-β activation is essential for naïve T cell conditioning by DCs in LNs [156]. Interestingly, αvβ8 integrin-deficient mice, either globally or specifically in DCs, spontaneously develop severe immune cell deficiencies due to the impairment of TGF-β1 activation [157]. Further work is required to determine the exact contribution of TGF-β and its regulators (LTBP, GARP, integrins) to pre-metastatic LN niche formation.

LN extracellular matrix remodeling in the pre-metastatic niche

While cancer-associated fibroblasts (CAFs) represent a major cellular component of most primary neoplasms [158], these cells have only been poorly described in metastatic organs, particularly in LNs to date. Interestingly, a recent study identified four CAF subtypes in metastatic LNs of breast cancer patients [159]. Two of these subtypes (CAF subtype 1 and subtype 4) produce TGF-β and CXCL12 and activate the NOTCH signaling pathway to promote tumor cell invasion. Intriguingly, the origin of those CAFs in LNs remains unclear [159, 160]. Additional studies are required to increase knowledge of putative CAF implications in pre-metastatic and metastatic LN niches.

ECM remodeling is a key event that contributes to metastatic organ pre-conditioning and to the formation of an appropriate environment for tumor seeding. ECM modifications in the pre-metastatic niche have already been described, in detail, for the lung, liver and bones but have been poorly documented in the case of LNs. Interestingly, organ specificities have been highlighted in terms of ECM remodeling [24]. Among the ECM proteins involved in the metastatic colonization of distant organs (lung, liver, and bone) are TNC, POSTN and versican, the large chondroitin sulfate

proteoglycan, which have been identified as key players [26, 161–163]. POSTN plays a major role in tissue remodeling by interacting with ECM proteins such as fibronectin, TNC and collagen types I, IV, V [164]. POSTN-knockout mice bearing breast tumors exhibit decreased MDSC accumulation in pre-metastatic lungs and percentages of CD4$^+$ and CD8$^+$ T cells were more prevalent in the lung, and immunosuppressive factors were reduced in them compared to levels in wild-type mice [104]. POSTN is thought to play its part in LN metastasis but has not been clearly demonstrated at the present time. Recently, POSTN has been identified in metastatic LNs from patients with cervical cancer [165]. CAFs expressing POSTN, impaired lymphatic integrity by activating the integrin-FAK/Src-VE-cadherin signaling pathway in LECs, thereby increasing metastatic dissemination. Interestingly, CAF-derived POSTN was not found in non-metastatic LNs, suggesting the importance of the role of POSTN in tumor cell dissemination [165]. Unfortunately, no evidence has been provided about POSTN in the LN pre-metastatic niche, and this needs further study. Increased fibrinogen deposition was found in tumor-draining LNs compared to control LNs [92]. Furthermore, enhanced production of ECM-remodeling factors such as LOX, MT1-MMP and TIMP-1 was detected in metastatic LNs from patients with oral cancer [166]. This was in line with the implication of LOX and MMPs in the liver and lung pre-metastatic niches [167–170]. For instance, MMP9 induced by primary tumors in lung endothelial cells and macrophages promotes the invasion of tumor cells into the lung [171]. MDSCs recruited in the lung are also an important source of MMP9 [172]. LOX can also promote the production of MMP9 and fibronectin by fibroblasts in the lung pre-metastatic niche [173]. Taken as a whole, these data highlight important matrix remodeling in LNs at different stages of the metastatic cascade. Additional studies are, however, still required to reveal the role of ECM-remodeling factors in the LN pre-metastatic niche.

Conclusions and perspectives

A pre-metastatic niche is now widely accepted as a specific tumor-induced microenvironment, favorable for disseminating tumor cells and metastasis formation [170]. The elaboration of a pre-metastatic niche before colonization by tumor cells is a complex process recognized as an initial key step in the metastatic cascade. Recent advances in this field have identified a panel of crucial molecular and cellular components contributing to pre-metastatic niche formation in various tumor models. Factors produced by primary tumors can potentially condition not only the LN microenvironment but also other distant organs, including the lung, liver, brain and bone [174]. The exposure of LNs to a higher concentration of tumor-secreted factors drained

by the lymph compared to other organs could explain, at least partially, the predominance of LN metastases in cancer prognosis and in metastatic dissemination [10]. The description of LN lymphangiogenesis and its role in the metastatic process is relatively recent. Only a small number of clinical studies to date have documented pre-metastatic lymphangiogenic variations in the sentinel LNs of patients with cervical, breast, lung and oral squamous carcinomas [2, 97, 175–177]. These studies supported the concept of the LN pre-metastatic niche and revealed that LV density was increased in pre-metastatic sentinels in comparison with non-sentinel LNs. Notably, LV remodeling is also associated with modifications in the immune landscape [2]. Therefore, LN lymphangiogenesis is viewed as a potential target to treat or prevent metastatic disease. In this context, and given the crucial role of the VEGF-C/VEGFR-3 signaling pathway in lymphangiogenesis, a majority of studies aim to develop therapeutic drugs targeting this pathway. A phase 1 clinical trial evaluated an antibody directed against VEGFR-3. Unfortunately, disease control was only observed for a small percentage of patients (19%) [178]. A lack of response of LN metastasis to treatment with inhibitors of VEGFR-2 and VEGFR-3 has also been shown in mouse models [179], but, to date, both pre-clinical and clinical data have failed to demonstrate the efficacy of VEGFR inhibitors on LN metastases. These data emphasize the importance of searching for other putative therapeutic targets. Another clinical trial has used VGX-100, a VEGF-C neutralizing antibody, but no data have been published yet (NCT01514123). Recently, simvastatin, a 3-hydroxy-3-methylglutaryl coenzyme A (HMG-CoA) reductase inhibitor, was tested for LN metastasis in mice. Its interest relies on its capacity to decrease inflammatory cytokine synthesis and circulating VEGF levels. Simvastatin appears to play a potential role in tumor lymphangiogenesis and LN metastasis, suggesting that its combination with other agents could reduce LN lymphangiogenesis and tumor progression [180]. As highlighted in this review, LN pre-metastatic niche formation not only relies on LN lymphangiogenesis but also results from important, but still poorly documented, remodeling of different cellular and matrix components. Therefore, it is probable that a narrow focus on a unique biological process such as lymphangiogenesis or one of these molecular pathways will be unsuccessful for therapeutic development.

A large number of questions remain unanswered. What are the dynamics of LN pre-metastatic formation? It is largely unknown how different ECM components interact in the pre-metastatic niche and exert cooperative/synergistic or antagonistic effects on metastatic tumor cells. Which markers or signatures could be used to stratify patients and/or predict their potential to form LN and distant metastases? Understanding how and when the key cross-talk between the primary tumor and LN is established to prime the organ is a

prerequisite to identify the best potential molecular target(s). Consequently, it is crucial that basic scientists and clinicians work together to explore all facets of the pre-metastatic LN niche for diagnostic, prognostic and therapeutic purposes.

Declarations

Conflict of interest The authors declare that no competing interests exist.

References

1. Chatterjee G, Pai T, Hardiman T et al (2018) Molecular patterns of cancer colonisation in lymph nodes of breast cancer patients. Breast Cancer Res 20:143. https://doi.org/10.1186/s13058-018-1070-3
2. Balsat C, Blacher S, Herfs M et al (2017) A specific immune and lymphatic profile characterizes the pre-metastatic state of the sentinel lymph node in patients with early cervical cancer. Oncoimmunology 6:1–10. https://doi.org/10.1080/2162402X.2016.1265718
3. Wakisaka N, Hasegawa Y, Yoshimoto S et al (2015) Primary tumor-secreted lymphangiogenic factors induce pre-metastatic lymphvascular niche formation at sentinel lymph nodes in oral squamous cell carcinoma. PLoS ONE 10:e0144056. https://doi.org/10.1371/journal.pone.0144056
4. Tuomas T, Kari A (2010) Lymphangiogenesis : molecular mechanisms and future promise. Cell 140:460–476. https://doi.org/10.1016/j.cell.2010.01.045
5. Maus RLG, Jakub JW, Hieken TJ et al (2019) Identification of novel, immune-mediating extracellular vesicles in human lymphatic effluent draining primary cutaneous melanoma. Oncoimmunology 8:1–10. https://doi.org/10.1080/2162402X.2019.1667742
6. Cho JK, Hyun SH, Choi N et al (2015) Significance of lymph node metastasis in cancer dissemination of head and neck cancer.

7. Stacker SA, Williams SP, Karnezis T et al (2014) Lymphangiogenesis and lymphatic vessel remodelling in cancer. Nat Rev Cancer 14:159–172. https://doi.org/10.1038/nrc3677
8. Padera TP, Meijer EFJ, Munn LL (2016) The lymphatic system in disease processes and cancer progression. Annu Rev Biomed Eng 18:125–158. https://doi.org/10.1146/annurev-bioeng-112315-031200
9. Petrova TV, Koh GY (2020) Biological functions of lymphatic vessels. Science 369:eaax4063. https://doi.org/10.1126/science.aax4063
10. Sleeman JP (2015) The lymph node pre-metastatic niche. J Mol Med 93:1173–1184. https://doi.org/10.1007/s00109-015-1351-6
11. Sleeman JP, Nazarenko I, Thiele W (2011) Do all roads lead to Rome? Routes to metastasis development. Int J Cancer 128:2511–2526. https://doi.org/10.1002/ijc.26027
12. Cady B (2007) Regional lymph node metastases, a singular manifestation of the process of clinical metastases in cancer: contemporary animal research and clinical reports suggest unifying concepts. Cancer Treat Res 135:185–201. https://doi.org/10.1007/978-0-387-69219-7_14
13. Fisher B, Jeong JH, Anderson S et al (2002) Twenty-five-year follow-up of a randomized trial comparing radical mastectomy, total mastectomy, and total mastectomy followed by irradiation. N Engl J Med 347:567–575. https://doi.org/10.1056/NEJMoa020128
14. Cascinelli N, Morabito A, Santinami M et al (1998) Immediate or delayed dissection of regional nodes in patients with melanoma of the trunk: a randomised trial. Lancet 351:793–796. https://doi.org/10.1016/S0140-6736(97)08260-3
15. Nathanson SD, Kwon D, Kapke A et al (2009) The role of lymph node metastasis in the systemic dissemination of breast cancer. Ann Surg Oncol 16:3396–3405. https://doi.org/10.1245/s10434-009-0659-2
16. Brown M, Assen FP, Leithner A et al (2018) Lymph node blood vessels provide exit routes for metastatic tumor cell dissemination in mice. Science 359:1408–1411. https://doi.org/10.1126/science.aal3662
17. Pereira ER, Kedrin D, Seano G et al (2018) Lymph node metastases can invade local blood vessels, exit the node, and colonize distant organs in mice. Science 359:1403–1407. https://doi.org/10.1126/science.aal3622
18. Kaplan RN, Riba RD, Zacharoulis S et al (2005) VEGFR1-positive haematopoietic bone marrow progenitors initiate the pre-metastatic niche. Nature 438:820–827. https://doi.org/10.1038/nature04186
19. Peinado H, Zhang H, Matei IR et al (2017) Pre-metastatic niches: organ-specific homes for metastases. Nat Rev Cancer 17:302–317. https://doi.org/10.1038/nrc.2017.6
20. Psaila B, Lyden D (2009) The metastatic niche: adapting the foreign soil. Nat Rev Cancer 9:285–293. https://doi.org/10.1038/nrc2621
21. Maru Y (2015) The lung metastatic niche. J Mol Med 93:1185–1192. https://doi.org/10.1007/s00109-015-1355-2
22. Houg DS, Bijlsma MF (2018) The hepatic pre-metastatic niche in pancreatic ductal adenocarcinoma. Mol Cancer 17:95. https://doi.org/10.1186/s12943-018-0842-9
23. Ren G, Esposito M, Kang Y (2015) Bone metastasis and the metastatic niche. J Mol Med 93:1203–1212. https://doi.org/10.1007/s00109-015-1329-4
24. Paolillo M, Schinelli S (2019) Extracellular matrix alterations in metastatic processes. Int J Mol Sci 20:4947. https://doi.org/10.3390/ijms20194947

Transl Oncol 8:119–125. https://doi.org/10.1016/j.tranon.2015.03.001

25. Williamson T, Sultanpuram N, Sendi H (2019) The role of liver microenvironment in hepatic metastasis. Clin Transl Med 8:21. https://doi.org/10.1186/s40169-019-0237-6

26. Malanchi I, Santamaria-Martínez A, Susanto E et al (2012) Interactions between cancer stem cells and their niche govern metastatic colonization. Nature 481:85–91. https://doi.org/10.1038/nature10694

27. Hirakawa S, Kodama S, Kunstfeld R et al (2005) VEGF-A induces tumor and sentinel lymph node lymphangiogenesis and promotes lymphatic metastasis. J Exp Med 201:1089–1099. https://doi.org/10.1084/jem.20041896

28. Hirakawa S, Brown LF, Kodama S et al (2007) VEGF-C-induced lymphangiogenesis in sentinel lymph nodes promotes tumor metastasis to distant sites. Blood 109:1010–1017. https://doi.org/10.1182/blood-2006-05-021758

29. Farnsworth RH, Lackmann M, Achen MG, Stacker SA (2014) Vascular remodeling in cancer. Oncogene 33:3496–3505. https://doi.org/10.1038/onc.2013.304

30. Aspelund A, Robciuc MR, Karaman S et al (2016) Lymphatic system in cardiovascular medicine. Circ Res 118:515–530. https://doi.org/10.1161/CIRCRESAHA.115.306544

31. Vaahtomeri K, Karaman S, Mäkinen T, Alitalo K (2017) Lymphangiogenesis guidance by paracrine and pericellular factors. Genes Dev 31:1615–1634. https://doi.org/10.1101/gad.303776.117

32. Fütterer A, Mink K, Luz A et al (1998) The lymphotoxin β receptor controls organogenesis and affinity maturation in peripheral lymphoid tissues. Immunity 9:59–70. https://doi.org/10.1016/S1074-7613(00)80588-9

33. Cherrier M, Eberl G (2012) The development of LTi cells. Curr Opin Immunol 24:178–183. https://doi.org/10.1016/j.coi.2012.02.003

34. Meier D, Bornmann C, Chappaz S et al (2007) Ectopic lymphoid-organ development occurs through interleukin 7-mediated enhanced survival of lymphoid-tissue-inducer cells. Immunity 26:643–654. https://doi.org/10.1016/j.immuni.2007.04.009

35. Dougall WC, Glaccum M, Charrier K et al (1999) RANK is essential for osteoclast and lymph node development. Genes Dev 13:2412–2424. https://doi.org/10.1101/gad.13.18.2412

36. Van De Pavert SA, Mebius RE (2010) New insights into the development of lymphoid tissues. Nat Rev Immunol 10:664–674. https://doi.org/10.1038/nri2832

37. Randall T, Carragher D, Rangel-Moreno J (2008) Development of secondary lymphoid organs. Annu Rev Immunol 26:627–650. https://doi.org/10.1146/annurev.immunol.26.021607.090257

38. Bovay E, Sabine A, Prat-Luri B et al (2018) Multiple roles of lymphatic vessels in peripheral lymph node development. J Exp Med 215:2760–2777. https://doi.org/10.1084/jem.20180217

39. Onder L, Ludewig B (2018) A fresh view on lymph node organogenesis. Trends Immunol 39:775–787. https://doi.org/10.1016/j.it.2018.08.003

40. Van De Pavert SA, Mebius RE (2014) Development of secondary lymphoid organs in relation to lymphatic vasculature. Adv Anat Embryol Cell Biol 214:81–91. https://doi.org/10.1007/978-3-7091-1646-3_7

41. Onder L, Mörbe U, Pikor N et al (2017) Lymphatic endothelial cells control initiation of lymph node organogenesis. Immunity 47:80-92.e4. https://doi.org/10.1016/j.immuni.2017.05.008

42. Fletcher AL, Acton SE, Knoblich K (2015) Lymph node fibroblastic reticular cells in health and disease. Nat Rev Immunol 15:350–361. https://doi.org/10.1038/nri3846

43. Rodda LB, Lu E, Bennett ML et al (2018) Single-cell RNA sequencing of lymph node stromal cells reveals niche-associated heterogeneity. Immunity 48:1014-1028.e6. https://doi.org/10.1016/j.immuni.2018.04.006

44. Harlé G, Kowalski C, Garnier L, Hugues S (2020) Lymph node stromal cells: mapmakers of t cell immunity. Int J Mol Sci 21:1–18. https://doi.org/10.3390/ijms21207785

45. Grant SM, Lou M, Yao L et al (2020) The lymph node at a glance—how spatial organization optimizes the immune response. J Cell Sci 133:1–7. https://doi.org/10.1242/jcs.241828

46. Girard JP, Moussion C, Förster R (2012) HEVs, lymphatics and homeostatic immune cell trafficking in lymph nodes. Nat Rev Immunol 12:762–773. https://doi.org/10.1038/nri3298

47. Gray EE, Cyster JG (2012) Lymph node macrophages. J. Innate Immun 4:424–436. https://doi.org/10.1159/000337007

48. Bellomo A, Gentek R, Bajénoff M, Baratin M (2018) Lymph node macrophages: Scavengers, immune sentinels and trophic effectors. Cell Immunol 330:168–174. https://doi.org/10.1016/j.cellimm.2018.01.010

49. Petrova TV, Koh GY (2018) Organ-specific lymphatic vasculature: from development to pathophysiology. J Exp Med 215:35–49. https://doi.org/10.1084/jem.20171868

50. Ulvmar MH, Mäkinen T (2016) Heterogeneity in the lymphatic vascular system and its origin. Cardiovasc Res 111:310–321. https://doi.org/10.1093/cvr/cvw175

51. Iftakhar-E-Khuda I, Fair-Mäkelä R, Kukkonen-Macchi A et al (2016) Gene-expression profiling of different arms of lymphatic vasculature identifies candidates for manipulation of cell traffic. Proc Natl Acad Sci U S A 113:10643–10648. https://doi.org/10.1073/pnas.1602357113

52. Fujimoto N, He Y, D'Addio M et al (2020) Single-cell mapping reveals new markers and functions of lymphatic endothelial cells in lymph nodes. PLoS Biol 18:e3000704. https://doi.org/10.1371/journal.pbio.3000704

53. Xiang M, Grosso RA, Takeda A et al (2020) A single-cell transcriptional roadmap of the mouse and human lymph node lymphatic vasculature. Front Cardiovasc Med. https://doi.org/10.3389/fcvm.2020.00052

54. Takeda A, Hollmén M, Dermadi D et al (2019) Single-cell survey of human lymphatics unveils marked endothelial cell heterogeneity and mechanisms of homing for neutrophils. Immunity 51:561-572.e5. https://doi.org/10.1016/j.immuni.2019.06.027

55. Cohen JN, Tewalt EF, Rouhani SJ et al (2014) Tolerogenic properties of lymphatic endothelial cells are controlled by the lymph node microenvironment. PLoS ONE 9:e87740. https://doi.org/10.1371/journal.pone.0087740

56. Ulvmar MH, Werth K, Braun A et al (2014) The atypical chemokine receptor CCRL1 shapes functional CCL21 gradients in lymph nodes. Nat Immunol 15:623–630. https://doi.org/10.1038/ni.2889

57. Cochran AJ, Huang RR, Lee J et al (2006) Tumour-induced immune modulation of sentinel lymph nodes. Nat Rev Immunol 6:659–670. https://doi.org/10.1038/nri1919

58. Roozendaal R, Mempel TR, Pitcher LA et al (2009) Conduits mediate transport of low-molecular-weight antigen to lymph node follicles. Immunity 30:264–276. https://doi.org/10.1016/j.immuni.2008.12.014

59. Martinez VG, Pankova V, Krasny L et al (2019) Fibroblastic reticular cells control conduit matrix deposition during lymph node expansion. Cell Rep 29:2810-2822.e5. https://doi.org/10.1016/j.celrep.2019.10.103

60. Novkovic M, Onder L, Bocharov G, Ludewig B (2020) Topological Structure and robustness of the lymph node conduit system. Cell Rep 30:893-904.e6. https://doi.org/10.1016/j.celrep.2019.12.070

61. Kelch ID, Bogle G, Sands GB et al (2019) High-resolution 3D imaging and topological mapping of the lymph node conduit system. PLoS Biol 17:1–25. https://doi.org/10.1371/journal.pbio.3000486

62. Reynoso GV, Weisberg AS, Shannon JP et al (2019) Lymph node conduits transport virions for rapid T cell activation. Nat Immunol 20:602–612. https://doi.org/10.1038/s41590-019-0342-0

63. Förster R, Davalos-Misslitz AC, Rot A (2008) CCR7 and its ligands: balancing immunity and tolerance. Nat Rev Immunol 8:362–371. https://doi.org/10.1038/nri2297

64. Ager A (2017) High endothelial venules and other blood vessels: critical regulators of lymphoid organ development and function. Front Immunol 8:1–16. https://doi.org/10.3389/fimmu.2017.00045

65. Pawlak JB, Caron KM (2020) Lymphatic programing and specialization in hybrid vessels. Front Physiol 11:114. https://doi.org/10.3389/fphys.2020.00114

66. Hynes RO, Naba A (2012) Overview of the matrisome—an inventory of extracellular matrix constituents and functions. Cold Spring Harb Perspect Biol 4:a004903–a004903. https://doi.org/10.1101/cshperspect.a004903

67. Walker C, Mojares E, Del Río HA (2018) Role of extracellular matrix in development and cancer progression. Int J Mol Sci 19:3028. https://doi.org/10.3390/ijms19103028

68. Høye AM, Erler JT (2016) Structural ECM components in the premetastatic and metastatic niche. Am J Physiol Cell Physiol 310:C955–C967. https://doi.org/10.1152/ajpcell.00326.2015

69. Eble JA, Niland S (2019) The extracellular matrix in tumor progression and metastasis. Clin Exp Metastasis 36:171–198. https://doi.org/10.1007/s10585-019-09966-1

70. Bourgot I, Primac I, Louis T et al (2020) Reciprocal interplay between fibrillar collagens and collagen-binding integrins: implications in cancer progression and metastasis. Front Oncol 10:1–28. https://doi.org/10.3389/fonc.2020.01488

71. Sixt M, Kanazawa N, Selg M et al (2005) The conduit system transports soluble antigens from the afferent lymph to resident dendritic cells in the T cell area of the lymph node. Immunity 22:19–29. https://doi.org/10.1016/j.immuni.2004.11.013

72. Robertson IB, Horiguchi M, Zilberberg L et al (2016) Latent TGF-β-binding proteins. Matrix Biol 47:44–53. https://doi.org/10.1016/j.matbio.2015.05.005

73. Sobocinski GP, Toy K, Bobrowski WF et al (2010) Ultrastructural localization of extracellular matrix proteins of the lymph node cortex: evidence supporting the reticular network as a pathway for lymphocyte migration. BMC Immunol 11:42. https://doi.org/10.1186/1471-2172-11-42

74. Malhotra D, Fletcher AL, Astarita J et al (2012) Transcriptional profiling of stroma from inflamed and resting lymph nodes defines immunological hallmarks. Nat Immunol 13:499–510. https://doi.org/10.1038/ni.2262

75. Hamidi H, Ivaska J (2018) Every step of the way: integrins in cancer progression and metastasis. Nat Rev Cancer. https://doi.org/10.1038/s41568-018-0038-z

76. González-González L, Alonso J (2018) Periostin: a matricellular protein with multiple functions in cancer development and progression. Front Oncol 8:1–15. https://doi.org/10.3389/fonc.2018.00225

77. Yokosaki Y, Monis H, Ghen J, Sheppard D (1996) Differential effects of the integrins α9β1, αvβ3, and αvβ6 on cell proliferative responses to tenascin. Roles of the β subunit extracellular and cytoplasmic domains. J Biol Chem 271:24144–24150. https://doi.org/10.1074/jbc.271.39.24144

78. Piao YJ, Kim HS, Hwang EH et al (2018) Breast cancer cell-derived exosomes and macrophage polarization are associated with lymph node metastasis. Oncotarget 9:7398–7410. https://doi.org/10.18632/oncotarget.23238

79. Tickner JA, Urquhart AJ, Stephenson SA et al (2014) Functions and therapeutic roles of exosomes in cancer. Front Oncol 4:1–8. https://doi.org/10.3389/fonc.2014.00127

80. Plebanek MP, Angeloni NL, Vinokour E et al (2017) Pre-metastatic cancer exosomes induce immune surveillance by patrolling monocytes at the metastatic niche. Nat Commun 8:1319. https://doi.org/10.1038/s41467-017-01433-3

81. Hood JL, San Roman S, Wickline SA (2011) Exosomes released by melanoma cells prepare sentinel lymph nodes for tumor metastasis. Cancer Res 71:3792–3801. https://doi.org/10.1158/0008-5472.CAN-10-4455

82. Zhou W, Fong MY, Min Y et al (2014) Cancer-secreted miR-105 destroys vascular endothelial barriers to promote metastasis. Cancer Cell 25:501–515. https://doi.org/10.1016/j.ccr.2014.03.007

83. Zeng Z, Li Y, Pan Y et al (2018) Cancer-derived exosomal miR-25-3p promotes pre-metastatic niche formation by inducing vascular permeability and angiogenesis. Nat Commun 9:5395. https://doi.org/10.1038/s41467-018-07810-w

84. Broggi MAS, Maillat L, Clement CC et al (2019) Tumor-associated factors are enriched in lymphatic exudate compared to plasma in metastatic melanoma patients. J Exp Med 216:1091–1107. https://doi.org/10.1084/jem.20181618

85. García-Silva S, Benito-Martín A, Sánchez-Redondo S et al (2019) Use of extracellular vesicles from lymphatic drainage as surrogate markers of melanoma progression and BRAFV600E mutation. J Exp Med 216:1061–1070. https://doi.org/10.1084/jem.20181522

86. Nogués L, Benito-Martin A, Hergueta-Redondo M, Peinado H (2018) The influence of tumour-derived extracellular vesicles on local and distal metastatic dissemination. Mol Aspects Med 60:15–26. https://doi.org/10.1016/j.mam.2017.11.012

87. Garmy-susini B, Avraamides CJ, Desgrosellier JS et al (2013) PI3K α activates integrin α 4 β 1 to establish a metastatic niche in lymph nodes. Proc Natl Acad Sci U S A 110:9042–9047. https://doi.org/10.1073/pnas.1219603110/

88. Lee AS, Kim DH, Lee JE et al (2011) Erythropoietin induces lymph node lymphangiogenesis and lymph node tumor metastasis. Cancer Res 71:4506–4517. https://doi.org/10.1158/0008-5472.CAN-10-3787

89. Dieterich LC, Detmar M (2016) Tumor lymphangiogenesis and new drug development. Adv Drug Deliv Rev 99:148–160. https://doi.org/10.1016/j.addr.2015.12.011

90. Ma Q, Dieterich LC, Detmar M (2018) Multiple roles of lymphatic vessels in tumor progression. Curr Opin Immunol 53:7–12. https://doi.org/10.1016/j.coi.2018.03.018

91. Karnezis T, Shayan R, Fox S et al (2012) The connection between lymphangiogenic signalling and prostaglandin biology: a missing link in the metastatic pathway. Oncotarget 3:890–903. https://doi.org/10.18632/oncotarget.593

92. Commerford CD, Dieterich LC, He Y et al (2018) Mechanisms of tumor-induced lymphovascular niche formation in draining lymph nodes. Cell Rep 25:3554-3563.e4. https://doi.org/10.1016/j.celrep.2018.12.002

93. Cordeiro OG, Chypre M, Brouard N et al (2016) Integrin-alpha IIb identifies murine lymph node lymphatic endothelial cells responsive to RANKL. PLoS ONE 11:1–16. https://doi.org/10.1371/journal.pone.0151848

94. Dieterich LC, Kapaklikaya K, Cetintas T et al (2019) Transcriptional profiling of breast cancer-associated lymphatic vessels reveals VCAM-1 as regulator of lymphatic invasion and permeability. Int J Cancer 145:2804–2815. https://doi.org/10.1002/ijc.32594

95. Brulois K, Rajaraman A, Szade A et al (2020) A molecular map of murine lymph node blood vascular endothelium at single cell resolution. Nat Commun. https://doi.org/10.1038/s41467-020-17291-5

96. Qian CN, Berghuis B, Tsarfaty G et al (2006) Preparing the "soil": the primary tumor induces vasculature reorganization

in the sentinel lymph node before the arrival of metastatic cancer cells. Cancer Res 66:10365–10376. https://doi.org/10.1158/0008-5472.CAN-06-2977

97. Chung MK, Do IG, Jung E et al (2012) Lymphatic vessels and high endothelial venules are increased in the sentinel lymph nodes of patients with oral squamous cell carcinoma before the arrival of tumor cells. Ann Surg Oncol 19:1595–1601. https://doi.org/10.1245/s10434-011-2154-9

98. Farnsworth RH, Karnezis T, Shayan R et al (2011) A role for bone morphogenetic protein-4 in lymph node vascular remodeling and primary tumor growth. Cancer Res 71:6547–6557. https://doi.org/10.1158/0008-5472.CAN-11-0200

99. Bekkhus T, Martikainen T, Olofsson A et al (2021) Article remodeling of the lymph node high endothelial venules reflects tumor invasiveness in breast cancer and is associated with dysregulation of perivascular stromal cells. Cancers 13:1–17. https://doi.org/10.3390/cancers13020211

100. Chen JY, Lai YS, Chu PY et al (2019) Cancer-derived VEGF-C increases chemokine production in lymphatic endothelial cells to promote CXCR2-dependent cancer invasion and MDSC recruitment. Cancers 11:1120. https://doi.org/10.3390/cancers11081120

101. Kitamura T, Qian BZ, Pollard JW (2015) Immune cell promotion of metastasis. Nat Rev Immunol 15:73–86. https://doi.org/10.1038/nri3789

102. Schaller J, Agudo J (2020) Metastatic colonization: escaping immune surveillance. Cancers 12:1–15. https://doi.org/10.3390/cancers12113385

103. Watanabe S, Deguchi K, Zheng R et al (2008) Tumor-induced CD11b + Gr-1 + myeloid cells suppress T cell sensitization in tumor-draining lymph nodes. J Immunol 181:3291–3300. https://doi.org/10.4049/jimmunol.181.5.3291

104. Wang Z, Xiong S, Mao Y et al (2016) Periostin promotes immunosuppressive premetastatic niche formation to facilitate breast tumour metastasis. J Pathol 239:484–495. https://doi.org/10.1002/path.4747

105. Wang Y, Ding Y, Guo N, Wang S (2019) MDSCs: key criminals of tumor pre-metastatic niche formation. Front Immunol 10:1–16. https://doi.org/10.3389/fimmu.2019.00172

106. Eisenblaetter M, Flores-Borja F, Lee JJ et al (2017) Visualization of tumor-immune interaction—target-specific imaging of S100A8/A9 reveals pre-metastatic niche establishment. Theranostics 7:2392–2401. https://doi.org/10.7150/thno.17138

107. Chafe SC, Lou Y, Sceneay J et al (2015) Carbonic anhydrase IX promotes myeloid-derived suppressor cell mobilization and establishment of a metastatic niche by stimulating G-CSF production. Cancer Res 75:996–1008. https://doi.org/10.1158/0008-5472.CAN-14-3000

108. Alicea-Torres K, Gabrilovich DI (2018) Biology of myeloid-derived suppressor cells. Oncoimmunology. https://doi.org/10.1007/978-3-319-62431-0_10

109. Vetsika EK, Koukos A, Kotsakis A (2019) Myeloid-derived suppressor cells: major figures that shape the immunosuppressive and angiogenic network in cancer. Cells 8:1647. https://doi.org/10.3390/cells8121647

110. Cochran AJ, Huang RR, Su A et al (2015) Is sentinel node susceptibility to metastases related to nodal immune modulation? Cancer J 21:39–46. https://doi.org/10.1097/PPO.0000000000000094

111. Lee JH, Torisu-Itakura H, Cochran AJ et al (2005) Quantitative analysis of melanoma-induced cytokine-mediated immunosuppression in melanoma sentinel nodes. Clin Cancer Res 11:107–112

112. Kumar V, Cheng P, Condamine T et al (2016) CD45 phosphatase inhibits STAT3 transcription factor activity in myeloid cells and

promotes tumor-associated macrophage differentiation. Immunity 44:303–315. https://doi.org/10.1016/j.immuni.2016.01.014

113. Holtzhausen A, Harris W, Ubil E et al (2019) TAM family receptor kinase inhibition reverses MDSC-mediated suppression and augments anti–PD-1 therapy in melanoma. Cancer Immunol Res 7:1672–1686. https://doi.org/10.1158/2326-6066.CIR-19-0008

114. Trovato R, Canè S, Petrova V et al (2020) The engagement between MDSCs and metastases: partners in crime. Front Oncol 10:1–16. https://doi.org/10.3389/fonc.2020.00165

115. Rodriguez PC, Hernandez CP, Quiceno D et al (2005) Arginase I in myeloid suppressor cells is induced by COX-2 in lung carcinoma. J Exp Med 202:931–939. https://doi.org/10.1084/jem.20050715

116. Srivastava MK, Sinha P, Clements VK et al (2010) Myeloid-derived suppressor cells inhibit T-cell activation by depleting cystine and cysteine. Cancer Res 70:68–77. https://doi.org/10.1158/0008-5472.CAN-09-2587

117. Yu J, Du W, Yan F et al (2013) Myeloid-derived suppressor cells suppress antitumor immune responses through IDO expression and correlate with lymph node metastasis in patients with breast cancer. J Immunol 190:3783–3797. https://doi.org/10.4049/jimmunol.1201449

118. Nagaraj S, Gupta K, Pisarev V et al (2007) Altered recognition of antigen is a mechanism of CD8+ T cell tolerance in cancer. Nat Med 13:828–835. https://doi.org/10.1038/nm1609

119. Molon B, Ugel S, Del Pozzo F et al (2011) Chemokine nitration prevents intratumoral infiltration of antigen-specific T cells. J Exp Med 208:1949–1962. https://doi.org/10.1084/jem.20101956

120. Zhu J, Powis De Tenbossche CG, Cané S et al (2017) Resistance to cancer immunotherapy mediated by apoptosis of tumor-infiltrating lymphocytes. Nat Commun. https://doi.org/10.1038/s41467-017-00784-1

121. Mohammadpour H, MacDonald CR, Qiao G et al (2019) B2 adrenergic receptor-mediated signaling regulates the immunosuppressive potential of myeloid-derived suppressor cells. J Clin Invest 129:5537–5552. https://doi.org/10.1172/JCI129502

122. Huang B, Pan PY, Li Q et al (2006) Gr-1+CD115+ immature myeloid suppressor cells mediate the development of tumor-induced T regulatory cells and T-cell anergy in tumor-bearing host. Cancer Res 66:1123–1131. https://doi.org/10.1158/0008-5472.CAN-05-1299

123. Wang J, Yang L, Yu L et al (2017) Surgery-induced monocytic myeloid-derived suppressor cells expand regulatory T cells in lung cancer. Oncotarget 8:17050–17058. https://doi.org/10.18632/oncotarget.14991

124. Tang F, Tie Y, Hong W et al (2020) Targeting myeloid-derived suppressor cells for premetastatic niche disruption after tumor resection. Ann Surg Oncol. https://doi.org/10.1245/s10434-020-09371-z

125. Liu Y, Cao X (2016) Immunosuppressive cells in tumor immune escape and metastasis. J Mol Med 94:509–522. https://doi.org/10.1007/s00109-015-1376-x

126. Liu Y, Cao X (2016) Characteristics and significance of the pre-metastatic niche. Cancer Cell 30:668–681. https://doi.org/10.1016/j.ccell.2016.09.011

127. Camara A, Cordeiro OG, Alloush F et al (2019) Lymph node mesenchymal and endothelial stromal cells cooperate via the RANK-RANKL cytokine axis to shape the sinusoidal macrophage niche. Immunity 50:1467-1481.e6. https://doi.org/10.1016/j.immuni.2019.05.008

128. Mondor I, Baratin M, Lagueyrie M et al (2019) Lymphatic endothelial cells are essential components of the subcapsular sinus macrophage niche. Immunity 50:1453-1466.e4. https://doi.org/10.1016/j.immuni.2019.04.002

129. Baratin M, Simon L, Jorquera A et al (2017) T cell zone resident macrophages silently dispose of apoptotic cells in the lymph node. Immunity 47:349-362.e5. https://doi.org/10.1016/j.immuni.2017.07.019

130. Asano K, Nabeyama A, Miyake Y et al (2011) CD169-positive macrophages dominate antitumor immunity by crosspresenting dead cell-associated antigens. Immunity 34:85–95. https://doi.org/10.1016/j.immuni.2010.12.011

131. Ohnishi K, Yamaguchi M, Erdenebaatar C et al (2016) Prognostic significance of CD169-positive lymph node sinus macrophages in patients with endometrial carcinoma. Cancer Sci 107:846–852. https://doi.org/10.1111/cas.12929

132. Saito Y, Ohnishi K, Miyashita A et al (2015) Prognostic significance of CD169+ lymph node sinus macrophages in patients with malignant melanoma. Cancer Immunol Res 3:1356–1363. https://doi.org/10.1158/2326-6066.CIR-14-0180

133. Shiota T, Miyasato Y, Ohnishi K et al (2016) The clinical significance of CD169-positive lymph node macrophage in patients with breast cancer. PLoS ONE 11:e0166680. https://doi.org/10.1371/journal.pone.0166680

134. Strömvall K, Sundkvist K, Ljungberg B et al (2017) Reduced number of CD169+ macrophages in pre-metastatic regional lymph nodes is associated with subsequent metastatic disease in an animal model and with poor outcome in prostate cancer patients. Prostate 77:1468–1477. https://doi.org/10.1002/pros.23407

135. Pucci F, Garris C, Lai CP et al (2016) SCS macrophages suppress melanoma by restricting tumor-derived vesicle-B cell interactions. Science 352:242–246. https://doi.org/10.1126/science.aaf1328

136. Ogawa F, Narumiya S, Majima M et al (2014) Prostanoid induces premetastatic niche in regional lymph nodes Find the latest version : prostanoid induces premetastatic niche in regional lymph nodes. J Clin Invest 124:4882–4894. https://doi.org/10.1172/JCI73530.tumor-specific

137. Rouhani JS (2014) Regulation of T-cell tolerance by lymphatic endothelial cells. J Clin Cell Immunol 05:242. https://doi.org/10.4172/2155-9899.1000242

138. Card CM, Yu SS, Swartz MA (2014) Emerging roles of lymphatic endothelium in regulating adaptive immunity. J Clin Invest 124:943–952. https://doi.org/10.1172/JCI73316

139. Cohen JN, Guidi CJ, Tewalt EF et al (2010) Lymph node-resident lymphatic endothelial cells mediate peripheral tolerance via Aire-independent direct antigen presentation. J Exp Med 207:681–688. https://doi.org/10.1084/jem.20092465

140. Tewalt EF, Cohen JN, Rouhani SJ, Engelhard VH (2012) Lymphatic endothelial cells - key players in regulation of tolerance and immunity. Front Immunol 3:305. https://doi.org/10.3389/fimmu.2012.00305

141. Habenicht LM, Kirschbaum SB, Furuya M et al (2017) Tumor regulation of lymph node lymphatic sinus growth and lymph flow in mice and in humans. Yale J Biol Med 90:403–415

142. Tewalt EF, Cohen JN, Rouhani SJ et al (2012) Lymphatic endothelial cells induce tolerance via PD-L1 and lack of costimulation leading to high-level PD-1 expression on CD8 T cells. Blood 120:4772–4782. https://doi.org/10.1182/blood-2012-04-427013

143. Jalkanen S, Salmi M (2020) Lymphatic endothelial cells of the lymph node. Nat Rev Immunol 20:566–578. https://doi.org/10.1038/s41577-020-0281-x

144. Lund AW, Duraes FV, Hirosue S et al (2012) VEGF-C promotes immune tolerance in B16 melanomas and cross-presentation of tumor antigen by lymph node lymphatics. Cell Rep 1:191–199. https://doi.org/10.1016/j.celrep.2012.01.005

145. Dubrot J, Duraes FV, Potin L et al (2014) Lymph node stromal cells acquire peptide-MHCII complexes from dendritic cells

and induce antigen-specific CD4+ T cell tolerance. J Exp Med 211:1153–1166. https://doi.org/10.1084/jem.20132000

146. Lucas ED, Tamburini BAJ (2019) Lymph node lymphatic endothelial cell expansion and contraction and the programming of the immune response. Front Immunol 10:36. https://doi.org/10.3389/fimmu.2019.00036

147. Wolfraim LA, Walz TM, James Z et al (2004) p21 Cip1 and p27 Kip1 act in synergy to alter the sensitivity of naive T cells to TGF-β-mediated G 1 arrest through modulation of IL-2 responsiveness. J Immunol 173:3093–3102. https://doi.org/10.4049/jimmunol.173.5.3093

148. Batlle E, Massagué J (2019) Transforming growth factor-β signaling in immunity and cancer. Immunity 50:924–940. https://doi.org/10.1016/j.immuni.2019.03.024

149. Ravi R, Noonan KA, Pham V et al (2018) Bifunctional immune checkpoint-targeted antibody-ligand traps that simultaneously disable TGFβ enhance the efficacy of cancer immunotherapy. Nat Commun 9:741. https://doi.org/10.1038/s41467-017-02696-6

150. Lodyga M, Hinz B (2019) TGF-β1—a truly transforming growth factor in fibrosis and immunity. Semin Cell Dev Biol 10:123–139. https://doi.org/10.1016/j.semcdb.2019.12.010

151. Campbell MG, Cormier A, Ito S et al (2020) Cryo-EM reveals integrin-mediated TGF-β activation without release from latent TGF-β. Cell 180:490-501.e16. https://doi.org/10.1016/j.cell.2019.12.030

152. Stockis J, Dedobbeleer O, Lucas S (2017) Role of GARP in the activation of latent TGF-β1. Mol Biosyst 13:1925–1935. https://doi.org/10.1039/c7mb00251c

153. Liénart S, Merceron R, Vanderaa C et al (2018) Structural basis of latent TGF-β1 presentation and activation by GARP on human regulatory T cells. Science 956:952–956. https://doi.org/10.1126/science.aau2909

154. Pang Y, Gara SK, Achyut BR et al (2013) TGF-β signaling in myeloid cells is required for tumor metastasis. Cancer Discov 3:936–951. https://doi.org/10.1158/2159-8290.CD-12-0527

155. Huang SC, Wei PC, Hwang-Verslues WW et al (2017) TGF-β1 secreted by Tregs in lymph nodes promotes breast cancer malignancy via up-regulation of IL-17RB. EMBO Mol Med 9:1660–1680. https://doi.org/10.15252/emmm.201606914

156. Mani V, Bromley SK, Äijö T et al (2019) Migratory DCs activate TGF-b to precondition naïve CD8+T cells for tissue-resident memory fate. Science 366:eaav5728. https://doi.org/10.1126/science.aav5728

157. Travis MA, Reizis B, Melton AC et al (2007) Loss of integrin αvβ8 on dendritic cells causes autoimmunity and colitis in mice. Nature 449:361–365. https://doi.org/10.1038/nature06110

158. Liu T, Zhou L, Li D et al (2019) Cancer-associated fibroblasts build and secure the tumor microenvironment. Front Cell Dev Biol 7:1–14. https://doi.org/10.3389/fcell.2019.00060

159. Pelon F, Bourachot B, Kieffer Y et al (2020) Cancer-associated fibroblast heterogeneity in axillary lymph nodes drives metastases in breast cancer through complementary mechanisms. Nat Commun 11:404. https://doi.org/10.1038/s41467-019-14134-w

160. Rodda LB, Lu E, Bennett ML et al (2018) Single-cell RNA sequencing of lymph node stromal resource single-cell RNA sequencing of lymph node stromal cells reveals niche-associated heterogeneity. Immunity 48:1014-1028.e6. https://doi.org/10.1016/j.immuni.2018.04.006

161. Oskarsson T, Acharyya S, Zhang XHF et al (2011) Breast cancer cells produce tenascin C as a metastatic niche component to colonize the lungs. Nat Med 17:867–874. https://doi.org/10.1038/nm.2379

162. O'Connell JT, Sugimoto H, Cooke VG et al (2011) VEGF-A and Tenascin-C produced by S100A4 + stromal cells are important for metastatic colonization. Proc Natl Acad Sci U S A 108:16002–16007. https://doi.org/10.1073/pnas.1109493108

163. Gao D, Joshi N, Choi H et al (2012) Myeloid progenitor cells in the premetastatic lung promote metastases by inducing mesenchymal to epithelial transition. Cancer Res 72:1384–1394. https://doi.org/10.1158/0008-5472.CAN-11-2905

164. Ratajczak-Wielgomas K, Dziegiel P (2015) The role of periostin in neoplastic processes. Folia Histochem Cytobiol 53:120–132. https://doi.org/10.5603/FHC.a2015.0014

165. Wei WF, Chen XJ, Liang LJ et al (2021) Periostin+cancer-associated fibroblasts promote lymph node metastasis by impairing the lymphatic endothelial barriers in cervical squamous cell carcinoma. Mol Oncol 15:210–227. https://doi.org/10.1002/1878-0261.12837

166. Fujita S, Sumi M, Tatsukawa E et al (2020) Expressions of extracellular matrix-remodeling factors in lymph nodes from oral cancer patients. Oral Dis 26:1424–1431. https://doi.org/10.1111/odi.13419

167. Owyong M, Chou J, van den Bijgaart RJE et al (2019) MMP9 modulates the metastatic cascade and immune landscape for breast cancer anti-metastatic therapy. Life Sci Alliance 2:1–16. https://doi.org/10.26508/lsa.201800226

168. Erler JT, Bennewith KL, Cox TR et al (2009) Hypoxia-induced lysyl oxidase is a critical mediator of bone marrow cell recruitment to form the pre-metastatic niche. Cancer Cell 15:35–44. https://doi.org/10.1016/j.ccr.2008.11.012

169. Cox TR, Erler JT (2011) Remodeling and homeostasis of the extracellular matrix: Implications for fibrotic diseases and cancer. Dis Model Mech 4:165–178. https://doi.org/10.1242/dmm.004077

170. Chin AR, Wang SE (2016) Cancer tills the premetastatic field: mechanistic basis and clinical implications. Clin Cancer Res 22:3725–3733. https://doi.org/10.1158/1078-0432.CCR-16-0028

171. Hiratsuka S, Nakamura K, Iwai S et al (2002) MMP9 induction by vascular endothelial growth factor receptor-1 is involved in lung-specific metastasis. Cancer Cell 2:289–300. https://doi.org/10.1016/S1535-6108(02)00153-8

172. Ghouse SM, Vadrevu SK, Manne S et al (2020) Therapeutic targeting of vasculature in the premetastatic and metastatic niches reduces lung metastasis. J Immunol 204:990–1000. https://doi.org/10.4049/jimmunol.1901208

173. Wu S, Zheng Q, Xing X et al (2018) Matrix stiffness-upregulated LOXL2 promotes fibronectin production, MMP9 and CXCL12

expression and BMDCs recruitment to assist pre-metastatic niche formation. J Exp Clin Cancer Res 37:1–12. https://doi.org/10.1186/s13046-018-0761-z

174. Aguado BA, Bushnell GG, Rao SS et al (2017) Engineering the pre-metastatic niche. Nat Biomed Eng 1:1–28. https://doi.org/10.1038/s41551-017-0077

175. Wakisaka N, Hasegawa Y, Yoshimoto S et al (2015) Primary tumor-secreted lymphangiogenic factors induce pre-metastatic lymphvascular niche formation at sentinel lymph nodes in oral squamous cell carcinoma. PLoS ONE 10:1–14. https://doi.org/10.1371/journal.pone.0144056

176. Kawai H, Minamiya Y, Ito M et al (2008) VEGF121 promotes lymphangiogenesis in the sentinel lymph nodes of non-small cell lung carcinoma patients. Lung Cancer 59:41–47. https://doi.org/10.1016/j.lungcan.2007.08.001

177. Zhao YC, Ni XJ, Wang MH et al (2012) Tumor-derived VEGF-C, but not VEGF-D, promotes sentinel lymph node lymphangiogenesis prior to metastasis in breast cancer patients. Med Oncol 29:2594–2600. https://doi.org/10.1007/s12032-012-0205-0

178. Saif MW, Knost JA, Chiorean EG et al (2016) Phase 1 study of the anti-vascular endothelial growth factor receptor 3 monoclonal antibody LY3022856/IMC-3C5 in patients with advanced and refractory solid tumors and advanced colorectal cancer. Cancer Chemother Pharmacol 78:815–824. https://doi.org/10.1007/s00280-016-3134-3

179. Padera TP, Kuo AH, Hoshida T et al (2008) Differential response of primary tumor versus lymphatic metastasis to VEGFR-2 and VEGFR-3 kinase inhibitors cediranib and vandetanib. Mol Cancer Ther 7:2272–2279. https://doi.org/10.1158/1535-7163.MCT-08-0182

180. Ji RC, Eshita Y, Kobayashi T et al (2018) Role of simvastatin in tumor lymphangiogenesis and lymph node metastasis. Clin Exp Metastasis 35:785–796. https://doi.org/10.1007/s10585-018-9940-8

Publisher's Note Springer Nature remains neutral with regard to jurisdictional claims in published maps and institutional affiliations.